Revisiting past excavations from South-Central Africa: palaeoenvironmental, biomolecular and geochronological analysis to improve archaeological understanding.

Chloë Baldreki

PhD

University of York

Chemistry

May 2024

Abstract

The South-Central African region contains many important archaeological and palaeoenvironmental sites, although the chronology of the region is not well understood. Most of the region's known sites have been excavated over the last 30 years. Since this time, additional biomolecular techniques have been developed, applicable to the region's fossil material.

A molluscan assemblage was extracted from Pleistocene sediments associated with Palaeolake Kafue, Zambia. Palaeoenvironmental analysis revealed varied past environments with terrestrial, marsh dwelling, and freshwater taxa. The first helicarionid to be listed from Zambia was also identified.

Dating is crucial to elucidate Pleistocene sites and to relate to mammalian (including hominin) evolutionary patterns. The shell of one commonly occurring terrestrial land snail, *Achatina* spp., was identified from Palaeolake Kafue, and was therefore investigated for its potential for the intra-crystalline protein degradation (IcPD) approach to amino acid geochronology (AAG). The three aragonitic layer (3AL) shell portion was shown to contain an intra-crystalline fraction of protein which appeared to adhere to closed system behaviour, showing predictable patterns of protein degradation. This biomineral therefore has potential for building AAGs across the African continent.

The IcPD approach to AAG was also undertaken on fossil tooth enamel from four taxa (bovid, equid, suid, rhinocerotid) from two Zambian archaeological sites: Twin Rivers and Mumbwa Caves. No direct dating of fossil material had been previously undertaken at Twin Rivers and these analyses revealed the complexity of this hilltop cave site's depositional history. A potential taxonomic effect was observed in fossil tooth enamel, with differences in peptide chain hydrolysis. This was also indicated by the difference in relative rates of racemisation for two amino acids during forced degradation experiments of Rhinocerotidae in comparison to previously published Elephantidae data. This data therefore demonstrates the need for taxa-specific AAGs from tooth enamel.

Due to the low levels of degradation induced over two years of isothermal heating at 60, 70 and 80 °C, some patterns of protein degradation were difficult to elucidate from IcPD and palaeoproteomic data. It was, however, possible to improve upon the known enamel proteome sequences of woolly rhino. Experimental samples and fossils displayed similar regions of peptide preservation in AMEL, suggesting the heating experiments undertaken in this study may be somewhat reflective of environmental diagenesis. Overall, it is therefore recommended that forced degradation experiments at these lower temperatures be undertaken for a minimum of 10 years to induce sufficient degradation for improved comparative analysis to fossils.

This thesis therefore demonstrates the value of revisiting archival material to improve archaeological understanding with updated palaeoenvironmental, biomolecular and geochronological analyses.

Table of Contents

List of Tables

List of Figures

14

19

Acknowledgments

There are many people I would like to thank for their help and support throughout my PhD. It has been an odd time to undertake a project, but one in which I couldn't have asked for more understanding and supportive supervisors. A massive thanks goes to Kirsty Penkman for all her wisdom (academic and otherwise!), enthusiasm and encouragement. I would also like to extend a huge thanks to Tom White for all his help, and for showing me the wonders of the NHMs mollusc collections. Big thanks also go to Larry Barham for his support and allowing me a glimpse into the archaeology of South-Central Africa, and to Mike Simms for facilitating my understanding of Palaeolake Kafue. I would also like to thank Sally Reynolds for her invaluable help reidentifying the taxonomy of the fossils and Jane Thomas-Oates and Jessie Hendy for their very useful TAP meeting discussions.

The NEaar group has been a wonderful place to undertake my project and I would like to thank Marc, Sam, Lucy, Sheila, Fazeelah, Martina, Ellie and Charllotte for making my time there so enjoyable. I would also like thank my (not so) new MAP lab colleagues, especially Adam and Tony, for their flexibility, support and patience!

At times, this thesis has turned me into a gremlin, and I would like to thank my friends and family for keeping me sane with all their love and laughter. Lastly, I would like to extend my humongous gratitude to Sam for coming on this (and every) adventure with me.

Declaration

I declare that this thesis is a presentation of original work, and I am the sole author, except where acknowledged in the relevant co-authored papers presented as chapters (2-4). This work has not previously been presented for a degree or other qualification at this University or elsewhere. All sources are acknowledged as references.

Parts of this thesis are presented as chapters in journal-style format. The work presented in chapter 2 was accepted for publication in *The Journal of Conchology* pending minor revisions in July 2024. The work presented in chapter 3 has resulted in the publication: Baldreki, C., Burnham, A., Conti, M., Wheeler, L., Simms, M.J., Barham, L., White, T.S. and Penkman, K., 2024. Investigating the potential of African land snail shells (Gastropoda: Achatininae) for amino acid geochronology. *Quaternary Geochronology*, *79*, p.101473. The work presented in chapter 4 has resulted in the publication: Baldreki, C., Dickinson, M., Reynolds, S., White, T.S., Barham, L. and Penkman, K., 2024. Old Fossils, New Information: Insights into Site Formation Processes of Two Pleistocene Cave Sequences in Zambia from Enamel Amino Acid Geochronology. *Open Quaternary, 10*(4), pp.1–17. Finally, the work presented in chapter 5 has been written in the style of a research paper, with a view to potential future publication.

Chapter 1. Introduction

Hominin evolution in Africa is complex and the ever-changing field of study is limited to the fossils and archaeology revealed thus far. The fluctuating past climates across Africa over the Pleistocene are also not well established. Relating environmental evolutionary drivers to hominin (and more widely, mammalian) evolutional then is especially challenging. The South-Central African region, though not well known for its high fossil preservation potential, still contains numerous interesting and important archaeological and paleoenvironmental sites. However, the region's chronology is not well understood. The aim of this thesis was therefore to employ the latest knowledge, expertise and biomolecular analyses on fossil material that had been previously excavated from sites within the region, with the goal of increasing archaeological site understanding.

This introduction therefore covers a brief summary of hominin evolution in Africa (section 1.1.1) and the potential role of climate (section 1.1.2). A summary of dating techniques applicable to archaeological sites in this region is then discussed (section 1.2), before discussion of ancient proteins (section 1.3) and the biomolecular techniques for geochronological (AAG, section 1.3.3) and palaeoproteomic (section 1.3.4) analysis.

1.1. The Quaternary

1.1.1. Human evolution

Africa has long been known to have played an integral role in the evolution of humankind, from the earliest hominins to the emergence of the genus *Homo* (see recent reviews e.g. Bergström *et al.*, 2021; Bobe and Wood 2022; Stringer, 2022). Evidence of the archaic Australopithecine hominins is currently only present within the Pliocene archaeological record of Africa. Such examples include the *Australopithecus afarensis* 'Lucy' skeleton (Johanson *et al.*, 1982), dated to 3.2 Ma (Walter, 1994) and the Laetoli footprints, dated to *ca*. 3.6 Ma (Leakey, 1981), showing fossilised volcanic ash footprints of two bipedal adults and a juvenile (Leakey and Hay, 1979). Evidence for the emergence of the genus *Homo* can also only be found in Africa (Villmoare *et al.*, 2015; DiMaggio *et al.*, 2015), with the first evidence of *H. habilis* discovered in Olduvai Gorge, Tanzania (Leakey *et al.*, 1964), dating to 1.8 Ma (Deino, 2012). Subsequent finds, such as the Afar cranium from Ethiopia, dated to 2.8 Ma (DiMaggio *et al.*, 2015) significantly pre-dated this first appearance.

The East African Rift System (EARS) has yielded multiple and frequently the earliest dated *Homo* species in the world including *H. habilis* (Leakey *et al.*, 1964, Johanson *et al.*, 1987), *H. erectus sensu lato* (Lepre and Kent, 2015) and (debatably; Hublin *et al.*, 2017; Richter *et al.*, 2017) *H. sapiens* (Day, 1969). The cave systems of South Africa have also yielded multiple notable hominin finds, including *H. naledi*, currently found only within the Rising Star cave system in South Africa (Berger *et*

al., 2015). With hominid fossils now found across the African continent (Fig. 1.1), recent studies have suggested the variable environmental preservation potential has played a dominant role in the African hominin fossil record. Subsequently, pan-African models of *Homo* evolution have been put forward (e.g. Hublin *et al.*, 2017) involving malleable metapopulations of multiple contemporaneous *Homo* species across the continent (Scerri *et al.*, 2019).
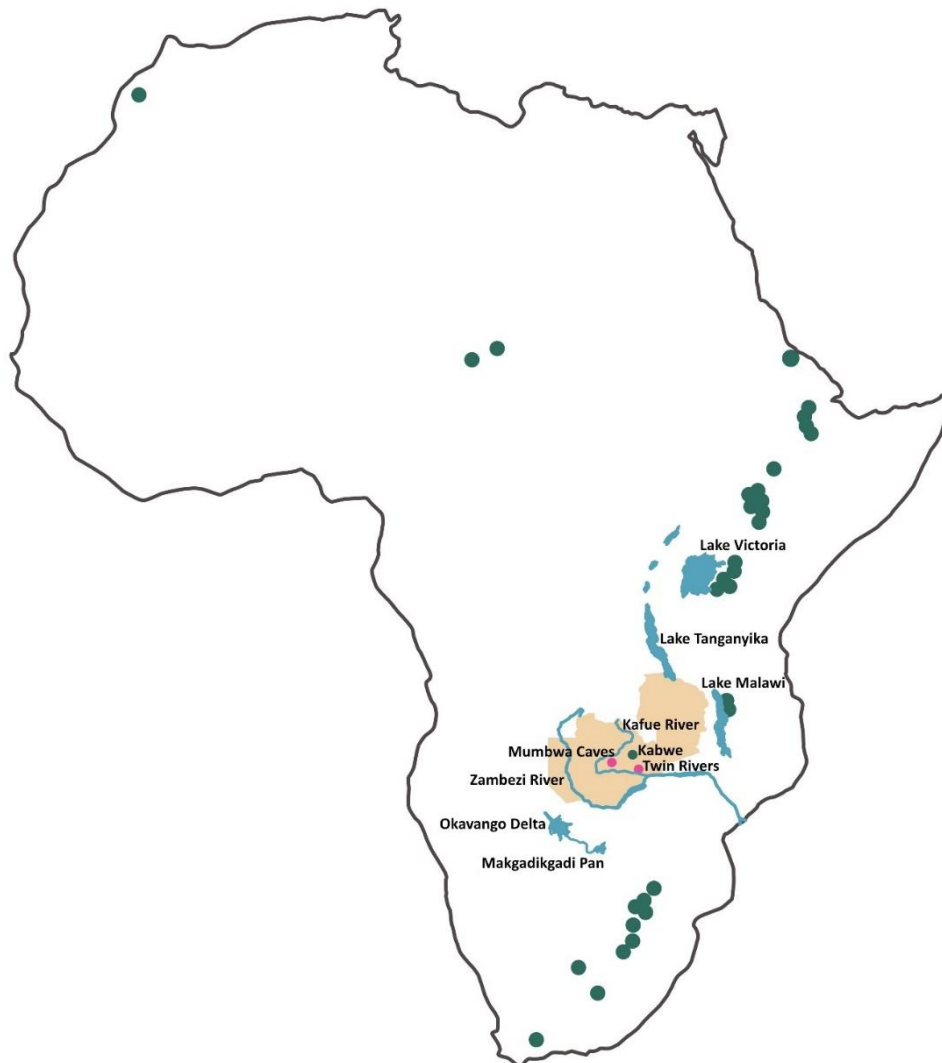
Figure 1.1. Map of Africa, highlighting the location of Zambia in yellow and major current water bodies in the South-Central African region. The two archaeological sites studied in this thesis, Mumbwa Caves and Twin Rivers, are displayed as pink circles. Locations of currently known hominin fossils (dating between ~7 Ma - 200 ka) are highlighted as green circles (Leaky *et al.*, 1964; Johanson *et al.*, 1982, 1987; Wood and Lonergan, 2008 and references therein; Simpson, 2013; Burger *et al.*, 2015; Lepre and Kent, 2015; Hublin *et al.*, 2017; Barr and Wood, 2024 and references therein).

1.1.1.1. South-Central Africa

Africa's South-Central region (the focus area of this PhD work) encompasses present day Zambia and adjacent areas of bordering countries (Angola, Namibia, Botswana, Zimbabwe, Mozambique, Malawi, Tanzania and Democratic Republic of Congo (DRC), Fig. 1.1). Whilst the region generally has a poorer fossil preservation potential, it has yielded hominin fossils, most notably the *Homo heidelbergensis* (*rhodesiensis*) Kabwe cranium. This has been recently dated to *ca*. 300 ka (Grün *et al.*, 2020), making it contemporaneous with *H. naledi* (Berger *et al.*, 2015) and archaic *H. sapiens* (Richter *et al.*, 2017). The region has also produced evidence for the transition from the Early to Middle Stone Age (Acheulian and Sangoan-Lupemban tool technologies respectively; Duller *et al.*, 2015), of early pigment use (~ 265 ka; Barham, 2002) and woodworking (>476 ka; Barham *et al.*, 2023). Two archaeological sites, Twin Rivers and Mumbwa Caves, are studied in this thesis and a brief overview of their archaeological is provided below.

Mumbwa Caves was first excavated in 1930's by Dart and Del Grande (1931) and Clark (1942) before a more thorough excavation across four field seasons from 1993 - 1996 by Barham (2000). The cave sequence (found within a freestanding dolomite outcrop) has shown evidence of intermittent use and occupation from >172 ka (dated at the base of the sequence by thermoluminescence) until recently (330 Cal BP as dated by radiocarbon). The archaeological assemblages, evidence of the caves period use, include microlithics, hearths and Middle Stone Age tools and their preparative debris (Barham, 2000).

Twin Rivers was first excavated in the 1950's by Clark (Clark, 1971; Clark and Brown 2001), followed by Barham in the late 1990's (Barham, 2000). The hilltop site contained six main breccia-bearing areas within its cave passages (although the cave roof collapsed at an unknown time, leaving the deposits exposed to weathering), termed A - F Blocks. Due to the breccias hardness, dynamite blasting was used in most areas of the early excavations (Clark and Brown 2001). The A Block sequence containing Early and Middle Stone Age tools, pigments and faunal fossils, was dated to ~170 - >400 ka using U-series dating on speleothem (Barham, 2000). As a hilltop site, the presence of rhinocerotid and giraffid fossils (among others) throughout the fossil assemblage is thought to have accumulated from predation and/or scavenging activity, including the possibility of hominin activity. During the Pleistocene, the hilltop site of Twin Rivers is thought to have overlooked Palaeolake Kafue, an extensive palaeo-wetland encompassing the Okavango delta, the Makgadikgadi pan and the Zambezi and Kafue rivers (Fig. 1.1; Simms and Davies, 2000).

The study of African palaeoenvironments across the Quaternary is considerably less well represented (and is especially lacking in South-Central Africa) compared to those within northern latitudes, which have had a relatively long history of local palaeoenvironmental study. One of the most popular theories on evolutionary drivers for hominin speciation, diversity and increased

cognitive abilities relates to the environmental stresses of the Quaternary's oscillating climates (e.g. Potts, 2012; Maslin *et al.*, 2015) and reconstruction of African palaeoenvironments is essential to our understanding of climate's role in hominin evolution (deMenocal, 2004).

1.1.2. Climate

The Quaternary is the most recent geological period of earth's history, covering the last 2.58 million years (Gibbard *et al.*, 2010). It is split into two epochs: the Pleistocene, ending at the start of the current interglacial (approximately 11,700 years BP), and from then, the Holocene, encompassing the present day (Walker *et al.*, 2009). The Quaternary is defined by episodic climate change: glacial-interglacial climate cycling in mid and high latitudes (Batchelor *et al.*, 2019) and arid-humid climate cycling in low latitudes (deMenocal, 2004).

The Milankovitch cycles (Fig. 1.2) describe earth's orbital oscillations, which play a significant role in the earth's climate fluctuations over the Quaternary (Campisano, 2012). These orbital oscillations include eccentricity (which describes the 100 ka yearly cycle between the earth's elliptical and almost circular orbit), obliquity (which describes the 41 ka yearly cycle of variation in the angle of the earth's tilt) and procession (a descriptor of the earth's wobble around its axis).

eccentricity   obliquity   procession
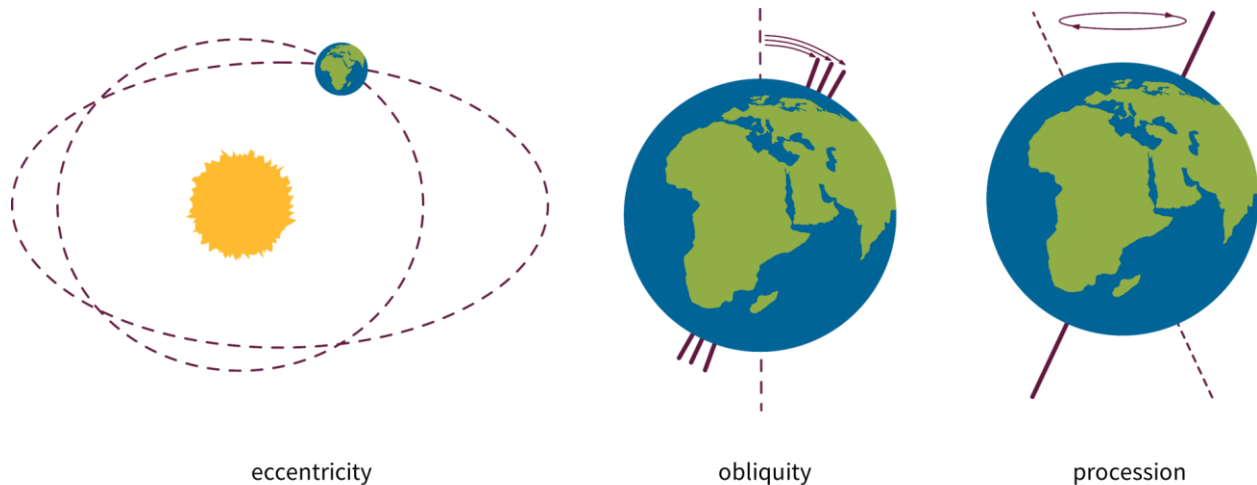
Figure 1.2. The Milankovitch cycles.

The intensity and distribution of solar radiation around the globe is directly affected by the combination of these three orbital cycles, with ice sheet growth and retraction in high latitudes (Hughes and Gibbard, 2018) and dust flux in low latitudes (deMenocal, 1995) correlating with these timescales during the Pleistocene. The complexity of regional climate fluctuations during the Quaternary, however, cannot only be described purely in astronomical terms, with additional feedback mechanisms influencing and contributing additional variables to both regional and global climates. These feedback mechanisms include variations in compositions and concentrations of

atmospheric gases, global winds and sea surface temperatures, and oceanic current directions and strengths (e.g. Demenocal *et al.*, 1993; Campisano, 2012).

In general terms, the Pleistocene climate oscillations across Africa are less well understood than within the northern hemisphere, where glacial and interglacial phases dominate the record. The arid-humid climate fluctuations resulted from a complex combination of environmental factors and occurred asynchronously across different regions of Africa (Blome *et al.*, 2012). These would have resulted in the expansion, contraction and alteration of habitats dependent on locality. However, in general, wetter, more humid climatic periods (known as pluvials) are evidenced in the expansion of lakes and watercourses, whilst interpluvials (periods of greater aridity) are often observed via the shrinkage or disappearance of lakes, rivers and their drainage systems.

1.1.2.1. Palaeoclimate reconstruction

Palaeoclimate reconstruction is a valuable endeavour for all regions across the globe, but is especially important in regions which have historically been less well studied, such as South-Central Africa. Assessment of habitats and how they change over time are pieced together with landscape evidence, biological records and chemical signatures to imply past habitats over the Quaternary.

Floral and faunal remains are often characteristic of specific habitats or ecozones (Villa *et al.*, 2010) and their presence or absence over time can infer shifts in habitat. For example, blesbok antelope found in the palaeoenvironmental record at Twin Rivers archaeological site in Zambia (Barham, 2000) are not observed north of the Limpopo River today. These faunal remains, characteristic of cooler, drier, savannah grassland-woodlands than the environments that are currently present in the region today (Clark and Brown, 2001) were also supported by the woody vegetation remains at Twin Rivers (Avery, 2003).

Genetic analysis of fauna found within a paleoenvironment can be used to investigate possible timings and/or reasons behind isolation of populations and resulting clades, and may indirectly help locate past climate refuges. For example, analysis of mitochondrial DNA (mtDNA) haplotypes in modern lions showed two distinct populations, despite only living 500 km apart (Moore *et al.*, 2016). Moore *et al.* (2016) suggested the ancestral lion population were wetland specialists originating from South-Central Africa, and that the savannah specialists of East Africa were a population isolated during an arid Pleistocene phase, becoming adapted to the savannah habitat. Pedersen *et al.*'s (2018) analysis of numerous populations of plains zebras suggested the Zambezi-Okavango wetland area of South-Central Africa was the most likely location of the ancestral population (*ca.* 370 ka), from which all current clades are descended. Studies such as these help to unravel changes in past environments, and can highlight potential regions of past diversification (such

as South-Central Africa) where the preservation potential of archaeological material may be lesser than elsewhere.

As well as mammalian fauna, molluscs are also highly useful environmental indicators, with many species adapted to specific environments (e.g. marine, freshwater, marsh wetlands and drylands). Some species are not only markers for watery environments but may also be indicative of the water's condition; for example, the shell form of the ostracod *Cyprideis torosa* is used as a water salinity indicator as its shell alters from smooth in hypersaline water, to noded in low salinity water (<~5 ‰) (Frenzel and Boomer, 2005). Such species are often studied in the context of estuarine sea level change in the northern hemisphere (e.g. Viehberg *et al.*, 2008; White *et al.,* 2013; Tsourou *et al.*, 2015), but can also be useful for the study of lakes in lower latitudes, where rapid evaporation of fresh water bodies can cause salinity crises (Schön *et al.*, 2000).

Chemical signatures from palaeobotanical remains in marine, lacustrine (Feakins *et al.*, 2007) and fluvial cores (Uno *et al.*, 2016; Johnson *et al.*, 2016) can also be used to infer climate information. For example, cuticular wax, used to protect a plant's leaves from excess water transpiration induced by extreme heat (Bueno *et al.*, 2019), is well preserved in cores over geological timescales (e.g. Kusch *et al.,* 2021). These plant waxes contain lipid biomarkers which can be used as proxies for aridity. Carbon isotope ratios ($\delta^{13}C$) are reflective of a plant's photosynthetic pathway. Typical of the C_3 pathway are trees, bushes, cool-season grasses and sedge, whilst warm-season grasses and sedge typically use the C_4 pathway (Uno *et al.*, 2016). δD_{wax} is an additional indicator of aridity from plant wax biomarkers, which measures the hydrogen isotope composition of precipitation (δD_p). Low rainfall gives rise to larger δD_{wax} values, whilst higher levels of precipitation result in smaller δD_{wax} values, allowing for hydroclimate interpretation. Used in combination these biomarkers help reconstruct palaeoenvironmental landscapes, which can often be related to the core chronologies (Tierney *et al.*, 2017).

The climatic information gained from cores have been interrelated with varying degrees of success. The African continent is large, and many regions have different dominant influences on their climates, giving rise to asynchronous climatic oscillations. One such example of this comes from geological climatic data from Lake Malawi in the South-Central African region, which indicated a shift towards greater humidity during a period of documented shift towards greater aridity in the horn of Africa (Johnson *et al.*, 2016). However, there are often relationships between lacustrine sedimentary cores within the same region, due to their closer synchronicity. For example, Lake Tanganyika and Lake Malawi from the South-Central African region both contain a hiatus in their core chronologies prior to *ca.* 94 ka. This hiatus also correlates with low lake levels from other African lakes, interpreted as a time of widespread mega droughts (Burnett *et al.*, 2011).

The ability to map past regional landscapes is essential to our understanding of past climates, and its role within faunal (including human) evolution. Placing regional climatic events into accurately

dated geological frameworks not only helps to elucidate the past, but is especially critical for future climate simulations and associated impacts on faunal and floral species. Widening the geographical and temporal range of palaeoenvironmental studies to less well studied regions such as South-Central Africa helps to enable a better understanding of the earth's complex climate system.

1.2. Dating techniques

Dating is integral to the study of human evolution, both with respect to archaeology and related palaeoenvironments. Techniques fall into two broad categories: numerical techniques, which provide singular numerical dates (with associated error ranges) and relative techniques, which are based on the relative age order of the material in question. No current individual technique of either type is able to span the entire Quaternary timescale for all sample types. They are therefore most powerful when used in a multifaceted approach, to elucidate the greatest information possible. The key techniques that are potentially applicable to the South-Central African region over the Pleistocene are therefore reviewed (sections 1.2.1 and 1.2.2).

1.2.1. Numerical dating techniques

Numerical dating techniques are highly useful tools, each with their own set of limitations and assumptions. It is therefore essential that each are viewed in the context of all available site information to assess the accuracy of the determined values.

1.2.1.1. Radiometric dating techniques

All radiometric dating techniques are based on the principle of radioactive decay of an unstable elemental isotope. Radioactive decay can occur in different ways including α decay (emission of an α particle), β decay (emission of an electron) or γ decay (emission of electromagnetic radiation). Radiometric dating techniques may be based on simple decay pathways (such as ^{14}C) or more complex chains involving multiple intermediates (such as ^{238}U and ^{235}U). Each exponential decay pathway has a half-life constant, which determines the upper limit of dating for each technique.

1.2.1.1.1. Radiocarbon dating

One of the most well-known radiometric dating techniques is radiocarbon dating. Developed in the 1940s by Willard Libby, the technique is based on the principle that unlike ^{12}C and ^{13}C (the stable isotopes of carbon found within the environment), ^{14}C undergoes exponential decay by β particle emission to become the more stable ^{14}N. ^{14}C is continuously produced in the atmosphere and becomes incorporated into living organisms in numerous ways, for example during plant

photosynthesis. Due to the constant cycle of production and decay, the ^{14}C in living organisms remains at a constant level, in equilibrium with the atmosphere. Once an organism dies and it is unable to replenish ^{14}C, the abundance decreases. By measuring the residual ^{14}C in a sample and using the known ^{14}C decay rate, a numerical age can be determined (reviewed in Walker, 2005).

^{14}C dating involves a number of assumptions. These include that (with the exception of ^{14}C undergoing constant decay) the ratio of carbon isotopes within samples remains unaltered, and that it is representative of the atmospheric carbon isotope ratio at the time of formation. This, however, does not always hold true, with many biological systems having a preferential uptake of carbon isotopes. Broadly speaking, plants undergoing photosynthesis preferentially uptake ^{12}C (Still and Rastogi, 2017), which if uncorrected, can result in an overestimation of the dates obtained. Conversely, ocean water preferentially absorbs ^{14}C, which can lead to higher ^{14}C accumulation in oceanic carbonates such as corals (Koweek *et al.*, 2019) and organisms which rely on marine resources, resulting in an underestimation of dates obtained using these materials. It is, however, possible to correct for preferential uptake with data normalisation when isotopic fractionation (δ^{13}C) within a sample is determined (Walker, 2005).

To complicate matters, where the sea surface is typically enriched with ^{14}C, the deeper sea is depleted in ^{14}C due to its inability to replenish the ^{14}C lost from decay by exchange with the atmosphere. This is known as the marine reservoir effect and gives rise to overestimation of age in deeper oceanic carbonates and organisms which rely on deeper marine resources (Alves *et al.*, 2018). The freshwater reservoir effect results in similar overestimation of ages and occurs where fresh water is rich in dissolved ancient limestone. Similar to the deep sea, ancient limestone contains depleted ^{14}C, lost through decay and cannot be not replenished by exchange with the atmosphere. Depleted ^{14}C ratios may then become incorporated into organisms within freshwater systems (Philippsen, 2013). Reservoir effects can be somewhat accounted for, but it should be noted that their effects can be highly variable and simple correction factors may not be suitable in all cases (Philippsen, 2013). Inaccurately old dates from terrestrial molluscs (as well as from freshwater species) are also commonplace. Molluscs ingest $CaCO_3$ to build their shells and where this comes from ancient limestone sources (depleted in ^{14}C), as with the freshwater reservoir effect, mollusc shells may have older apparent ages (e.g. Rubin *et al.*, 1963; Goodfriend and Stipp, 1983; Forman *et al.*, 2021).

Relatedly, the original assumption that atmospheric carbon isotopic composition remains stable was shown not to be accurate, with evidence that it varies over time due to changes in cosmic ray intensities (e.g. Beck *et al.*, 2001 and references therein). Detailed work by the IntCal Working Group (IWG) over recent years have pieced together atmospheric ^{14}C concentrations from a number of sources (including dendrochronology, corals, forams and speleothems) to provide the field with ^{14}C atmospheric concentration calibration curves (Reimer *et al.*, 2020).

Other than these assumptions, radiocarbon's biggest potential source of error is

contamination, which can drastically alter the accuracy and precision of the dates determined, particularly for older samples (e.g. Olson, 1963; Wood, 2015). Radiocarbon is not alone in the potential for error; as with all numerical techniques it is especially important not to assume the result obtained is an absolute value, especially where it conflicts with additional evidence.

Radiocarbon dating is used extensively due to the wide range of organic samples it is applicable to, but its greatest disadvantage for this study is its maximum reliable dating range. This is because the half-life of ^{14}C (the time taken for the radioactivity of half a samples ^{14}C atoms to have completely decayed) is 5730 ± 40 years (Godwin, 1962), with an upper limit of analysis of up to 10 half-lives, resulting in a maximum dating capability of up to *ca*. 60 ka (Behre and van der Plicht, 1992). It therefore is only able to provide reliable dating information for the most recent *ca*. 2% of the Quaternary, leaving many sites in the South-Central African region without effectively dated sequences past this time.

1.2.1.1.2. Uranium-series (U-series)

U-series dating exploits the radioactive decay of ^{238}U to ^{206}Pb and ^{235}U to ^{207}Pb and through complex decay chains involving multiple isotopic elements. Within these elongated chains, the ^{230}Th/^{234}U isotopic ratio is most commonly used for dating and provides dating information up to ~500 ka (the most recent *ca*. 20% of the Quaternary period), extending the timeframe of dating by ten-fold in comparison to radiocarbon. U-series dating is typically undertaken on carbonates from either marine (e.g. corals (e.g. Chutcharavan and Dutton, 2021)) or terrestrial origins (e.g. speleothem (Spötl and Boch, 2019)). Uranium is found within these carbonates due to its water solubility, becoming incorporated into the crystal structure of the carbonate as it grows.

U-series dating relies on two basic assumptions: 1) that the carbonate samples adhere to closed-system behaviour post deposition, and 2) that the daughter isotopes are entirely created by the radioactive decay chains. In the case of the latter assumption, contamination from detrital material can lead to inaccuracies in true age estimates, with possible contamination of both parent and daughter isotopes. Detrital contamination can however be accounted for using a ^{232}Th/^{230}Th correction factor, as unlike ^{230}Th, ^{232}Th is not a decay product. Contamination is especially problematic where a sample has not adhered to closed system behaviour, which is observed in many sample types, such as molluscs (McLaren and Rowe, 1996), while uptake post deposition is especially common in bone and teeth (Pike *et al*., 2002). Contamination also rarely occurs uniformly within a sample, with uranium uptake occurring on the surface of the sample and subsequent diffusion towards the interior (Grün *et al*., 2010). As these types of samples are commonly found in the archaeological and palaeoenvironmental records, significant work has been undertaken to develop uptake models in an attempt to correct for open system behaviour; however, it is still worth bearing in mind that each of these models have their own series of assumptions (Sambridge *et al*., 2012).

One advantage of U-series is the direct dating of bones and teeth (although often best considered as providing a minimum age estimate (Pike *et al.*, 2002)). Direct dating is especially important in cases where contextual information has been completely lost, such as with the Kabwe (*Homo heidelbergensis* (r*hodesiensis*)) cranium from Zambia (Grün *et al.*, 2020). In comparison to bone and teeth, speleothem is considered to better adhere to the closed-system assumptions made in calculating dates from U-series analysis (Aubert *et al.*, 2012). However, dating speleothem has an alternative limitation, in that it is an indirect method for dating associated archaeological and/or palaeoenvironmental deposits and challenges interpreting dating can arise from this.

U-series has, however, been successfully undertaken at sites in Zambia, including Twin Rivers (Barham, 2000), where speleothem over and underlying the archaeological deposits were dated, helping to provide valuable site information.

1.2.1.1.3. Potassium-Argon (K-Ar) and Argon-Argon (Ar-Ar)

Argon isotope dating, based on the radioactive decay pathway of ^{40}K to ^{40}Ar, is a considerably longer lived isotopic radiometric dating technique, able to cover the Quaternary (Guillou *et al.*, 2021). It is applicable to volcanic rock formations under the principle that whilst molten, volcanic rock releases ^{40}Ar (g) produced from ^{40}K decay; upon solidification, a closed system is formed with ^{40}Ar becoming trapped and increasing over time as ^{40}K decays. $^{40}K/^{40}Ar$ ratios and subsequent age calculations can be determined in two ways: K-Ar and Ar-Ar. In both cases the concentration of ^{40}Ar is measured by mass spectrometry by melting the rock to release the gaseous ^{40}Ar trapped within. During K-Ar analysis, ^{40}K is directly measured from a separate subsample, either by atomic absorption spectrophotometry or flame photometry. During Ar-Ar analysis, ^{40}K is indirectly measured from the same sample used to determine the ^{40}Ar content, through the measurement of ^{39}Ar. ^{39}Ar is produced from the stable ^{39}K isotope during sample irradiation and as the proportions of ^{39}Ar to ^{39}K and ^{39}K to ^{40}K are known, it is possible to calculate the ^{40}K content. Based on the ^{40}K half-life of ~ 1250 million years (Kossert *et al.*, 2022), the resulting $^{40}K/^{40}Ar$ ratio allows calculation of time since the last volcanic activity.

One of argon dating's greatest limitations is its sample type, being only applicable to volcanic rock. Like all techniques, it also has a number of assumptions. The first is homogeneity of the sample, especially important for K-Ar analysis where separate subsamples are used to determine ^{40}K and ^{40}Ar. Related to this, it is also assumed that ^{40}Ar is a reliable indicator of time since volcanism; both that all ^{40}Ar was released prior to solidification post volcanic event and that the rock then maintained closed system behaviour, with no release of ^{40}Ar through weathering or subsequent heating events. Were either of these assumptions not accurate, over and under estimation of age would result respectively. The likelihood of weathering can, however, be investigated with the observation of secondary minerals, indicative of recrystallisation (e.g. Popov *et al.*, 2020). Over estimation can also occur when

older mineral fractions become incorporated into the volcanic output (lava/ash), but can also be investigated through analysis of the whole rock in comparison to separate mineral fractions (Kelley, 2002). The final assumption made in argon dating presumes all ^{40}Ar results from ^{40}K decay. ^{40}Ar is however present in the atmosphere and through measurement of ^{36}Ar, an atmospheric correction is applied resulting from their known proportions.

One of argon dating's biggest advantages is its maximum reliable dating range resulting from ^{40}K's long-lived half-life and in contrast to radiocarbon, its depth of coverage allows dating across the hominin evolutionary timescale. Volcanism has been prevalent within the east African rift system over the Quaternary and K-Ar dating has been able to help elucidate dates on a number of interesting fossils (e.g. Leakey, 1981; Phillips *et al.*, 2023). However, due to the lack of volcanism in many regions of Africa, argon isotope dating remains limited in its capability, including within South-Central Africa.

1.2.1.4. Luminescence dating

A number of numerical dating techniques fall under the luminescence category including thermoluminescence (TL), optically stimulated luminescence (OSL) and infrared stimulated luminescence (IRSL). Luminescence dating can be undertaken on multiple sample types including a number of minerals (typically quartz and feldspar), volcanic rock, fired pottery and burnt flint artefacts, as well as calcitic biominerals (such as opercula (Duller and Roberts, 2018)). Each luminescence technique uses a different source to stimulate the release of luminescence: heat (TL), light (OSL) or infrared (IRSL). The intensity of stimulation required is proportional to the quantity of absorbed natural radiation since the sample was last exposed to a heat source, sunlight or during biomineralisation. This final exposure event, often described as "bleaching" or "zeroing", is assumed to remove all trapped electrons from the sample's crystal structure defects prior to deposition. Of the luminescence dating techniques, OSL, developed in the 1980's by Huntley *et al.*, (1985), has been applied successfully across a number of sites globally and within Africa. It has proved to be a particularly successful technique on wind-blown sand dunes, such as those in the Namib Desert (Bristow *et al.*, 2007), in part due to this sediment type's adherence to one of luminescence dating's main assumptions, that the sample is fully bleached (or zeroed) at the time of deposition, due to ample exposure to sunlight.

To determine an age estimate by luminescence dating, the total radiation absorbed by the sample during deposition is calculated in the laboratory and termed the equivalent dose (D_e). The dose rate (the amount of environmental radiation the sample received per year) must also be known in order to calculate an age estimate for a sample. The environmental radiation can be determined in two ways (Duller, 2008a). An 'in field' measurement uses a portable gamma spectrometer which measures the sedimentary radiation directly from the sample location, after the sample core has been

removed. Alternatively (or additionally) extra sediment can be sampled for laboratory analysis of the radioactive elemental composition (potassium, uranium and thorium's decay chains), using a technique such as inductively coupled plasma mass spectrometry (ICP-MS). Variations in dose rates determined from individual grains are assumed to result from minor variations in sedimentary radiation and should therefore result in only very small differences between the D_e values measured. It is known, however, that different sedimentary types have different compositions and concentrations of radioactive elements (Badawy *et al.*, 2018). The assumption of only minor variations in environmental radiation therefore generally holds true for sites with little variation between sedimentary types, but the assumption and its part in the calculation can become complex for sites where the sedimentary record is less uniform. To add to the complexity, dose rates may also change over time. This is especially common at sites where variations in water content have occurred. Uranium, for example, is water soluble and may be removed or deposited into the sediment by water flow, altering the equilibrium of both the uranium and thorium decay chains, hence altering the radioactivity of the sediment (Degering and Degering, 2020).

Sedimentary water content is also required for luminescence calculations and is measured from the surrounding sediment, or an assumed average is used where the depositional environmental history is not known. OSL dating undertaken on fluvial sediments can therefore be challenging as a result of these and other assumptions, such as no post depositional mixing having occurred (Rittenour, 2008). Incomplete bleaching is also relatively common within fluvial sediments due to insufficient sunlight filtering through the river water (Wallinga, 2002). However, single grain OSL is able to identify incomplete bleaching in samples, enabling only appropriate grains to be chosen for analysis (Duller, 2008b).

OSL has been used successfully at numerous sites within South-Central Africa, such as at Kalambo Falls (Duller *et al.*, 2015; Barham *et al.*, 2023) and Twin Rivers (Barham, 2000) in Zambia. Ultimately the success of luminescence dating is determined by how accurate the estimations in dose rate and water content are for each sample. It can, however, still provide very useful information, even when associated with large error ranges, for sites like many within South-Central Africa which have very poor chronology. It is a reminder that results from all dating techniques should always be critically assessed and as with many other techniques discussed, luminescence dating evidence is most compelling when used in conjunction with a variety of other dating techniques.

1.2.1.5. Electron spin resonance (ESR) dating

Electron spin resonance (ESR) (also but less commonly known as electron paramagnetic (EPR)) dating was first used as a dating technique in 1975 (Ikeya and Ohmura, 1983). Similar to luminescence dating, ESR measures the trapped electrons within a sample; however, in ESR it is the

paramagnetic properties of a sample that provide a measure of age. This is possible as the strength of the resonance (produced from exciting the trapped electrons using a magnetic field) is proportional to the number of electrons present since the onset of electron trapping. ESR can be undertaken on a number of sample types including corals, enamel, molluscs and speleothems, and has a maximum dating range of up to 2 Ma, theoretically providing the ability to date sites over the majority of the Quaternary timescale (Rink, 1997).

The assumptions made in ESR are very similar to those previously discussed in luminescence dating, and relate to the palaeodose and annual dose rate. The palaeodose is calculated in the laboratory (much like the equivalent dose in luminescence dating) and can vary due to the sample type analysed. Variations in the depositional environment such as the sediment type, uniformity and water content can once again lead to a variable history of environmental radioactivity and can cause errors with the estimated annual dose rate (Walker, 2005). Similar to U-series dating, ESR is also based on the assumption that samples adhere to closed-system behaviour. As stated in section 1.2.1.1.2, radioactive elements may be exchanged between the enamel surface and the depositional environment. Subsequent diffusion towards the interior of the sample then results in uneven distributions of radioactive elements within the sample (Grün et al., 2010) and variable dating results. In calcium carbonate ($CaCO_3$) biominerals such as molluscs, erroneous results can arise from open-system behaviour in terms of mineral diagenesis, resulting in leaching and/or uptake of radioactive elements from the depositional environment. Aragonite is a meta-stable polymorph of $CaCO_3$ and over geological timescales may convert to calcite, the thermodynamically stable polymorph of $CaCO_3$. If this occurs the assumption of maintenance of a closed system no longer holds true and the reliability of the dates obtained becomes questionable (Rink, 1997).

Limitations to the precision of ESR are openly discussed in many reviews (e.g. Rink, 1997; Skinner, 2011; Duval, 2018) and in papers with published results (Duval et al., 2012), allowing easier critical assessment of the accuracy of the dates obtained. This is especially helpful when comparing determined ages from additional independent dating techniques. Due to the commonality of fossil teeth at archaeological and palaeoenvironmental sites of interest and it's wider Quaternary coverage, ESR dating on enamel has been carried out at a number of sites across Africa (e.g. Schwarcz et al., 1993; Douka et al., 2014), including on important hominin fossils from the South-Central African region (Grün et al., 2020), providing dating for archaeological sites much deeper into the Quaternary timescale, significantly past the upper limit of many other techniques.

1.2.2. Relative dating techniques:

Numerical dating techniques have undoubtedly provided the ability to pinpoint key archaeological and palaeoenvironmental events in time, but where the assumptions required to accurately calculate a date (discussed in detail for each technique in section 1.2.1 above) are invalid, the resulting dates can become effectively meaningless. The second category of dating techniques classed as 'relative' fall into two further subcategories which frequently inter-relate. Age equivalence techniques provide marker horizons allowing inter-site correlation, whilst chronological techniques are based on stratigraphic horizons overlaying one another in a chronological fashion (Walker, 2005). Relative techniques can be calibrated with numerical dating techniques and may contain additional palaeoenvironmental information (section 1.2.1), able to further expand our understanding of regional and global climates over the Quaternary.

1.2.2.1. Age equivalence

Age equivalent techniques have typically been used deeper in earth's history to characterise geological boundaries associated with large-scale shifts in global climates. Where reliable numerical dating of age equivalence markers can be undertaken at any one site, this in theory provides dating for all.

1.2.2.1.1. Tephrostratigraphy

During volcanic eruptions ash is expelled into the atmosphere and can be carried large distances resulting in distal tephra deposition. In the majority of (although not all (Lane *et al.*, 2012)) cases, each volcanic eruption results in a distinct geochemical composition of deposited tephra and identification of cryptotephra is carried out using both the physical and chemical properties, relatable to the volcanic centre (Lowe, 2011). Preservation of ash layers are dependent on a number of factors including the magnitude (e.g. Di Roberto *et al.*, 2020) and type of the volcanic eruption, the wind direction (e.g. Davies *et al.*, 2016) and strength at the time of eruption and the location of deposition. Preservation of ash deposits are possible in lake and marine sediments (e.g. McLean *et al.*, 2018; Abbott *et al.*, 2018), on peat surfaces (e.g. Fontijn *et al.*, 2014) and in glacier ice (e.g. Fontijn *et al.*, 2014), but post-depositional processes such as at peat and bog surfaces can result in patchy coverage (Payne and Gehrels, 2010). As well as providing age equivalence, tephra can be numerically dated using argon dating, discussed in section 1.2.1.1.3.

Tephrostratigraphy's major limitation, however, is its regional specificity (regional examples provided in Fig. 1.3), and whilst highly useful in East Africa, it is not applicable to many other regions in Africa, including the South-Central region.
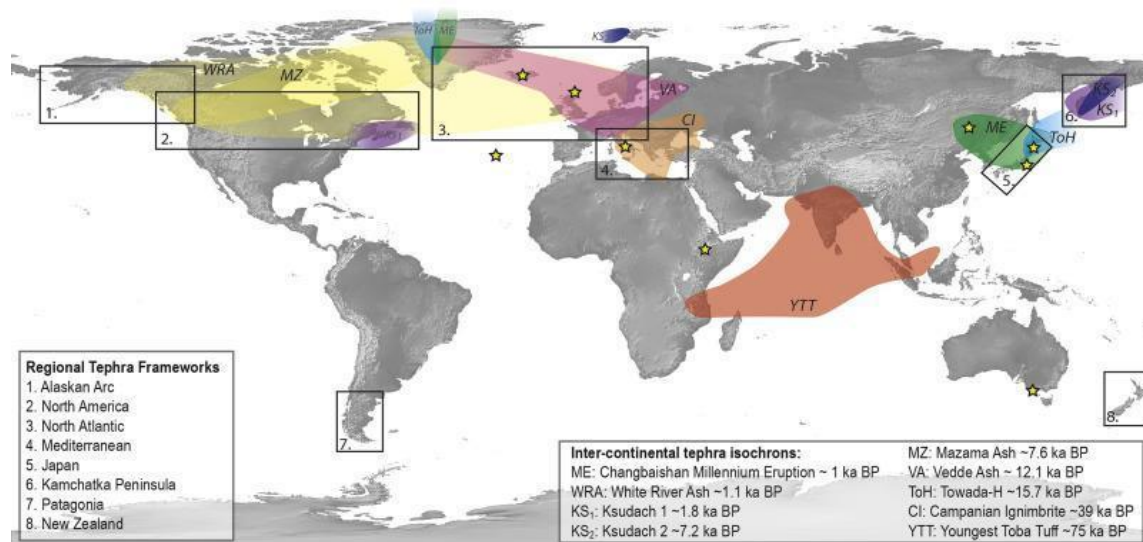
Figure 1.3. Taken from Lane *et al*., 2017, coloured envelopes enclose areas where tephra deposits have been found and geochemically correlated across more than one continent. Boxes indicate established regional tephrostratigraphic records, where tephra isochrons are widely used for palaeoenvironmental, archaeological and volcanological research.

1.2.2.1.2. Palaeomagnetism

Palaeomagnetism is the sedimentary record of changes to the earth's magnetic field (Sternberg, 1997). It is recorded in a number of ways, including: 1) within ferromagnetic minerals (haematite and magnetite) which lock in the earth's geomagnetic field at the time of sediment formation (known as natural remanent magnetism (NRM)), 2) within volcanic rock, upon heating (known as thermoremanent magnetism (TRM) and 3) within unconsolidated sediment whilst accumulating on the ocean floor (known as depositional or detrital remanent magnetism (DRM)) (Tarling, 1975). Palaeomagnetism is applicable across the world, including within the South-Central African region. Examples within Africa include its use at Sterkfontein Cave, where deposits containing *Australopithecus africanus* fossils were related to specific, known age geomagnetic field events, corroborating additional dating at the site (Herries and Shaw, 2011).

1.2.2.1.3. Biostratigraphy

Deeper into geological time, biostratigraphic analysis can be used to provide marker horizons. For example, faunal markers are used to mark the Permian-Triassic Boundary in the Karoo Basin, South Africa (Viglietti *et al*., 2016), whilst pollen analysis has been used to denote vegetational transitions at the Miocene-Pliocene boundary in South-Western Africa (Hoetzel *et al*., 2015). Biostratigraphy is further discussed in section 1.2.2.2.3, as it is also commonly used as a chronological method.

1.2.2.2. Relative stratigraphic methods

Whilst within individual sites there can be chronological events observed by both tephrostratigraphy (termed tephrochronology) and palaeomagnetism, they are most frequently used as age equivalent marker horizons. Within the Quaternary, biostratigraphy is more commonly used as a relative dating method, and frequently entwined with palaeoenvironmental analysis. In addition to biostratigraphy a number of commonly used chronological methods are also discussed.

1.2.2.2.1. Marine Oxygen Isotope Record

The marine oxygen isotope record is a stratigraphic record based on oceanic sediment cores which has been used to categorise regional and global climatic stages. Climatic conditions can be inferred from the relative abundance of two oxygen isotopes (^{16}O and ^{18}O), analysed from the $CaCO_3$ skeletons of microfossils (foraminifera) within the ocean sediment core. Inference is based on the principle that ^{16}O (the 'lighter' naturally occurring oxygen isotope) evaporates in greater abundance from the oceans in comparison to ^{18}O (the 'heavier' naturally occurring oxygen isotope). During glacials, the ^{16}O enriched evaporated water becomes incorporated into ice sheets and glaciers, depleting the oceans of ^{16}O, giving rise to 'heavier' oxygen isotope ratio ($\delta^{18}O$) within the microfossils found in oceanic sediment cores. Conversely, during interglacials the ^{16}O enriched evaporated water is cycled back into the oceans, giving rise to 'lighter' $\delta^{18}O$ values (Shackleton, 1967). Shackleton and Opdyke (1973; 1976) categorised the cyclical patterns into marine oxygen isotope stages (MIS), which are numbered from the top down, where interglacials are categorised by odd numbers and glacials by even numbers.

A significant advantage of the marine oxygen isotope record is that it provides a chronology of global climatic events that extends beyond the Quaternary timescale, irrespective of the location of oceanic coring. As a stratigraphic technique, however, care must be taken in sampling of the core. Variations in the rate of sedimentation mean regular intervals of core sampling may result in different timescales of sedimentation. Care with interpretation is therefore key, not only in terms of sedimentation rate variability, but because, whilst cores have been sampled with no apparent depositional hiatus, events may be missing entirely from the stratigraphy, due to deep oceanic currents removing sediment or from bioturbation (Shackleton, 2006). The marine oxygen isotope record is primarily dated in one of two ways. The core can be orbitally-tuned against the astronomical Milankovitch cycles (described in section 1.1.2). As the frequency of each of the earth's oscillations (eccentricity, obliquity and precession) is known, they can be correlated to the oxygen isotope ratio cycles observed in the microfossils within the oceanic cores. MIS can then be deduced which work back from the present day, covering geological timescales (e.g. Imbrie *et al.*, 1984; Shackleton *et al.*, 1990). Alternatively (or additionally) palaeomagnetism can be employed to obtain a

magnetostratigraphy of oceanic sediment cores, usually with detrital remnant magnetism (DRM) measurement. Care must be taken with interpretation of DRM, as in tandem with sedimentation rate variability and hiatuses discussed above, sediment consolidation variability, if particularly slow, can cause significant lags in the geomagnetic signal (Walker, 2005). Likewise, testing for leads and lags against orbital-tuning can be problematic, with the possibility of misinterpretation especially likely over short timescale chronologies (Blaauw, 2012).

The marine oxygen isotope record has been instrumental in our understanding of the glacial-interglacial oscillations of the global climate over a geological timescale, but it is not able to provide any information on where ice sheets and glaciers were located and therefore their growth and retraction patterns, or how this would have influenced regional climates. It remains a powerful tool when orbitally-tuned against the Milankovitch cycles, correlated with palaeomagnetism and calibrated against numerical dating techniques, but its biggest strength lies in its relationship with ice-core chronologies, terrestrial biostratigraphy, and environmental proxies.

1.2.2.2.2. Ice-Core Chronologies

Ice core chronologies provide another stratigraphic record of highly useful environmental information from the mid-Pleistocene to the present (Lambert *et al.*, 2008). As glacier ice accumulates annually it's possible to establish a chronology from the depth and stratigraphy of the core. Similar to all relative dating techniques, care must be taken with the interpretation of the stratigraphy. Annual layers tend to become more diffuse deeper within cores, increasing the error margins associated with the chronology and the palaeoenvironmental proxy, which can be especially problematic at low snow accumulation sites (Walker, 2005). Variations in the annual snow quantity and wind scouring can also lead to gaps within the chronology and further complications can arise from ice deformations, causing disruptions to the stratigraphy. Interpretation can be assisted where numerical dating techniques are employed to calibrate the chronology, such as U-series dating undertaken on dust trapped within ice-cores (Aciego *et al.*, 2011). Independent marker horizons such as tephra from large-scale volcanic eruptions can also be a useful tool to date and to correlate different stratigraphic records (Abbott and Davies, 2012). The challenges of dating and interpreting ice cores are highlighted by a number of cores from the Tibetan Plateau which contain apparent conflicting $\delta^{18}O$ warming and cooling trends. Little numerical dating could be employed throughout the cores, so whilst the possibility of regional discrepancies was discussed, interpretation was suggested to be the most likely cause of the differences (Hou *et al.*, 2019).

Trace atmospheric gases trapped within the ice cores can also be used to assist dating when compared to orbital parameters. As stated previously with regard to the marine oxygen isotope record, testing for leads and lags associated with orbital tuning can be problematic and can cause misleading results, especially over short timescale chronologies (Blaauw, 2012). Variations in

concentrations of greenhouse gases such as CO_2 and CH_4 appear to coincide with known climate fluctuations, suggesting they play a likely role with global feedback mechanisms and amplify orbital forcing (Raynaud *et al.*, 1993). Other trace gases have also been linked to large regional events. For example, trace CH_3Cl concentrations from an Antarctic core (spanning 2000 years) were shown to play a complex role within the biogeochemical cycle involving tropical vegetation and biomass burning (Williams *et al.*, 2007). Antarctic ice deformations known as blue ice (where deep layers are contorted and driven up) have revealed rare chronologies dating back to 2.7 Ma BP (Voosen, 2017). The trace gases contained within the ice allow a rare glimpse into atmospheric conditions over the Quaternary timescale, and when compared against orbital parameters are used to improve global climate modelling simulations (Rubino *et al.*, 2019). Analysis of trace isotopes can also be undertaken. For example, the study of $\delta^{15}N$ in Greenland ice cores display the changes to the global nitrogen cycle (Geng *et al.*, 2014) and the study of lead isotope ratios in an ice core from the Yukon was able to locate the anthropogenic source of coal combustion (Gross *et al.*, 2012). Identifying the original source of particulate matter has also helped reveal global wind patterns from dust transportation (Fischer *et al.*, 2007) and melt layers within the chronology are also indicative of summer temperatures (Abram *et al.*, 2013). Combined, all this information assists with the reconstruction of temperatures, wind patterns, precipitation, volcanic activity and the influence of human activity over the Quaternary on a global scale and can often also help to elucidate the factors affecting regional climates across the globe. However, their use depends on the original deposition of snow and its long-term preservation as ice, which is limited in Africa.

Presently, the African continent contains only three locations (all within East Africa) where glaciers can be found. Ice coring has taken place at two of these locations, Mount Kenya (Thompson and Hastenrath, 1981) and Mount Kilimanjaro (Thompson *et al.*, 2002), whilst the Ruwenzori mountains climate and glacial history has been primarily studied by lake cores (Jackson *et al.*, 2020). African glaciers are, however, in a precarious position, highlighted by the *ca*. 80% decrease in the aerial extent of Kilimanjaro's ice cover observed at the time of study (~2.6 km^2 in 2000 in comparison to ~12 km^2 in 1912), severely limiting opportunities for study (Thompson *et al.*, 2002).

1.2.2.2.3. Terrestrial Biostratigraphy

Whilst the marine oxygen isotope record and ice-core chronologies have and continue to provide global frameworks displaying the oscillating climates of the Quaternary, they provide very little information regarding low latitude regional climates such as within South-Central Africa.

Terrestrial biostratigraphy builds a chronology of palaeoenvironmental landscapes within the stratigraphy by employing both the presence, evolution and extinction of floral and faunal remains (Walker, 2005). Biozones are built from sections of the stratigraphy with fossils characteristic of a

specific type of palaeoenvironmental landscape. These fossils may include both large and small mammalian fauna, invertebrates and molluscs, flora and pollen. Within a region, distinct stratigraphic biozones can then be correlated, regardless of the sedimentary type they are found within.

Terrestrial biostratigraphy can also often be correlated with marine oxygen-isotope stages and/or ice-core events where known global climatic shifts are observed in each record (Shackleton, 2006). Biozones may also be associated with archaeological material, and broad dates may be applied from the biozone to the archaeology (or vice versa). Palaeoecological inferences are commonly undertaken at archaeological sites, and numerous examples can be found within the South-Central African region (e.g. Gwisho Hot Springs (Fagan *et al.*, 1966), Twin Rivers (Bishop and Reynolds, 2000), Mumbwa Caves (Avery, 2000), Kabwe (Avery, 2002)). In addition to inferring paleoclimates, faunal and floral fossils may also be excellent samples for many of the numerical dating techniques (discussed in section 1.2.1) and for amino acid geochronology (discussed in section 1.2.2.2.4 below), allowing further calibration of the chronology. Terrestrial biostratigraphy is an important technique from which to build a framework for palaeoenvironmental and/or archaeological study, and is a particularly useful foundation to build from in regions with poorly dated chronologies such as within South-Central Africa.

1.2.2.2.4. Amino Acid Geochronology

Amino acid geochronology (AAG) is primarily used as a relative dating technique and relies on the predictable breakdown of fossil protein over time. Proteins are biological molecules found throughout nature, which play numerous roles essential for life. They play a central role in biomineralisation processes and in doing so, some become trapped into the crystal structure or onto the crystal surface they help to organise and form (Chang and Evans, 2015). This in turn stabilises and protects the protein from the burial environment on death. There is substantial evidence of biomineralisation proteins and their building block amino acids surviving throughout the Quaternary within the geological record, with rare cases of protein sequences found into the Miocene, such as in ostrich eggshell from the Linxia Basin, northeastern Tibetan Plateau in China dating to 6.5 Ma (Demarchi *et al.*, 2022). Protein degradation is dependent on a number of factors including temperature and biomineral type, and AAGs are built regionally for each biomineral where a similar temperature history has occurred. Regional aminozones may then be calibrated using numerical dating techniques (allowing the potential to determine numerical dates from AAG data) and/or correlated to deep-sea records and climate signals (Penkman, 2010), with extrapolation of chronologies able to provide dating covering the entirety of the Quaternary period and potentially beyond. Biominerals are relatively abundant at archaeological and palaeoenvironmental sites across all regions of the globe, making them excellent samples for analysis. Amino acid dating therefore

provides an exciting opportunity to elucidate archaeological and/or palaeoenvironmental timeframes in regions with poorly dated chronologies such as South-Central Africa.

As one of the main focuses of this PhD project, AAG is discussed in further detail in section 1.3.3 below, after a more general introduction to ancient proteins and their potential for additional insights to the Quaternary scientist.

1.3. Ancient proteins

Ancient amino acids were first identified within fossil shells by Abelson in 1954 and shortly thereafter it was hypothesised that the diagenesis of proteins trapped within biominerals might be used as a principle for dating (Abelson, 1955). Subsequent studies continued to investigate this possibility through proteins' constituent amino acids, resulting in the relative dating technique amino acid geochronology (AAG; discussed in section 1.3.3). Techniques capable of identifying ancient protein preserved in its higher structure were fairly limited until the development of soft ionisation mass spectrometry (Ostrom *et al.*, 2000). Since the early 2000s, the field of palaeoproteomics has blossomed and is now undertaken on a wide range of materials for an array of purposes (see recent reviews Hendy *et al.*, 2018c; Warinner *et al.*, 2022). The most relevant applications to this study (taxonomic identification, investigation of evolutionary relationships and sex determination) are discussed in section 1.3.4. As AAG and palaeoproteomics can often be undertaken on the same material, they offer the opportunity to study ancient proteins and their degradation pathways, to provide multiple lines of complementary information (Demarchi *et al.*, 2016; Presslee *et al.*, 2019; 2021; Cappellini *et al.*, 2019; Welker *et al.*, 2020).

1.3.1. Amino acids and proteins

Amino acids are the building blocks of proteins. Structurally, amino acids contain a central α-carbon, bonded to a hydrogen, an amine, a carboxyl and an R group (unique to each amino acid; Fig. 1.4).
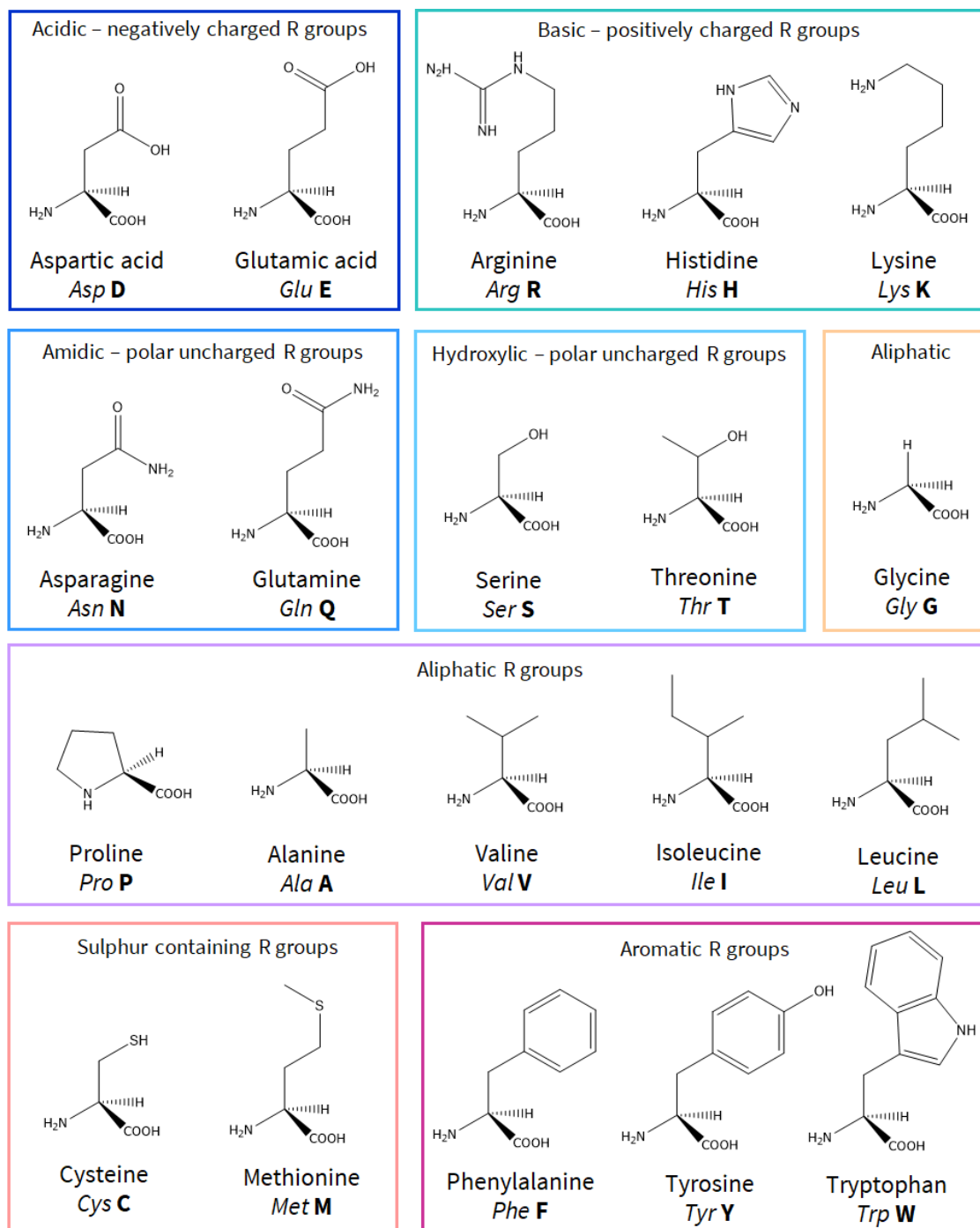
Figure 1.4. Structure of the twenty naturally occurring amino acids, including their three-letter code (italicised) and single letter code (bold).

When free in a neutral pH solution, amino acids are zwitterionic, with a protonated, positively charged amine group and a deprotonated, negatively charged carboxyl group (Fig. 1.5). The overall ionic charge varies with pH for each amino acid, with many amino acids containing R groups which may also become charged by gaining or losing protons in acidic or basic solutions (Fig. 1.5).
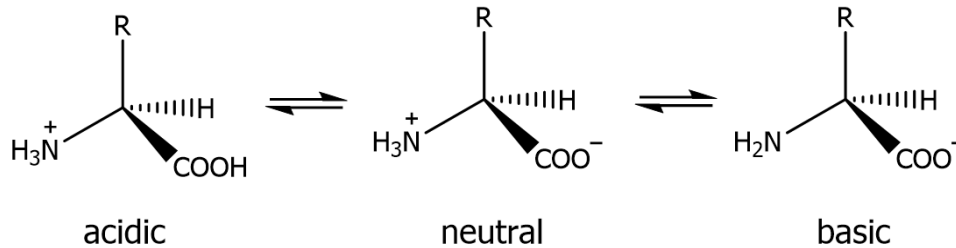
Figure 1.5. Generic amino acid ionic forms under different pH conditions.

The sequence of amino acids in a peptide chain forms the primary structure of a protein. During spontaneous folding, this sequence helps direct both the secondary structures (formed through non-R group interactions e.g. a-helices and β-pleated sheets) and the tertiary structure (overall 3D arrangement of the protein, largely driven by R-group interactions) (Schulz and Schirmer, 2013).

1.3.2. Proteins in biominerals

Proteins are essential to life and have a vast array of functions in nature. They are central to the biomineralisation process, both in terms of directing biomineral architecture (e.g. Belcher *et al.*, 1996; Shin *et al*., 2020) and in modulating the mineral's properties through their incorporation (e.g. Nudelman and Sommerdijk, 2012). Biominerals are often targeted for ancient protein analysis for two main reasons. Firstly, biominerals have high fossil preservation potential and are therefore frequently found within archaeological and palaeoenvironmental sites, providing a common material for analysis of endogenous ancient protein. In addition to this, preservation of ancient protein is thought to be greatly improved within biominerals from a combination of the stabilising effect of interactions with the mineral surface (Demarchi *et al*., 2016) as well as the physical protection offered by the mineral structure from influences of the burial environment (capable of impacting rates of diagenesis (e.g. Smith, 1987)). The two biominerals applicable to this project, gastropod shell and tooth enamel, are each discussed in detail below.

1.3.2.1. Gastropod shell

Gastropods encompass a huge class of molluscs, spanning numerous ecological habitats including terrestrial, freshwater and marine environments. In gastropods, the shell is formed during embryonic development, termed a protoconch, and continues to grow sequentially throughout the animal's life (McDougall and Degnan, 2018). Gastropods build their shells from calcium carbonate ($CaCO_3$), though across this class, there is great diversity in architecture, ranging from single to multi layered and variable use of polymorphic crystal structures of $CaCO_3$ (calcite, aragonite or in rare cases vaterite) (Checa, 2018 and references therein).

Gastropods have a long evolutionary history and can be found far back in the geological record (Frýda et al., 2008). The organic component trapped within the $CaCO_3$ crystal structure has been used for multiple archaeological and palaeoenvironmental purposes e.g. radiocarbon dating (Rowson et al., 2024), isotope analysis (Wiese et al., 2020) and has been used extensively for amino acid geochronology (e.g. Ortiz et al., 2006; Roberts et al., 2008; New et al., 2019). Published proteomes for gastropods are relatively limited, making palaeoproteomic work more challenging, however, the shells of many species have been studied by mass spectrometry, including a peptide mass fingerprinting approach to species identification (see section 1.3.4.1.1).

In addition to shell, many gastropods also make additional biomineral structures. For example, many freshwater and marine species also build opercula, a 'trapdoor' to close the shell opening. Temporary opercular, termed epiphragm, are also created by terrestrial hibernating species, whilst most molluscs also produce mineralised eggs. Some species also have radula (tongue/teeth; Vortsepneva et al., 2023) and gizzard plates (part of the digestive system; Malaquias and Cervera, 2006). Less commonly, some species of terrestrial molluscs also produce love darts used in reproduction (Lodi and Koene, 2016). These biominerals vary in abundance in the fossil record, however, gastropod shell is found within fossil deposits of the South-Central African region and their study is the focus of chapters 2 and 3.

1.3.2.2. Tooth enamel

Enamel forms the outermost layer of the tooth microstructure, protecting the dentine, pulp and root within (Fig. 1.6). Enamel's inorganic component, calcium hydroxyapatite ($Ca_{10}(PO_4)_6(OH)_2$, is highly mineralised (>95%) making it the hardest mammalian biomineral (Lacruz et al., 2017).
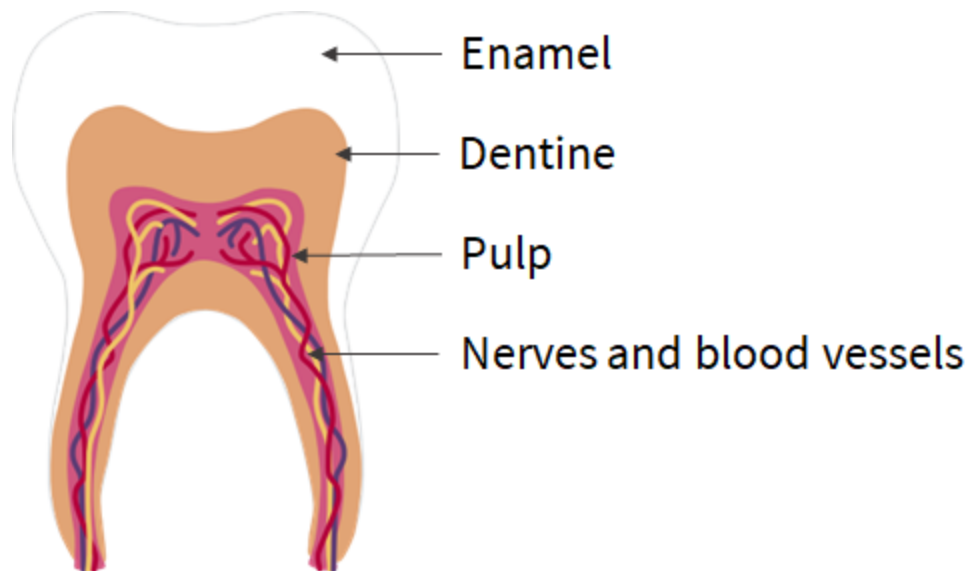
Figure 1.6. Cross sectional representation of the basic microstructure of a 'living' mammalian (human) molar tooth.

Mineralisation of enamel (amelogenesis) occurs in two main stages, secretion and maturation. In the first stage, ameloblast cells secrete extracellular matrix proteins (EMPs) including amelogenin (AMEL), ameloblastin (AMBN) and enamelin (ENAM) (Gil-Bona and Bidlack, 2020). Nucleation of the hydroxyapatite crystals is thought to occur at the dentine enamel junction (DEJ), with elongation occurring at 90°, directed by the EMPs. During this secretory stage, similar amounts (by weight) of protein, mineral and water are present in the enamel, giving rise to a soft structure. During a brief transition stage, around a quarter of the ameloblast cells are thought to die and the production of EMPs is downregulated (Smith and Warshawsky, 1977). The second major stage of enamel formation, maturation, then takes place. In this stage the mineral crystals increase in both width and length, forming long rods running from the DEJ to the enamel surface. As these mineral crystals increase in size, matrix metalloproteinase-20 (MMP20) and kallikrein-4 (KLK4) enzymes work to remove EMPs to allow dense crystal development (Simmer and Fincham, 1995). The enamel proteome, however, is not entirely removed during the maturation process and remnants of biomineralisation proteins become trapped within the forming enamel crystal structure. Such incorporation has been shown to beneficially modulate the properties of enamel (He and Swain, 2008).

The enamel proteome is relatively small, comprised of a handful of enamel-specific proteins (Gil-Bona and Bidlack, 2020), although several nonspecific proteins have also been identified, e.g. serum albumin, antithrombin and ubiquitin (Castiblanco et al., 2015). In mature enamel, amelogenin dominates the proteome. In mammals, amelogenin is coded for on both the X and Y chromosome, giving rise to sex-specific protein isoforms, differing by amino acid sequence. Sex determination has therefore been studied through proteomic analysis and has proved highly useful to the archaeological

46

community (e.g. Lugli *et al.*, 2019; Cintas-Peña *et al.*, 2023), with applicability beyond (Parker *et al.*, 2021). As the densest mineral in the mammalian body, tooth enamel has high preservation potential, and the proteins trapped within have also provided the opportunity to study evolutionary relationships between extinct and extant taxa (Cappellini *et al.*, 2019; Welker *et al.*, 2020) and build amino acid geochronologies (Dickinson *et al.*, 2019). Mammalian tooth enamel is a common fossil in archaeological deposits within South-Central Africa and enamel AAG is therefore the focus of chapters 4 and 5.

1.3.3. Amino acid geochronology

Amino acid geochronology (AAG) is a direct, relative dating technique which utilises the predictable degradation of proteins within fossil biominerals (such as gastropod shell and tooth enamel), studied at the constituent amino acid level.

1.3.3.1. A brief history of AAG

Shortly after protein was first identified in fossil shells by Abelson in 1954, it was suggested that diagenesis of proteins trapped within biominerals could be used as a principle for dating (Abelson, 1955). In 1967 this was shown to be plausible when Hare and Abelson analysed fossil bivalves and observed an increase in amino acid racemisation (AAR; see section 1.3.3.3.1) correlated with age (Hare and Ableson, 1967). The early application of this technique to fossil bone resulted in a few controversial studies where the racemisation results contradicted other dating techniques and/or site understanding (e.g. Bada, 1985; Blackwell *et al.*, 1990), leading the community to question its reliability and accuracy. During this time, analysis was undertaken on the South-Central African Kabwe cranium, which yielded an aspartic acid D/L = 0.55. The study calibrated this value to produce a age of 110 ka (Bada *et al.*, 1974). As this fossil was discovered in a working mine, little stratigraphic information was recorded and preserved, and verification of this surprisingly young AAR date proved highly challenging due to the lack of appropriate additional dating techniques available at the time. U-series dating has only recently been undertaken on the cranium, giving rise to a much earlier result of 299 ± 25 ka (Grün *et al.*, 2020). Since the 1970's, studies on bone have revealed the non-linear breakdown of collagen (Dobberstein *et al.*, 2009), in addition to the minerals open-system behaviour (i.e. its increased likelihood of contamination and reaction rate influences from the depositional environment (Bravenec *et al.*, 2018)) and the AAR date of 110 ka is therefore very unlikely to be reliable. Subsequent work on this technique has focused on improving its reliability and robustness by establishing stringent data screening approaches (e.g. Kaufman, 2006; Ortiz *et al.*, 2018) and the development of the intra-crystalline protein degradation (IcPD) laboratory methodology approach (Sykes *et al.*, 1995; Penkman *et al.*, 2008).

Forced degradation experiments have a long history of study in AAG for comparison to fossil diagenesis (e.g. Bada and Schroeder, 1972; Kimber and Griffin, 1987; Canoira *et al.*, 2003; Dobberstein *et al.*, 2009; Crisp *et al.*, 2013; Tomiak *et al.*, 2013; Ortiz *et al.*, 2017; Dickinson *et al.*, 2019). Isothermal heating in laboratory-controlled conditions is typically employed to artificially accelerate protein degradation, allowing investigation of mechanisms for comparison to fossil protein diagenesis. Improving understanding of fossil protein diagenesis within the natural environment is key in validating the endogeneity and degradation state of samples.

1.3.3.2. Intra-crystalline protein degradation

Intra-crystalline protein degradation (IcPD) is an AAG approach which targets protein trapped within the crystal structure of fossil biominerals. Building on studies in the 1970s showing that organic material resistant to chemical oxidation appeared to be trapped within crystals (Towe and Thomson, 1972; Crenshaw ,1972), IcPD protocols were developed in the 1990s and 2000s and includes a sample pretreatment step with a strong chemical oxidiser to target what is termed the intra-crystalline fraction of protein (Fig. 1.7) (Sykes *et al.*, 1995; Penkman, 2005).
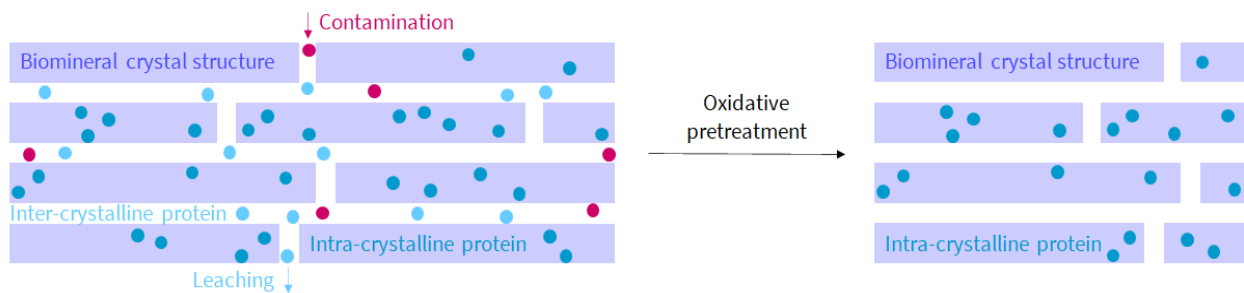
Figure 1.7. Generic schematic representation of protein within fossil biominerals.

In many biominerals, this fraction of protein has been shown to behave as a closed-system (e.g. gastropods (Sykes *et al.*, 1995; Penkman *et al.*, 2008; Demarchi *et al.*, 2013a), ostrich eggshell (Crisp *et al.*, 2013), coral (Hendy *et al.*, 2012), foraminifera (Wheeler *et al.*, 2021) and enamel (Dickinson *et al.*, 2019)), although this is not the case for all fossil biominerals (e.g. Orem and Kaufman, 2011; Demarchi *et al.*, 2015; Ortiz *et al.*, 2017). Where closed-system behaviour is maintained, leaching of endogenous protein, contamination by exogenous protein and most additional environmental impacts on protein degradation are removed (Towe, 1980). Such environmental impacts on rates of racemisation (section 1.3.3.3.1) include soil pH (Hare and Mitterer, 1969; Friedman and Liardon, 1985), water concentration (Hare, 1974) and the presence of metal ions (Smith and Evans, 1980). For biominerals which adhere to closed-system behaviour, the use of the intra-crystalline approach has helped to improve the accuracy and precision, and reduce data variability, increasing the reliability and robustness of the geochronologies obtained (e.g. Brooks *et al.*, 1990; Penkman *et al.*, 2008; Hendy *et al.*, 2012).

1.3.3.3. Protein degradation pathways

Ancient proteins undergo a myriad of protein degradation processes during diagenesis, and it is possible to investigate a number of these from the IcPD approach to AAG. These include amino acid racemisation (section 1.3.3.3.1), peptide chain hydrolysis (section 1.3.3.3.2) and decomposition reactions (section 1.3.3.3.3), discussed below.

1.3.3.3.1. Racemisation

All amino acids (except for glycine, where R = H) contain a stereogenic centre at the α-carbon, which results in two possible enantiomeric forms (Fig. 1.8). These enantiomers are labelled from their resulting rotation of a plane of polarised light, where L = *laevo* (left) and D=*dextro* (right). As enantiomers are chemically identical, neither form is thermodynamically favoured whilst free in solution. Two amino acids (isoleucine and threonine) also have an additional stereocenter on their β-carbon (Fig. 1.8), resulting in four stereoisomers; two enantiomers (chemically identical isomers, e.g. L-isoleucine and D-isoleucine, Fig. 1.8) and two diastereoisomers (chemically non-identical isomers, e.g. L-isoleucine and D-alloisoleucine, Fig. 1.8). Their conversion is termed epimerisation.
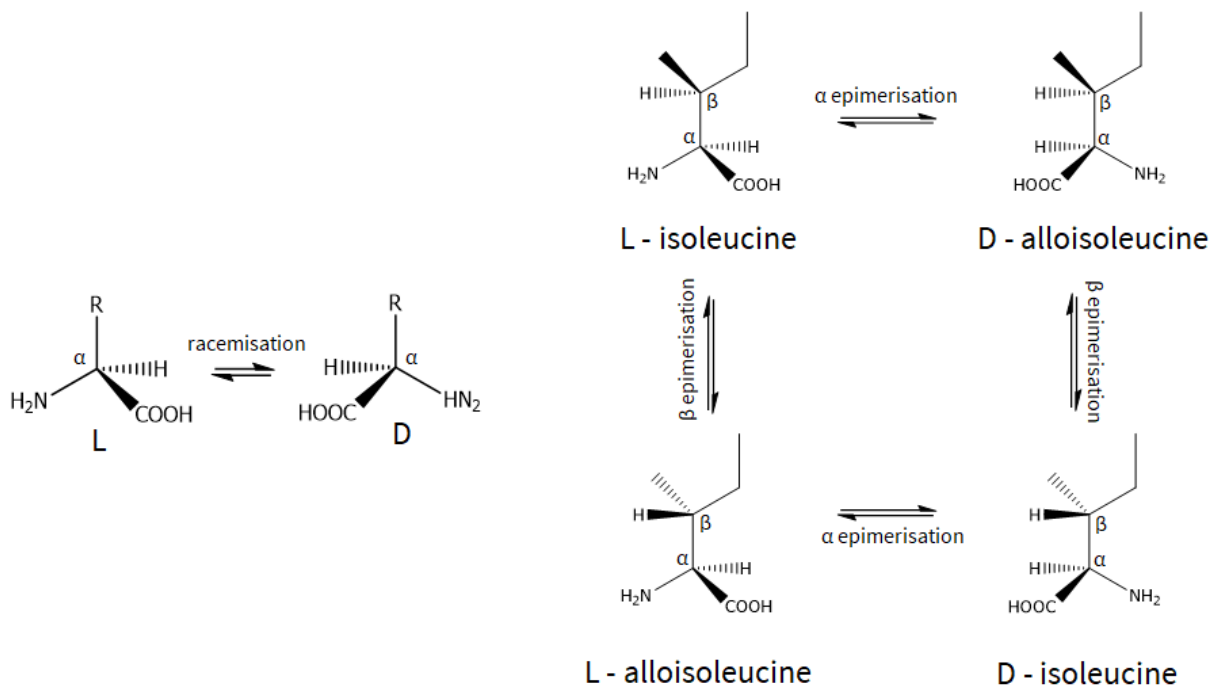
Figure 1.8. Top - racemisation of amino acids with a single stereogenic centre (α). Bottom - epimerisation of an amino acid with two stereogenic centres (α, β).

In living organisms, enantiomeric control of amino acids within proteins is exerted, with proteins built almost exclusively from L-enantiomers. This ensures the desired enantiomeric form is maintained for protein function. This biological control ceases after death, at which point the amino acids become able to racemise. There are a few interesting exceptions to the exclusive synthesis of proteins from L-enantiomers, including bacteria which use some D-amino acids to build and regulate their peptidoglycan cell walls (Cava *et al.*, 2011). D-amino acids have also been implicated in many diseases including ischemia, epilepsy, neurodegenerative disorders (Genchi, 2017) and schizophrenia (Fuchs *et al.*, 2005).

The mechanism of racemisation for free amino acids is thought to involve base catalysed hydrogen abstraction, forming a planar sp^2 hybridised carbanion, followed by addition of a proton from either plane (Fig. 1.9). As neither plane is thermodynamically favoured, the system tends towards an equilibrium where D/L = 1 (Neuberger, 1948).
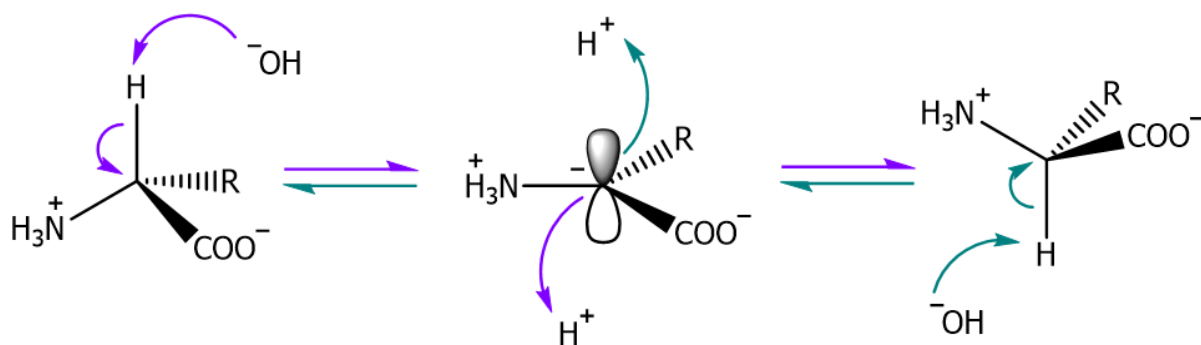
Figure 1.9. The mechanism of base catalysed free amino acid racemisation (Neuberger, 1948).

The rate of racemisation is influenced by the stability of the intermediate carbanion (Matsuo *et al.*, 1967). In free amino acids, this carbanion is resonance stabilised by the carboxylic acid group and inductively stabilised by the positively charged amine group (Neuberger, 1948), with variability in rates of racemisation arising from each amino acid's different R groups (Smith and Evans, 1980; Smith and Reddy, 1989). Inductive effects are also considered to play a major role in the stability of the carbanion. In general, the greater electron withdrawing effect of an R group, the slower the rate of racemisation, due to increased stabilisation of the intermediate carbanion. In heated neutral pH solutions, Smith *et al.*, (1978) found the relative rates of racemisation were Asp>Glu>Phe>Ala>Leu>Ile>Val, indicating that the relative rates cannot be fully explained by inductive effects alone, and that resonance stabilisation and both steric and solvents effects also play a role (Smith *et al.,* 1978).

Racemisation can also occur under strong acidic conditions, although it is thought to proceed via a different mechanism, involving enolisation, with proton addition to an amino acid's carboxy group resulting in a planar intermediate (Fig. 1.10). As with the base catalysed mechanism, a proton

may then be added either side of the plane resulting in a mixture of D and L enantiomers. Once again rates vary between amino acids resulting from the R groups' ability to electronically stabilise the intermediate, or from steric effects (Frank *et al.*, 1981).
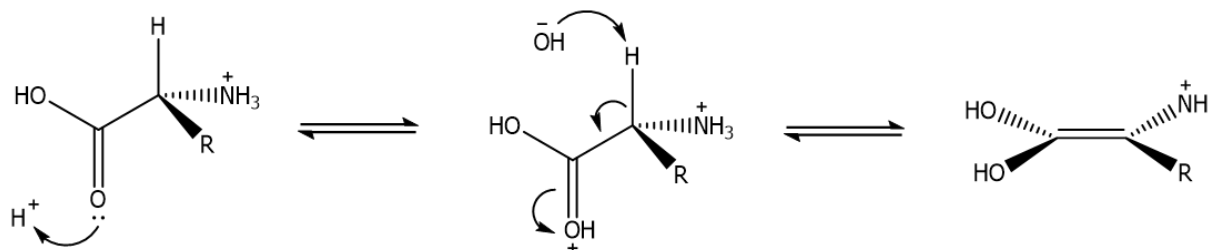
Fig. 1.10. The mechanism of acid catalysed free amino acid racemisation.

The majority of amino acids require conformational freedom to racemise and are not able to do so when bound within a peptide chain (Mitterer and Kriausakul, 1984). Terminal amino acids are able to racemise, and at the N-terminus this is thought to proceed via a reversible diketopiperazines (DKP) cyclisation (Fig. 1.11; Steinberg and Bada, 1981).
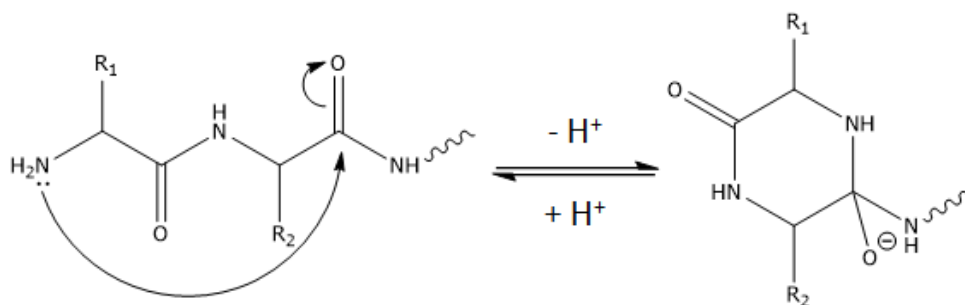
Figure 1.11. Reversible N-terminal diketopiperazine cyclisation mechanism (Steinberg and Bada, 1981).

In-chain racemisation has, however, been observed for asparagine, aspartic acid and serine (Stephenson and Clarke, 1989; Takahashi *et al.*, 2010; Demarchi *et al.*, 2013b). In the case of asparagine and aspartic acid, the ability to reversibly form a five-membered succinimide ring is thought to play a key role in the in-chain racemisation mechanism (Fig. 1.12), as well as asparagine's propensity to deamidate to aspartic acid.
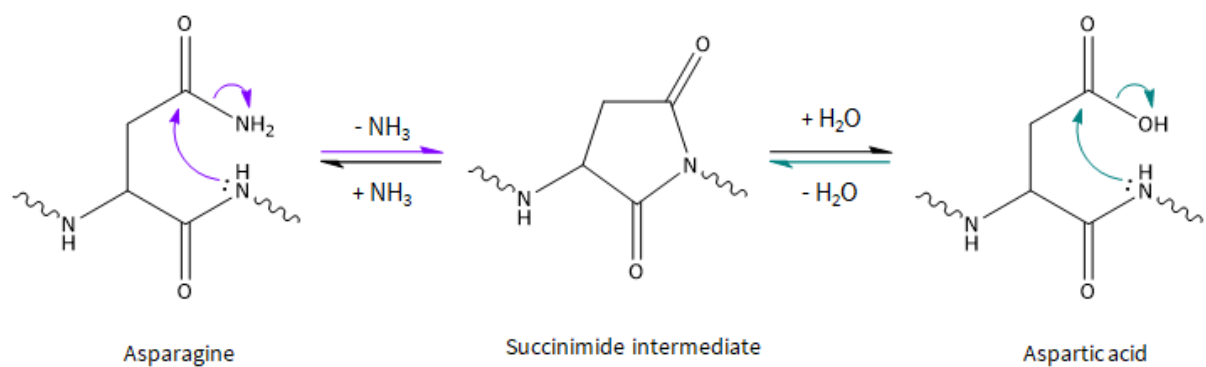
Figure 1.12. Reversible succinimide ring mechanism for asparagine and aspartic acid (Stephenson and Clarke, 1989).

A number of variables have been shown to affect the rates of amino acid racemisation. Kinetic studies have displayed the effect of temperature on rates of racemisation both for free amino acids (Smith and Evans, 1980) and those within biominerals (e.g. Hare and Mitterer, 1969; Brooks *et al.*, 1990; Canoira *et al.*, 2003; Dickinson *et al.*, 2019). For simple di- and tri- peptides, neighbouring amino acids were shown to alter rates of racemisation (Mitterer and Kriausakul, 1984), which for proteins would be further compounded by their secondary and tertiary structures. Relating to this, a taxonomic effect has been previously described (e.g. Miller and Brigham-Grette, 1989; Penkman *et al.*, 2008; Ortiz *et al.*, 2013) resulting from taxonomic differences in each protein's primary amino acid sequence. For proteins within biominerals, additional interactions, for example with the mineral surface and solvent (water) effect have also been shown to affect rates of protein degradation (Demarchi *et al.*, 2016). These studies highlight the importance of building taxa-specific amino acid geochronologies regionally to account for taxonomic and regional climatic temperature differences.

1.3.3.3.2. Peptide chain hydrolysis

Alongside racemisation, an additional protein degradation mechanism which can be studied using IcPD analysis is peptide chain hydrolysis. The condensation reaction involved in building a protein's primary sequence is a reversible reaction (hydrolysis) which occurs during protein diagenesis (Fig. 1.13). Peptide bond hydrolysis may occur at the C- or N-terminus of the peptide sequence (freeing individual amino acids), or mid peptide chain (resulting in two shorter peptides).
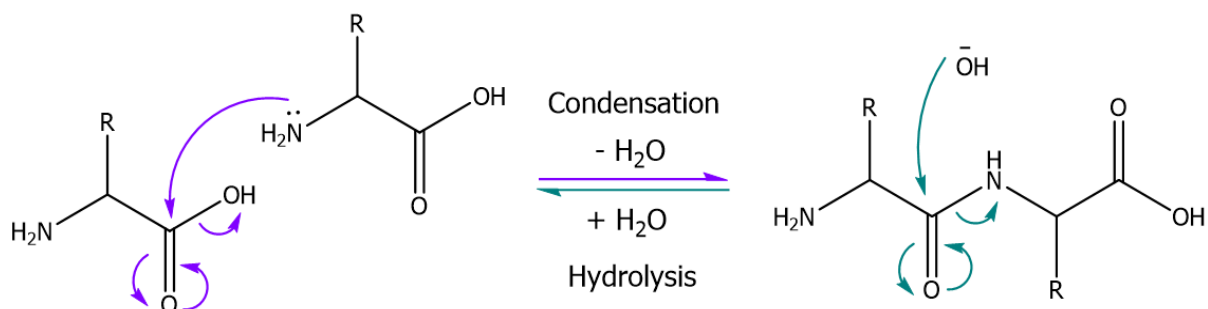
Figure 1.13. The reversible peptide bond mechanism.

The rate of hydrolysis is dependent on a number of factors. These include the concentration of water molecules (Pan *et al.*, 2011) and their physical access to different areas of the peptide chain, both in terms of their tertiary protein structure and any additional interactions with a mineral surface (Demarchi *et al.*, 2016). Amino acid R groups also influence the chemical stability of reaction intermediates, which in turn alters relative rates of peptide bond hydrolysis. Additional influences from the burial environment such as pH (Liardon and Ledermann, 1986) and temperature (Bada, 1985) have also been shown to affect rates. In broad terms, the extent of hydrolysis in fossil proteins increases with time. However, its reaction kinetics are highly variable (Walton, 1998) and the extent of hydrolysis cannot be used reliably on its own to indicate fossil biomineral age. Hydrolysis is, however, routinely investigated from IcPD analysis by calculating the percentage of free amino acids (%FAA) to corroborate the likelihood of closed-system behaviour.

1.3.3.3.3. Decomposition reactions

There are a number of different amino acid decomposition reactions, which occur during protein, peptide and amino acid degradation. Some of these decomposition reactions include deamidation, decarboxylation and condensation (Vallentyne, 1964; Bada *et al.*, 1978; Walton, 1998). The majority of decomposition reactions cannot be directly observed from IcPD data, but may be indirectly apparent from loss of amino acid signal, i.e. decreasing amino acid concentrations. As degradation pathways occur simultaneously, in some cases the decomposition of free amino acids may inhibit racemic equilibrium being achieved at high extents of protein degradation (Schroeder and Bada, 1977) and decreasing levels of %FAA (Vallentyne, 1964).

R group deamidation occurs in two amino acids, asparagine and glutamine, resulting in the formation of aspartic acid and glutamic acid respectively. This reaction also readily occurs in strongly acidic conditions and is therefore induced during the hydrolysis and demineralisation stages of the IcPD protocol. As the decomposition products are indistinguishable from the naturally occurring aspartic acid and glutamic acid by HPLC, these amino acids are grouped and termed Asx and Glx (Hill, 1965). Unfortunately, it is therefore not possible to study their individual degradation trends by IcPD

analysis, but they can, however, be examined through mass spectrometric analysis of peptides (discussed in section 1.3.4).

Two decomposition reactions which can be investigated through IcPD analysis are threonine and serine degradation. During protein diagenesis dehydration of both amino acids results in the production of alanine (Bada *et al.*, 1978); trends in [Ser]/[Ala] can therefore be investigated to corroborate the likelihood of closed system behaviour of the intra-crystalline protein fraction (Penkman *et al.*, 2008).

1.3.3.4. Amino acid analysis

AAG now routinely utilises reverse phase high performance liquid chromatography (RP-HPLC) with fluorescence detection to quantify amino acids. The IcPD approach uses an analytical method created by Kaufman and Manley (1998) and adapted slightly by Penkman (2005), which allows determination of the racemic proportions of up to 11 amino acids and the concentrations and relative compositions of up to 15 amino acids (Fig. 1.14).
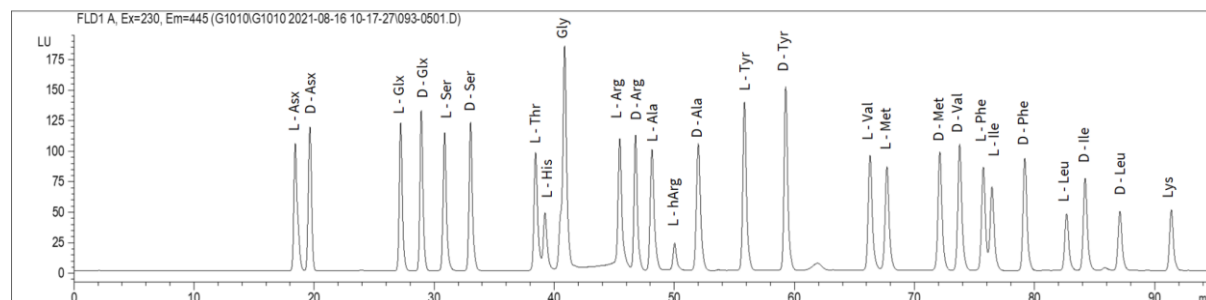
Figure 1.14. Example chromatogram of a sample standard.

Prior to the development of this method, two techniques were commonly used to measure amino acid racemisation. More commonly, HPLC analysis was undertaken with ion-exchange (IEx) separation which focused on the analysis of just one amino acid chiral pair, the epimerisation of L-isoleucine to D-alloisoleucine (Fig. 1.8, section 1.3.3.3.1), referred to as the A/I value. In living nature, isoleucine (Ile) is found almost exclusively in its L enantiomeric form (and conveniently for amino acid dating), in fossils L- Ile epimerises solely to D-aIle, with D-Ile and L-aIle not found within fossils due to their instability (Bada *et al.*, 1986). As diastereoisomers, L-Ile and D-aIle were easy to chemically separate by IEx-HPLC due to their non-chemically identical nature (e.g. Kaufman and Sejrup, 1995; Miller *et al.*, 1999). The alternative analytical technique was gas chromatography (GC), which had the advantage of being able to analyse multiple amino acid chiral pairs, but took considerably more preparation and was therefore less favoured due to its time intensive methodology (e.g. Kvenvolden *et al.*, 1973; Kaufman and Manley, 1998). Isoleucine epimerisation is still analysed using the IcPD analytical methodology, although as racemisation occurs for the majority of amino acids analysed,

54

racemisation is usually used as a catch-all term, encompassing racemisation and isoleucine epimerisation. In comparison to early A/I value determination, HPLC analysis of multiple intra-crystalline amino acids has widened the array of protein degradation mechanisms available for study (such as relative rates of racemisation, peptide chain hydrolysis and decomposition reactions), and allowed a wider study of endogenous protein diagenesis at the constituent amino acid level (e.g. Penkman *et al.*, 2008; Crisp *et al.*, 2013; Tomiak *et al.*, 2013; Ortiz *et al.*, 2018; Dickinson *et al.*, 2019).

1.3.4. Palaeoproteomics

Palaeoproteomics is still a relatively young field, which studies ancient peptides, with an aim to identify specific proteins. Whilst less informative than ancient DNA (aDNA), proteins contain an abundance of biological information and have been shown to consistently preserve longer than aDNA (Van Der Valk *et al.*, 2021; Kjær *et al.*, 2022; Demarchi *et al.*, 2016; 2022), being capable of surviving across the globe well into the Quaternary and in rare cases beyond (e.g. Demarchi *et al.*, 2016; 2022; Buckley *et al.*, 2019). Studies have now been undertaken on a wide range of materials including (but not limited to) bone (e.g. Buckley *et al.*, 2009; Welker *et al.*, 2015), ivory (e.g. Gilbert *et al.*, 2024), eggshell (e.g. Demarchi *et al.*, 2016; 2022), mollusc shell (e.g. Sakalauskaite *et al.*, 2020), enamel (e.g. Cappellini *et al.*, 2019; Lugli *et al.*, 2019; Cintas-Peña *et al.*, 2023), dental calculus (e.g. Warinner *et al.*, 2015; Hendy *et al.*, 2018a), soft tissues such as the brain (e.g. Maixner *et al.*, 2013), coprolites (e.g. Runge *et al.*, 2021), cooking and storage vessels (e.g. Solazzo *et al.*, 2008; Hendy *et al.*, 2018b) and textiles such as leather, silk and wool (e.g. Brandt *et al.*, 2020; Gong *et al.*, 2016; Solazzo *et al.*, 2013a). Such studies have been undertaken for a variety of purposes, revealing evolutionary relationships, past diets, diseases, technologies and informing best preservation strategies for art and museum artefacts, to name a few.

1.3.4.1. Peptide analysis by mass spectrometry

For many palaeoproteomic applications, to produce peptides suitable for detection by a mass spectrometer, standard laboratory protocols are required to reduce, alkylate and digest the protein (Shuken, 2023). These steps first reduce (break apart) the disulphide bonds which stabilise the protein's secondary and tertiary structures, before the addition of an alkyl group to stop these bonds reforming. Reduction and alkylation help to improve both detection of cysteine containing peptides and the access of subsequent digestive enzymes (Suttapitugsakul *et al.*, 2017; Evans, 2019). One of the most commonly used enzymes, trypsin (Warinner *et al.*, 2022), cleaves at the C-terminal side of arginine and lysine. For samples where a very high degree of protein diagenesis (peptide bond hydrolysis) is expected, and for tooth enamel, where enzymatic digestion of enamel proteins occurs

during enamel maturation (section 1.3.2.2), enzyme free protocols are often successfully employed (e.g. Cappellini *et al.*, 2019; Madupe *et al.*, 2023; Taurozzi *et al.*, 2024).

Current palaeoproteomic studies tend to utilise two main MS approaches; either as a standalone technique using matrix assisted laser desorption ionisation time of flight (MALDI-ToF) MS, or in tandem with chromatography (LC-MS/MS). In both cases peptides are detected in the mass spectrometer as ions based on their mass to charge ratio (m/z). The choice of technique is normally based upon the research goal, which ranges from established high-throughput applications such as ZooMS (zooarchaeology by mass spectrometry), to highly specialised research interests and therefore analysis (Cleland and Schroeter, 2018).

1.3.4.1.1. Peptide mass fingerprinting

ZooMS is a low cost, high-throughput method which uses MALDI-ToF mass spectrometry to identify taxa (Buckley *et al.*, 2009; Collins *et al.*, 2010). It is a peptide mass fingerprinting approach (PMF) allowing the taxonomic identification of collagenous biominerals (typically bone, occasionally tooth dentine, ivory and antler), based upon diagnostic tryptic peptides in a mass spectrum. The degree to which taxonomic identifications are possible is related in part to the limitations of the taxonomic variability of collagenous proteins, which whilst divergent are relatively well conserved, in addition to the database against which the mass spectra are compared. This database continues to grow with further research (e.g. Janzen *et al.*, 2021; Codlin *et al.*, 2022; Dierickx *et al.*, 2022).

Similar PMF approaches to taxonomically identify material have also been taken with eggshell (e.g. Presslee *et al.*, 2017; Demarchi *et al.,* 2020), mollusc shell (Sakalauskaite *et al.*, 2020) and keratinous tissues (such as hair, wool, horn, claws and others) (Solazzo *et al.*, 2013b).

1.3.4.1.2. Tandem mass spectrometry

Tandem mass spectrometry (MS/MS; Fig. 1.15) involves the introduction of an additional fragmentation and detection component (MS2) for ions detected in the first scan (MS1). This approach is undertaken to more accurately identify the peptides observed in the MS1. During fragmentation by collision induced dissociation (CID), peptide (amide) bonds are broken, giving rise to shorter peptide fragments. The peptide fragment yields either a b or y ion, where the cleavage has occurred on the C- or N- side of the peptide bond respectively (Fig. 1.15).
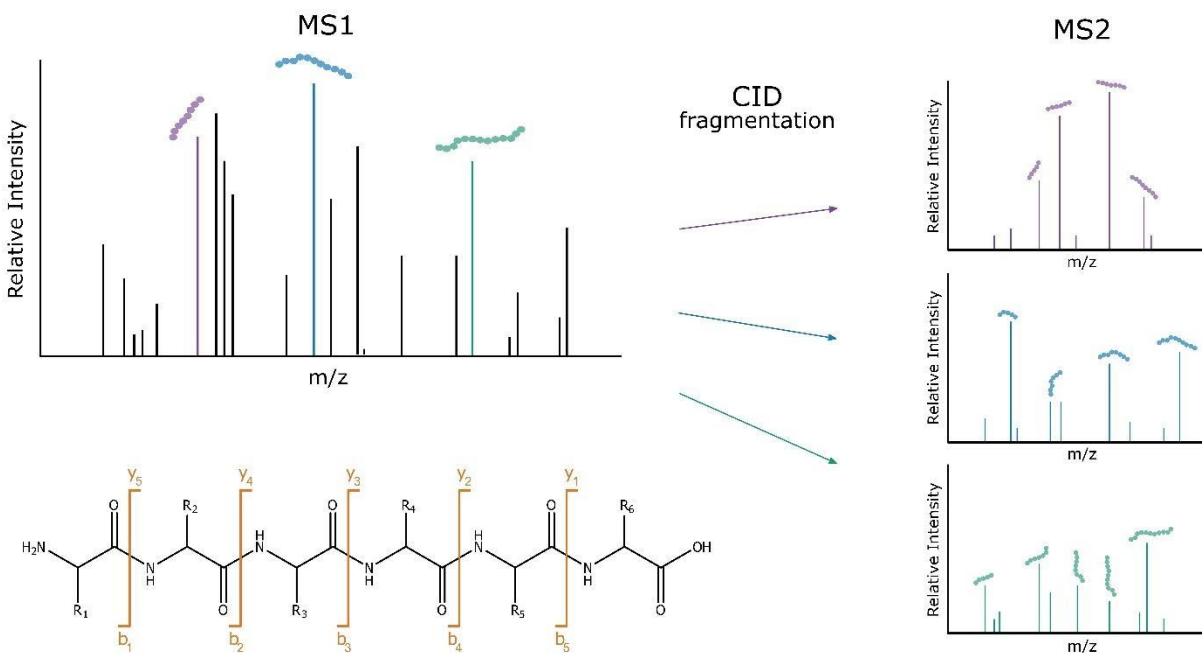
Figure. 1.15 Schematic of tandem mass spectrometry.

Tandem mass spectrometry has been undertaken using MALDI-ToF instruments for ancient protein analysis (e.g. Tripković *et al*., 2013; Bona *et al*., 2014), but is most frequently used in conjunction with liquid chromatography. LC-MS/MS becomes necessary for more complex mixtures to allow separations of sample components along a gradient. For analysis of ancient proteins, the data dependent analysis (DDA) approach to MS is most often used. DDA involves the selection of the most intense peptide ions in the MS1 for fragmentation in the MS2 (Fig. 1.15). Currently, the DDA approach is most appropriate, and tends to yield the best results, for samples which: a) contain a low protein complexity (<1000 proteins), b) where post translational modifications (PTMs) and/or diagenetoforms (diagenetic modifications, Cleland *et al*., 2021) are important, and/or c) where manual validation of the mass spectra is desired. In most cases, all three criteria occur in palaeoproteomic studies.

Once data has been acquired, it is searched against a database. Ideally this database contains the sequences for all plausible proteins within a sample, including common laboratory contaminants, and no others (Chiang *et al*., 2024). Database searching software also undertake false discovery rate (FDR) statistical testing for peptides which are matched to protein sequences (peptide spectral matches, PSMs), by searching against the reverse of all sequences included in the database (a decoy database), improving the confidence in the peptide and protein identifications obtained.

1.3.4.2. Protein degradation pathways

As previously discussed in section 1.3.3.3, ancient proteins undergo a host of protein degradation processes during diagenesis. Some diagenetic mechanisms which are possible to study

by IcPD, such as peptide bond hydrolysis (section 1.3.3.3.2), can be inferred from a different perspective by palaeoproteomic data. From MS analysis the peptide length can be used to infer peptide chain hydrolysis, with a greater number of short peptides expected for more highly degraded samples (Cleland et al., 2021). Other mechanisms, which cannot be studied through IcPD data, such as deamidation of asparagine and glutamine, are possible to investigate through palaeoproteomic data. Many diagenetic modifications (or diagenetoforms; Cleland et al., 2021), including deamidation, are possible to identify by including as a variable peptide modification in a database searches. The extent of deamidation has a relationship with protein diagenesis, but it is not linear and high variability is often observed between samples (e.g. Robinson and Robinson, 2004; Ramsøe et al., 2020; Chowdhury and Buckley, 2022). An additional parameter which can also help to corroborate ancient protein identification from palaeoproteomic data is the assessment of regions of protein preservation and long-surviving peptides (Demarchi et al., 2016). Used in combination, these approaches allow the palaeoproteomic data to be scrutinised from multiple angles, providing the ability to interpret the data more confidently.

As with IcPD, forced degradation experiments on archaeologically relevant material can be used to investigate protein diagenesis by mass spectrometry. These studies typically cover a broader range of sample types and research focus than those undertaken for AAG (e.g. silk degradation to assist artefact conservation (Chen et al., 2020), experimental burial of wool fabrics to understand preservation potential (Solazzo et al., 2013a), cooking experiments to study protein alterations and ceramic binding (Barker et al., 2018)) and are therefore more context dependent. They do, however, provide the same opportunity to study protein diagenesis on an accelerated timescale and to help validate the likelihood of ancient protein.

1.3.5. Ancient proteins summary

Proteins are biologically informative molecules, which have the potential to be preserved for millions of years (Umamaheswaran and Dutta, 2024). Remnants from the oldest ancient proteins published to date (e.g. Penkman et al., 2013 Saitta et al., 2024; Demarchi et al., 2016, 2022; Buckley et al., 2019) have all been analysed from biominerals, acting as excellent repositories for ancient endogenous protein. Ancient proteins from biominerals can be studied through multiple techniques, including AAG and palaeoproteomics, offering complementary data on the same material (e.g. Presslee et al., 2019; 2021), providing multiple lines of highly useful information. Analysis of ancient protein from biominerals using the latest approaches has not been explored in the South-Central African region, where a number of biominerals, most abundantly, terrestrial gastropod shell and tooth enamel, are frequently found at archaeological and palaeoenvironmental sites within the region.

1.4. Aims

The aim of this thesis is therefore to explore the potential of previously excavated material from the South-Central African region for palaeoenvironmental analysis (objective 1), biomolecular analysis (objectives 2, 3 and 4) and geochronological analysis (objectives 2 and 3), to improve archaeological understanding within this region. The specific objectives are as follows:

1. To extract molluscan material from sediments associated with Ancient Lake Kafue, Zambia, to undertake palaeoenvironmental analysis (chapter 2, research paper accepted for publication in *The Journal of Conchology* pending minor revisions in July 2024), and investigate whether the mollusc species present were appropriate for building an amino acid geochronology).

2. To investigate the suitability of the giant African land snail (*Achatina* sp. and *Lissachatina* sp.) shell (present within the excavated sediments detailed in chapter 2) for building an AAG using the IcPD approach for the South-Central African region (chapter 3, research paper published in *Quaternary Geochronology* under the citation: Baldreki, C., Burnham, A., Conti, M., Wheeler, L., Simms, M.J., Barham, L., White, T.S. and Penkman, K., 2024. Investigating the potential of African land snail shells (Gastropoda: Achatininae) for amino acid geochronology. *Quaternary Geochronology, 79*, pp.101473).

3. To investigate the use of another biomineral found in Quaternary deposits in the region, mammalian tooth enamel, from two archaeological sites in Zambia for building taxa-specific geochronologies for the South-Central African region. Additionally, to investigate the use of the IcPD approach to AAG using tooth enamel for elucidating cave site depositional histories (chapter 4, research paper published in *Open Quaternary* under the citation: Baldreki, C., Dickinson, M., Reynolds, S., White, T.S., Barham, L. and Penkman, K., 2024. Old Fossils, New Information: Insights into Site Formation Processes of Two Pleistocene Cave Sequences in Zambia from Enamel Amino Acid Geochronology. *Open Quaternary, 10*(4), pp.1–17).

4. To investigate the use of forced degradation experiments on Rhinocerotidae enamel through chiral amino acid and palaeoproteomic analysis, to better understand markers of intra-crystalline protein degradation (chapter 5).

1.5. References

Abbott, P.M. and Davies, S.M., 2012. Volcanism and the Greenland ice-cores: the tephra record. *Earth-Science Reviews, 115*(3), pp.173-191.

Abbott, P.M., Griggs, A.J., Bourne, A.J., Chapman, M.R. and Davies, S.M., 2018. Tracing marine cryptotephras in the North Atlantic during the last glacial period: Improving the North Atlantic marine tephrostratigraphic framework. *Quaternary Science Reviews, 189*, pp.169-186.

Abelson, P.H., 1955. Organic constituents of fossils. *Carnegie Inst. Wash. Year Book, 54*, pp.107-109.

Abram, N.J., Mulvaney, R., Wolff, E.W., Triest, J., Kipfstuhl, S., Trusel, L.D., Vimeux, F., Fleet, L. and Arrowsmith, C., 2013. Acceleration of snow melt in an Antarctic Peninsula ice core during the twentieth century. *Nature Geoscience, 6*(5), pp.404-411.

Aciego, S., Bourdon, B., Schwander, J., Baur, H. and Forieri, A., 2011. Toward a radiometric ice clock: uranium ages of the Dome C ice core. *Quaternary Science Reviews, 30*(19-20), pp.2389-2397.

Alves, E.Q., Macario, K., Ascough, P. and Bronk Ramsey, C., 2018. The worldwide marine radiocarbon reservoir effect: definitions, mechanisms, and prospects. *Reviews of Geophysics, 56*(1), pp.278-305.

Aubert, M., Pike, A.W., Stringer, C., Bartsiokas, A., Kinsley, L., Eggins, S., Day, M. and Grün, R., 2012. Confirmation of a late middle Pleistocene age for the Omo Kibish 1 cranium by direct uranium-series dating. *Journal of Human Evolution, 63*(5), pp.704-710.

Avery, D.M., 2000. Chapter 6 Past and present ecological and environmental information from micromammals in Barham, L.S., 2000. *The Middle Stone Age of Zambia, South Central Africa*. Western academic & specialist Press. pp.63-72.

Avery, D.M., 2002. Taphonomy of micromammals from cave deposits at Kabwe (Broken Hill) and Twin Rivers in Central Zambia. *Journal of Archaeological Science, 29*(5), pp.537-544.

Avery, D.M., 2003. Early and Middle Pleistocene environments and hominid biogeography; micromammalian evidence from Kabwe, Twin Rivers and Mumbwa Caves in central Zambia. *Palaeogeography, Palaeoclimatology, Palaeoecology, 189*(1-2), pp.55-69.

Bada, J.L., 1985. Amino acid racemization dating of fossil bones. *Annual Review of Earth and Planetary Sciences, 13*(1), pp.241-268.

Bada, J.L. and Schroeder, R.A., 1972. Racemization of isoleucine in calcareous marine sediments: kinetics and mechanism. *Earth and Planetary Science Letters, 15*(1), pp.1-11.

Bada, J.L., Schroeder, R.A., Protsch, R. and Berger, R., 1974. Concordance of collagen-based radiocarbon and aspartic-acid racemization ages. *Proceedings of the National Academy of Sciences, 71*(3), pp.914-917.

Bada, J.L., Shou, M.Y., Man, E.H., and Schroeder, R.A. 1978. Decomposition of hydroxy amino acids in foraminiferal tests: Kinetics, mechanism and geochronological implications. *Earth Planetary Science Letters, 41*(1), pp.67-76.

Bada, J.L., Zhao, M., Steinberg, S. and Ruth, E., 1986. Isoleucine stereoisomers on the Earth. *Nature, 319*(6051), pp.314-316.

Badawy, W.M., Duliu, O.G., Frontasyeva, M.V., El Samman, H. and Faanhof, A., 2018. Environmental radioactivity of soils and sediments: Egyptian sector of the Nile valley. *Isotopes in environmental and health studies, 54*(5), pp.535-547.

Baldreki, C., Burnham, A., Conti, M., Wheeler, L., Simms, M.J., Barham, L., White, T.S. and Penkman, K., 2024. Investigating the potential of African land snail shells (Gastropoda: Achatininae) for amino acid geochronology. *Quaternary Geochronology*, *79*, pp.101473.

Barham, L.S., 2000. *The Middle Stone Age of Zambia, South Central Africa*. Western academic & specialist Press.

Barham, L., 2002. Systematic pigment use in the Middle Pleistocene of south-central Africa. *Current anthropology, 43*(1), pp.181-190.

Barham, L., Duller, G.A.T., Candy, I., Scott, C., Cartwright, C.R., Peterson, J.R., Kabukcu, C., Chapot, M.S., Melia, F., Rots, V. and George, N., 2023. Evidence for the earliest structural use of wood at least 476,000 years ago. *Nature, 622*(7981), pp.107-111.

Barker, A., Dombrosky, J., Venables, B. and Wolverton, S., 2018. Taphonomy and negative results: An integrated approach to ceramic-bound protein residue analysis. *Journal of Archaeological Science, 94*, pp.32-43.

Barr, W.A. and Wood, B., 2024. Spatial sampling bias influences our understanding of early hominin evolution in eastern Africa. *Nature Ecology & Evolution*, pp.1-8.

Batchelor, C.L., Margold, M., Krapp, M., Murton, D.K., Dalton, A.S., Gibbard, P.L., Stokes, C.R., Murton, J.B. and Manica, A., 2019. The configuration of Northern Hemisphere ice sheets through the Quaternary. *Nature communications, 10*(1), p.3713.

Beck, J.W., Richards, D.A., Lawrence, R., Silverman, B.W., Smart, P.L., Donahue, D.J., Hererra-Osterheld, S., Burr, G.S., Calsoyas, L., Timothy, A.J. and Jull, 2001. Extremely large variations of atmospheric ^{14}C concentration during the last glacial period. *Science, 292*(5526), pp.2453-2458.

Behre, K.E. and van der Plicht, J., 1992. Towards an absolute chronology for the last glacial period in Europe: radiocarbon dates from Oerel, northern Germany. *Vegetation History and Archaeobotany, 1*, pp.111-117.

Belcher, A.M., Wu, X.H., Christensen, R.J., Hansma, P.K., Stucky, G.D. and Morse, D.E., 1996. Control of crystal phase switching and orientation by soluble mollusc-shell proteins. *Nature, 381*(6577), pp.56-58.

Berger, L.R., Hawks, J., de Ruiter, D.J., Churchill, S.E., Schmid, P., Delezene, L.K., Kivell, T.L., Garvin, H.M., Williams, S.A., DeSilva, J.M. and Skinner, M.M., 2015. *Homo naledi*, a new species of the genus *Homo* from the Dinaledi Chamber, South Africa. *elife, 4*, p.e09560.

Bergström, A., Stringer, C., Hajdinjak, M., Scerri, E.M. and Skoglund, P., 2021. Origins of modern human ancestry. *Nature*, *590*(7845), pp.229-237.

Bishop, L.C. and Reynolds, S.C., 2000. Chapter 11 Fauna from Twin Rivers in Barham, L.S., 2000. *The Middle Stone Age of Zambia, South Central Africa*. Western academic & specialist Press. pp.217-222.

Blaauw, M., 2012. Out of tune: the dangers of aligning proxy archives. *Quaternary Science Reviews, 36*, pp.38-49.

Blackwell, B., Rutter, N. W., Debénath, A. 1990. Amino acid racemization in mammalian bones and teeth from La Chaise-de-Vouthon (Charente), France. *Geoarchaeology, 5*(2), pp.121-147.

Bobe, R. and Wood, B., 2022. Estimating origination times from the early hominin fossil record. *Evolutionary Anthropology: Issues, News, and Reviews, 31*(2), pp.92-102.

Bona, A., Papai, Z., Maasz, G., Toth, G.A., Jambor, E., Schmidt, J., Toth, C., Farkas, C. and Mark, L., 2014. Mass spectrometric identification of ancient proteins as potential molecular biomarkers for a 2000-year-old osteogenic sarcoma. *PLoS One*, *9*(1), p.e87215.

Brandt, L.Ø., Ebsen, J.A. and Haase, K., 2020. Leather shoes in early Danish cities: choices of animal resources and specialization of crafts in Viking and medieval Denmark. *European Journal of Archaeology*, *23*(3), pp.428-450.

Bravenec, A.D., Ward, K.D. and Ward, T.J., 2018. Amino acid racemization and its relation to geochronology and archaeometry. *Journal of separation science, 41*(6), pp.1489-1506.

Bristow, C.S., Duller, G.A.T. and Lancaster, N., 2007. Age and dynamics of linear dunes in the Namib Desert. *Geology, 35*(6), pp.555-558.

Brooks, A.S., Hare, P.E., Kokis, J.E., Miller, G.H., Ernst, R.D. and Wendorf, F., 1990. Dating Pleistocene archeological sites by protein diagenesis in ostrich eggshell. *Science, 248*(4951), pp.60-64.

Buckley, M., Collins, M., Thomas-Oates, J. and Wilson, J.C., 2009. Species identification by analysis of bone collagen using matrix-assisted laser desorption/ionisation time-of-flight mass spectrometry. *Rapid Communications in Mass Spectrometry: An International Journal Devoted to the Rapid Dissemination of Up-to-the-Minute Research in Mass Spectrometry*, *23*(23), pp.3843-3854.

Buckley, M., Lawless, C. and Rybczynski, N., 2019. Collagen sequence analysis of fossil camels, *Camelops* and c.f. *Paracamelus*, from the Arctic and sub-Arctic of Plio-Pleistocene North America. *Journal of proteomics*, *194*, pp.218-225.

Bueno, A., Alfarhan, A., Arand, K., Burghardt, M., Deininger, A.C., Hedrich, R., Leide, J., Seufert, P., Staiger, S. and Riederer, M., 2019. Effects of temperature on the cuticular transpiration barrier of two desert plants with water-spender and water-saver strategies. *Journal of Experimental Botany, 70*(5), pp.1613-1625.

Burnett, A.P., Soreghan, M.J., Scholz, C.A. and Brown, E.T., 2011. Tropical East African climate change and its relation to global climate: a record from Lake Tanganyika, Tropical East Africa, over the past 90+ kyr. *Palaeogeography, Palaeoclimatology, Palaeoecology, 303*(1-4), pp.155-167.

Campisano, C.J., 2012. Milankovitch cycles, paleoclimatic change, and hominin evolution. *Nature Education Knowledge, 3*(5).

Canoira, L., García-Martínez, M.J., Llamas, J.F., Ortíz, J.E. and Torres, T.D., 2003. Kinetics of amino acid racemization (epimerization) in the dentine of fossil and modern bear teeth. *International journal of chemical kinetics, 35*(11), pp.576-591.

Cappellini, E., Welker, F., Pandolfi, L., Ramos-Madrigal, J., Samodova, D., Rüther, P.L., Fotakis, A.K., Lyon, D., Moreno-Mayar, J.V., Bukhsianidze, M. and Rakownikow Jersie-Christensen, R., 2019. Early Pleistocene enamel proteome from Dmanisi resolves *Stephanorhinus* phylogeny. *Nature, 574*(7776), pp.103-107.

Castiblanco, G.A., Rutishauser, D., Ilag, L.L., Martignon, S., Castellanos, J.E. and Mejía, W., 2015. Identification of proteins from human permanent erupted enamel. *European journal of oral sciences*, *123*(6), pp.390-395.

Cava, F., Lam, H., De Pedro, M.A. and Waldor, M.K., 2011. Emerging knowledge of regulatory roles of D-amino acids in bacteria. *Cellular and Molecular Life Sciences, 68*, pp.817-831.

Chang, E.P. and Evans, J.S., 2015. Pif97, a von Willebrand and Peritrophin biomineralization protein, organizes mineral nanoparticles and creates intracrystalline nanochambers. *Biochemistry, 54*(34), pp.5348-5355.

Checa, A.G., 2018. Physical and biological determinants of the fabrication of molluscan shell microstructures. *Frontiers in Marine Science*, *5*, p.353.

Chen, R., Hu, M., Zheng, H., Yang, H., Zhou, L., Zhou, Y., Peng, Z., Hu, Z. and Wang, B., 2020. Proteomics and immunology provide insight into the degradation mechanism of historic and artificially aged silk. *Analytical chemistry, 92*(3), pp.2435-2442.

Chiang, Y., Welker, F. and Collins, M.J., 2024. Spectra without stories: reporting 94% dark and unidentified ancient proteomes. *Open Research Europe, 4*(71), p.71.

Chowdhury, M.P. and Buckley, M., 2022. Trends in deamidation across archaeological bones, ceramics and dental calculus. *Methods*, *200*, pp.67-79.

Chutcharavan, P.M. and Dutton, A., 2021. A global compilation of U-series-dated fossil coral sea-level indicators for the Last Interglacial period (Marine Isotope Stage 5e). *Earth System Science Data, 13*(7).

Cintas-Peña, M., Luciañez-Triviño, M., Montero Artús, R., Bileck, A., Bortel, P., Kanz, F., Rebay-Salisbury, K. and García Sanjuán, L., 2023. Amelogenin peptide analyses reveal female leadership in Copper Age Iberia (c. 2900–2650 BC). *Scientific Reports, 13*(1), p.9594.

Clark, J.D., 1942. Further excavations (1939) at Mumbwa Caves, Northern Rhodesia. *Transactions of the Royal Society of South Africa, 29*(3), pp.133-201.

Clark, J.D., 1971. Human behavioral differences in southern Africa during the later Pleistocene. *American Anthropologist, 73*(5), pp.1211-1236.

Clark, J.D. and Brown, K.S., 2001. The Twin Rivers Kopje, Zambia: stratigraphy, fauna, and artefact assemblages from the 1954 and 1956 excavations. *Journal of Archaeological Science, 28*(3), pp.305-330.

Cleland, T.P. and Schroeter, E.R., 2018. A comparison of common mass spectrometry approaches for paleoproteomics. *Journal of proteome research, 17*(3), pp.936-945.

Cleland, T.P., Schroeter, E.R. and Colleary, C., 2021. Diagenetiforms: a new term to explain protein changes as a result of diagenesis in paleoproteomics. *Journal of proteomics, 230*, pp.103992.

Codlin, M.C., Douka, K. and Richter, K.K., 2022. An application of zooms to identify archaeological avian fauna from Teotihuacan, Mexico. *Journal of Archaeological Science, 148*, p.105692.

Collins, M., Buckley, M., Grundy, H.H., Thomas-Oates, J., Wilson, J. and van Doorn, N., 2010. ZooMS: the collagen barcode and fingerprints. *Spectroscopy Europe, 22*, pp.2-2.

Crenshaw, M.A., 1972. The soluble matrix from *Mercenaria mercenaria* shell. *Biomineralisation, 6*, pp.6-11.

Crisp, M., Demarchi, B., Collins, M., Morgan-Williams, M., Pilgrim, E. and Penkman, K., 2013. Isolation of the intra-crystalline proteins and kinetic studies in *Struthio camelus* (ostrich) eggshell for amino acid geochronology. *Quaternary Geochronology, 16*, pp.110-128.

Dart, R.A. and Del Grande, N., 1931. The ancient iron-smelting cavern at Mumbwa. *Transactions of the Royal Society of South Africa, 19*, pp.379-427.

Davies, L.J., Jensen, B.J., Froese, D.G. and Wallace, K.L., 2016. Late Pleistocene and Holocene tephrostratigraphy of interior Alaska and Yukon: Key beds and chronologies over the past 30,000 years. *Quaternary Science Reviews, 146*, pp.28-53.

Day, M.H., 1969. Early *Homo sapiens* remains from the Omo River region of south-west Ethiopia: Omo human skeletal remains. *Nature, 222*(5199), pp.1135-1138.

Degering, D. and Degering, A., 2020. Change is the only constant-time-dependent dose rates in luminescence dating. *Quaternary Geochronology, 58*, p.101074.

Deino, A.L., 2012. 40Ar/39Ar dating of Bed I, Olduvai Gorge, Tanzania, and the chronology of early Pleistocene climate change. *Journal of Human Evolution, 63*(2), pp.251-273.

Demarchi, B., Rogers, K. Fa, D. A., Finlayson, C. J., Milner, N., Penkman, K. E. H., 2013a. Intra-crystalline protein diagenesis (IcPD) in *Patella vulgata*. Part I: Isolation and testing of the closed system. *Quaternary Geochronology, 16*, pp.144-157.

Demarchi, B., Collins, M., Bergström, E., Dowle, A., Penkman, K., Thomas-Oates, J., Wilson, J., 2013b. New experimental evidence for in-chain amino acid racemization of serine in a model peptide. *Analytical Chemistry, 85*(12), pp.5835-5842 236.

Demarchi, B., Clements, E., Coltorti, M., Van De Locht, R., Kröger, R., Penkman, K. and Rose, J., 2015. Testing the effect of bleaching on the bivalve *Glycymeris*: A case study of amino acid geochronology on key Mediterranean raised beach deposits. *Quaternary Geochronology, 25*, pp.49-65.

Demarchi, B., Hall, S., Roncal-Herrero, T., Freeman, C. L., Woolley, J., Crisp, M. K., Wilson, J., Fotakis, A., Fischer, R., Kessler, B. M., Jersie-Christensen, R. R., Olsen, J. V., Haile, J., Thomas, J., Marean, C. W., Parkington, J., Presslee, S., Lee-Thorp, J., Ditchfield, P., Hamilton, J. F., Ward, M. W., Wang, C. M., Shaw, M. D., Harrison, T., Dominguez-Rodrigo, M., Macphee, R. D. E., Kwekason, A., Ecker, M., Horwitz, L. K., Chazan, M., Kroger, R., Thomas-Oates, J., Harding, J. H., Cappellini, E., Penkman, K., Collins, M. J., 2016. Protein sequences bound to mineral surfaces persist into deep time. *elife, 5*, p.e17092.

Demarchi, B., Presslee, S., Sakalauskaite, J., Fischer, R., and Best, J., 2020. The role of birds at Çatalhöyük revealed by the analysis of eggshell. *Quaternary International, 543*, pp.50-60.

Demarchi, B., Mackie, M., Li, Z., Deng, T., Collins, M.J. and Clarke, J., 2022. Survival of mineral-bound peptides into the Miocene. *Elife, 11*, p.e82849.

deMenocal, P.B., Ruddiman, W.F. and Pokras, E.M., 1993. Influences of high-and low-latitude processes on African terrestrial climate: Pleistocene eolian records from equatorial Atlantic Ocean Drilling Program site 663. *Paleoceanography, 8*(2), pp.209-242.

deMenocal, P.B., 1995. Plio-pleistocene African climate. *Science, 270*(5233), pp.53-59.

deMenocal, P., 2004. African climate change and faunal evolution during the Pliocene–Pleistocene. *Earth and Planetary Science Letters*, *220*(1-2), pp.3-24.

Di Roberto, A., Albert, P.G., Colizza, E., Del Carlo, P., Di Vincenzo, G., Gallerani, A., Giglio, F., Kuhn, G., Macrì, P., Manning, C.J. and Melis, R., 2020. Evidence for a large-magnitude Holocene eruption of Mount Rittmann (Antarctica): A volcanological reconstruction using the marine tephra record. *Quaternary Science Reviews, 250*, p.106629.

Dickinson, M.R., Lister, A.M. and Penkman, K.E., 2019. A new method for enamel amino acid racemization dating: a closed system approach. *Quaternary Geochronology, 50*, pp.29-46.

Dierickx, K., Presslee, S., Hagan, R., Oueslati, T., Harland, J., Hendy, J., Orton, D., Alexander, M. and Harvey, V.L., 2022. Peptide mass fingerprinting of preserved collagen in archaeological fish bones for the identification of flatfish in European waters. *Royal Society Open Science*, *9*(7), p.220149.

DiMaggio, E.N., Campisano, C.J., Rowan, J., Dupont-Nivet, G., Deino, A.L., Bibi, F., Lewis, M.E., Souron, A., Garello, D., Werdelin, L. and Reed, K.E., 2015. Late Pliocene fossiliferous sedimentary record and the environmental context of early *Homo* from Afar, Ethiopia. *Science, 347*(6228), pp.1355-1359.

Dobberstein, R.C., Collins, M.J., Craig, O.E., Taylor, G., Penkman, K.E. and Ritz-Timme, S., 2009. Archaeological collagen: Why worry about collagen diagenesis?. *Archaeological and Anthropological Sciences, 1*, pp.31-42.

Douka, K., Jacobs, Z., Lane, C., Grün, R., Farr, L., Hunt, C., Inglis, R.H., Reynolds, T., Albert, P., Aubert, M. and Cullen, V., 2014. The chronostratigraphy of the Haua Fteah cave (Cyrenaica, northeast Libya). *Journal of Human Evolution, 66*, pp.39-63.

Duller, G.A., 2008a. Luminescence Dating: guidelines on using luminescence dating in archaeology.

Duller, G.A., 2008b. Single-grain optical dating of Quaternary sediments: why aliquot size matters in luminescence dating. *Boreas, 37*(4), pp.589-612.

Duller, G.A., Tooth, S., Barham, L. and Tsukamoto, S., 2015. New investigations at Kalambo Falls, Zambia: Luminescence chronology, site formation, and archaeological significance. *Journal of Human Evolution, 85*, pp.111-125.

Duller, G.A. and Roberts, H.M., 2018. Seeing snails in a new light. *Elements: An International Magazine of Mineralogy, Geochemistry, and Petrology, 14*(1), pp.39-43.

Duval, M., Falguères, C., Bahain, J.J., Grün, R., Shao, Q., Aubert, M., Dolo, J.M., Agusti, J., Martinez-Navarro, B., Palmqvist, P. and Toro-Moyano, I., 2012. On the limits of using combined U-series/ESR method to date fossil teeth from two Early Pleistocene archaeological sites of the Orce area (Guadix-Baza basin, Spain). *Quaternary Research, 77*(3), pp.482-491.

Duval, M., 2018. Dating and electron spin resonance (ESR). *The encyclopedia of archaeological sciences*, pp.1-6.

Evans, C.A., 2019. Reducing complexity? Cysteine reduction and S-alkylation in proteomic workflows: Practical considerations. *Mass Spectrometry of Proteins: Methods and Protocols*, pp.83-97.

Fagan, B.M., Van Noten, F.L. and Vynckier, J.R., 1966, December. Wooden Implements from Late Stone Age Sites at Gwisho Hot-springs, Lochinvar, Zambia. In *Proceedings of the Prehistoric Society* (Vol. 32, pp. 246-261). Cambridge University Press.

Feakins, S.J., Eglinton, T.I. and deMenocal, P.B., 2007. A comparison of biomarker records of northeast African vegetation from lacustrine and marine sediments (ca. 3.40 Ma). *Organic Geochemistry, 38*(10), pp.1607-1624.

Fischer, H., Fundel, F., Ruth, U., Twarloh, B., Wegner, A., Udisti, R., Becagli, S., Castellano, E., Morganti, A., Severi, M. and Wolff, E., 2007. Reconstruction of millennial changes in dust emission, transport and

regional sea ice coverage using the deep EPICA ice cores from the Atlantic and Indian Ocean sector of Antarctica. *Earth and Planetary Science Letters, 260*(1-2), pp.340-354.

Fontijn, K., Lachowycz, S.M., Rawson, H., Pyle, D.M., Mather, T.A., Naranjo, J.A. and Moreno-Roa, H., 2014. Late Quaternary tephrostratigraphy of southern Chile and Argentina. *Quaternary Science Reviews, 89*, pp.70-84.

Forman, S.L., Hockaday, W., Liang, P. and Ramsey, A., 2021. Radiocarbon age offsets, ontogenetic effects, and potential old carbon contributions from soil organic matter for pre-bomb and modern detritivorous gastropods from central Texas, USA. *Palaeogeography, Palaeoclimatology, Palaeoecology, 583*, p.110671.

Frank, H., Woiwode, W., Nicholson, G. and Bayer, E., 1981. Determination of the rate of acidic catalyzed racemization of protein amino acids. *Liebigs Annalen der Chemie, 1981*(3), pp.354-365.

Frenzel, P. and Boomer, I., 2005. The use of ostracods from marginal marine, brackish waters as bioindicators of modern and Quaternary environmental change. *Palaeogeography, Palaeoclimatology, Palaeoecology, 225*(1-4), pp.68-92.

Friedman, M., Liardon, R., 1985. Racemization kinetics of amino acid residues in alkali-treated soybean proteins. *Journal of Agricultural and Food Chemistry, 33*(4), pp.666-672.

Frýda, J., Nützel, A. and Wagner, P.J., 2008. Paleozoic gastropoda. *Phylogeny and Evolution of the Mollusca*, pp.239-270.

Fuchs, S.A., Berger, R., Klomp, L.W. and De Koning, T.J., 2005. D-amino acids in the central nervous system in health and disease. *Molecular genetics and metabolism, 85*(3), pp.168-180.

Gibbard, P.L., Head, M.J., Walker, M.J., 2010. Formal ratification of the Quaternary System/Period and the Pleistocene Series/Epoch with a base at 2.58 Ma. *Journal of Quaternary Science, 25*(2), pp.96-102.

Gil-Bona, A. and Bidlack, F.B., 2020. Tooth enamel and its dynamic protein matrix. *International Journal of Molecular Sciences, 21*(12), p.4458.

Geng, L., Alexander, B., Cole-Dai, J., Steig, E.J., Savarino, J., Sofen, E.D. and Schauer, A.J., 2014. Nitrogen isotopes in ice core nitrate linked to anthropogenic atmospheric acidity change. *Proceedings of the National Academy of Sciences, 111*(16), pp.5808-5812.

Genchi, G., 2017. An overview on D-amino acids. *Amino acids, 49*, pp.1521-1533.

Gilbert, C., Krupicka, V., Galluzzi, F., Popowich, A., Bathany, K., Claverol, S., Arslanoglu, J. and Tokarski, C., 2024. Species identification of ivory and bone museum objects using minimally invasive proteomics. *Science Advances*, *10*(4), p.eadi9028.

Godwin, H., 1962. Half-life of radiocarbon. *Nature, 195*(4845), pp.984-984.

Gong, Y., Li, L., Gong, D., Yin, H. and Zhang, J., 2016. Biomolecular evidence of silk from 8,500 years ago. *PLoS One*, *11*(12), pp.e0168042.

Goodfriend, G.A. and Stipp, J.J., 1983. Limestone and the problem of radiocarbon dating of land-snail shell carbonate. *Geology, 11*(10), pp.575-577.

Gross, B.H., Kreutz, K.J., Osterberg, E.C., McConnell, J.R., Handley, M., Wake, C.P. and Yalcin, K., 2012. Constraining recent lead pollution sources in the North Pacific using ice core stable lead isotopes. *Journal of Geophysical Research: Atmospheres, 117*(D16).

Grün, R., Aubert, M., Hellstrom, J. and Duval, M., 2010. The challenge of direct dating old human fossils. *Quaternary International, 223*, pp.87-93.

Grün, R., Pike, A., McDermott, F., Eggins, S., Mortimer, G., Aubert, M., Kinsley, L., Joannes-Boyau, R., Rumsey, M., Denys, C. and Brink, J., 2020. Dating the skull from Broken Hill, Zambia, and its position in human evolution. *Nature, 580*(7803), pp.372-375.

Guillou, H., Nomade, S. and Scao, V., 2021. The ^{40}K/^{40}Ar and ^{40}Ar/^{39}Ar Methods. *Paleoclimatology*, pp.73-87.

Hare, P.E., 1974. Amino acid dating of bone - the influence of water. *Carnegie Institute of Washington Year Book*, 73, pp.576-81.

Hare, P.E., Abelson, P.H., 1967. Racemisation of amino acids in fossil shells. *Carnegie Institute of Washington Year Book, 66*, pp.526-528.

Hare, P.E., Mitterer, R.M. 1969. Laboratory simulation of amino acid diagenesis in fossils. *Carnegie Institute Washington Year Book, 67*, pp.205-208.

He, L.H. and Swain, M.V., 2008. Understanding the mechanical behaviour of human enamel from its structural and compositional characteristics. *Journal of the mechanical behavior of biomedical materials*, *1*(1), pp.18-29.

Hendy, E.J., Tomiak, P.J., Collins, M.J., Hellstrom, J., Tudhope, A.W., Lough, J.M. and Penkman, K.E., 2012. Assessing amino acid racemization variability in coral intra-crystalline protein for geochronological applications. *Geochimica et Cosmochimica* Acta, 86, pp.338-353.

Hendy, J., Warinner, C., Bouwman, A., Collins, M.J., Fiddyment, S., Fischer, R., Hagan, R., Hofman, C.A., Holst, M., Chaves, E. and Klaus, L., 2018a. Proteomic evidence of dietary sources in ancient dental calculus. *Proceedings of the Royal Society B: Biological Sciences*, *285*(1883), pp.20180977.

Hendy, J., Colonese, A.C., Franz, I., Fernandes, R., Fischer, R., Orton, D., Lucquin, A., Spindler, L., Anvari, J., Stroud, E. and Biehl, P.F., 2018b. Ancient proteins from ceramic vessels at Çatalhöyük West reveal the hidden cuisine of early farmers. *Nature communications*, *9*(1), pp.4064.

Hendy, J., Welker, F., Demarchi, B., Speller, C., Warinner, C. and Collins, M.J., 2018c. A guide to ancient protein studies. *Nature ecology & evolution, 2*(5), 791-799.

Herries, A.I. and Shaw, J., 2011. Palaeomagnetic analysis of the Sterkfontein palaeocave deposits: Implications for the age of the hominin fossils and stone tool industries. *Journal of human evolution, 60*(5), pp.523-539.

Hill, R.L., 1965. Hydrolysis of proteins. *Advances in Protein Chemistry*, *20*, pp.37-107.

Hoetzel, S., Dupont, L.M. and Wefer, G., 2015. Miocene–Pliocene vegetation change in south-western Africa (ODP Site 1081, offshore Namibia). *Palaeogeography, Palaeoclimatology, Palaeoecology, 423*, pp.102-108.

Hou, S., Zhang, W., Pang, H., Wu, S.Y., Jenk, T.M., Schwikowski, M. and Wang, Y., 2019. Apparent discrepancy of Tibetan ice core $\delta^{18}O$ records may be attributed to misinterpretation of chronology. *The Cryosphere, 13*(6), pp.1743-1752.

Hublin, J.J., Ben-Ncer, A., Bailey, S.E., Freidline, S.E., Neubauer, S., Skinner, M.M., Bergmann, I., Le Cabec, A., Benazzi, S., Harvati, K. and Gunz, P., 2017. New fossils from Jebel Irhoud, Morocco and the pan-African origin of *Homo sapiens*. *Nature, 546*(7657), pp.289-292.

Hughes, P.D. and Gibbard, P.L., 2018. Global glacier dynamics during 100 ka Pleistocene glacial cycles. *Quaternary Research, 90*(1), pp.222-243.

Huntley, D.J., Godfrey-Smith, D.I. and Thewalt, M.L., 1985. Optical dating of sediments. *Nature, 313*(5998), pp.105-107.

Ikeya, M. and Ohmura, K., 1983. Comparison of ESR ages of corals from marine terraces with ^{14}C and [230]Th/[234]U ages. *Earth and Planetary Science Letters, 65*(1), pp.34-38.

Imbrie, J., Hays, J.D., Martinson, D.G., McIntyre, A., Mix, A.C., Morley, J.J., Pisias, N.G., Prell, W.L. and Shackleton, N.J., 1984. The orbital theory of Pleistocene climate: support from a revised chronology of the marine d^{18}O record.

Jackson, M.S., Kelly, M.A., Russell, J.M., Doughty, A.M., Howley, J.A., Zimmerman, S.R. and Nakileza, B., 2020. Holocene glaciation in the Rwenzori Mountains, Uganda. *Climate of the past Discussions, 2020*, pp.1-38.

Janzen, A., Richter, K.K., Mwebi, O., Brown, S., Onduso, V., Gatwiri, F., Ndiema, E., Katongo, M., Goldstein, S.T., Douka, K. and Boivin, N., 2021. Distinguishing African bovids using Zooarchaeology by Mass Spectrometry (ZooMS): New peptide markers and insights into Iron Age economies in Zambia. *PLoS One*, *16*(5), p.e0251061.

Johanson, D.C., Lovejoy, C.O., Kimbel, W.H., White, T.D., Ward, S.C., Bush, M.E., Latimer, B.M. and Coppens, Y., 1982. Morphology of the Pliocene partial hominid skeleton (AL 288-1) from the Hadar formation, Ethiopia. *American Journal of Physical Anthropology*, *57*(4), pp.403-451.

Johanson, D.C., Masao, F.T., Eck, G.G., White, T.D., Walter, R.C., Kimbel, W.H., Asfaw, B., Manega, P., Ndessokia, P. and Suwa, G., 1987. New partial skeleton of *Homo habilis* from Olduvai Gorge, Tanzania. *Nature, 327*(6119), pp.205-209.

Johnson, T.C., Werne, J.P., Brown, E.T., Abbott, A., Berke, M., Steinman, B.A., Halbur, J., Contreras, S., Grosshuesch, S., Deino, A. and Scholz, C.A., 2016. A progressively wetter climate in southern East Africa over the past 1.3 million years. *Nature, 537*(7619), pp.220-224.

Kaufman, D.S., 2006. Temperature sensitivity of aspartic and glutamic acid racemization in the foraminifera *Pulleniatina*. *Quaternary Geochronology, 1*(3), pp.188-207.

Kaufman, D. S. and Manley, W. F., 1998. A new procedure for determining DL amino acid ratios in fossils using reverse phase liquid chromatography. *Quaternary Science Reviews, 17*(11), pp.987-1000.

Kaufman, D.S. and Sejrup, H.P., 1995. Isoleucine epimerization in the high-molecular-weight fraction of Pleistocene Arctica. *Quaternary Science Reviews, 14*(4), pp.337-350.

Kelley, S., 2002. K-Ar and Ar-Ar dating. *Reviews in Mineralogy and Geochemistry, 47*(1), pp.785-818.

Kimber, R.W.L. and Griffin, C.V., 1987. Further evidence of the complexity of the racemization process in fossil shells with implications for amino acid racemization dating. *Geochimica et Cosmochimica Acta, 51*(4), pp.839-846.

Kjær, K.H., Winther Pedersen, M., De Sanctis, B., De Cahsan, B., Korneliussen, T.S., Michelsen, C.S., Sand, K.K., Jelavić, S., Ruter, A.H., Schmidt, A.M. and Kjeldsen, K.K., 2022. A 2-million-year-old ecosystem in Greenland uncovered by environmental DNA. *Nature, 612*(7939), pp.283-291.

Kossert, K., Amelin, Y., Arnold, D., Merle, R., Mougeot, X., Schmiedel, M. and Zapata-García, D., 2022. Activity standardization of two enriched ^{40}K solutions for the determination of decay scheme parameters and the half-life. *Applied Radiation and Isotopes, 188*, p.110362.

Koweek, D.A., Forden, A., Albright, R., Takeshita, Y., Mucciarone, D.A., Ninokawa, A. and Caldeira, K., 2019. Carbon isotopic fractionation in organic matter production consistent with benthic community composition across a coral reef flat. *Frontiers in Marine Science, 5,* p.520.

Kusch, S., Mollenhauer, G., Willmes, C., Hefter, J., Eglinton, T.I. and Galy, V., 2021. Controls on the age of plant waxes in marine sediments–A global synthesis. *Organic Geochemistry*, *157*, p.104259.

Kvenvolden, K.A., Peterson, E., Wehmiller, J. and Hare, P.E., 1973. Racemization of amino acids in marine sediments determined by gas chromatography. *Geochimica et Cosmochimica Acta, 37*(10), pp.2215-2225.

Lacruz, R.S., Habelitz, S., Wright, J.T. and Paine, M.L., 2017. Dental enamel formation and implications for oral health and disease. *Physiological reviews, 97*(3), pp.939-993.

Lane, C.S., Blockley, S.P., Mangerud, J.A.N., Smith, V.C., Lohne, Ø.S., Tomlinson, E.L., Matthews, I.P. and Lotter, A.F., 2012. Was the 12.1 ka Icelandic Vedde Ash one of a kind?. *Quaternary Science Reviews, 33*, pp.87-99.

Lane, C.S., Lowe, D.J., Blockley, S.P., Suzuki, T. and Smith, V.C., 2017. Advancing tephrochronology as a global dating tool: applications in volcanology, archaeology, and palaeoclimatic research. *Quaternary Geochronology, 40*, pp.1-7.

Lambert, F., Delmonte, B., Petit, J.R., Bigler, M., Kaufmann, P.R., Hutterli, M.A., Stocker, T.F., Ruth, U., Steffensen, J.P. and Maggi, V., 2008. Dust-climate couplings over the past 800,000 years from the EPICA Dome C ice core. *Nature, 452*(7187), pp.616-619.

Leakey, L.S., Tobias, P.V. and Napier, J.R., 1964. A new species of the genus *Homo* from Olduvai Gorge. *Nature, 202*(4927), pp.7-9.

Leakey, M.D., 1981. Tracks and tools. *Philosophical Transactions of the Royal Society of London. B, Biological Sciences, 292*(1057), pp.95-102.

Leakey, M.D. and Hay, R.L., 1979. Pliocene footprints in the Laetolil Beds at Laetoli, northern Tanzania. *Nature, 278*(5702), pp.317-323.

Lepre, C.J. and Kent, D.V., 2015. Chronostratigraphy of KNM-ER 3733 and other Area 104 hominins from Koobi Fora. *Journal of Human Evolution*, *86*, pp.99-111.

Liardon, R., Ledermann, S., 1986. Racemization kinetics of free and protein-bound amino acids under moderate alkaline treatment. *Journal of Agricultural and Food Chemistry, 34*(3), pp.557–565.

Lodi, M. and Koene, J.M., 2016. The love-darts of land snails: integrating physiology, morphology and behaviour. *Journal of Molluscan Studies*, *82*(1), pp.1-10.

Lowe, D.J., 2011. Tephrochronology and its application: a review. *Quaternary Geochronology, 6*(2), pp.107-153.

Lugli, F., Di Rocco, G., Vazzana, A., Genovese, F., Pinetti, D., Cilli, E., Carile, M.C., Silvestrini, S., Gabanini, G., Arrighi, S. and Buti, L., 2019. Enamel peptides reveal the sex of the Late Antique 'Lovers of Modena'. *Scientific reports*, *9*(1), pp.13130.

Madupe, P.P., Koenig, C., Patramanis, I., Rüther, P.L., Hlazo, N., Mackie, M., Tawane, M., Krueger, J., Taurozzi, A.J., Troché, G.B. and Kibii, J., 2023. Enamel proteins reveal biological sex and genetic variability within southern African *Paranthropus. bioRxiv*, pp.2023-3007.

Malaquias, M.A.E. and Cervera, J.L., 2006. The genus Haminoea (Gastropoda: Cephalaspidea) in Portugal, with a review of the European species. *Journal of Molluscan Studies*, *72*(1), pp.89-103.

Maslin, M.A., Shultz, S. and Trauth, M.H., 2015. A synthesis of the theories and concepts of early human evolution. *Philosophical Transactions of the Royal Society B: Biological Sciences, 370*(1663), p.20140064.

Matsuo, H., Kawazoe, Y., Sato, M., Ohnishi, M. & Tatsuno, T., 1967. Studies on racemization of amino acids and their derivatives 1. On Deuterium-Hydrogen exchange reaction of amino acids derivatives in basic media. *Chemical & Pharmaceutical Bulletin. 15*(4), pp.391-398.

Maixner, F., Overath, T., Linke, D., Janko, M., Guerriero, G., van den Berg, B.H., Stade, B., Leidinger, P., Backes, C., Jaremek, M. and Kneissl, B., 2013. Paleoproteomic study of the Iceman's brain tissue. *Cellular and Molecular Life Sciences, 70*, pp.3709-3722.

McDougall, C. and Degnan, B.M., 2018. The evolution of mollusc shells. *Wiley interdisciplinary reviews: developmental biology, 7*(3), p.e313.

McLaren, S.J. and Rowe, P.J., 1996. The reliability of uranium-series mollusc dates from the western Mediterranean basin. *Quaternary Science Reviews, 15*(7), pp.709-717.

McLean, D., Albert, P.G., Nakagawa, T., Suzuki, T., Staff, R.A., Yamada, K., Kitaba, I., Haraguchi, T., Kitagawa, J., Members, S.P. and Smith, V.C., 2018. Integrating the Holocene tephrostratigraphy for East Asia using a high-resolution cryptotephra study from Lake Suigetsu (SG14 core), central Japan. *Quaternary Science Reviews, 183*, pp.36-58.

Miller, G.H. and Brigham-Grette, J., 1989. Amino acid geochronology: resolution and precision in carbonate fossils. *Quaternary International, 1*, pp.111-128.

Mitterer, R.M. and Kriausakul, N., 1984. Comparison of rates and degrees of isoleucine epimerization in dipeptides and tripeptides. *Organic Geochemistry, 7*(1), pp.91-98.

Miller, G.H., Beaumont, P.B., Deacon, H.J., Brooks, A.S., Hare, P.E. and Jull, A.J.T., 1999. Earliest modern humans in southern Africa dated by isoleucine epimerization in ostrich eggshell. *Quaternary Science Reviews, 18*(13), pp.1537-1548.

Moore, A.E., Cotterill, F.P., Winterbach, C.W., Winterbach, H.E., Antunes, A. and O'Brien, S.J., 2016. Genetic evidence for contrasting wetland and savannah habitat specializations in different populations of lions (*Panthera leo*). *Journal of Heredity, 107*(2), pp.101-103.

Neuberger, A., 1948. Stereochemistry of amino acids. *Advances in Protein Chemistry 4*, pp.297-383.

New, E., Yanes, Y., Cameron, R.A., Miller, J.H., Teixeira, D. and Kaufman, D.S., 2019. Aminochronology and time averaging of Quaternary land snail assemblages from colluvial deposits in the Madeira Archipelago, Portugal. *Quaternary Research, 92*(2), pp.483-496.

Nudelman, F. and Sommerdijk, N.A., 2012. Biomineralization as an inspiration for materials chemistry. *Angewandte Chemie International Edition*, *51*(27), pp.6582-6596.

Olson, E.A., 1963. *The problem of sample contamination in radiocarbon dating*. Columbia University.

Orem, C.A. and Kaufman, D.S., 2011. Effects of basic pH on amino acid racemization and leaching in freshwater mollusk shell. *Quaternary Geochronology, 6*(2), pp.233-245.

Ortiz, J.E., Torres, T., Yanes, Y., Castillo, C., Nuez, J.D.L., Ibáñez, M. and Alonso, M.R., 2006. Climatic cycles inferred from the aminostratigraphy and aminochronology of Quaternary dunes and palaeosols from the eastern islands of the Canary Archipelago. *Journal of Quaternary Science: Published for the Quaternary Research Association, 21*(3), pp.287-306.

Ortiz, J.E., Sánchez-Palencia, Y., Gutiérrez-Zugasti, I., Torres, T. and González-Morales, M., 2018. Protein diagenesis in archaeological gastropod shells and the suitability of this material for amino acid racemisation dating: *Phorcus lineatus* (da Costa, 1778). *Quaternary Geochronology, 46*, pp.16-27.

Ortiz, J.E., Torres, T. and Pérez-González, A., 2013. Amino acid racemization in four species of ostracodes: taxonomic, environmental, and microstructural controls. *Quaternary Geochronology, 16*, pp.129-143.

Ortiz, J.E., Torres, T., Sánchez-Palencia, Y. and Ferrer, M., 2017. Inter-and intra-crystalline protein diagenesis in Glycymeris shells: Implications for amino acid geochronology. *Quaternary Geochronology, 41*, pp.37-50.

Ostrom, P.H., Schall, M., Gandhi, H., Shen, T.L., Hauschka, P.V., Strahler, J.R. and Gage, D.A., 2000. New strategies for characterizing ancient proteins using matrix-assisted laser desorption ionization mass spectrometry. *Geochimica et Cosmochimica Acta, 64*(6), pp.1043-1050.

Pan, B., Ricci, M. S., Trout, B. L., 2011. A Molecular Mechanism of Hydrolysis of Peptide Bonds at Neutral pH Using a Model Compound. *The Journal of Physical Chemistry B, 115*(19), pp.5958-5970.

Parker, G.J., McKiernan, H.E., Legg, K.M. and Goecker, Z.C., 2021. Forensic proteomics. *Forensic Science International: Genetics, 54*, p.102529.

Payne, R. and Gehrels, M., 2010. The formation of tephra layers in peatlands: an experimental approach. *Catena, 81*(1), pp.12-23.

Pedersen, C.E.T., Albrechtsen, A., Etter, P.D., Johnson, E.A., Orlando, L., Chikhi, L., Siegismund, H.R. and Heller, R., 2018. A southern African origin and cryptic structure in the highly mobile plains zebra. *Nature Ecology & Evolution, 2*(3), pp.491-498.

Penkman, K.E.H., 2005. Amino acid geochronology: a closed system approach to test and refine the UK model. PhD thesis, University of Newcastle.

Penkman, K. E. H., Kaufman, D. S., Maddy, D., Collins, M. J., 2008. Closed-system behaviour of the intra-crystalline fraction of amino acids in mollusc shells. *Quaternary Geochronology, 31*(2), pp.2-25.

Penkman, K. E. H., 2010. Amino acid geochronology: Its impact on our understanding of the Quaternary stratigraphy of the British Isles. *Journal of Quaternary Science 25*(4), pp.501-514.

Penkman, K.E., Preece, R.C., Bridgland, D.R., Keen, D.H., Meijer, T., Parfitt, S.A., White, T.S. and Collins, M.J., 2013. An aminostratigraphy for the British Quaternary based on *Bithynia* opercula. *Quaternary Science Reviews, 61*, pp.111-134.

Philippsen, B., 2013. The freshwater reservoir effect in radiocarbon dating. *Heritage Science, 1*, pp.1-19.

Phillips, D., Matchan, E.L., Gleadow, A.J., H. Brown, F., A. McDougall, I., Cerling, T.E., G. Leakey, M., Hergt, J.M. and Leakey, L.N., 2023. $^{40}Ar/^{39}Ar$ eruption ages of Turkana Basin tuffs: millennial-scale resolution constrains palaeoclimate proxy tuning models and hominin fossil ages. *Journal of the Geological Society, 180*(4), pp.jgs2022-171.

Pike, A.W.G. and Hedges, R.E.M., 2002. U-series dating of bone using the diffusion-adsorption model. *Geochimica et Cosmochimica Acta, 66*(24), pp.4273-4286.

Popov, D.V., Spikings, R.A., Scaillet, S., O'Sullivan, G., Chew, D., Badenszki, E., Daly, J.S., Razakamanana, T. and Davies, J.H., 2020. Diffusion and fluid interaction in Itrongay pegmatite (Madagascar): Evidence from in situ $^{40}Ar/^{39}Ar$ dating of gem-quality alkali feldspar and UPb dating of protogenetic apatite inclusions. *Chemical Geology, 556*, p.119841.

Potts, R., 2012. Evolution and environmental change in early human prehistory. *Annual Review of Anthropology, 41*, pp.151-167.

Presslee, S., Wilson, J., Woolley, J., Best, J., Russell, D., Radini, A., Fischer, R., Kessler, B., Boano, R., Collins, M. and Demarchi, B., 2017. The identification of archaeological eggshell using peptide markers. *STAR: Science & Technology of Archaeological Research, 3*(1), pp.89-99.

Presslee, S., Slater, G.J., Pujos, F., Forasiepi, A.M., Fischer, R., Molloy, K., Mackie, M., Olsen, J.V., Kramarz, A., Taglioretti, M. and Scaglia, F., 2019. Palaeoproteomics resolves sloth relationships. *Nature Ecology & Evolution*, *3*(7), pp.1121-1130.

Presslee, S., Penkman, K., Fischer, R., Richards-Slidel, E., Southon, J., Hospitaleche, C.A., Collins, M. and MacPhee, R., 2021. Assessment of different screening methods for selecting palaeontological bone samples for peptide sequencing. *Journal of proteomics, 230*, p.103986.

Ramsøe, A., van Heekeren, V., Ponce, P., Fischer, R., Barnes, I., Speller, C. and Collins, M.J., 2020. DeamiDATE 1.0: Site-specific deamidation as a tool to assess authenticity of members of ancient proteomes. *Journal of archaeological science, 115*, pp.105080.

Raynaud, D., Jouzel, J., Barnola, J.M., Chappellaz, J., Delmas, R.J. and Lorius, C., 1993. The ice record of greenhouse gases. *Science, 259*(5097), pp.926-934.

Reimer, P.J., Austin, W.E., Bard, E., Bayliss, A., Blackwell, P.G., Ramsey, C.B., Butzin, M., Cheng, H., Edwards, R.L., Friedrich, M. and Grootes, P.M., 2020. The IntCal20 Northern Hemisphere radiocarbon age calibration curve (0–55 cal kBP). *Radiocarbon, 62*(4), pp.725-757.

Richter, D., Grün, R., Joannes-Boyau, R., Steele, T.E., Amani, F., Rué, M., Fernandes, P., Raynal, J.P., Geraads, D., Ben-Ncer, A. and Hublin, J.J., 2017. The age of the hominin fossils from Jebel Irhoud, Morocco, and the origins of the Middle Stone Age. *Nature, 546*(7657), pp.293-296.

Rittenour, T.M., 2008. Luminescence dating of fluvial deposits: applications to geomorphic, palaeoseismic and archaeological research. *Boreas, 37*(4), pp.613-635.

Rink, W.J., 1997. Electron spin resonance (ESR) dating and ESR applications in Quaternary science and archaeometry. *Radiation measurements, 27*(5-6), pp.975-1025.

Roberts, D.L., Bateman, M.D., Murray-Wallace, C.V., Carr, A.S. and Holmes, P.J., 2008. Last interglacial fossil elephant trackways dated by OSL/AAR in coastal aeolianites, Still Bay, South Africa. *Palaeogeography, Palaeoclimatology, Palaeoecology, 257*(3), pp.261-279.

Robinson, N.E. and Robinson, A., 2004. *Molecular clocks: deamidation of asparaginyl and glutaminyl residues in peptides and proteins*. Althouse press.

Rowson, B., Law, M., Miller, J., White, T., Shipton, C., Crowther, A., Ndiema, E., Petraglia, M. and Boivin, N.L., 2024. A Quaternary sequence of terrestrial molluscs from East Africa: a record of diversity, stability, and abundance since Marine Isotope Stage 5 (78,000 BP). *Archiv für Molluskenkunde, 153*(1), pp.61-86.

Rubin, M., Likins, R.C. and Berry, E.G., 1963. On the validity of radiocarbon dates from snail shells. *The Journal of Geology, 71*(1), pp.84-89.

Rubino, M., Etheridge, D.M., Thornton, D.P., Howden, R., Allison, C.E., Francey, R.J., Langenfelds, R.L., Steele, L.P., Trudinger, C.M., Spencer, D.A. and Curran, M.A., 2019. Revised records of atmospheric trace gases CO_2, CH_4, N_2O and $\delta^{13}C$-CO_2 over the last 2000 years from Law Dome, Antarctica. *Earth System Science Data, 2019, 11*(2), pp.473-492.

Runge, A.K.W., Hendy, J., Richter, K.K., Masson-MacLean, E., Britton, K., Mackie, M., McGrath, K., Collins, M., Cappellini, E. and Speller, C., 2021. Palaeoproteomic analyses of dog palaeofaeces reveal a preserved dietary and host digestive proteome. *Proceedings of the Royal Society B*, *288*(1954), pp.20210020.

Sakalauskaite, J., Marin, F., Pergolizzi, B. and Demarchi, B., 2020. Shell palaeoproteomics: First application of peptide mass fingerprinting for the rapid identification of mollusc shells in archaeology. *Journal of Proteomics*, *227*, pp.103920.

Saitta, E.T., Vinther, J., Crisp, M.K., Abbott, G.D., Wheeler, L., Presslee, S., Kaye, T.G., Bull, I., Fletcher, I., Chen, X. and Vidal, D., 2024. Non-avian dinosaur eggshell calcite can contain ancient, endogenous amino acids. *Geochimica et Cosmochimica Acta, 365*, pp.1-20.

Sambridge, M., Grün, R. and Eggins, S., 2012. U-series dating of bone in an open system: the diffusion-adsorption-decay model. *Quaternary Geochronology, 9*, pp.42-53.

Scerri, E.M., Chikhi, L. and Thomas, M.G., 2019. Beyond multiregional and simple out-of-Africa models of human evolution. *Nature ecology & evolution, 3*(10), pp.1370-1372.

Schön, I., Verheyen, E. and Martens, K., 2000. Speciation in ancient lake ostracods: comparative analysis of Baikalian *Cytherissa* and Tanganyikan *Cyprideis*. *Internationale Vereinigung für theoretische und angewandte Limnologie: Verhandlungen*, *27*(5), pp.2674-2677.

Schroeder, R.A. and Bada, J.L., 1977. Kinetics and mechanism of the epimerization and decomposition of threonine in fossil foraminifera. *Geochimica et Cosmochimica Acta, 41*(8), pp.1087-1095.

Schulz, G.E. and Schirmer, R.H., 2013. *Principles of protein structure*. Springer Science & Business Media.

Schwarcz, H.P., Grün, R. and Tobias, P.V., 1994. ESR dating studies of the australopithecine site of Sterkfontein, South Africa. *Journal of Human Evolution, 26*(3), pp.175-181.

Shackleton, N., 1967. Oxygen isotope analyses and Pleistocene temperatures re-assessed. *Nature, 215*(5096), pp.15-17.

Shackleton, N.J. and Opdyke, N.D., 1973. Oxygen isotope and palaeomagnetic stratigraphy of Equatorial Pacific core V28-238: Oxygen isotope temperatures and ice volumes on a 105 year and 106 year scale. *Quaternary research, 3*(1), pp.39-55.

Shackleton, N.J. and Opdyke, N.D., 1976. Oxygen-isotope and paleomagnetic stratigraphy of Pacific core V28-239 late Pliocene to latest Pleistocene. *Memoir of the Geological Society of America, 145*, pp.449-464.

Shackleton, N.J., Berger, A. and Peltier, W.R., 1990. An alternative astronomical calibration of the lower Pleistocene timescale based on ODP Site 677. *Earth and environmental science transactions of the royal society of Edinburgh, 81*(4), pp.251-261.

Shackleton, N.J., 2006. Formal Quaternary stratigraphy—What do we expect and need?. *Quaternary Science Reviews, 25*(23-24), pp.3458-3462.

Shin, N.Y., Yamazaki, H., Beniash, E., Yang, X., Margolis, S.S., Pugach, M.K., Simmer, J.P. and Margolis, H.C., 2020. Amelogenin phosphorylation regulates tooth enamel formation by stabilizing a transient amorphous mineral precursor. *Journal of Biological Chemistry, 295*(7), pp.1943-1959.

Shuken, S.R., 2023. An introduction to mass spectrometry-based proteomics. *Journal of Proteome Research, 22*(7), pp.2151-2171.

Simmer, J.P. and Fincham, A.G., 1995. Molecular mechanisms of dental enamel formation. *Critical Reviews in Oral Biology & Medicine*, *6*(2), pp.84-108.

Simms, M.J. and Davies, P., 2000. Appendix 7. Preliminary report on the sediments and molluscs of Lake Patrick. In: Barham LS (Ed.) *The Middle Stone Age of Zambia, South Central Africa*. Western Academic & Specialist Press. pp.275 – 280.

Simpson, S.W., 2013. Before Australopithecus: the earliest hominins. *A companion to paleoanthropology*, pp.417-433.

Skinner, A.R., 2011. Current topics in ESR dating. *Radiation measurements, 46*(9), pp.749-753.

Smith, G.G., Evans, R.C., 1980. The effect of structure and conditions on the rate of racemisation of free and bound amino acids. *Biogeochemistry of Amino Acids*, pp.257-282.

Smith, G.G. and Reddy, G.V., 1989. Effect of the side chain on the racemization of amino acids in aqueous solution. *The Journal of Organic Chemistry, 54*(19), pp.4529-4535.

Smith, C.E. and Warshawsky, H., 1977. Quantitative analysis of cell turnover in the enamel organ of the rat incisor. Evidence for ameloblast death immediately after enamel matrix secretion. *The Anatomical Record*, *187*(1), pp.63-97.

Smith, G.G., Williams, K.M. and Wonnacott, D.M., 1978. Factors affecting the rate of racemization of amino acids and their significance to geochronology. *The Journal of Organic Chemistry, 43*(1), pp.1-5.

Solazzo, C., Dyer, J.M., Clerens, S., Plowman, J., Peacock, E.E. and Collins, M.J., 2013a. Proteomic evaluation of the biodegradation of wool fabrics in experimental burials. *International Biodeterioration & Biodegradation*, *80*, pp.48-59.

Solazzo, C., Fitzhugh, W.W., Rolando, C. and Tokarski, C., 2008. Identification of protein remains in archaeological potsherds by proteomics. *Analytical Chemistry*, *80*(12), pp.4590-4597.

Solazzo, C., Wadsley, M., Dyer, J.M., Clerens, S., Collins, M.J. and Plowman, J., 2013b. Characterisation of novel α-Keratin peptide markers for species identification in keratinous tissues using mass spectrometry. *Rapid Communications in Mass Spectrometry, 27*(23), pp.2685-2698.

Spötl, C. and Boch, R., 2019. Uranium series dating of speleothems. In *Encyclopedia of caves* (pp. 1096-1102). Academic Press.

Steinberg, S. and Bada, J.L., 1981. Diketopiperazine formation during investigations of amino acid racemization in dipeptides. *Science, 213*(4507), pp.544-545.

Stephenson, R.C., Clarke, S., 1989. Succinimide formation from aspartyl and asparaginyl peptides as a model for the spontaneous degradation of proteins. *The Journal of Biological Chemistry, 264*(11), pp.6164–70.

Sternberg, R.S., 1997. Archaeomagnetic dating. In *Chronometric dating in archaeology* (pp. 323-356). Boston, MA: Springer US.

Still, C. and Rastogi, B., 2017. What drives carbon isotope fractionation by the terrestrial biosphere?. Journal of Geophysical Research: *Biogeosciences, 122*(11), pp.3108-3110.

Stringer, C., 2022. The development of ideas about a recent African origin for *Homo sapiens*. *Journal of Anthropological Sciences= Rivista di Antropologia: JASS, 100*.

Suttapitugsakul, S., Xiao, H., Smeekens, J. and Wu, R., 2017. Evaluation and optimization of reduction and alkylation methods to maximize peptide identification with MS-based proteomics. *Molecular BioSystems*, *13*(12), pp.2574-2582.

Sykes, G.A., Collins, M.J. and Walton, D.I., 1995. The significance of a geochemically isolated intracrystalline organic fraction within biominerals. *Organic Geochemistry, 23*(11-12), pp.1059-1065.

Tarling, D.H., 1975. Archaeomagnetism: the dating of archaeological materials by their magnetic properties. *World archaeology, 7*(2), pp.185-197.

Taurozzi, A.J., Rüther, P.L., Patramanis, I., Koenig, C., Sinclair Paterson, R., Madupe, P.P., Harking, F.S., Welker, F., Mackie, M., Ramos-Madrigal, J. and Olsen, J.V., 2024. Deep-time phylogenetic inference by paleoproteomic analysis of dental enamel. *Nature Protocols*, pp.1-32.

Thompson, L.G. and Hastenrath, S., 1981. Climatic ice core studies at Lewis Glacier, Mount Kenya. Z. Gletscherkd. *Glazialgeol, 17*(1), pp.115-123.

Thompson, L.G., Mosley-Thompson, E., Davis, M.E., Henderson, K.A., Brecher, H.H., Zagorodnov, V.S., Mashiotta, T.A., Lin, P.N., Mikhalenko, V.N., Hardy, D.R. and Beer, J., 2002. Kilimanjaro ice core records: evidence of Holocene climate change in tropical Africa. *Science, 298*(5593), pp.589-593.

Tierney, J.E., deMenocal, P.B. and Zander, P.D., 2017. A climatic context for the out-of-Africa migration. *Geology, 45*(11), pp.1023-1026.

Tomiak, P. J., Penkman, K. E H., Hendy, E. J., Demarchi, B., Murrells, S., Davis, S., McCullagh, P., Collins, M. J. 2013. Testing the limitations of artificial protein degradation kinetics using known-age massive *Porites* coral skeletons. *Quaternary Geochronology, 16*, pp.87-109.

Towe, K.M., 1980. Preserved organic ultrastructure: an unreliable indicator for Paleozoic amino acid biogeochemistry. *Biogeochemistry of Amino Acids*, pp.65-74.

Towe, K.M. and Thompson, G.R., 1972. The structure of some bivalve shell carbonates prepared by ion-beam thinning: A Comparison Study. *Calcified tissue research, 10*, pp.38-48.

Tripković, T., Charvy, C., Alves, S., Lolić, A.Đ., Baošić, R.M., Nikolić-Mandić, S.D. and Tabet, J.C., 2013. Identification of protein binders in artworks by MALDI-TOF/TOF tandem mass spectrometry. *Talanta*, *113*, pp.49-61.

Tsourou, T., Drinia, H. and Anastasakis, G., 2015. Ostracod assemblages from holocene middle shelf deposits of southern Evoikos gulf (Central Aegean Sea, Greece) and their palaeoenvironmental implications. *Micropaleontology*, pp.85-99.

Umamaheswaran, R. and Dutta, S., 2024. Preservation of proteins in the geosphere. *Nature Ecology & Evolution*, pp.1-8.

Uno, K.T., Polissar, P.J., Kahle, E., Feibel, C., Harmand, S., Roche, H. and Demenocal, P.B., 2016. A Pleistocene palaeovegetation record from plant wax biomarkers from the Nachukui Formation, West Turkana, Kenya. *Philosophical Transactions of the Royal Society B: Biological Sciences, 371*(1698), p.20150235.

Vallentyne, J.R., 1964. Biogeochemistry of organic matter—II Thermal reaction kinetics and transformation products of amino compounds. *Geochimica et Cosmochimica Acta, 28*(2), pp.157-88.

Van Der Valk, T., Pečnerová, P., Díez-del-Molino, D., Bergström, A., Oppenheimer, J., Hartmann, S., Xenikoudakis, G., Thomas, J.A., Dehasque, M., Sağlıcan, E. and Fidan, F.R., 2021. Million-year-old DNA sheds light on the genomic history of mammoths. *Nature*, *591*(7849), pp.265-269.

Viehberg, F.A., Frenzel, P. and Hoffmann, G., 2008. Succession of late Pleistocene and Holocene ostracode assemblages in a transgressive environment: A study at a coastal locality of the southern Baltic Sea (Germany). *Palaeogeography, Palaeoclimatology, Palaeoecology, 264*(3-4), pp.318-329.

Viglietti, P.A., Smith, R.M., Angielczyk, K.D., Kammerer, C.F., Fröbisch, J. and Rubidge, B.S., 2016. The Daptocephalus Assemblage Zone (Lopingian), South Africa: a proposed biostratigraphy based on a new compilation of stratigraphic ranges. *Journal of African Earth Sciences, 113*, pp.153-164.

Villa, P., Goni, M.F.S., Bescós, G.C., Grün, R., Ajas, A., Pimienta, J.C.G. and Lees, W., 2010. The archaeology and paleoenvironment of an Upper Pleistocene hyena den: an integrated approach. *Journal of Archaeological Science, 37*(5), pp.919-935.

Villmoare, B., Kimbel, W.H., Seyoum, C., Campisano, C.J., DiMaggio, E.N., Rowan, J., Braun, D.R., Arrowsmith, J.R. and Reed, K.E., 2015. Early *Homo* at 2.8 Ma from Ledi-Geraru, Afar, Ethiopia. *Science, 347*(6228), pp.1352-1355.

Voosen, P., 2017. 2.7-million-year-old ice opens window on past. *Science, 357*(6352), pp.630-6311.

Vortsepneva, E., Mikhlina, A. and Kantor, Y., 2023. Main patterns of radula formation and ontogeny in Gastropoda. *Journal of Morphology*, *284*(1), p.e21538.

Walker, M., 2005. *Quaternary dating methods*. John Wiley & Sons.

Walker, M., Johnsen, S., Rasmussen, S.O., Popp, T., Steffensen, J.P., Gibbard, P., Hoek, W., Lowe, J., Andrews, J., Björck, S. and Cwynar, L.C., 2009. Formal definition and dating of the GSSP (Global Stratotype Section and Point) for the base of the Holocene using the Greenland NGRIP ice core, and selected auxiliary records. *Journal of Quaternary Science, 24*(1), pp.3-17.

Wallinga, J., 2002. Optically stimulated luminescence dating of fluvial deposits: a review. *Boreas, 31*(4), pp.303-322.

Walter, R.C., 1994. Age of Lucy and the first family: single-crystal ^{40}Ar/^{39}Ar dating of the Denen Dora and lower Kada Hadar members of the Hadar Formation, Ethiopia. *Geology, 22*(1), pp.6-10.

Walton, D., 1998. Degradation of intracrystalline proteins and amino acids in fossil brachiopods. *Organic Geochemistry, 28*(6), pp.389-410.

Warinner, C., Speller, C. and Collins, M.J., 2015. A new era in palaeomicrobiology: prospects for ancient dental calculus as a long-term record of the human oral microbiome. *Philosophical Transactions of the Royal Society B: Biological Sciences*, *370*(1660), pp.20130376.

Warinner, C., Korzow Richter, K. and Collins, M.J., 2022. Paleoproteomics. *Chemical reviews, 122*(16), pp.13401-13446.

Welker, F., Collins, M.J., Thomas, J.A., Wadsley, M., Brace, S., Cappellini, E., Turvey, S.T., Reguero, M., Gelfo, J.N., Kramarz, A. and Burger, J., 2015. Ancient proteins resolve the evolutionary history of Darwin's South American ungulates. *Nature*, *522*(7554), pp.81-84.

Welker, F., Ramos-Madrigal, J., Gutenbrunner, P., Mackie, M., Tiwary, S., Rakownikow Jersie-Christensen, R., Chiva, C., Dickinson, M.R., Kuhlwilm, M., de Manuel, M. and Gelabert, P., 2020. The dental proteome of *Homo antecessor*. *Nature, 580*(7802), pp.235-238.

Wheeler, L.J., Penkman, K.E. and Sejrup, H.P., 2021. Assessing the intra-crystalline approach to amino acid geochronology of *Neogloboquadrina pachyderma* (sinistral). *Quaternary Geochronology, 61*, p.101131.

White, T.S., Preece, R.C. and Whittaker, J.E., 2013. Molluscan and ostracod successions from Dierden's Pit, Swanscombe: insights into the fluvial history, sea-level record and human occupation of the Hoxnian Thames. *Quaternary Science Reviews*, *70*, pp.73-90.

Wiese, R., Hartmann, K., Gummersbach, V.S., Shemang, E.M., Struck, U. and Riedel, F., 2020. Lake highstands in the northern Kalahari, Botswana, during MIS 3b and LGM. *Quaternary International, 558*, pp.10-18.

Williams, M.B., Aydin, M., Tatum, C. and Saltzman, E.S., 2007. A 2000 year atmospheric history of methyl chloride from a South Pole ice core: Evidence for climate-controlled variability. *Geophysical research letters, 34*(7).

Wood, R., 2015. From revolution to convention: the past, present and future of radiocarbon dating. *Journal of Archaeological Science, 56*, pp.61-72.

Wood, B. and Lonergan, N., 2008. The hominin fossil record: taxa, grades and clades. *Journal of Anatomy*, *212*(4), pp.354-376.

Chapter 2. Notes on Pleistocene and Recent non-marine Mollusca from Zambia

This chapter was accepted for publication in *The Journal of Conchology* pending minor revisions in July 2024. The suggested revisions have been incorporated into this chapter. Extraction of Mollusca from the sediments was carried out by CB; taxonomic identification was carried out by CB and TW; interpretation within the context of Palaeolake Kafue, and writing, was carried out by CB with guidance from LB, MS, KP and TW.

The purpose of this study was to extract Mollusca from sediments associated with Palaeolake Kafue which had been previously excavated by LB, in order to undertake palaeoenvironmental analysis and assess whether any present species may be appropriate for building amino acid geochronologies.

Authorship

Chloë Baldreki[1]*, Lawrence Barham[2], Michael J. Simms[3], Kirsty E.H. Penkman[1], Tom S. White[4]

[1] Department of Chemistry, University of York, UK
[2] Department of Archaeology, Classics and Egyptology, University of Liverpool, UK
[3] Senior Curator of Geology, National Museums Northern Ireland
[4] Principal Curator, non-Insect Invertebrates, Natural History Museum, London, UK

Key words

Land snails, South-Central Africa, taxonomy, palaeoenvironments

Abstract

Pleistocene and Recent non-marine molluscan faunas from Zambia, and from South-Central Africa more generally, are relatively poorly understood. Many extant species have been reported only from single localities, often the type localities from which they were first described, and their distributions and ecological preferences are unknown. Fossil assemblages have seldom been documented in any detail, partly because early archaeological investigations often disregarded non-marine molluscs as invasive elements of the fossil record. Here, we present new data from the late Middle to Late Pleistocene Palaeolake Kafue lacustrine sequence, situated in the landscape below the archaeological site of Twin Rivers Kopje, Zambia, where non-marine mollusc shells are preserved in cemented carbonate-rich sediments. The composition of this fauna, its palaeoecological significance and relevance to the archaeological and hydrological records of the Lake Kafue Basin are discussed.

We also briefly review the molluscan fauna of Zambia as a basis for future research in the region. Type specimens of *Achatina craven* E.A. Smith, 1881, *A. morrelli* Preston, 1905, *A. morrelli* var. *kafuensis* Melvill & Ponsonby, 1907 and *A. tavaresiana* Morelet, 1866 are illustrated.

2.1. Introduction

The use of fossil non-marine mollusc assemblages as part of multi-disciplinary reconstructions of past environments and climates has a long pedigree, but their potential in this regard varies dramatically around the world depending on local preservation conditions and traditions of research. Pleistocene molluscs have long been a staple of Quaternary research in temperate regions with predominantly calcareous bedrock (such as parts of North-West Europe), but in other parts of the world they have been largely unresearched (cf. White *et al*., 2017). This is the case for the South-Central Africa region, which encompasses present day Zambia and adjacent areas of bordering countries (Angola, Namibia, Botswana, Zimbabwe, Mozambique, Malawi, Tanzania and Democratic Republic of the Congo (DRC); Fig. 2.1). Although the Pleistocene remains understudied, earlier (Neogene, Pliocene) sequences in East Africa have been documented and represent a potentially useful source of comparative data (e.g. Verdcourt, 1987; Pickford, 1995; Tattersfield, 2011; Tattersfield *et al*., 2024).
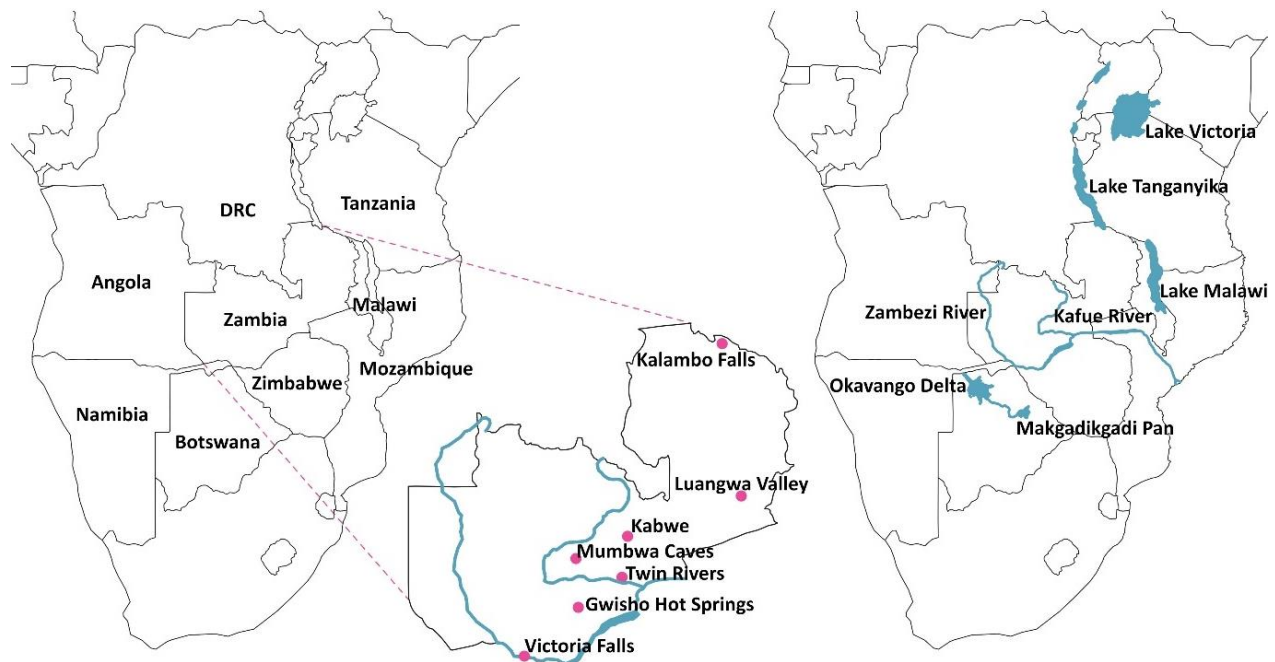
Figure 2.1. Left: Map of southern Africa highlighting the South-Central African region; Centre: Map of Zambia highlighting relevant archaeological sites; Right: Map of southern Africa highlighting current major water bodies.

Archaeological sites in Zambia range in age from ~1.1 million years old (Barham *et al.*, 2011) to the historic present (Fletcher *et al.*, 2022). The region has preserved the earliest evidence to date of a wooden structure, dated to >476 ka (Barham *et al.*, 2023) and the transition from Early to Middle Stone Age tool technologies is recorded in the north and south of the country (Duller *et al.*, 2015; Richter *et al.*, 2022). Twin Rivers Kopje has also preserved evidence of pigment use associated with Middle Pleistocene deposits (Barham, 2002). The famous hominin cranium recovered from Kabwe (Broken Hill), attributed to *Homo heidelbergensis/rhodesiensis*; *Homo bodoensis* (Woodward, 1921; Stringer, 2012; Roksandic *et al.*, 2022) has also been dated to the Middle Pleistocene (~300 ka, Grün *et al.*, 2020). However, the relationship between these important changes apparent in the archaeological and fossil records and the regional climatic record are difficult to assess given the small number of well-stratified sites with reliable chronological data.

With the exception of malacological studies focusing on biomedical topics, particularly the transmission of schistosomiasis (e.g. Wright, 1956; Richards, 1970; Brown and Rollinson, 1996; Stensgaard *et al.*, 2019), little attention has been given to the taxonomic study of Pleistocene or Recent non-marine Mollusca in Zambia, and the most extensive studies have focused on the endemic aquatic faunas in major lakes on or close to the Zambian border, such as Lake Malawi (Genner *et al.*, 2007) and Lake Tanganyika (Michel *et al.*, 2004). The most recent checklist summarising the land snail fauna of Zambia was compiled over 35 years ago (van Bruggen, 1988; see also van Bruggen 1993), and this review included fewer than 45 localities scattered across a country with an area of more than 750,000 km^2. Although the faunas of neighbouring countries have been studied and reviewed in more detail (e.g. van Bruggen and Meredith, 1984; Verdcout, 2004; Seddon *et al.*, 2005; Herbert and Kilburn, 2004; van Bruggen 2008), a similar paucity of modern records is apparent for the majority of neighbouring central southern African countries, with little development in the way of regional distribution maps for common terrestrial species, making it difficult to infer their ecological tolerances. Additional obstacles to their study arise from the recent colonial history of sub-Saharan Africa, with international borders and nomenclature having changed significantly since the first research on regional molluscan faunas was undertaken at the end of the 19th century, requiring care when interpreting earlier publications and labels associated with museum specimens (e.g. Fig. 2.2).
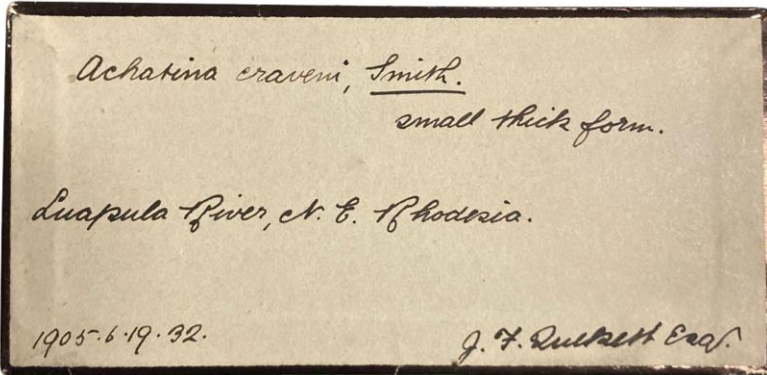
Figure 2.2. NHM label for an *Achatina craveni* specimen collected in 1905 from the Luapula River, North East Rhodesia (Zambia).

Early malacological syntheses for central and southern Africa were compiled by Pilsbry (1919), who reviewed the terrestrial Mollusca collected by the American Museum Congo Expedition (1909–1915), and Connolly (1939), whose work was focussed on South Africa and the Cape. German malacologists also contributed some early records from eastern Africa (e.g. Thiele, 1911). Zambia, formerly known as Northern Rhodesia, falls between these three regions but was neglected in terms of malacological research. Indeed, van Bruggen (1988) was able to find only a handful of papers on Zambian molluscs, of which only one (Germain, 1920) specifically focussed on "Rhodésie septentrionale" [Northern Rhodesia]. Other more localised records include the southern part of Lake Tanganyika (Bourguignat, 1885), relevant parts of British Central Africa (Smith, 1893), a single new species from the Zambezi River (Preston, 1905) and a small collection made in North-Eastern Rhodesia (Melvill and Standen, 1907).

A related issue stems from the tendency to assess molluscan faunas in terms of modern geopolitical boundaries, compiling checklists for individual countries rather than for broader regions defined using environmental criteria. This is difficult to avoid as the focus of this paper on Zambia demonstrates, but is worth acknowledging. The presence or absence of species in such lists might therefore be predicated entirely on the amount of effort focussed on a particular country (or region, such as a national park), and is unlikely to represent an accurate record of its distribution across a wider region. Checklists are also often compiled uncritically from published records or museum specimens, some of which may date to the early 19th century. Verification of these records can be impossible unless the original specimens can be examined, and the precision of the locality data must be taken at face value. As a result of the sporadic study in this region, and more broadly across Africa, it is not uncommon to encounter numerous *taxa inquirenda* and synonymised names; this is particularly true of Achatinidae, a group that contains a plethora of old names that are often difficult to match to specimens. Caution is therefore required in using them for any comparative analysis. Nonetheless, the most comprehensive published checklist for Zambia (van Bruggen, 1988) provides a

useful starting point for species that could potentially be preserved in late Middle and Late Pleistocene archaeological and palaeoenvironmental contexts in this region.

Similar issues are evident when it comes to palaeontological studies of Pleistocene molluscan material from Zambia and neighbouring countries. These have often been focussed on marine or estuarine sequences (e.g. Sessa *et al.*, 2013; Kilburn and Tankard, 1975; Langejans *et al.*, 2017) or records from large lake basins (e.g.Cooper *et al.*, 1989; van Damme and Gautier, 2013), with few detailed records from fluvial or other non-marine habitats. Herbert (2010) mentioned 'subfossil' shells from localities in South Africa and Namibia that were tentatively identified as *Vertigo antivertigo* (Draparnaud, 1801) and *Zonitoides nitidus* (O.F. Müller, 1773), although these records remain enigmatic. Many archaeological publications have emphasised the use of molluscs as food (e.g. Thackeray, 1988; Taylor *et al.*, 2011; Taylor, 2014) or decoration (e.g. Fagan and van Noten 1971; Phillipson, 1976; Bouzouggar *et al.* 2007; Miller *et al.*, 2018), rather than their potential to elucidate past environments (cf. Faulkner *et al.*, 2021). Shells have been used for dating with mixed success (see examples in Grine, 2016), with well-documented limitations in using shell biomineral for radiocarbon and electron spin resonance (ESR) dating techniques (e.g. Pigati *et al.*, 2010, 2013; Philippsen, 2013; Douka, 2017; Duval *et al.*, 2020). The fossil record for the South-Central African region is extremely sparse, and mollusc fossils have probably been encountered more often than has been documented.

Part of this lack of study is probably due to long-standing traditions of research, with Mollusca either not recorded or retained. Quarrying in the 1920s at Kabwe (Broken Hill) led to the discovery of well-preserved hominin fossils and significant fossil mammal assemblages (most notably micromammals), but there were no reported molluscan assemblages (Avery, 2003), suggesting either that these fossils were not preserved or that they were not deemed sufficiently important to sample. Another reason for the apparent reticence to use molluscan data gleaned from archaeological sequences is a common misconception that land snails are an intrusive part of the fossil record. Numerous archaeological papers refer to the "burrowing" habit of giant African land snail species, often dismissing potential data from these fossils as being unreliable due to potential bioturbation (e.g. Biittner *et al.*, 2017). Whilst it is true that most large snail species seek shelter from high temperatures by burying themselves in loose surface sediment or amongst damp leaf litter, they have no capacity to tunnel deeply into well consolidated sedimentary sequences in the same way obligate burrowing animals, such as rabbits and hares, are able to (e.g. Fowler *et al.*, 2004; Robbins *et al.*, 2008; Pelletier *et al.*, 2017). They therefore should not be disregarded for this reason. There are few (if any) terrestrial snail taxa that actively burrow below the subsoil, although members of the genera *Cecilioides* and *Coilostele* exploit cracks and root hollows to significant depths and have consequently

been routinely excluded in interpretations of Pleistocene land snail faunas for decades (e.g. Evans, 1972).

Non-marine molluscs can act as excellent palaeoenvironmental markers, with taxa inhabiting environments ranging from freshwater bodies, marshes and fens, and vegetated terrestrial habitats. Recording their presence can provide valuable climatic and ecological information, especially in areas where the palaeoenvironmental record is scant, providing evidence for climatic oscillations, one suggested driver of mammalian (including hominin) evolution (e.g. Chan *et al.*, 2019; Tatterfield *et al.*, 2024). Several recent archaeological excavations have recognised the benefits of including analyses of molluscan assemblages, in addition to macro and micro mammals, to provide palaeoenvironmental context. One of the most detailed long records to include Pleistocene non-marine Mollusca is from Panga-ya-Saidi, Kenya (Shipton *et al.*, 2018; Rowson *et al.*, 2024). Here, well-preserved molluscan assemblages excavated from a long sequence within a rock shelter provide a record of local environmental change spanning the last ~60,000 years.

In this paper we therefore summarise the Pleistocene terrestrial record from Zambia and neighbouring parts of South-Central Africa, and provide an initial regional context for fossil assemblages obtained from sediments at the base of the archaeological site at Twin Rivers Kopje associated with Palaeolake Kafue.

2.2. Materials and Methods

2.2.1. Palaeolake Kafue near Twin Rivers Kopje, Zambia

Sedimentary successions associated with Palaeolake Kafue have yielded some of the only late Middle – Late Pleistocene molluscan assemblages documented from Zambia, although the precise dating remains somewhat problematic (see Baldreki *et al.*, 2024 for further discussion). Two calcareous lacustrine sequences containing fossil non-marine Mollusca were found directly below (Site 1; Fig. 2.3), and within 16 km (Site 19; Fig. 2.3), of the archaeological site of Twin Rivers Kopje in Zambia, ~30 km southwest of Lusaka (Fig. 2.1). The succession of clays, limestones and sands are interpreted as evidence of a fluctuating sequence of lacustrine and terrestrial deposits reflecting palaeolake expansion and contraction. At its maximum extent, the lake is estimated to have covered 17,000 km^2, making it comparable in size to present day Lake Nyanza [Victoria] (Simms and Davies, 2000).
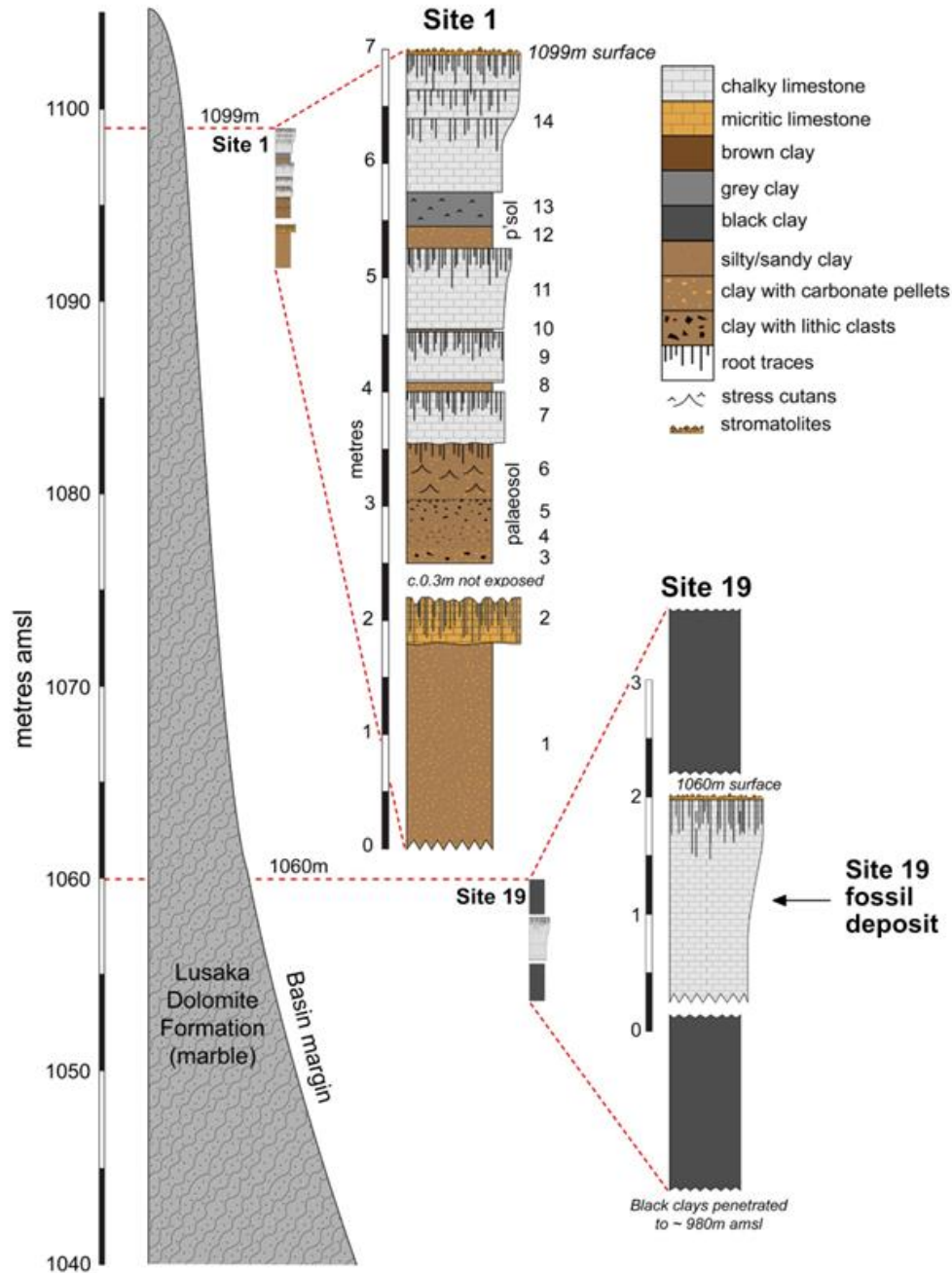
Figure 2.3. Palaeolake Kafue, excavation site sequences.

The non-marine Mollusca from Site 1 were briefly documented by Simms (Simms and Davies 2000), although only one terrestrial snail was identified to species level (*Achatina tavaresiana* Morelet, 1866 [as *A. tavaresiense*]). The fauna from Site 1 also included specimens identified as belonging to the genus *Vertigo*. This genus has a predominantly Holarctic distribution across North America, central/East Asia and Europe (cf. Adam, 1954 for African records), but it has now been shown that some African taxa (e.g. *Afripupa* Pilsbry & C.M. Cooke, 1920) are synonymous with *Vertigo* (Nekola and

90

Coles, 2016; Nekola *et al.*, 2018). All other identifications were to family level and included the aquatic families Lymnaeidae and Planorbidae and the terrestrial groups Succineidae, Euconulidae, "Subulinidae" and Achatinidae. None of the fossil shells were figured, and the original specimens identified from Site 1 have been lost (P. Davies, pers. comm.), meaning that the identities of the specimens (in particular those identified as *A. tavaresiana* and *Vertigo* sp.) cannot be independently confirmed.

All the material identified as part of this study was recovered from fossiliferous calcareous sediments at Site 19. The internal stratigraphic position of the molluscs within the chalky limestone was not recorded and the assemblage is therefore best considered as a single time-equivalent population (although this may span a considerable time window). These sediments may correlate with the palaeosols of Beds 3-6 at Site 1, which indicate a significant retreat of the lake shoreline from its highstand position at Site 1. The Site 19 mollusc assemblage is, therefore, inferred to be somewhat older than the Site 1 assemblages that were recovered from calcareous sediments above Bed 6, as discussed by Simms and Davies (2000). See Baldreki *et al.*, (2024) for further site relationship interpretations.

2.2.2. Extraction Methodology

The blocks of sediment containing molluscan remains from Site 19 were heavily indurated and cemented and were essentially very young limestone. This presented a significant challenge to the extraction of thin non-marine mollusc shells, since they were resistant to most of the standard methods of disaggregating stubborn sediment, and they could not be treated with acids due to the likelihood of shell damage. The blocks were soaked in water and disaggregation was manually encouraged. Some samples were treated with anionic surfactant (household dish soap) in an attempt to improve sediment breakdown, but this proved of limited use. Loosened sediment was sieved with a 300 µm mesh, rinsed with water and left to air dry for ~24 hours. Mollusc shells (whole and fragments) were collected with tweezers and the remaining sediment blocks were placed back in water to soak. The soaking, sieving and mollusc collection was repeated multiple times, but the assemblages were hard won.

2.3. Results

2.3.1 Identification of fossil shells

The new shell materials were extracted from heavily cemented calcareous sediments from Site 19 (Fig. 2.3), some of which was used as the basis for assessment of the suitability of achatinid shell for amino acid geochronology (Baldreki *et al.*, 2024). The only taxon identified to species level in published records from the site is *Achatina tavaresiana* (Simms and Davies, 2000; Fig. 2.4). The shell characters of Achatininae are notoriously labile, and even fresh specimens can be difficult to identify with certainty. However, the distributions of *Achatina*, which is restricted to West Africa, and *Lissachatina*, which is restricted to East Africa (Fontanilla, 2010), strongly suggest that identification of the Lake Kafue shells as *Achatina* is incorrect (F. Naggs, pers. comm.). Molecular data clarifying the genetic and biogeographical distributions of Achatininae is forthcoming (Fontanilla *et al.*, in press).
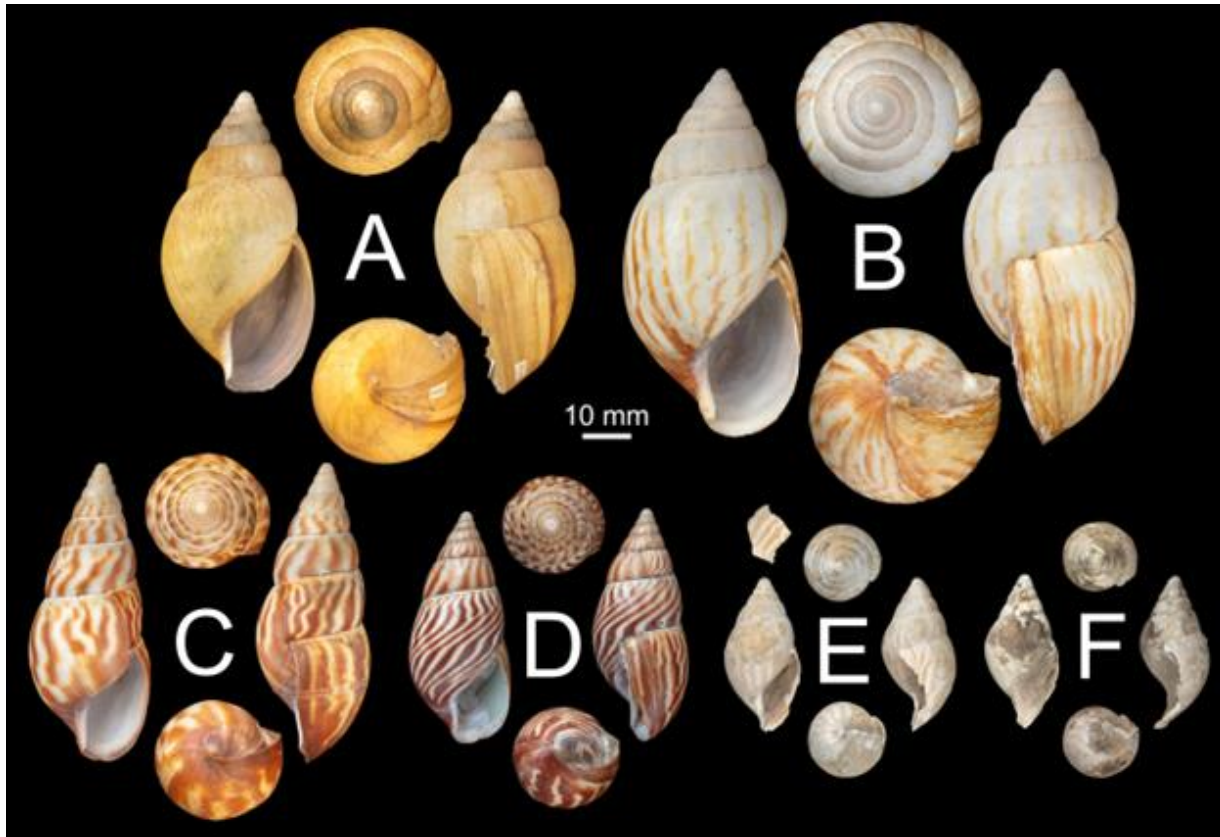
Figure 2.4. Comparison of two fossil specimens from Site 19 associated with Palaeolake Kafue (E: PK.S19.4 (ZM.LV.AR.9888) and F: PK.S19.3 (ZM.LV.AR.9887)) to museum specimens of A: *Achatina tavaresiana* Morelet, 1866 (NHMUK 1893.2.3.151, syntype); B: *Achatina craveni* (NHMUK 1880.12.22.2, syntype); C: *Achatina morrelli* Preston, 1905 (NHMUK 1907.11.21.89); D: *Achatina morrelli* var. *kafuensis* Melvill and Ponsonby, 1907 (NHMUK 1905.6.19.25, figured syntype).

The taxonomic positioning of species within Achatinidae is complex, and whilst several studies have attempted to identify and discuss classifications for the subgenera, this has not yet been fully resolved. In his revision of the genus *Achatina*, Bequaert (1950) placed *A. tavaresiana* in the subgenus *Achatina* (*Achatina*). This was distinguished from his new subgenus *Lissachatina* on the basis of microsculpture on the nepionic whorls. In *Achatina* these are covered with "granulations in closely set, regular, spiral and vertical rows'', but in *Lissachatina* they are smooth (cf. Bequaert, 1950: 12–13 and 49). This dichotomy appeared to separate the western and central African species with sculptured apices as *Achatina*, from the eastern African taxa with smooth apices as *Lissachatina*. However, Mead (1991, 1995) subsequently noted that these sculptural differences were unreliable, and so added additional shell characters and, for some species, features of the genital anatomy (in particular the penial sheath) to further refine the distinction between *Achatina* and *Lissachatina*.

Mead (1991) also noted an emerging tendency to identify achatinid species on the basis of weaker morphological characters, such as shell sculpture, if the locality of the specimen was well documented. This highlights an obvious and inherent problem for fossil material, such as the specimens from Palaeolake Kafue, in that species distributions may have been different in the past. Confident identification of fossil achatinid shells is especially problematic given that the shells are often worn (e.g. Fig. 2.4) and anatomical details of the soft body are unavailable to the taxonomist. Zambia is therefore an interesting place to attempt to identify fossil achatinid specimens, since it is situated at the interface between the "eastern" and "western" biogeographical provinces first proposed by Bequaert (1950). The Zambian fossil record could therefore potentially provide evidence for the expansion and contraction of the ranges of *Achatina* and *Lissachatina* species as a response to Quaternary climate change. However, in the absence of full molecular analyses, these systematic issues remain problematic, and we therefore assign only provisional identities to the fossil shells from sediments associated with Palaeolake Kafue.

Additional problems arise from misidentification of material and failure to consult type specimens when making taxonomic judgements. The type specimens of *A. tavaresiana* and *A. craveni* E.A. Smith, 1881, both of which have been examined for this work (Fig. 2.4), are clearly conchologically distinct. *Achatina tavaresiana* exhibits granulose sculpture on its nepionic whorls that would place it in the subgenus *Achatina* (*sensu* Bequaert, 1950), but also the "half-domed" apex characteristic of *Lissachatina* (*sensu* Mead, 1995), which illustrates the contradictory nature of the published evidence. *Achatina craveni* has a smooth, fully rounded apex, which would place it in either *Lissachatina sensu* Bequaert or *Achatina sensu* Mead. MolluscaBase currently places both species in *Achatina* (MolluscaBase Eds 2024), although the authority for this is unclear; Brown and Evans (2021) figured a specimen as "*Cochlitoma tavaresiana* (Morelet, 1866)" but provided no further details for this generic placement. The placement of *A. tavaresiana* in *Lissachatina* by Bequaert (1950) appears to have been overruled by Mead (1995), who moved it back to *Achatina* on the basis of the form of the apex. In his

checklist of Zambian land snails, van Bruggen (1988) listed only *L. craveni* as part of the Recent Zambian fauna, also noting its distinctness from *A. tavaresiana*. In contrast, Crowley and Pain (1964) had suggested that the two species are synonymous. In the absence of molecular data, these problems remain unresolved (Fontanilla *et al.*, in press).

A further taxonomic issue relates to another species recorded in Zambia, *Achatina morrelli* Preston, 1905, which was listed as a synonym of *A. capelloi* Furtado, 1886 by Bequaert (1950: 49) and placed in the subgenus *Lissachatina*. Brown and Evans (2021: 63) preferred instead to retain *A. morrelli* as a distinct species of *Achatina*, noting that shells they had examined and identified as this taxon were clearly different to *L. capelloi*. However, examination of the type of *A. morrelli* (NHMUK 1907.11.21.89; Fig. 2.4) shows that it is clearly a *Lissachatina*, and it superficially resembles the type of *A. capelloi* figured by Furtado (1886). The type of *A. capelloi* has not been located, so its generic position remains provisional, but the synonymy proposed by Bequaert (1950) appears sound. Brown and Evans (2021) provided two unnumbered figures of shells labelled as "*A. morrelli*", which are a closer match to *A. morrelli kafuensis* Melvill and Standen (1907), but the distinctness of this Zambian taxon remains unclear until its taxonomic position can be confirmed.

Additional species identified in the Pleistocene assemblage include several juvenile specimens of *Afroguppya rumrutiensis* (Preston, 1911) (Fig. 2.5B), a tropical East African species with a range extending from Kenya, through Tanzania, Malawi, Zambia, Zimbabwe and Mozambique (de Winter and van Bruggen, 1992; Herbert and Kilburn, 2004), although the conspecificity of specimens collected across this large area requires confirmation. van Bruggen (1988) noted that this species has been recorded primarily in East Africa, but he acknowledged the possibility of it being found further west in central Africa. It has been recorded living in Zambia at only a single locality, the Chowo forest on the eastern border with Malawi (van Bruggen, 1988), so the Pleistocene record from the Palaeolake Kafue site appears to be the westernmost record of this species yet reported. Although the fossil specimens are all juvenile or broken shells, the distinctive microsculpture characteristic of *A. rumrutiensis* can clearly be seen on the upper whorls (Fig. 2.5C). In South Africa this species has been recorded in leaf litter, under stones and amongst vegetation in a range of habitats including forest and thicket, and is evidently tolerant of somewhat drier conditions (Herbert and Kilburn, 2004).

A single shell identified as *Vertigo* sp. (Fig. 2.5G) is potentially significant, although the nature of the sediments mean that the mouth cannot be cleared to allow identification to species level. It is possible that it is *V. antivertigo*, which has been reported as an enigmatic 'subfossil' in South Africa and Namibia (Herbert, 2010) and could therefore be the same species identified to genus level by Simms (Simms and Davies, 2000). However, it is also possible that it represents *V. congoensis garambae* Adam, 1854 or *V. bisulcata* (Jickeli, 1873). The environmental implications of this specimen therefore remain unclear. Two specimens of *Helicarion* cf. *issangoensis* Thiele, 1911 were also identified from the Site 19 Palaeolake Kafue (Fig. 2.5F). The type locality "Issango Ferry" refers to the

94

ferry that crossed the Semiliki (formerly Issango) River during the latter part of the expedition to the African interior undertaken by Franz Stuhlmann in 1891 (Thiele, 1911). This species was not recorded in the checklist of land snail species compiled by van Bruggen (1988). The only other record of a species from the genus in Zambia was *Helicarion nyassanus* var. *excellens* (Melvill and Standen, 1907), but this has not been recorded since the early 20th century. It is possible that these taxa are conspecific, but a revision of southern African *Helicarion* is beyond the scope of this paper. Several specimens of *Ceciliodes* sp. were also recovered. Members of this burrowing genus are routinely excluded from Pleistocene palaeoenvironmental reconstructions (cf. Evans, 1972) because their burrowing habit makes them a rare example of a non-marine mollusc that could be invasive to an archaeological or geological context. These shells probably entered the fossil record via the numerous root holes and fissures evident in the sediments, but whether they are contemporaneous with the other material is unclear. van Bruggen (1988) listed *C. gokweanus* (Boettger, 1870) as the only species recorded from Zambia but also noted that the Afrotropical *Cecilioides* are poorly known.
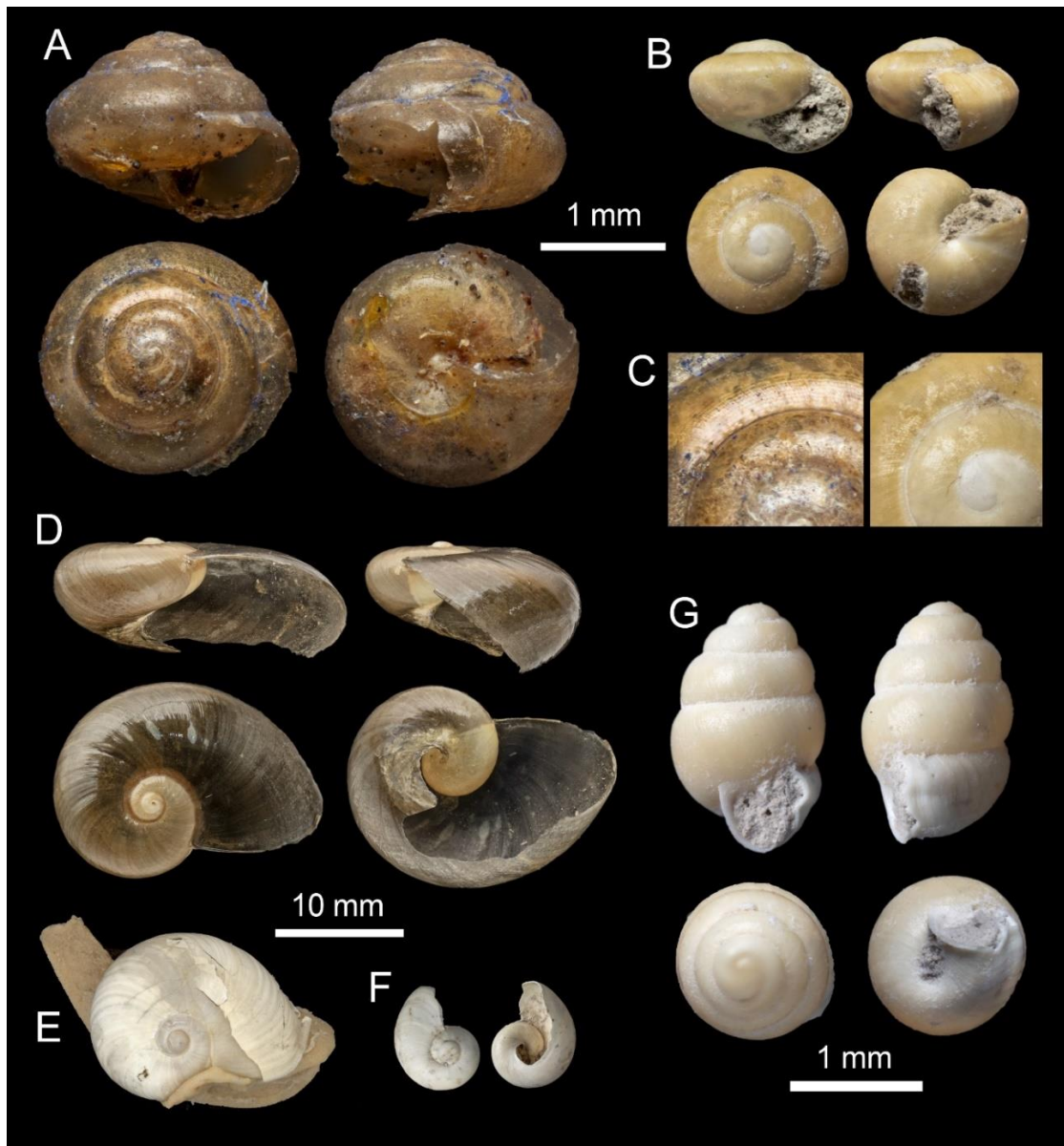
Figure 2.5. A–C: *Afroguppya rumrutiensis* (Preston, 1911) (A: NHMUK 20210195, Mt. Kinangop, Abedare Range, Kenya; B: Palaeolake Kafue fossil specimen PK.S19.26; B: comparison of shell microsculpture on apical whorls). D–F: *Helicarion issangoensis* Thiele, 1911 (D: NHMUK 1937.12.30.1420; E: syntype, ZMB/Moll-109970; F: Palaeolake Kafue fossil specimen PK.S19.7). G: *Nesopupa* sp. (Palaeolake Kafue fossil specimen).

2.3.2. Palaeoenvironmental implications

Despite the small size and low species diversity of the molluscan fauna derived from the Palaeolake Kafue Site 19 sediments, some general inferences about the local environment can be made. It is difficult to characterise the vegetation precisely, although the *Helicarion* is a potential indicator of shade/tree cover. The *Vertigo* specimen (Fig. 2.5G) could be associated with woodland

(e.g. *V. bisulcata* (Jickeli, 1873); see Tattersfield *et al.*, 2024) or, if an identification as *Vertigo antivertigo* can be confirmed, rather wetter environments. However, the assemblage provides a general impression of a well-vegetated environment proximal to a large body of water and is wholly in keeping with the interpretation of the sediments representing a lake margin (Simms and Davies, 2000). Two freshwater taxa were identified, although the specimens were fragmentary juvenile shells that could not be identified with confidence to species level; five specimens represented Planorbidae and three represented Lymnaeidae. The most common shells represented were Succineidae, with over 40 countable specimens recovered; these were again mostly juvenile shells that could not be identified to species level. In northern Europe, this family is strongly associated with marshy habitats close to bodies of water. However, this is not the case in sub-Saharan Africa, where succineids can be found places that are (at least seasonally) remarkably dry, such as grasslands on the southern Serengeti (Tattersfield *et al.* 2024). Pickford (1995) considered African Succineidae to be characteristic of "seasonally waterlogged ground, even in semi-arid to arid country". Nevertheless, given the proximity of Site 19 to Palaeolake Kafue, it seems clear that waterlogged conditions were at least seasonally available.

The most common terrestrial species represented was *Afroguppya rumrutiensis* (Preston, 1912), with 26 countable specimens identified. This species has a generally east African distribution, with records from South Africa (KwaZulu Natal), Zimbabwe, Malawi, Tanzania and Kenya (van Bruggen, 1988; de Winter and van Bruggen, 1992), although van Bruggen (1988) noted the possibility that it might occur further west. The record from this assemblage represents the first Pleistocene record of the species in Zambia. This species was also recorded in relatively low numbers at the Late Pleistocene cave site of Panga ya Saidi, Kenya, where much richer faunas have been recovered from a sequence spanning a period of ~80,000 years (Rowson *et al.*, 2024). It says much about current knowledge of African non-marine Mollusca that even a comparatively rich sequence like Panga ya Saidi was difficult to interpret due to the limited knowledge of the habitat preferences of extant species (Rowson *et al.*, 2024).

2.4. Discussion

The South-Central African region's current ecology, reflective of its topography, is diverse. Zambia contains tropical deciduous woodlands across its high central plateau, which grade to dryland savannah on the margins of the Kalahari basin. Several major river systems (e.g. Kafue and Zambezi rivers; Fig. 2.1) and lakes (Bangweulu, Mweru and Tanganyika; Fig. 2.1) are present in Zambia, and large wetlands occur seasonally in much of the north of the country. Today, the Twin Rivers Kopje overlooks the Kafue River floodplain to the south-east and the Lusaka dolomite plateau to the north-west, giving rise to a mixed grassland-woodland habitat typical of these ecozones, but

during the Middle Pleistocene it would have overlooked a vast lake (Clark and Brown, 2001; Barham *et al.*, 2000).

The Zambian non-marine molluscan fauna is poorly known. The checklist compiled by van Bruggen (1988) included 56 terrestrial taxa; of these, 25 were reported for the first time, and most of these new records were from the Chowo Forest, an area on the Zambia–Malawi border that had recently been subject of an intensive survey. Few other areas of Zambia have been similarly investigated for terrestrial molluscs, and those that have are usually on the borders with neighbouring countries where surveys have been carried out (e.g. Smith, 1893; Muratov, 2010). Some of the localities included by Smith (1893) are now in eastern Zambia, including the western part of the Nyika Plateau, hence the inclusion by van Bruggen (1988) of some of the taxa recorded in his checklist of the Zambian terrestrial fauna. This collection bias is likely to be the reason why many widely distributed families such as Maizaniidae, Veronicellidae and Ariophantidae are not represented in published checklists for Zambia. It is notable that *Helicarion* (*Gymnarion) issangoensis*, recorded at Palaeolake Kafue Site 19, is a member of the last-mentioned group and this represents its first record in Zambia.

Molluscan assemblages have also only rarely been reported from archaeological sites in Zambia. Apart from the sequences associated with Palaeolake Kafue, only one gastropod species was reported from the Twin Rivers archaeological site (G block; Barham, 2000), whilst in the Luangwa Valley only a brief mention of the recovery of land snail artefacts amongst other organic material was reported from late Holocene deposits (Fletcher *et al.*, 2022). At the site of Mumbwa Caves in central Zambia, mollusc fragments were reported with human remains (Dart and Del Grande, 1931) and from early Holocene deposits, but these were not described (Barham, 2000). A more detailed account of Mollusca was recorded at the mid-Holocene site of Gwisho Hot Springs, including several of taxa identified to species level (e.g. *Achatina schinziana* Mousson, 1888, *Aspatharia sinuate* von Martens, 1883, *Burtoa nilotica* Pfeiffer, 1861, *Lanistes ellipticus* von Martens 1866, as well as fragments representing the unionid genus *Cafferia* Simpson, 1990; however, the discussion was focused on their use as food and decoration rather than their palaeoecological potential. Similarly, at the Later Stone Age archaeological sites of Kalemba, Thandwe and Makwe, *Achatina* shells were again discussed with reference to beads and decoration, but not in terms of any paleoenvironmental implications (Phillipson, 1976).

In general terms, climate oscillations across Africa during the Pleistocene are less well understood than those of middle to high latitudes in the northern hemisphere, where glacial and interglacial phases dominate the record (Maslin *et al.*, 2014). In Africa, regional arid-humid fluctuations occurred as a result of a complex combination of environmental factors, such as ice sheet volume in the northern hemisphere, global sea surface temperatures, precipitation volume and patterns, and trade winds (Demenocal *et al.*, 1993; Weij *et al.*, 2024). These fluctuations happened asynchronously across different regions (Blome *et al.*, 2012) and would have resulted in expansion,

contraction, and alteration of habitats dependent on locality. In Zambia, evidence for phases of lake expansion and contraction in the latter part of the Middle Pleistocene for Palaeolake Kafue has been previously reported (Simms and Davies, 2000).

The taxa identified here from recent studies of Pleistocene sediments associated with Palaeolake Kafue show evidence of varied climatic conditions, including wetter conditions than the present prevailing climate. More catholic terrestrial taxa, such as *Achatina* spp. and *Afroguppya rumrutiensis*, were found alongside taxa that potentially indicate wetter environments, such as *Vertigo* sp. and *Succinea* sp., and obligate freshwater taxa such as *Planorbis* sp. These findings, whilst not currently providing much insight into changes in the local climate and environment through time, nevertheless represent an important datapoint for future regional studies of the Zambian Pleistocene malacofauna.

2.4. Conclusions

Zambia lies at a central crossroads between major biogeographical provinces in central southern Africa and its extant and fossil molluscan faunas are potentially critical to understanding changing distributions of species in response to climate change during at least the last half million years. The Pleistocene non-marine molluscan assemblage extracted from sediments preserved at Palaeolake Kafue in southern Zambia included freshwater taxa (Lymnaeidae and Planorbidae), species indicative of vegetation at the lake-margin (Succineidae), and terrestrial species, some of which represent the first records in the Zambian Pleistocene record (*Afroguppya rumrutiensis* and *Helicarion issangoensis*). Although the assemblage is not large enough to make significant claims about past climatic and environmental conditions, it represents an important record for continued research in this area. This study also provides the first record of *Helicarion issangoensis* from Zambia and highlights the need for detailed studies of both the Recent faunas (through ecological surveys and examination of museum collections) and the Pleistocene fossil record in underrepresented regions of research, such as within South-Central Africa.

Acknowledgements

2.5. References

Adam, W., 1954. Études sur les mollusques de l'Afrique centrale et des regions voisines 1. Vertiginidae et Valloniidae. Volume Jubilaire Victor Van Straelen. Tome II. Institut Royal d'Histoire Naturelle de Belgique. pp. 725–817.

Avery, D.M., 2003. Early and Middle Pleistocene environments and hominid biogeography; micromammalian evidence from Kabwe, Twin Rivers and Mumbwa Caves in central Zambia. *Palaeogeography, Palaeoclimatology, Palaeoecology, 189* (1–2), pp.55–69.

Baldreki, C., Burnham, A., Conti, M., Wheeler, L., Simms, M.J., Barham, L., White, T.S. and Penkman, K., 2024. Investigating the potential of African land snail shells (Gastropoda: Achatininae) for amino acid geochronology. *Quaternary Geochronology, 79*, p.101473.

Barham, L.S., 2000. *The Middle Stone Age of Zambia, South Central Africa*. Western academic & specialist Press.

Barham, L.S., Simms, M., Gilmour, M., Debenham, N., 2000. Chapter 10 Twin Rivers, excavation and behavioural record in Barham, L.S., 2000. *The Middle Stone Age of Zambia, South Central Africa*. Western academic & specialist Press. pp.165-216.

Barham, L., 2002. Systematic pigment use in the Middle Pleistocene of south-central Africa. *Current anthropology, 43*(1), pp.181-190.

Barham, L., 2011. Clarifying Some Fundamental Errors in Herries'"A Chronological Perspective on the Acheulian and Its Transition to the Middle Stone Age in Southern Africa: The Question of the Fauresmith". *International Journal of Evolutionary Biology*, *2012*.

Barham, L., Duller, G.A.T., Candy, I., Scott, C., Cartwright, C.R., Peterson, J.R., Kabukcu, C., Chapot, M.S., Melia, F., Rots, V. and George, N., 2023. Evidence for the earliest structural use of wood at least 476,000 years ago. *Nature, 622*(7981), pp.107-111.

Bequaert, J.C., 1951. Studies in the Achatininae, a group of African land snails. *Bulletin of the Museum of Comparative Zoology at Harvard College, 105*(1), pp.1-216.

Biittner, K.M., Sawchuk, E.A., Miller, J.M., Werner, J.J., Bushozi, P.M. and Willoughby, P.R., 2017. Excavations at Mlambalasi Rockshelter: A terminal Pleistocene to recent Iron Age record in southern Tanzania. *African Archaeological Review, 34*(2), pp.275-295.

Blome, M.W., Cohen, A.S., Tryon, C.A., Brooks, A.S. and Russell, J., 2012. The environmental context for the origins of modern human diversity: a synthesis of regional variability in African climate 150,000–30,000 years ago. *Journal of human evolution, 62*(5), pp.563-592.

Bourguignat, J.R., 1885. *Notice prodromique sur les mollusques terrestres et fluviatiles recueillis par M. Victor Giraud dans la région méridionale du Lac Tanganika*. Tremblay.

Bouzouggar, A., Barton, N., Vanhaeren, M., d'Errico, F., Collcutt, S., Higham, T., Hodge, E., Parfitt, S., Rhodes, E., Schwenninger, J.L. and Stringer, C., 2007. 82,000-year-old shell beads from North Africa and implications for the origins of modern human behavior. *Proceedings of the National Academy of Sciences, 104*(24), pp.9964-9969.

Brown, K. and Evans, M. 2021., *The Achatinid Landshells of Southern Africa*. ConchBooks, Harxheim, Germany.

Brown, D.S. and Rollinson, D., 1996. Aquatic snails of the *Bulinus africanus* group in Zambia identified according to morphometry and enzymes. *Hydrobiologia, 324*, pp.163-177.

Chan, E.K., Timmermann, A., Baldi, B.F., Moore, A.E., Lyons, R.J., Lee, S.S., Kalsbeek, A.M., Petersen, D.C., Rautenbach, H., Förtsch, H.E. and Bornman, M.S., 2019. Human origins in a southern African palaeo-wetland and first migrations. *Nature, 575*(7781), pp.185-189.

Clark, J.D. and Brown, K.S., 2001. The Twin Rivers Kopje, Zambia: stratigraphy, fauna, and artefact assemblages from the 1954 and 1956 excavations. *Journal of Archaeological Science, 28*(3), pp.305-330.

Connolly, M.W., 1939. *A Monographic Survey of South African non-marine Mollusca*. Trustees of the South African Museum, Cape Town.

Cooper, J.A.G., Kilburn, R.N. and Kyle, R., 1989. A late Pleistocene molluscan assemblage from Lake Nhlange, Zululand, and its palaeoenvironmental implications. *South African journal of geology, 92*(2), pp.73-83.

Crowley, T.E. and Pain, T., 1964. *Achatina* (*Lissachatina*) *tavaresiana* Morelet; its synonymy and distribution. *Revue de Zoologie et de Botanique Africaines,* 64(1-2), pp.121–131.

Dart, R.A. and Grande, N. del., 1931. The ancient iron-smelting cavern at Mumbwa*. Transactions of the Royal Society of South Africa, 19*, pp.379–427.

Demenocal, P.B., Ruddiman, W.F. and Pokras, E.M., 1993. Influences of high-and low-latitude processes on African terrestrial climate: Pleistocene eolian records from equatorial Atlantic Ocean Drilling Program site 663. *Paleoceanography, 8*(2), pp.209-242.

de Winter, A.J. and van Bruggen, A.C., 1992. Systematic position and distribution of the African land snails *Afropunctum seminium* (Morelet) and *'Guppya'rumrutiensis* (Preston)(Mollusca, Gastropoda Pulmonata: Euconulidae), with the description of two new taxa. *Proceedings of the Koninklijke Nederlandse Akademie van Wetenschappen. Serie C: Biological and medical sciences, 95*, pp.515-533.

Douka, K., 2017. Radiocarbon dating of marine and terrestrial shell. *Molluscs in Archaeology: Methods, Approaches and Applications*, p.381.

Duller, G.A., Tooth, S., Barham, L. and Tsukamoto, S., 2015. New investigations at Kalambo Falls, Zambia: Luminescence chronology, site formation, and archaeological significance. *Journal of Human Evolution, 85*, pp.111-125.

Duval, M., Arnold, L.J. and Rixhon, G., 2020. Electron spin resonance (ESR) dating in Quaternary studies: evolution, recent advances and applications. *Quaternary International, 556*, pp.1-10.

Fagan, B.M. and van Noten, F.L., 1971. The hunter gatherers of Gwisho, Musée Royal de l'Afrique Centrale, Tervuren.

Evans, J.G., 1972. *Land Snails in Archaeology*. Seminar Press, London and New York.

Faulkner, P., Miller, J.M., Quintana Morales, E.M., Crowther, A., Shipton, C., Ndiema, E., Boivin, N. and Petraglia, M.D., 2021. 67,000 years of coastal engagement at Panga ya Saidi, eastern Africa. *Plos one, 16*(8), p.e0256761.

Fletcher, R., Barham, L., Duller, G. and Jain, M., 2022. Nothing set in stone: Chaines operatoires of later stone age sequences from the Luangwa valley and Muchinga Escarpment, Zambia. *South African Archaeological Bulletin* 77(217), pp.89–114.

Fontanilla, I.K.C., 2010. *Achatina* (*Lissachatina*) *fulica* Bowdich: its molecular phylogeny, genetic variation in global populations, and its possible role in the spread of the rat lungworm *Angiostrongylus cantonensis* (Chen). PhD thesis, University of Nottingham.

Fontanilla, I.K.C., Naggs, F., Tang, C., Herbert, D.G. and Wade, C.M., In press. Radiation of Giant Snails across sub-Saharan Africa: the molecular phylogenetic evidence. *Molecular Phylogenetics and Evolution*.

Fowler, K.D., Greenfield, H.J. and van Schalkwyk, L.O., 2004. The effects of burrowing activity on archaeological sites: Ndondondwane, South Africa. *Geoarchaeology: An International Journal, 19*(5), pp.441-470.

Furtado, A., 1886. Coquilles terrestres et fluviatiles de l'exploration Africaine de M.M. Capello et Ivens (1884–1885). *Journal de Conchyliologie 34*(2), pp.138-152.

Genner, M.J., Todd, J.A., Michel, E., Erpenbeck, D., Jimoh, A., Joyce, D.A., Piechocki, A. and Pointier, J.P., 2007. Amassing diversity in an ancient lake: evolution of a morphologically diverse parthenogenetic gastropod assemblage in Lake Malawi. *Molecular Ecology, 16*(3), pp.517-530.

Germain, L., 1920. Contributions a la Faune Malacologique de l'Afrique équatoriale LX. Sur quelques mollusques de la Rhodésie septentrionale. *Bulletin du Muséum National d'Histoire Naturelle, 26*, pp.239–244.

Grine, F.E., 2016. The Late Quaternary hominins of Africa: The skeletal evidence from MIS 6-2. *Africa from MIS 6-2: population dynamics and paleoenvironments*, pp.323-381.

Grün, R., Pike, A., McDermott, F., Eggins, S., Mortimer, G., Aubert, M., Kinsley, L., Joannes-Boyau, R., Rumsey, M., Denys, C. and Brink, J., 2020. Dating the skull from Broken Hill, Zambia, and its position in human evolution. *Nature, 580*(7803), pp.372-375.

Herbert, D. and Kilburn, R., 2004. *A field guide to the land snails and slugs of eastern South Africa*. Natal Museum, Pietermaritzburg, South Africa, pp.1-336.

Herbert, D., 2010. The introduced terrestrial Mollusca of South Africa. SANBI Biodiversity Series 15. South African National Biodiversity Institute, Pretoria.

Kilburn, R.N. and Tankard, A.J., 1975. Pleistocene molluscs from the west and south coasts of the Cape Province, South Africa. *Annals of the South African Museum*, 67(6), pp.183–226.

Langejans, G.H., Dusseldorp, G.L. and Thackeray, J.F., 2017. Pleistocene molluscs from Klasies River (South Africa): Reconstructing the local coastal environment. *Quaternary International, 427*, pp.59-84.

Maslin, M.A., Brierley, C.M., Milner, A.M., Shultz, S., Trauth, M.H. and Wilson, K.E., 2014. East African climate pulses and early human evolution. *Quaternary Science Reviews, 101*, pp.1-17.

Mead, A.R., 1991. Anatomical criteria in the systematics of the Achatinidae (Pulmonata). In: Meier-Brook C (Ed.) *Proceedings of the 10th International Malacological Congress*, Tubingen, pp.549–553.

Mead, A.R., 1995. Anatomical studies reveal new phylogenetic interpretations in *Lissachatina* (Pulmonata: Achatinidae). *Journal of Molluscan Studies*, 61(2), pp.257–73.

Melvill, J.C. and Standen, R., 1907. Notes on a collection of terrestrial and fluviatile Mollusca, made in North-Eastern Rhodesia, during 1905, by Mr. Sheffield A. Neave, M.A., B.Sc. *Memoirs and Proceedings of the Manchester Literary & Philosophical* Society, 51(4) pp.1–16.

Michel, E.L., Todd, J.A., Cleary, D.F., Kingma, I.R., Cohen, A.S. and Genner, M.J., 2004. Scales of endemism: challenges for conservation and incentives for evolutionary studies in a gastropod species flock from Lake Tanganyika. *Journal of Conchology, Special Publication, 3*, pp.155–72.

Miller, J.M., Sawchuk, E.A., Reedman, A.L. and Willoughby, P.R., 2018. Land snail shell beads in the sub-Saharan archaeological record: when, where, and why? *African Archaeological Review, 35*, pp.347–378.

Muratov, I.V., 2010. Terrestrial molluscs of Cabo Delgado and adjacent inland areas of north-eastern Mozambique. *African Invertebrates, 51*(2), pp.255–288.

Nekola, J.C. and Coles, B.F., 2016. Supraspecific taxonomy in the Vertiginidae (Gastropoda, Stylommatophora). *Journal of Molluscan Studies, 82*, pp.208–212.

Nekola, J.C., 2018. A phylogenetic overview of the genus *Vertigo* O.F. Müller, 1773 (Gastropoda: Pulmonata: Pupillidae: Vertiginidae). *Malacologia, 62*(1), pp.21–161.

Pelletier, M., Royer, A., Holliday, T.W., Discamps, E., Madelaine, S. and Maureille, B., 2017. Rabbits in the grave! Consequences of bioturbation on the Neandertal "burial" at Regourdou (Montignac-sur-Vézère, Dordogne). *Journal of human evolution, 110*, pp.1-17.

Philippsen, B., 2013. The freshwater reservoir effect in radiocarbon dating. *Heritage Science, 1*, pp.1–9.

Phillipson, D.W., 1976. *The Prehistory of eastern Zambia*. British Institute in Eastern Africa, Nairobi.

Pickford, M., 1995. Fossil land snails of East Africa and their palaeoecological significance. *Journal of African Earth Sciences 20*(3-4), pp.167-226.

Pigati, J.S., Rech, J.A. and Nekola, J.C., 2010. Radiocarbon dating of small terrestrial gastropod shells in North America. *Quaternary Geochronology, 5*(5), pp.519-532.

Pigati, J.S., McGeehin, J.P., Muhs, D.R. and Bettis III, E.A., 2013. Radiocarbon dating late Quaternary loess deposits using small terrestrial gastropod shells. *Quaternary Science Reviews, 76*, pp.114-128.

Pilsbry, H.A. and Lang, H., 1919. A Review of the Land Mollusks of the Belgian Congo: chiefly based on the collections of the American Museum Congo Expedition, 1909-1915. Trustees of the American Museum of Natural History, New York.

Preston, H.B., 1905. Description of a new *Achatina* from the Zambesi. *Proceedings of the Malacological Society of London, 6*, p.244.

Richards, C.S., 1970. Genetics of a molluscan vector of schistosomiasis. *Nature, 227*(5260) pp.806–10.

Richter, M., Tsukamoto, S., Chapot, M.S., Duller, G.A. and Barham, L.S., 2022. Electron spin resonance dating of quartz from archaeological sites at Victoria Falls, Zambia. *Quaternary Geochronology, 72*, p.101345.

Robbins, L.H., Campbell, A.C., Murphy, M.L., Brook, G.A., Liang, F., Skaggs, S.A., Srivastava, P., Mabuse, A.A. and Badenhorst, S., 2008. Recent archaeological research at Toteng, Botswana: early domesticated livestock in the Kalahari. *Journal of African Archaeology, 6*(1), pp.131-149.

Roksandic, M., Radović, P., Wu, X.J. and Bae, C.J., 2022. Resolving the "muddle in the middle": The case for *Homo bodoensis* sp. nov. *Evolutionary Anthropology*: *Issues, News, and Reviews, 31*(1) pp.20–29.

Rowson, B., Law, M., Miller, J., White, T., Shipton, C., Crowther, A., Ndiema, E., Petraglia, M. and Boivin, N.L., 2024. A Quaternary sequence of terrestrial molluscs from East Africa: a record of diversity, stability, and abundance since Marine Isotope Stage 5 (78,000 BP). *Archiv für Molluskenkunde, 153*(1), pp.61-86.

Seddon, M.B., Tattersfield, P., Herbert, D.G., Rowson, B., Lange, C.N., Ngereza, C. and Warui, C.M., 2005. Diversity of African forest mollusc faunas: what we have learned since Solem (1984). *Records of the Western Australian Museum Supplement 68*, pp.103-113.

Sessa, J.A., Callapez, P.M., Dinis, P.A. and Hendy, A.J., 2013. Paleoenvironmental and paleobiogeographical implications of a Middle Pleistocene mollusc assemblage from the marine terraces of Baía das Pipas, southwest Angola. *Journal of Paleontology, 87*(6), pp.1016-1040.

Shipton, C., Roberts, P., Archer, W., Armitage, S.J., Bita, C., Blinkhorn, J., Courtney-Mustaphi, C., Crowther, A., Curtis, R., Errico, F.D. and Douka, K., 2018. 78,000-year-old record of Middle and Later Stone Age innovation in an East African tropical forest. *Nature Communications, 9*(1), p.1832.

Simms, M.J. and Davies, P., 2000. Appendix 7. Preliminary report on the sediments and molluscs of Lake Patrick. In: Barham LS (Ed.) *The Middle Stone Age of Zambia, South Central Africa*. Western Academic & Specialist Press. pp.275 – 280.

Smith, E.A., 1893. On a collection of land and freshwater shells transmitted by Mr. H.H. Johnston C.B. from British Central Africa. *Proceedings of the Zoological Society of London*, pp.632–641.

Stensgaard, A.S., Vounatsou, P., Sengupta, M.E. and Utzinger, J., 2019. Schistosomes, snails and climate change: current trends and future expectations. *Acta tropica, 190*, pp.257-268.

Stringer, C., 2012. The status of *Homo heidelbergensis* (Schoetensack 1908). *Evolutionary Anthropology: Issues, News, and Reviews, 21*(3), pp.101-107.

Tattersfield, P., Rowson, B., Ngereza, C.F. and Harrison, T., 2024. Laetoli, Tanzania: Extant terrestrial mollusc faunas shed new light on climate and palaeoecology at a Pliocene hominin site. *PLoS ONE 19*(5), p.e0302435.

Taylor, V.K., Barton, R.N.E., Bell, M., Bouzouggar, A., Collcutt, S., Black, S. and Hogue, J.T., 2011. The Epipalaeolithic (Iberomaurusian) at Grotte des Pigeons (Taforalt), Morocco: a preliminary study of the land Mollusca. *Quaternary International, 244*(1), pp.5-14.

Taylor, V.K., 2014. Land snail middens in the Late Pleistocene and early Holocene in North Africa: a case study from Taforalt (Grotte des Pigeons), Morocco. PhD thesis, University of Reading.

Thackeray, J.F., 1988. Molluscan fauna from Klasies River, South Africa. *The South African Archaeological Bulletin*, pp.27-32.

Thiele, J., 1911. Mollusken der deutschen Zentral-Afrika-Expedition. Wissenschaftliche Ergebnisse der deutschen Zentral-Afrika-Expedition, 1907–1908. *Band III, Zoologie I. Klinkhardt & Biermann, Leipzig*, pp.175–214.

van Bruggen, A.C., 1988. A record of the genus *Cerastua* (Mollusca, Gastropoda, Pulmonata: Enidae) from Zambia, with a preliminary list of the terrestrial molluscs of that country. *Proceedings of the Koninklijke Nederlandse Akademie van Wetenschappen, Series C*: *Biological and Medical Sciences, 91*, pp.1–17.

van Bruggen, A.C., 1993. *Cerastua* in the south revisited, a new taxon in Malawi and Zambia (Mollusca, Gastropoda, Pulmonata: Enidae). *Proceedings of the Koninklijke Nederlandse Akademie van Wetenschappen, Series C: Biological and Medical Sciences 96,* pp.143-149.

van Bruggen, A.C., 2008. New studies on the land molluscs of Malawi, a second interim progress report. Prolegomena for a new checklist. *Basteria 72,* pp.353-368.

van Bruggen, A.C. and Meredith H.M., 1984. A preliminary analysis of the land molluscs of Malawi. In: Solem A, van Bruggen AC (Eds) World-wide snails: Biogeographical studies on non-marine Mollusca. EJ Brill / W Backhuys, Leiden, pp.156–171.

van Damme, D. and Gautier, A., 2013. Lacustrine mollusc radiations in the Lake Malawi Basin: experiments in a natural laboratory for evolution. *Biogeosciences, 10*(9), pp.5767–5778.

Verdcourt, B., 2004, October. New and little known species of terrestrial Mollusca from East Africa and Congo (Kinshasa). In Annales historico-naturales Musei nationalis hungarici (Vol. 96, pp. 299-315).

Weij, R., Sniderman, J.K., Woodhead, J.D., Hellstrom, J.C., Brown, J.R., Drysdale, R.N., Reed, E., Bourne, S. and Gordon, J., 2024. Elevated Southern Hemisphere moisture availability during glacial periods. *Nature, 626*(7998), pp.319-326.

White, T.S., Bridgland, D.R., Limondin-Lozouet, N. and Schreve, D.C., 2017. Fossils from Quaternary fluvial archives: Sources of biostratigraphical, biogeographical and palaeoclimatic evidence. *Quaternary Science Reviews, 166*, pp.150-176.

Woodward, A.S., 1921. A new cave man from Rhodesia, South Africa. *Nature, 108*(2716), pp.371–372.

Wright, C.A., 1956. A note on the ecology of some Molluscan intermediate hosts of African schistosomiasis. *Annals of Tropical Medicine & Parasitology, 50*(4), pp.346–349.

Chapter 3. Investigating the potential of African land snail shells (Gastropoda: Achatininae) for amino acid geochronology

The fossil Achatininae analysed in this chapter resulted from the sediment extraction undertaken in chapter 2. Taxonomic identification of these specimens was undertaken by CB and TW; all laboratory analysis was undertaken by CB, with the exception of the 110 °C forced degradation experiments, which were undertaken by AB under the guidance of CB, MC and KP; the SEM image in figure 3.2 was undertaken by AB under the guidance of MC; all data analysis was carried out by CB with guidance from KP; interpretation and writing within the context of Palaeolake Kafue was carried out by CB with guidance from LB, MS, TW and KP; interpretation and writing within the context of the forced degradation experiments was carried out by CB with guidance from KP and LW.

The purpose of this study was to investigate whether common regional land snail shells extracted from the sediments associated with Palaeolake Kafue (chapter 2) would be appropriate for building regional amino acid geochronologies.

Authorship

Chloë Baldreki[1]*, Andrew Burnham[1], Martina Conti[1], Lucy Wheeler[1], Michael J. Simms[2], Lawrence Barham[3], Tom S. White[4], Kirsty Penkman[1]

[1] Department of Chemistry, University of York, UK
[2] Senior Curator of Geology, National Museums Northern Ireland
[3] Department of Archaeology, Classics and Egyptology, University of Liverpool, UK
[4] Principal Curator, non-Insect Invertebrates, Natural History Museum, London, UK

Abstract

Aragonitic calcium carbonate ($CaCO_3$) terrestrial mollusc shells with complex shell microstructures, such as those in the African subfamily Achatininae, have the potential to be used to build amino acid geochronologies across the African continent. However, as different microstructural shell layers are likely to have different protein compositions, sampling strategies need to be developed to identify the most appropriate shell portion to target. To test possible variability in

protein degradation rates between microstructural layers, sampling of a single microstructural shell layer (the 'nacreous' layer) was compared to sampling all three aragonitic layers ('3AL') in modern and fossil shells. Reliable isolation of the nacreous layer in all samples proved impractical, and additional complications arose due to mineral diagenesis induced by sampling with a drill. Pleistocene fossils of *Lissachatina* sp. and modern specimens of *Achatina tavaresiana* Morelet, 1866 were shown to have an intra-crystalline protein fraction. The 3AL shell portion adhered more closely to closed system behaviour in heated modern, and fossil, samples. The intra-crystalline protein degradation (IcPD) patterns of Achatininae fossil samples were not consistent with IcPD in forced degradation experiments at high temperatures in the laboratory. However, reliable degradation trends were observed in the 3AL shell portion, demonstrating the potential of fossil achatinids for building relative amino acid geochronologies across Africa.

Key words

AAR, racemisation, Quaternary, dating, gastropod shell, Africa

3.1. Introduction

The shells of non-marine molluscs have potential to be used for amino acid geochronologies (AAG), a dating technique which exploits the time-dependent diagenesis of proteins (e.g., racemisation, hydrolysis and degradation of amino acids) contained within biominerals (Abelson, 1955; Hare and Mitterer, 1967; Penkman *et al.*, 2008; Hearty and Kaufman, 2009). AAG studies within the African continent to date have primarily focussed on ostrich eggshell (e.g., Brooks *et al.*, 1990; Miller *et al.*, 1992; Murray-Wallace *et al.*, 2015), with a paucity of studies based on other biominerals. Globally, the shells of terrestrial gastropod molluscs have been used for AAG in various locations (e.g. *Actinella nitidiuscula* in Madeira (New *et al.*, 2019); *Trochoidea seetzeni* in Israel (Goodfriend, 1991); *Cerion* sp. in the Bahamas (Hearty and Kaufman, 2009); *Rabdotus mooreanus* in the USA (Ellis *et al.*, 1996) and a variety of taxa in Europe e.g. *Theba* sp. in the Canary Islands (Ortiz *et al.*, 2006) and *Trichia* sp. and *Cepea* sp. in the UK (Bowen *et al.*, 1989)), but in Africa very few studies based on terrestrial gastropod molluscs have been published (e.g. *Trophidophora* sp. land snails in South Africa (Roberts *et al.*, 2008)). There is therefore scope for developing amino acid geochronologies using understudied biominerals, such as the shells of common land snail species in the subfamily Achatininae, which occur across Africa (Fontanilla, 2010) and include regions where ostrich eggshell is not present (Barham and Debenham, 2000).

Achatininae is a subfamily of medium-large land snails native to the African continent. The sizable shells (up to 20 cm in some species) of achatinids have an extensive fossil record (Solem, 1979) that extends back at least as far as the Miocene (Pickford, 1995; Pickford 2008), with some probable

but contested records from the Eocene (Neubert and van Damme, 2012; Pickford *et al.*, 2014; Hammouda, *et al.*, 2017). Achatininae fossils have the potential to provide both palaeoecological and palaeoclimatic data (White *et al.*, 2017; Taylor *et al.*, 2011), as well as age estimation, for example via radiocarbon dating (e.g., Wojcieszak *et al.*, 2023 and references therein) and AAG. Species of the genus *Achatina* (Fig. 3.1A) have a current distribution across sub-Saharan West Africa (Fontanilla, 2010; *contra* older works such as Hodasi, 1984; Raut and Barker, 2002), while those of the genus *Lissachatina* (Fig. 3.1B) occur in central-eastern Africa (Fontanilla, 2010). Achatinids occupy a wide range of habitats, from equatorial rainforest to open savannah and the semi-desert environments of south and southwest Africa. Some, most notably *Lissachatina fulica* Bowdich, 1822, have become invasive crop-pests where introduced in many other parts of the world (Vijayan *et al.*, 2022), leading to the suggestion that they could represent useful index fossils for the Anthropocene (Hausdorf, 2018).
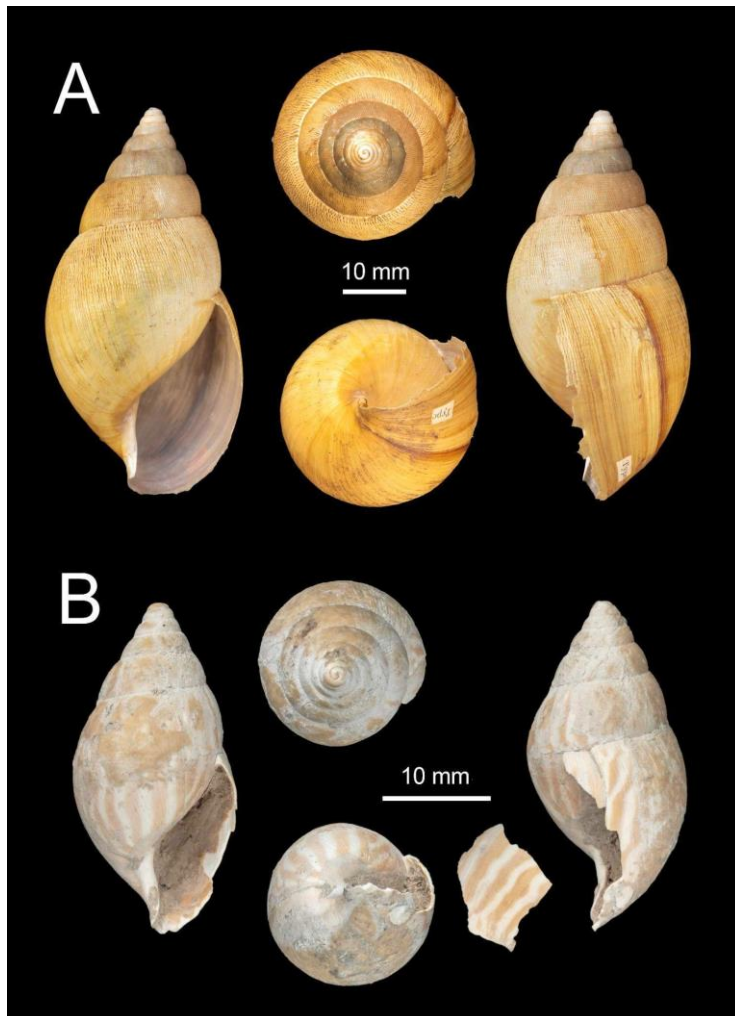
Figure 3.1. A - *Achatina tavaresiana* Morelet, 1866 (syntype, NHMUK 1893.2.4.151). B - *Lissachatina* sp. (fossil specimen PK.S19.4, from Palaeolake Kafue (Site 19) near Twin Rivers kopje).

The shells of achatinid land snails consist of a CaCO$_3$ biomineral with an aragonitic crystal structure (de Paula and Silveira, 2009). In this study, shells of modern *Achatina tavaresiana* were observed to contain the same four-layered microstructure (Fig. 3.2) as those previously reported for *Lissachatina fulica* (Chaki *et al.*, 1992). The microstructural layers, visible by scanning electron microscopy (SEM), include the periostracum (composed primarily of organic material and easily removed using a Dremel drill) and three aragonitic CaCO$_3$ layers (in this study termed '3AL': prismatic, cross-lamellar and nacreous).
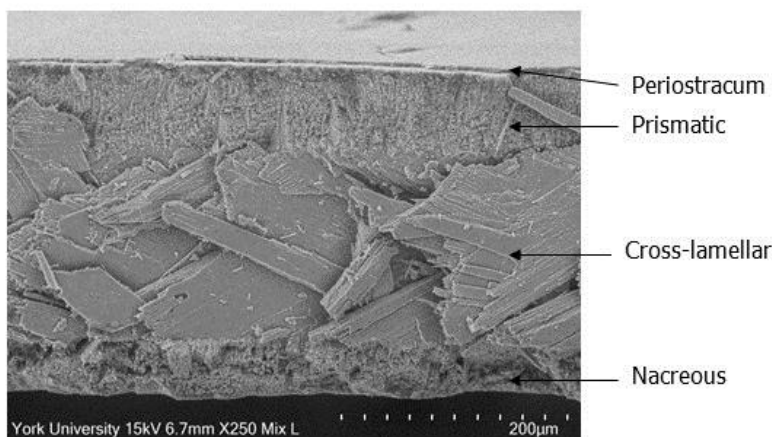
Figure 3.2. SEM image (x250) of a modern *Achatina tavaresiana* shell, showing four microstructural layers: the periostracum, prismatic, cross-lamellar and nacreous.

The complex structures of achatinid shells, and indeed those of many other mollusc taxa (e.g. the bivalve genera *Mytilus* (Hare, 1963), *Arctica* (Haugen and Sejrup, 1990) and *Glycymeris* (Demarchi *et al.*, 2015; Ortiz *et al.*, 2017)) presents two major challenges for AAG. The first is the possibility of microstructural protein differences: if different proteins control the architecture of the three aragonitic microstructural layers, then intra-specimen and/or inter-individual differences in the relative proportions of each layer would lead to variations in the relative abundance of these proteins. If these proteins break down at different rates due to differences in their peptide sequences (Smith and Evans, 1980; Mitterer and Kriausakul, 1984; Ortiz *et al.*, 2013), the chronological signal obtained from protein diagenesis could become convoluted (Ortiz *et al.*, 2013). The second challenge relates to mineral stability; aragonite is a metastable polymorph of calcium carbonate, which although kinetically stable can undergo conversion to the calcite polymorph over geological timescales (Brand and Morrison, 1987). Polymorphic conversion can lead to any originally entrapped amino acids not adhering to closed system behaviour and becoming compromised during rearrangement (opening and subsequent closing) of the crystal structure (Penkman *et al.*, 2007; Penkman *et al.*, 2010). To assess the potential impact of these issues, this study analysed samples taken from a single layer

(nacreous) and from across all three aragonitic layers (3AL: prismatic, cross-lamellar and nacreous; Fig. 3.2). The nacreous layer was selected due to sampling practicalities. Being the innermost layer, it was the easiest to obtain, with reliable sampling of the cross-lamellar and prismatic layers rendered impractical due to the overall thinness of the shell (~ 250 µm, Fig.3.2).

One AAG approach shown to improve the reliability of the data in some mollusc shells is intra-crystalline protein degradation (IcPD) analysis. This approach targets protein trapped within the crystal matrix of biominerals, which may be isolated with a strong chemical oxidant (Sykes *et al.*, 1995). This intra-crystalline protein fraction has been shown to operate as a closed system in many biominerals (e.g. gastropods (Penkman *et al.*, 2008; Demarchi *et al.*, 2013a), ostrich eggshell (Crisp *et al.*, 2013), coral (Hendy *et al.*, 2012), tooth enamel (Dickinson *et al.*, 2019) and the calcareous tests of foraminifera (Millman *et al.*, 2022)), and where this is the case, leaching of endogenous protein, contamination by exogenous protein and additional environmental impacts on protein degradation are minimised (Smith, 1987; Towe, 1980). In some biominerals, the IcPD approach to AAG has been shown to improve both the accuracy and precision of the data, increasing the reliability and robustness of the geochronologies obtained (Sykes *et al.*, 1995; Penkman *et al.*, 2008; Bosch *et al.*, 2015; Ortiz *et al.*, 2015). Oxidative treatment, however, is not always appropriate or necessary and, in these cases, stringent data screening approaches have also been used successfully for many AAG studies (e.g. Kaufman, 2006; Kosnik *et al.*, 2008; Ortiz *et al.*, 2018).

In this study we therefore evaluate the suitability of different shell layers in Achatininae shell for AAG using IcPD analysis and consider its potential to build amino acid geochronologies across Africa in the future. We assess two sampling strategies (single layer vs multi-layer) and investigate mineral stability by XRD analysis (section 3.3.1.3). We investigate whether an intra-crystalline fraction of protein is present via bleaching experiments (section 3.3.1.1), and whether this fraction behaves as a closed system through analysis of IcPD in forced degradation experiments on modern shells, and within fossils of Middle Pleistocene age (section 3.3.1.2). Finally, we evaluate the ability of these elevated temperature experiments to mimic the protein degradation observed in achatinid fossils, and therefore whether it is possible to use kinetic parameters derived from high temperature experiments to estimate age or burial temperature in Achatininae (section 3.2.2, SI section 3.5.4.).

3.2. Materials and Methods

3.2.1. Materials

In this study four modern and seven fossil specimens were sampled (table 3.1; in the absence of a universally accepted definition of the term "fossil", here we use the term to refer to preserved shell material within sediment). The modern specimens, obtained from historical collections in the Natural History Museum, London (NHM), all represent the West African species *Achatina taveresiana* Morelet, 1866. No record was made about how these specimens were collected, but the usual practice for high quality museum specimens is live collection and their pristine condition suggests this was the case. This species was chosen because shells identified as *A. tavaresiana* had previously been recorded from the Palaeolake Kafue (formerly known as Palaeolake Patrick) sequence (Simms, 2000). The fossils included in this study originated from sediments associated with Palaeolake Kafue (Site 19 chalky limestone (Fig. 3.3B), described in detail in SI section 3.5.1), close to the Twin Rivers archaeological site in Zambia. The internal stratigraphic position of the molluscs within the chalky limestone was not recorded, although those recovered *in situ* were all from about the top 30 cm of the deposit. The fossil achatinid shells studied here are therefore considered as a single time-equivalent population, although may span a considerable time window.

The age of these lacustrine limestones is poorly constrained, but some inferences can be made from radiometric dates recovered from two nearby sites: the Twin Rivers kopje and the Casavera Stream, both on the margins of Palaeolake Kafue. Various uranium-series (U-series) dates from Twin Rivers were obtained from calcite speleothem layers, ranging from >400 ka to ~140 ka. Two other U-series dates have been published for the Casavera stream 'fossil' tufa deposits (near Site 1, Fig. 3.3B) and these have an age range of ~200–400 ka (Barham *et al*., 2000: 179). An in-depth discussion of contextual information about the palaeolake and its dating is provided in the SI (section 3.5.1). While it is not currently possible to further constrain the Site 19 sediments in age, from all the available information they are assumed to be Middle Pleistocene.
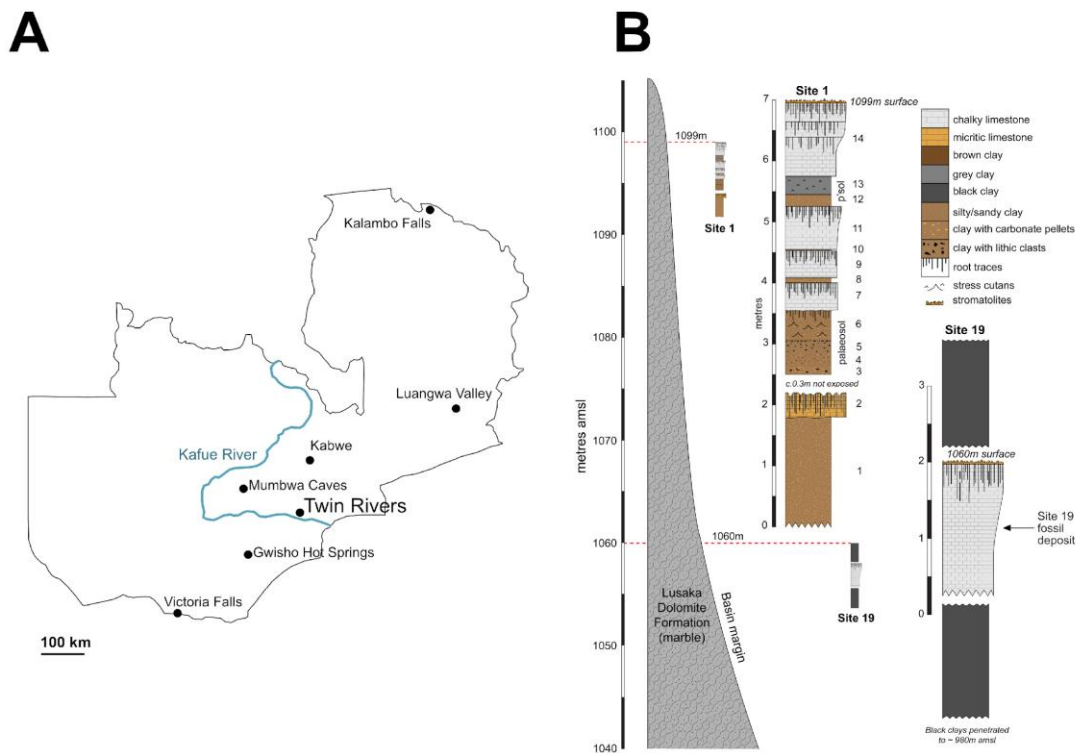
Figure 3.3. A - Map of Zambia highlighting key archaeological sites and the modern Kafue River course. B – Stratigraphic sections showing the relationship between two relevant Palaeolake Kafue sites: Site 1, and Site 19. The fossils analysed in this study came from a single chalky limestone stratigraphic section (arrowed) within Site 19. Site 19 (S15˚33'21.1", E28˚02'50.1", altitude 1060 m amsl) is associated with Palaeolake Kafue, close to Twin Rivers archaeological site (S15°31, E28°11).

Because of significant restrictions on in-person research and access to museum collections caused by the COVID-19 pandemic in 2020 and 2021, formal identification of the fossil specimens was only possible after the laboratory experiments had been carried out. The fossils were identified as *Lissachatina* sp*.* based on the known biogeography of Achatininae, although the worn condition of the fossils and difficulty in using shell characters to identify achatinids prevented species-level identification (Mead, 1991; chapter 2). Shell specimens previously identified as *A. tavaresiana* from the Palaeolake Kafue sequences (Simms, 2000) were examined, but it is not clear which of these were used to diagnose *A. tavaresiana* and the surviving specimens were either small fragments of shell or internal casts that could not be identified to species level. Given the known distributions of *Achatina* and *Lissachatina*, their previous identification is unlikely to be correct. Regardless, the species represented are assumed to be sufficiently closely related within the subfamily Achatininae for comparative IcPD analysis.

Table 3.1. Modern *Achatina tavaresiana* samples obtained from the Natural History Museum (NHM), London, and fossil *Lissachatina* sp. samples now archived in Livingstone Museum, Zambia, analysed in this study.

Sample ID	Museum registration number	Locality	Specimen type
PK.S19.3	ZM.LV.AR.9887	Site 19, Palaeolake Kafue	fossil
PK.S19.4	ZM.LV.AR.9888	Site 19, Palaeolake Kafue	fossil
PK.S19.20.1	ZM.LV.AR.9889	Site 19, Palaeolake Kafue	fossil
PK.S19.44	ZM.LV.AR.9890	Site 19, Palaeolake Kafue	fossil
PK.S19.45	ZM.LV.AR.9891	Site 19, Palaeolake Kafue	fossil
PK.S19.47	ZM.LV.AR.9892	Site 19, Palaeolake Kafue	fossil
PK.S19.48	ZM.LV.AR.9893	Site 19, Palaeolake Kafue	fossil
MA.NHM.UG.1	NHMUK20230327	Uganda	modern
MA.NHM.SC.1	NHMUK20230328	Seychelles	modern
MA.NHM.MR.1	NHMUK20230329	Mauritius	modern
MA.NHM.TZ.1	NHMUK20230330	Tanzania	modern

Modern ostrich eggshell (OES) and shells of the terrestrial gastropod *Cepaea* sp. were used as calcite and aragonite $CaCO_3$ XRD reference material respectively (Feng *et al.*, 2001; Kowalewska-Groszkowska *et al.*, 2018).

3.2.2. Fossil cleaning

All fossil Achatininae shells excavated from Site 19 were filled with solidified sediment. The shells were soaked in water and where possible, the sediment manually removed. The outermost shell whorl of each fossil specimen was taken for sampling.

3.2.3. Sampling

In order to identify an optimal sampling strategy, all shells in this study (four modern (for bleaching and elevated temperature experiments) and seven fossil specimens) were sampled for both their nacreous and three aragonitic layer (3AL) shell portions (table 3.1). Shell periostracum was removed with an abrasive rotary burr on a handheld rotary tool (Dremel drill). The shell was washed and sonicated in water (ultrapure, 18.2 MΩ cm^{-1}) to remove any remaining powder before being air-dried. All specimens were sampled on the outermost whorl of each shell. Two shell portions were sampled from separate areas of this outermost whorl: the three aragonitic layers (3AL; comprising the prismatic, cross-lamellar and nacreous layers) and the nacreous layer. The 3AL portion was finely powdered with an agate pestle and mortar. The nacreous was removed from a separate area of each shell with an abrasive rotary burr on a handheld rotary tool (Dremel drill) and collected as a very fine powder. A cautious approach to removal of the nacreous was undertaken, but, since the

microstructural layers were difficult to view both by eye and under standard laboratory microscope magnification, it is therefore possible non-nacreous layers were also incorporated. For this reason, this shell portion is termed the 'nacreous'. Whilst particle size has been shown to affect the variability of data obtained for coarse particles (500-1000 µm) in some shell species (e.g. *Patella*, Demarchi *et al.*, 2013a), Penkman *et al.*, (2008) found that particle size was shown not to affect the final concentration, the rate at which the intra-crystalline fraction was reached, or the data variability for shells of the bivalves *Corbicula* and *Margaritifera* or the gastropod *Bithynia*. As a fine powder (< 500 µm by eye) was collected for both the 3AL and 'nacreous' shell portions, no sieving was undertaken, in order to minimise the risk of loss of valuable material which occurs during the sieving process.

3.2.4. Isolation of the intra-crystalline protein fraction

To test whether an intra-crystalline fraction of protein was present within modern *A. tavaresiana* shell, bleaching experiments were undertaken following adapted methods of Sykes *et al.*, (1995) and Penkman *et al.*, (2008). Bleach (a strong chemical oxidant - 12% NaOCl (Fisher Scientific, analytical grade), 50 µL/mg) was added to ca. 20 mg of powdered sample (in separate 2 mL plastic microcentrifuge tubes (Eppendorf)) and left on a rotor (constant, mild agitation) for 24, 48 and 72 hours, to test the impacts of bleaching time. The bleach was removed by pipette and each sample was washed five times with water (ultrapure, 18.2 MΩ cm^{-1}), before a final wash with methanol (Sigma-Aldrich, HPLC-grade) and left to air dry. Given the results presented in section 3.3.1.1, for all subsequent elevated temperature and fossil IcPD analysis, an optimised bleaching time of 48 hours was used.

3.2.5. Elevated temperature experiments

Elevated temperature experiments on modern biominerals have routinely been used to investigate protein degradation on an accelerated timescale for comparative analysis to the geological diagenesis observed in fossils (e.g., Bada and Schroeder, 1972; Kimber and Griffin, 1987; Canoira *et al.*, 2003; Penkman *et al.*, 2008; Demarchi *et al.*, 2013a; Tomiak *et al.*, 2013; Ortiz *et al.*, 2017; Dickinson *et al.*, 2019).

Following powdering (section 3.2.3) and bleaching (section 3.2.4), approximately 10 mg of modern shell was suspended in 300 µL water (ultrapure, 18.2 MΩ cm^{-1}) and isothermally heated for the times and temperatures given in table 3.2. These samples were undertaken in experimental triplicate. 300 µL of water was used to enable comparative analysis to previous studies (e.g., Penkman *et al.*, 2008; Demarchi *et al.*, 2013a; Tomiak *et al.*, 2013; Crisp *et al.*, 2013) and the conditions are assumed not to affect the intra-crystalline fraction of protein, where closed-system behaviour has been

adhered to. The water was removed by pipette and the samples were left to air dry prior to preparation for analysis (section 3.2.6).

Table 3.2. Elevated temperature experiment conditions for the 3AL and 'nacreous' portions of modern *Achatina* shell. Due to sample constraints, only the two starred heating times at 140 °C were undertaken for *Achatina* 'nacreous'.

Temperature (°C)	Heating time (days)																
60	-	-	-	-	-	-	-	-	-	50	90	150	-	240	365	417	548
70	-	-	-	-	-	-	20	-	-	50	-	150	-	240	365	-	548
80	-	-	-	-	-	10	20	30	-	50	90	150	200	240	365	-	548
110	-	1	-	-	5	10	20	30	40	50	-	-	-	-	-	-	-
140	0.08	1*	2	3*	-	-	-	-	-	-	-	-	-	-	-	-	-

3.2.6. Amino acid analysis

Following the methods of Penkman *et al*., (2008), *ca*. 5 mg (accurate masses recorded) subsamples were weighed out for analysis of the free amino acid fraction (FAA) and the total hydrolysable amino acid fraction (THAA). FAA subsamples were demineralised in 2 M HCl (minimum possible volume) and placed into a centrifugal evaporator for *ca*. 24 hours. THAA subsamples were demineralised in 7 M HCl (20 µL/mg), the vials flushed with N_2 and heated to 110 °C for 24 hours, prior to drying in a centrifugal evaporator (*ca*. 24 hours). All subsamples were rehydrated (10 µL/mg) in a solution of internal standard (L-homo-arginine, 0.01 M), hydrochloric acid (0.01 M) and sodium azide (1.5 mM). Separation of the chiral isomers of the amino acids was carried out by fluorescence detection reverse phase high performance liquid chromatography (RP-HPLC; Fig. 3.4) using a modified Kaufman and Manley (1998) method (Penkman, 2005). As experimental replicates were prepared, no analytical replicates were undertaken; analytical replicates have been shown to account for only a small portion of the total variability, hence the use of subsample experimental replicates also encompasses analytical variability (Powell *et al.*, 2013).
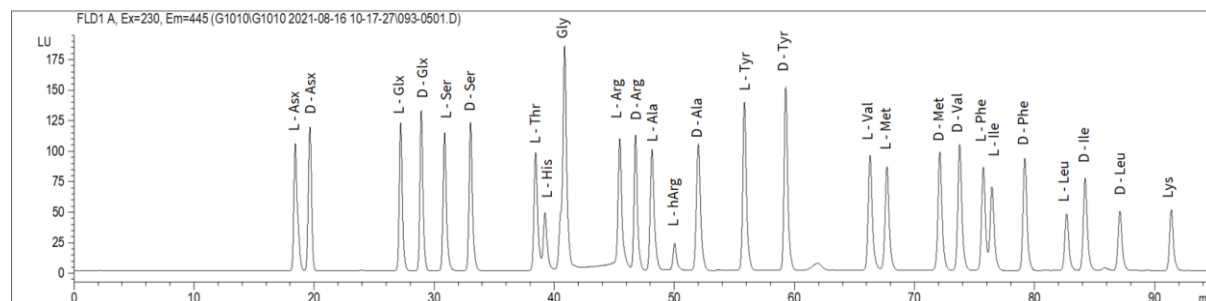
Figure 3.4. Example chromatogram of a standard.

Total amino acid concentration and relative composition calculations were carried out for Asx, Glx, Ser, L-Thr, L-His, Gly, Arg, Ala, Tyr, Val, Met, Phe, Ile and Leu. In the case of Thr and His only the L enantiomer is resolved by this chromatographic method, whilst Gly contains no stereogenic centre and therefore does not have L/D enantiomers (Fig. 3.4). Sufficient concentration and chromatographic resolution were achieved for the calculation of racemisation and percentage free values for Asx, Glx, Ser, Ala, Val, Phe within the achatinid shells (see SI Data).

3.2.7. Assessment of mineral diagenesis

Crystal structure polymorphism was analysed by X-ray diffraction (XRD) analysis. This was to test for mineral diagenesis, specifically the conversion of aragonite, the metastable polymorph of $CaCO_3$, to calcite, as mineral diagenesis can result in the targeted intra-crystalline protein becoming compromised from rearrangement (opening and subsequent closing) of the crystal structure (Preece and Penkman, 2005; Penkman *et al*., 2010). Analysis was undertaken on two instruments (due to availability at time of analysis of the samples). Approximately 10 mg of powdered sample was flattened onto a specimen holder (Malvern or Bruker silicon single crystal low background specimen folder for small specimen amounts) with a glass microscope slide. XRD analysis was carried out using two methods adapted from Lesbani *et al*., (2013). On the Pananalytical Eeris diffractometer, each sample was scanned between 5 – 70° 2θ at a scanning speed of 0.2° s^{-1}; on the Bruker D8 diffractometer, each sample was scanned between 0 – 120° 2θ using a 0.05 degree increment with a measurement time of 0.1 seconds per step.

3.3. Results and Discussion

3.3.1. Assessment of suitability for IcPD analysis

3.3.1.1. Assessment of intra-crystalline protein fraction - bleaching experiments

Bleaching experiments were undertaken to first assess whether an intra-crystalline fraction of protein was present within achatinid shell, and if so, to determine the optimal exposure time. The concentration of all hydrolysable amino acids decreased within both the 3AL shell portion and the 'nacreous' layer of *A. tavaresiana* shell post-exposure to bleach (Fig. 3.5, SI Fig. 3.1). No appreciable difference in concentration was observed between the bleach times investigated. The stable concentrations of amino acids remaining post-bleaching are therefore hypothesised to be the protected intra-crystalline fraction (Sykes *et al*., 1995), with the unbleached samples also containing an inter-crystalline fraction that is exposed to the environment.
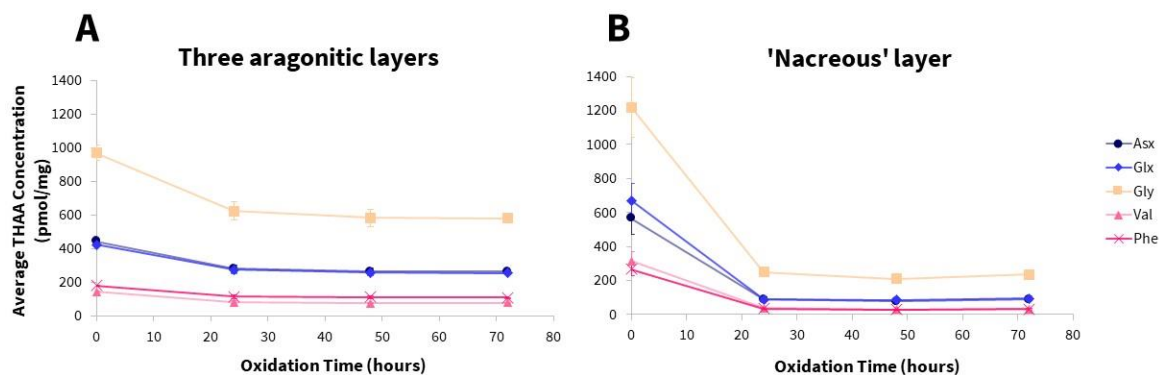
Figure 3.5. Average THAA concentration for five example amino acids in modern *Achatina tavaresiana* shell portions (A - 3AL, B - 'nacreous' layer); powdered shell was analysed unbleached (0 hours) and exposed to NaOCl, strong chemical oxidant, for 24, 48 and 72 hours. Error bars represent the standard deviation about the mean for subsample experimental triplicates. Within 24 hours a decreased, stable concentration of amino acids was achieved in both shell portions, defined as the intra-crystalline protein fraction.

No significant differences in protein composition were observed between the unbleached and any of the bleached (24, 48 and 72 hours) 3AL shell samples (Fig. 3.6A). It is therefore likely that the inter- and intra-crystalline protein fractions contain similar protein compositions and have minimal contamination in these samples. There was, however, a difference in composition upon bleaching for the 'nacreous' samples (Fig. 3.6B). This could be due to different proteins within the inter- and intra-crystalline fractions, and/or as a result of the sampling method of obtaining Achatininae 'nacreous'. As the 'nacreous' is drilled off the shell as a powder (unlike 3AL shell sampling which uses a pestle and mortar), contamination from proteins within the cross-lamellar layer is possible. Nonetheless, it is worth noting that minimal differences were observed between the samples which were bleached for 24, 48 and 72 hours (Fig. 3.6B), indicating the bleach successfully removed any contamination and the inter-crystalline protein from the 'nacreous' sample.

As far as we are aware, no studies have been undertaken to characterise the proteins in the individual microstructural layers of achatinid shell. The differences in relative amino acid abundance between 3AL shell portion and 'nacreous' (Fig. 3.6, e.g. Gly 24% ± 1% in the 3AL and 29% ± 1% in the 'nacreous', for all samples exposed to bleach) can therefore be used to indicate a difference in protein composition between the two shell portions.

119
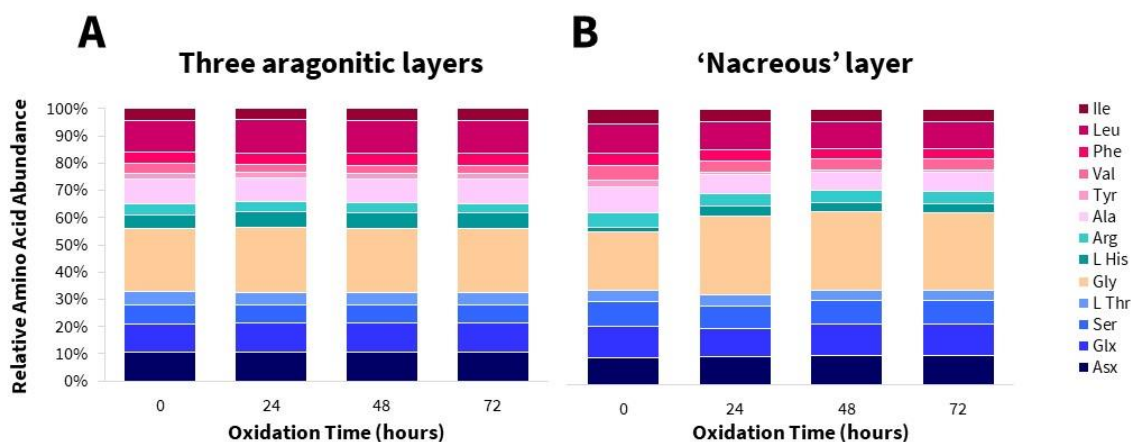
Figure 3.6. Relative amino acid composition of the THAA fraction in modern *Achatina tavaresiana* shell portions (A - 3AL, B - 'nacreous' layer) after the shell was exposed to NaOCl, a strong chemical oxidant, for 0, 24, 48 and 72 hours.

The bleaching experiments therefore indicate that an intra-crystalline fraction of protein is present within Achatininae shell, which was successfully isolated by exposure to NaOCl, a strong chemical oxidant. For all subsequent experiments and analyses, a bleaching time of 48 hours was chosen, consistent with methodologies of other shell material (Penkman *et al*., 2008; Demarchi *et al*., 2013a).

3.3.1.2. Assessment of closed system behaviour

After establishing that Achatininae shell has an intra-crystalline fraction of protein present within the 'nacreous' and 3AL shell portions (section 3.3.1.1), we then assessed whether degradation within this fraction was consistent with closed-system behaviour.

3.3.1.2.1. Elevated temperature kinetic experiments – racemisation and hydrolysis

Elevated temperature kinetic experiments are used to investigate protein degradation on an accelerated timescale for comparison with the diagenesis observed in fossils (e.g., Bada, 1972; Kriausakul and Mitterer, 1978; Kimber and Griffin, 1987; Canoira *et al.,* 2003; Kaufman, 2006; Clarke and Murray-Wallace, 2006) and can also be used to test closed-system behaviour of any intra-crystalline protein fraction (Penkman *et al.,* 2008; Hendy *et al*., 2012; Demarchi *et al.*, 2013a; Dickinson *et al*., 2019). In achatinid shell, it is likely that different proteins are contained within the different aragonitic layers (prismatic, cross-lamellar and nacreous) as a result of having controlled the distinct $CaCO_3$ architecture (section 3.3.1.1). The peptide sequence, unique to each protein, influences protein degradation and rates of amino acid racemisation (Smith and Evans, 1980; Mitterer and Kriausakul, 1984; Ortiz *et al*., 2013). As sampling was undertaken on both the 3AL shell portion and the 'nacreous'

layer, elevated temperature experiments can therefore also be used to investigate the protein degradation within different microstructural shell portions.

As expected for protein degradation, at each elevated temperature, the extent of racemisation increased with time for all amino acids (Figs. 3.7 and 3.8, SI Figs. 3.2 and 3.3). In general, greater variability in the extent of racemisation (D/L) was observed for amino acids in the 'nacreous' layer in comparison to the 3AL shell portion (e.g., Fig. 3.7). This may be a sampling issue (section 3.2.3) or because the 'nacreous' intra-crystalline protein fraction doesn't operate as a closed system (Ortiz *et al.*, 2017; Wheeler *at al.*, 2021). For the majority of the temperatures (Fig. 3.7, SI Fig. 3.2), similar trends for both the 3AL and 'nacreous' layer were observed to the reported relative racemisation rates for free amino acids (Asp>Phe>Ala>Glu>Val) (Smith and Evans, 1980). In proteins, with the exception of Ser and Asx (Demarchi *et al.*, 2013b), the majority of amino acids are not able to freely racemise in chain, requiring greater conformational freedom (terminal or free) to do so. Any differences in the relative rates of racemisation here (in comparison to free amino acids) are likely as a result of additional influential factors for proteins within biominerals, such as the peptide sequence and biomineral interactions (e.g., Demarchi *et al.*, 2016).
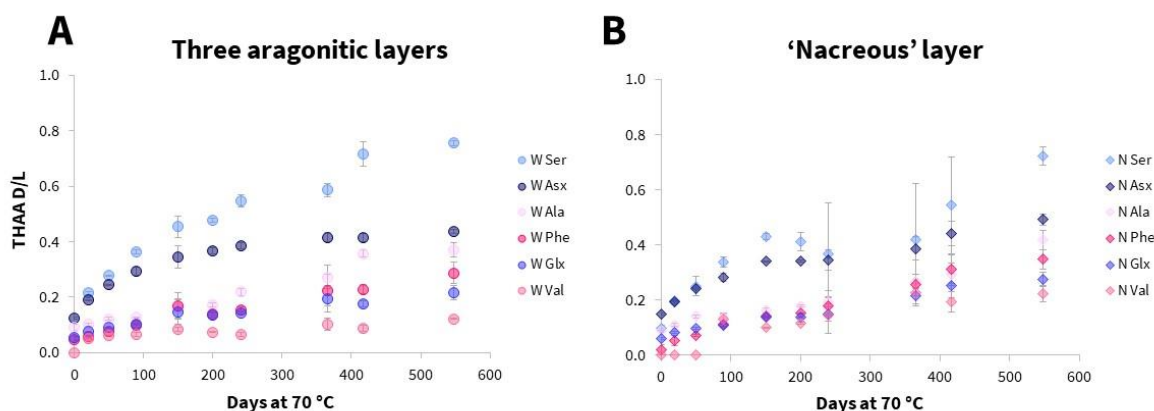
Figure 3.7. The extent of racemisation for the hydrolysable amino acids in the 3AL shell portion (A) and the 'nacreous' layer (B) of modern *Achatina tavaresiana* shell, during isothermal heating at 70 °C. Error bars represent the standard deviation about the mean for subsample experimental triplicates. An increase in racemisation was observed for all amino acids, at different relative rates.

Additionally, as expected the extent of racemisation (D/L) increased for all amino acids with increasing temperature (e.g., Asx in Fig. 3.8A, SI Fig. 3.3). Similar patterns of degradation were also observed for peptide chain hydrolysis (e.g., Asx in Fig. 3.8B, SI Fig. 3.4). Interestingly, at 70°C and 80°C, Asx in the 3AL appeared to hydrolyse much faster than in the 'nacreous' layer (Fig. 3.8B). At 110 °C, Asx in the 3AL also showed a different hydrolysis pattern to the 'nacreous' layer (Fig. 3.8B). These temperature-related differences were also observed for the other amino acids studied (Glx, Ser, Ala,

Val, Phe; SI Fig. 3.4). Differences between the 'nacreous' layer and 3AL peptide chain hydrolysis rates may be because of primary protein sequence differences (with respect to both the relative peptide bond strengths arising from different neighbouring amino acids in the peptide chain (Hill, 1965), and/or to the different mineral surface interactions and solvent (water) effects (Demarchi *et al.*, 2016)).
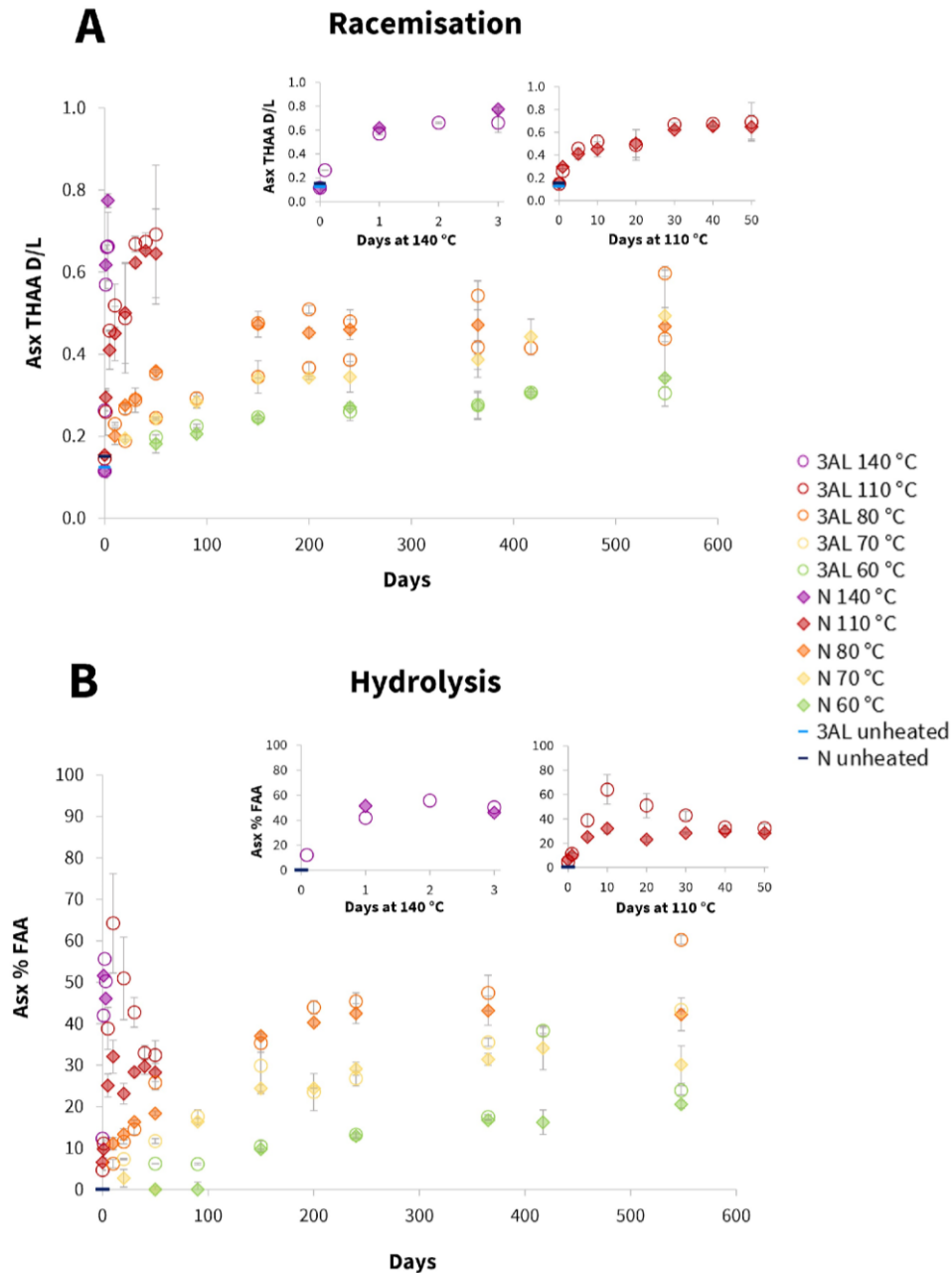
Figure 3.8. The extent of racemisation (A) and peptide chain hydrolysis (B) in Asx in bleached of modern *Achatina tavaresiana* shell during isothermal heating at 60, 70, 80, 110 and 140 °C. Error bars represent the standard deviation about the mean for subsample experimental triplicates. An increase in racemisation and hydrolysis was observed for Asx in respect to both time and temperature.

3.3.1.2.2. FAA vs THAA in artificially degraded shells and fossils

From IcPD analysis, closed system behaviour can be inferred in several ways including from a strong positive correlation between the FAA and THAA extent of racemisation (Penkman *et al.*, 2008). In general, the 3AL displayed a stronger positive correlation between the free and hydrolysable amino acid fractions for the majority of amino acids (four best chromatographically separated amino acids given in Fig. 3.9), in both modern heated and fossil samples. Greater variability in the extent of racemisation was observed in the 'nacreous', especially within the THAA for both the modern heated and fossil samples (Fig. 3.9), indicating either inconsistent sampling or poorer adherence to closed-system behaviour (discussed in detail below in sections 3.3.1.3-4).
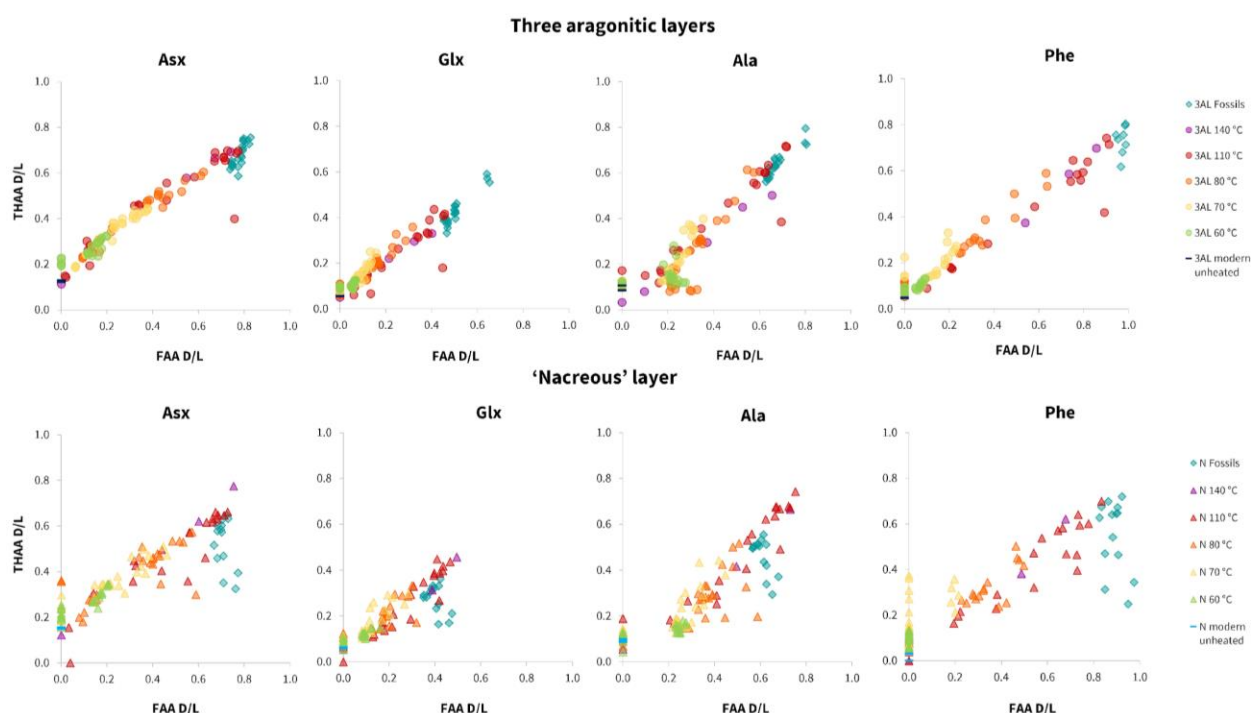
Figure 3.9. Intra-crystalline free (FAA) vs total hydrolysable (THAA) racemisation values (D/L) in four amino acids (Asx, Glx, Ala, Phe) from elevated temperature experiments on modern *Achatina tavaresiana* shell at 60, 70, 80, 110, and 140 °C and unheated, and from *Lissachatina* sp. fossils. Upper: 3AL; lower: 'nacreous' layer. For any data points plotted at 0 (on the x and/or y axis), the concentration of the D isomer was below the limit of detection.

A range of relatively high racemisation values were obtained for the fossil *Lissachatina* sp. samples (Fig. 3.9), either because they represent a range of ages within the Middle Pleistocene (consistent with section 3.2.1 and SI section 3.1) and/or resulting from the fossils having experienced different temperature histories. The latter may occur for fossils of similar age which have experienced different integrated burial temperatures (Wehmiller *et al.*, 2000) or through heating events such as cooking (Wojcieszak *et al.*, 2023). Consideration of temperature histories is therefore an important

factor to consider for future studies where relative chronologies, which rely on the extent of racemisation as a marker for regional time, are being built. However, as these fossil samples are used to represent naturally aged samples (rather than being of known specific ages), their data is useful here for making comparisons to experimentally degraded material.

3.3.1.2.3. Shell microstructural layer differences between modern heated and fossils

During elevated temperature experiments, the majority of amino acids from both the 3AL and 'nacreous' layer racemised at a similar relative rate between 60 °C (Fig. 3.10B) — 110 °C. One exception was observed, valine, which racemised more quickly in the 'nacreous' layer at every temperature (e.g., Fig. 3.10A and 3.10B). At 140 °C, systematic differences in the extent of relative racemisation were observed between the 3AL and 'nacreous' layer for a number of amino acids (Fig. 3.10A). The naturally degraded fossils showed a different trend to the elevated temperature experiments, contrary to the 140 °C data, with the majority of amino acids more highly racemised in the 3AL shell portion than in the nacreous layer (Fig. 3.10C). There are a few possible reasons for this. One explanation is that the conditions used for the accelerated degradation experiments (powdered, bleached shell in water) don't reflect the environmental degradation conditions experienced by shells (here from Site 19 chalky limestone, Fig. 3.2B), and therefore the degradation mechanisms may be influenced by these environmental differences. However, this would not be the case if the intra-crystalline fraction of protein within achatinid shell truly displayed closed-system behaviour, as theoretically all external influences except temperature are removed. Another explanation for the divergent relative racemisation rates at different temperatures, is that different protein degradation mechanisms may be occurring at high temperatures compared to those experienced by the fossils at lower environmental temperatures; this has been observed before in other biominerals (e.g. coral (Tomiak *et al.*, 2013) and the marine bivalve *Pecten* (Pierini *et al.*, 2016)).

124
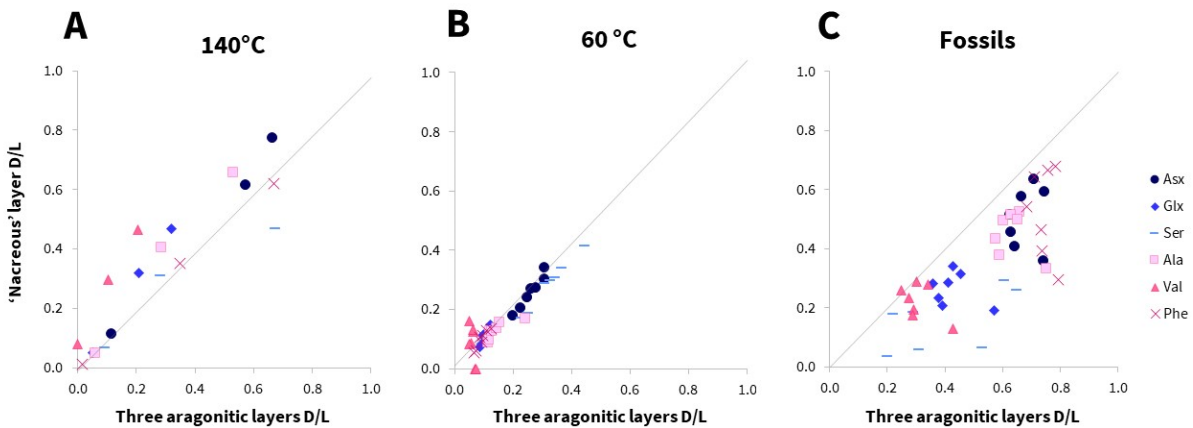
Figure 3.10. Comparison between the mean extent of racemisation for THAA of modern *Achatina tavaresiana* shell during elevated temperature experiments at 140 °C (A) and 60 °C (B) and *Lissachatina* sp. fossils (C). The central grey line marks a theoretical 1:1 ratio; for data above this, amino acids are racemising quicker in the 'nacreous' layer; below, those in the 3AL are faster. Importantly this relationship changes between the high temperature experiments and fossil samples at lower burial temperatures.

For the 3AL, the relative amino acid compositions of the fossil shells were largely comparable to those with similar extents of Glx racemisation from the heating experiments and dissimilar to the modern, unheated sample (Fig. 3.11A). These include markers of protein degradation such as the decomposition of Ser to Ala (Bada *et al.*, 1978), with lower %Ser and higher %Ala for increasingly degraded samples (SI Fig. 3.6). The total amino acid concentrations observed in the fossils were in general lower than those observed in the modern heated samples, but not dissimilar to the concentrations observed to those heated to 60, 70 and 80 °C for the longer time periods (SI Fig. 3.5). This further indicates that the intra-crystalline fraction of the 3AL shell portion behaves as a closed system. The concentration (SI Fig. 3.5) and relative composition of the 'nacreous' layer shell portion (Fig. 3.11B) was more variable between fossils; when considered in combination with the wider spread of racemisation values observed (Fig. 3.9), it is likely that the protein in this shell portion is a less reliable marker of time for building AAGs than the 3AL shell portion.
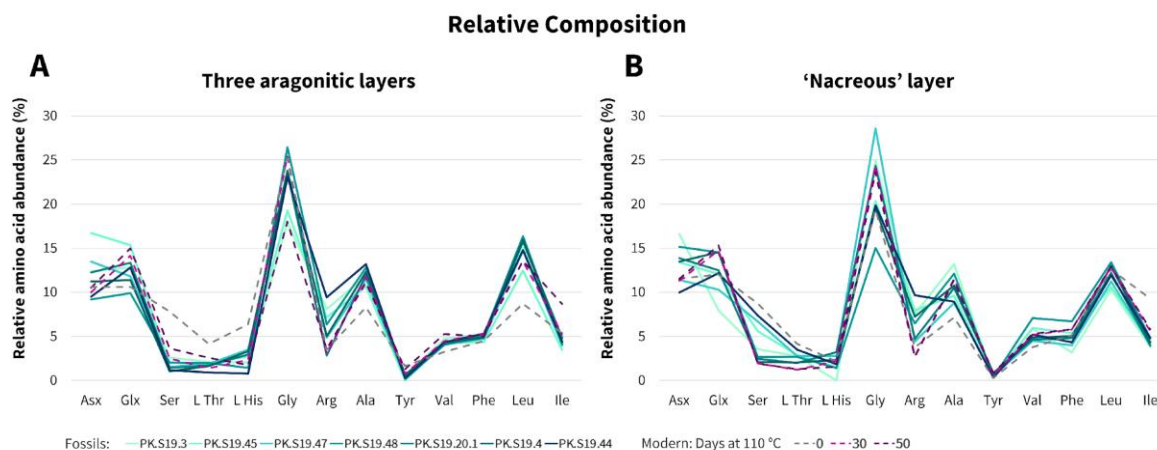
Figure 3.11. Comparison of the mean relative amino acid abundances for the total hydrolysable amino acids (THAA) in the 3AL (A) and 'nacreous' (B) shell portions of the *Lissachatina* sp*.* fossil samples and *Achatina tavaresiana* modern unheated and samples with similar extents of Glx racemisation from heating to 110 °C. The fossil samples have been colour-coded in order of increasing extent of Glx racemisation from the 3AL shell portion (darker teal = higher Glx D/L).

The apparent adherence to closed-system behaviour in the 3AL showcases the potential suitability of 3AL portion of Achatininae shell for future IcPD analysis to build regional AAGs across Africa.

3.3.1.3. Assessment of mineral diagenesis

XRD analysis was undertaken to assess the aragonitic CaCO$_3$ crystal structure of modern and fossil Achatininae (de Paula and Silveira, 2009). Whilst kinetically stable, aragonite may undergo conversion to the calcite polymorph over geological timescales (Brand and Morrison, 1987), potentially leading to the target intra-crystalline fraction of amino acids becoming compromised from rearrangement (opening and subsequent closing) of the crystal structure (Penkman *et al*., 2010). XRD analysis of the powdered (via drilling for 'nacreous' and pestle and mortar for the 3AL) fossil Achatininae shell samples resulted in diffractograms which largely matched the aragonitic reference, but with evidence of a weak calcitic diffraction peak from at ~ 29° 2Ө for a number of samples (Fig. 3.12).
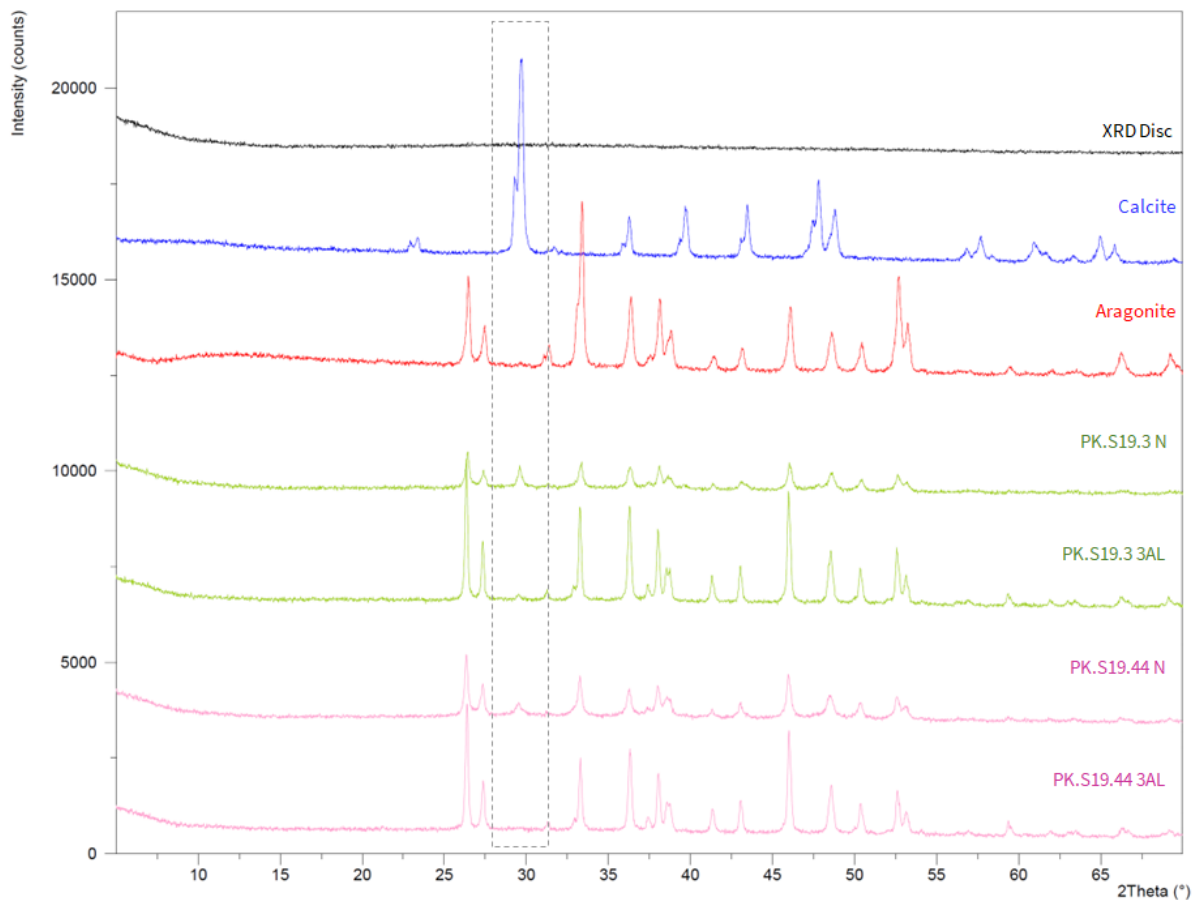
Figure 3.12. Diffractograms of two fossil *Lissachatina* sp. shells, sampled from both the 3AL and 'nacreous' (N) of each shell in comparison to calcite and aragonite $CaCO_3$ references. The dashed box highlights the dominant calcitic diffraction peak at ~ 29° 2θ; this shouldn't be present in an aragonitic sample but is present in both fossil 'nacreous' layers. Please note, the diffractograms have been offset on the y axis for visibility and the spectral counts left for relative scale.

Evidence for the presence of calcite in the fossil samples was very weakly observable in 2/7 3AL samples (e.g. PK.S19.3 W, Fig. 3.12) and in 4/7 'nacreous' samples (e.g. PK.S19.3 N and PK.S19.44 N, Fig. 3.12). This indicated that thermodynamic conversion of aragonite to calcite may have occurred in some of the fossil samples. There was, however, no clear relationship between the presence of calcite and the extent of subsample replicate variability. As only a portion of each fossil sample was analysed by XRD prior to IcPD analysis, it is not possible to say with certainty that where it was not observed, mineral diagenesis may not have occurred in another sampled part of the shell. Additionally, whether the presence of calcite resulted from mineral diagenesis during the fossils' burial history is difficult to assess, since evidence of calcite was also observed in modern Achatininae shell 'nacreous' (but not 3AL), both prior to and during elevated temperature experiments (Fig. 3.13). In the 'nacreous' this may be induced by the sampling process, the mechanical pressure and heat of

drilling off the 'nacreous' from the inside of the shell (Foster *et al.*, 2008). Given this, we recommend that sampling by drilling is minimised wherever possible in this shell material to avoid induced remineralisation.
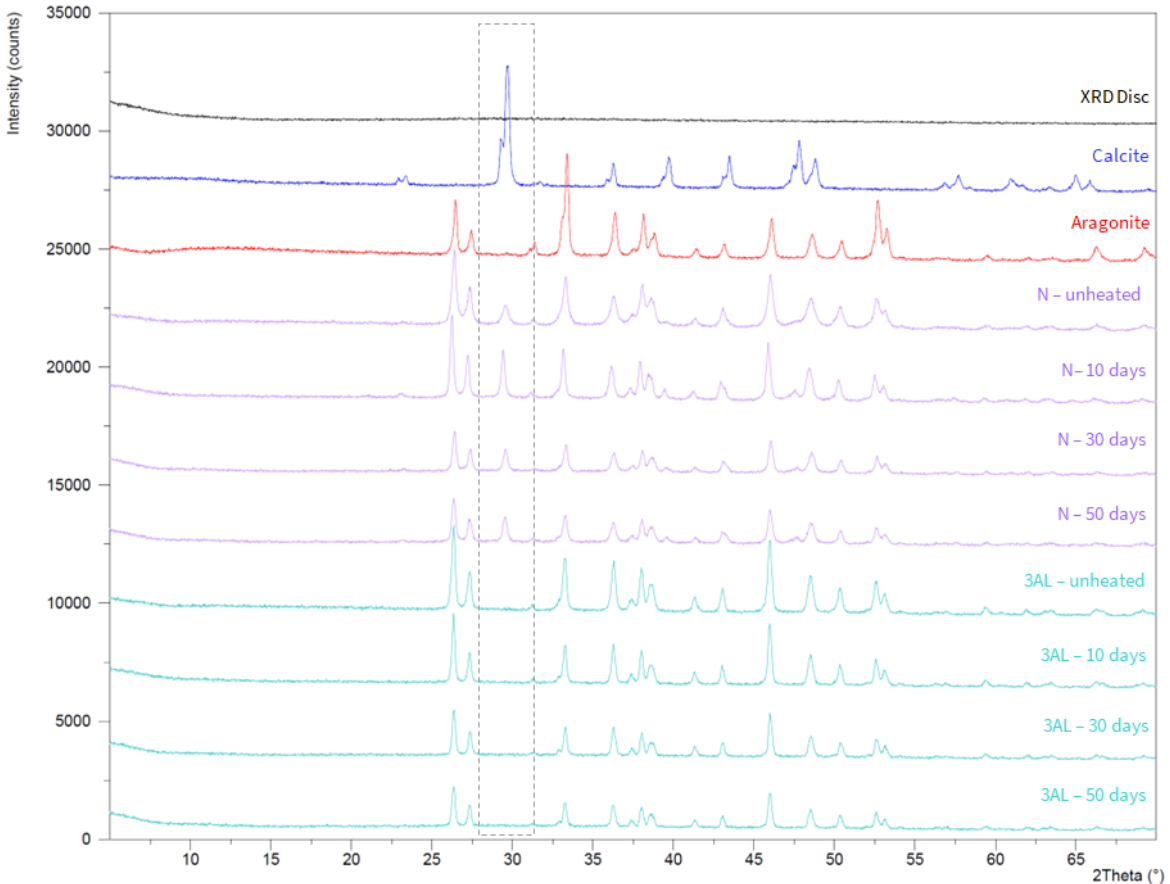
Figure 3.13. Diffractograms of modern *Achatina tavaresiana* shell 3AL and 'nacreous' samples heated to 110°C for 0, 10, 30 and 50 days. The dashed box highlights the dominant calcitic diffraction peak at ~ 29° 2Ɵ. The calcite peak was present in all nacreous samples, but not the 3AL samples. Please note, the diffractograms have been offset on the y axis for visibility and the spectral counts left for relative scale.

3.3.1.4. Sampling considerations and recommendations

Evidence that different proteins may be found in the 'nacreous' to other microstructural layers in achatinid shell was observed from the relative amino acid abundances in section 3.3.1.1. Whilst targeting a single layer, such as the nacreous, would theoretically be preferred in order to reduce the possibility of different proteins within different microstructural layers confusing the chronological signal, we do not recommend this sampling strategy for Achatininae shell for two reasons. Firstly, achatinid shell is ~ 250 μm thick (Fig. 3.2). Whilst the microstructural layers are clear under the magnification of a SEM (Fig. 3.2), distinguishing the boundary between the nacreous and cross-

lamellar layers is rarely possible by eye. This results in the need to sample the nacreous very cautiously to minimise accidental sampling of the cross-lamellar layer. Taking this approach therefore requires much more shell to be sampled to obtain sufficient 'nacreous' for analysis. Secondly, the mechanical pressure and heat from the rotary drill during sampling may give rise to thermodynamic conversion of aragonite to calcite (section 3.3.1.3). If this occurs, it becomes difficult to assess the fossil's mineral diagenetic history (i.e., whether closed-system behaviour has been adhered to, and subsequently whether racemisation values are a reliable signal of endogenous protein degradation). Due to the potential size of achatinid shells, fossils may often be found incomplete, with only apices or body whorls present. Additionally, the fossils studied here contained solidified sediment which was challenging to remove. As it was beyond the scope of this study to investigate intra-specimen variability, we sampled all specimens on the outermost whorl of each shell. We therefore currently recommend that future studies sample only the 3AL shell portion from the outermost whorl, where consistent degradation patterns and closed-system behaviour was observed in both modern heated and fossil samples (3.3.1.2), and for its relative ease of consistent sampling, known to reduce the potential for intra-shell variability (Murray-Wallace, 1995; Hearty and Kaufman, 2009).

3.3.2. Kinetic behaviour

Numerical age estimates were calculated from fossil amino acid racemisation data through the application of mathematical models that use accelerated degradation experiments and/or calibration using additional dating techniques. Mathematical models have been used with mixed results (e.g., Tomiak *et al.*, 2013 and references therein), but have been successfully employed for a number of biominerals (e.g., Clarke and Murray-Wallace, 2006, Wehmiller *et al.*, 2012; Torres *et al.*, 2014). In these cases, meaningful extrapolation has been possible where the high temperature protein degradation experiments mimic the mechanisms occurring in naturally degraded fossils. The disparity between the 'nacreous' layer and 3AL relative racemisation patterns in section 3.3.1.3 provides potential evidence that this is not the case for achatinids. To explore this further, we have investigated the predictions for fossil age and temperature made by two commonly used mathematical models (Clarke and Murray-Wallace, 2006). Data from our high temperature (60 – 140 °C) experiments were modelled using apparent reversible first order kinetics (RFOK$_a$) and constrained power law kinetics (CPK); see supplementary information (SI section 3.5.4) for a detailed description. Linearisation of the experimental data using these models was variable, with some amino acids achieving very high levels of linearity (e.g., Ala, Fig. 3.14B), whilst others had poor fit (e.g., Asx, Fig. 3.14A). This poor fit of Asx results from its rapid initial racemisation rate (likely due to its ability to racemise when bound in a peptide chain (Demarchi *et al.*, 2013b)), and from the observed Asx signal being a combination of

aspartic acid and asparagine, giving rise to a more complex 'observed' rate signal (e.g. Goodfriend *et al.*, 1992).
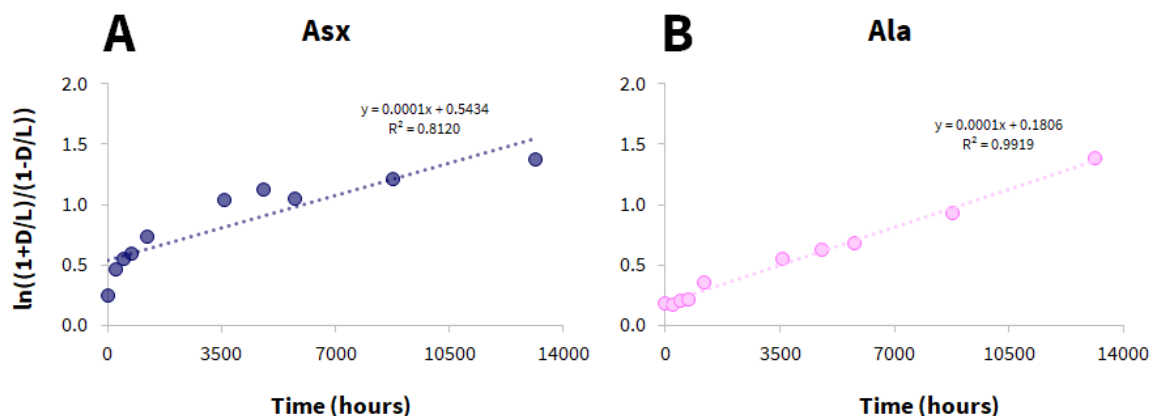
Figure 3.14. Assessment of fit for the linearised relationship between the time spent at 80 °C and transformed D/L values for Asx (A) and Ala (B) using RFOK (SI equation 3.2), for hydrolysed 3AL. The linearity of transformed D/L values was variable between amino acids, indicating $RFOK_a$ is not a suitable kinetic model to describe all amino acid racemisation within the intra-crystalline fraction of Achatininae shell.

In making the assumption that the reaction pathways are the same at all temperatures and undertaking accelerated degradation experiments at a minimum of three temperatures, it is possible to calculate the activation energy (E_a) for racemisation using the Arrhenius equation (SI equation 3.4). Activation energies were calculated for all amino acids where 'good' linearity ($R^2 > 0.97$ as suggested by Crisp *et al.*, (2013)) was achieved through the mathematical transformations (Ala, table 3.3 and Phe SI table 3.1). In general, where very high levels of linearity ($R^2 > 0.995$) were observed, there was little difference in the resulting activation energies from $RFOK_a$ and CPK (e.g., Ala ~ 96 kJ mol^{-1} for both, table 3.3). Interestingly a greater discrepancy was observed for the calculated activation energy for Ala racemisation in the 'nacreous' (96.8 kJ mol^{-1} using $RFOK_a$ vs. 119.0 kJ mol^{-1} using CPK), even though very high levels of linearity were observed for both kinetic models. Variability between activation energies calculated using different mathematical models has previously been reported (Crisp *et al.*, 2013; Tomiak *et al.*, 2013; Dickinson *et al.,* 2019), and this may be due to the validity of the mathematical transformations to each dataset, which encompasses issues due to different reaction pathways being made available at higher temperatures.

Table 3.3. Activation energies of Ala racemisation calculated from the Arrhenius equation (4) using data from five elevated temperature experiments (60, 70, 80, 110, 140 °C) on modern *Achatina tavaresiana* shell.

Amino acid	Shell fraction	Kinetic model	n	Model fit (R^2)	E_a (kJ mol^{-1})
Ala	3AL	$RFOK_a$	n/a	0.996	95.7
		CPK	1.2	0.998	97.5
	'Nacreous'	$RFOK_a$	n/a	0.988	96.8
		CPK	1.9	0.990	119.0

3.3.2.1. Plausibility of predicted fossil ages and diagenetic temperatures

To explore a best-case scenario, we used amino acids with good model fits (high R^2 values), to gauge whether these mathematical models could be used to calculate plausible numerical ages or past climate temperatures for the fossils based on their extent of racemisation. Although there is no direct evidence for the age of the shell material from Site 19, there is strong circumstantial evidence (discussed in section 3.2.1, SI section 3.1) that the sediments at Sites 1 and 19 are broadly coeval in age with the occupation of the Twin Rivers kopje and are probably later Middle Pleistocene in age. Assigning an arbitrary date of 200 ka to two of the fossils (with the highest and lowest racemisation values) resulted in extrapolated integrated climate temperatures between - 7.0 and - 11.3 °C when using Ala (table 4). If the samples are older (400 ka), then the extrapolated temperatures are even lower (from between -10.8°C and -15.4 °C, depending on the model). Given this requires the site to be below freezing for its history, this is an incredibly unlikely range for the average integrated temperature of the sediment for Palaeolake Kafue, Zambia. Likewise, whilst Lusaka's current mean annual temperature (20.4 °C) would be an overestimation of the average regional temperature during the Pleistocene climate oscillations, the calculated ages using this temperature estimate are a factor of ten lower than their expected age and fall within the Holocene (table 3.4).

Table 3.4. 'Kinetic age' and 'kinetic temperature' calculations using two fossils from both their 3AL and 'nacreous' (N) for Ala. 'Kinetic ages' were calculated using Lusaka, Zambia's current mean annual temperature (MAT, 20.4 °C). 'Kinetic temperatures' were calculated using arbitrary fossil ages of 200 ka and 400 ka for these Late Middle Pleistocene fossils. Note that the 'kinetic age' and 'kinetic temperature' outputs from the mathematical models do not agree with the palaeoenvironmental information for these fossils and should not be interpreted as accurate values for this site.

Fossil ID	Shell fraction	'Kinetic age' (years) using current MAT: 20.4°C	'Kinetic temperature' (°C) using fossil age: 200 ka	'Kinetic temperature' (°C) using fossil age: 400 ka
PK.S19.44	3AL	2705	-8.6	-12.7
	N	1673	-9.1	-12.9
PK.S19.45	3AL	1724	-11.3	-15.4
	N	2468	-7.0	-10.8

The highly implausible results produced by the RFOK$_a$ and CPK models for the achatinids studied here (table 3.4, SI table 3.1) may be due to protein decomposition pathways being different at lower environmental (burial) temperatures than they are under the high temperature experiments in the intra-crystalline fraction of this biomineral (discussed in section 3.3.1.2.3), as has been observed for some other biominerals (e.g. Tomiak *et al.*, 2013). Whilst the assumption is that the intra-crystalline protein fraction is not influenced by any external factors other than temperature, in this case it is also possible that the conditions used for the accelerated degradation experiments (powdered, bleached shell in 300 µL water), were not a good proxy for naturally degraded shell samples. Experimental influences may therefore have rendered these samples inappropriate for extrapolation in this case. Nevertheless, the consistent patterns of racemisation in Achatininae (section 3.3.1.2) mean this taxa still holds potential for building relative amino acid geochronologies across Africa in future.

3.4. Conclusion

The shells of land snails in the subfamily Achatininae (modern *Achatina tavaresiana* and fossil *Lissachatina* sp.), which have complex multi-layered CaCO$_3$ shell microstructures, were assessed for their potential suitability for building amino acid geochronologies using IcPD analysis. Comparison was made between the three aragonitic layer (3AL) shell portion and the 'nacreous' layer alone in order to assess the most appropriate sampling strategy. Achatininae shell was shown to have an intra-crystalline fraction of protein, which appeared to adhere to closed-system behaviour in the 3AL shell portion. The 'nacreous' layer did not adhere well to closed system behaviour, possibly due to complications arising from difficulties sampling the very thin shell (~ 250 µm thick) and potential mineral diagenesis during drilling. We therefore recommend using the 3AL shell portion for further research involving achatinid shells. Predictable protein degradation, in terms of racemisation and

hydrolysis, was observed during elevated temperature experiments, with respect to both temperature and time. Different relative rates of racemisation were observed for proteins in the 'nacreous' layer and 3AL in modern shells for different elevated temperatures, and showed a different pattern of behaviour in the fossils. This prevented accurate extrapolation of fossil parameters from mathematical modelling of high temperature kinetic experiments. Although numerical dating of achatinid fossils using two kinetic models was not possible, the consistent degradation patterns and closed-system behaviour of the 3AL shell portion showed that this shell type has the potential to provide chronological data on Pleistocene timescales for many regions across the African continent. Such frameworks would be highly beneficial to archaeologists and Quaternary scientists working at timescales beyond the reach of radiocarbon dating, and in areas of Africa where ostrich eggshell is not present. A larger study of well-constrained fossils from sequences across the region is required to test the full feasibility for amino acid geochronology.

Acknowledgements

3.5. References

Abelson, P.H., 1955. Organic constituents of fossils. *Carnegie Inst. Wash. Year Book, 54*, pp.107-109.

Allen, A.P., Kosnik, M.A. and Kaufman, D.S., 2013. Characterizing the dynamics of amino acid racemization using time-dependent reaction kinetics: a Bayesian approach to fitting age-calibration models. *Quaternary Geochronology, 18*, pp.63-77.

Bada, J.L. and Schroeder, R.A., 1972. Racemization of isoleucine in calcareous marine sediments: kinetics and mechanism. *Earth and Planetary Science Letters, 15*(1), pp.1-11.

Bada, J.L. and Schroeder, R.A., 1975. Amino acid racemization reactions and their geochemical implications. *Naturwissenschaften, 62*, pp.71-79.

Bada, J.L., Shou, M.Y., Man, E.H., and Schroeder, R.A. 1978. Decomposition of hydroxy amino acids in foraminiferal tests: Kinetics, mechanism and geochronological implications. *Earth Planetary Science Letters, 41*(1), pp.67-76.

Barham, L.S., 1998. Possible early pigment use in south-central Africa. Current Anthropology, 39(5), pp.703-710.

Barham, L.S., 2000. *The Middle Stone Age of Zambia, South Central Africa*. Western academic & specialist Press.

Barham and Debenham, 2000. Chapter 3 Mumbwa Caves Chronology in Barham, L.S., 2000. *The Middle Stone Age of Zambia, South Central Africa*. Western academic & specialist Press. pp.43-50.

Barham, L.S., Simms, M., Gilmour, M., Debenham, N., 2000. Chapter 10 Twin Rivers, excavation and behavioural record in Barham, L.S., 2000. *The Middle Stone Age of Zambia, South Central Africa*. Western academic & specialist Press. pp.165-216.

Barham, L.S. and Smart, P.L., 1996. Current events: An early date for the Middle Stone Age of central Zambia. *Journal of Human Evolution, 30*(3), pp.287-290.

Bishop, L.C. and Reynolds, S.C., 2000. Chapter 11 Fauna from Twin Rivers in Barham, L.S., 2000. *The Middle Stone Age of Zambia, South Central Africa*. Western academic & specialist Press. pp. 217-222.

Bosch, M.D., Mannino, M.A., Prendergast, A.L., O'Connell, T.C., Demarchi, B., Taylor, S.M., Niven, L., Van Der Plicht, J. and Hublin, J.J., 2015. New chronology for Ksâr 'Akil (Lebanon) supports Levantine route of modern human dispersal into Europe. *Proceedings of the National Academy of Sciences, 112*(25), pp.7683-7688.

Bowen, D.Q., Hughes, S., Sykes, G.A. and Miller, G.H., 1989. Land-sea correlations in the Pleistocene based on isoleucine epimerization in non-marine molluscs. *Nature, 340*(6228), pp.49-51.

Brand, U. and Morrison, J.O., 1987. Paleoscene# 6. Biogeochemistry of fossil marine invertebrates. *Geoscience Canada, 14*(2), pp.85-107.

Brooks, A.S., Hare, P.E., Kokis, J.E., Miller, G.H., Ernst, R.D. and Wendorf, F., 1990. Dating Pleistocene archeological sites by protein diagenesis in ostrich eggshell. *Science, 248*(4951), pp.60-64.

Canoira, L., García-Martínez, M.J., Llamas, J.F., Ortíz, J.E. and Torres, T.D., 2003. Kinetics of amino acid racemization (epimerization) in the dentine of fossil and modern bear teeth. *International journal of chemical kinetics, 35*(11), pp.576-591.

Casanova, J., Hillaire-Marcel, C., 1992. Chronology and paleohydrology of late Quaternary high lake levels in the Manyara basin (Tanzania) from isotopic data (^{18}O, ^{13}C, ^{14}C, Th/U) on fossil stromatolites. *Quaternary Research, 38(*2), pp.205–226.

Chaki, K.K., Misra, K.K. and Sur, R.K., 1992. The surface morphology of the shell in active and in aestivating *Achatina fulica* (Bowdich) and *Pila globosa* (Swainson). *Proc. 9th Eur. Malac. Cong*, pp.97-102.

Clarke, S.J. and Murray-Wallace, C.V., 2006. Mathematical expressions used in amino acid racemisation geochronology—a review. *Quaternary Geochronology, 1*(4), pp.261-278.

Crisp, M., Demarchi, B., Collins, M., Morgan-Williams, M., Pilgrim, E. and Penkman, K., 2013. Isolation of the intra-crystalline proteins and kinetic studies in *Struthio camelus* (ostrich) eggshell for amino acid geochronology. *Quaternary Geochronology, 16*, pp.110-128.

de Paula, S.M. and Silveira, M., 2009. Studies on molluscan shells: contributions from microscopic and analytical methods. *Micron, 40*(7), pp.669-690.

Demarchi, B., Rogers, K. Fa, D. A., Finlayson, C. J., Milner, N., Penkman, K. E. H., 2013a. Intra-crystalline protein diagenesis (IcPD) in *Patella vulgata*. Part I: Isolation and testing of the closed system. *Quaternary Geochronology, 16*, pp.144-157.

Demarchi, B., Collins, M., Bergström, E., Dowle, A., Penkman, K., Thomas-Oates, J., Wilson, J., 2013b. New experimental evidence for in-chain amino acid racemization of serine in a model peptide. *Analytical Chemistry, 85*(12), pp.5835-5842 236.

Demarchi, B., Hall, S., Roncal-Herrero, T., Freeman, C. L., Woolley, J., Crisp, M. K., Wilson, J., Fotakis, A., Fischer, R., Kessler, B. M., Jersie-Christensen, R. R., Olsen, J. V., Haile, J., Thomas, J., Marean, C. W.,

Parkington, J., Presslee, S., Lee-Thorp, J., Ditchfield, P., Hamilton, J. F., Ward, M. W., Wang, C. M., Shaw, M. D., Harrison, T., Dominguez-Rodrigo, M., Macphee, R. D. E., Kwekason, A., Ecker, M., Horwitz, L. K., Chazan, M., Kroger, R., Thomas-Oates, J., Harding, J. H., Cappellini, E., Penkman, K., Collins, M. J., 2016. Protein sequences bound to mineral surfaces persist into deep time. *elife, 5*, p.e17092.

Demarchi, B., Clements, E., Coltorti, M., Van De Locht, R., Kröger, R., Penkman, K. and Rose, J., 2015. Testing the effect of bleaching on the bivalve *Glycymeris*: A case study of amino acid geochronology on key Mediterranean raised beach deposits. *Quaternary Geochronology, 25*, pp.49-65.

Dickinson, M.R., Lister, A.M. and Penkman, K.E., 2019. A new method for enamel amino acid racemization dating: a closed system approach. *Quaternary Geochronology, 50*, pp.29-46.

Ellis, G.L., Goodfriend, G.A., Abbott, J.T., Hare, P.E. and Von Endt, D.W., 1996. Assessment of integrity and geochronology of archaeological sites using amino acid racemization in land snail shells: examples from central Texas. *Geoarchaeology, 11*(3), pp.189-213.

Feng, Q.L., Zhu, X., Li, H.D. and Kim, T.N., 2001. Crystal orientation regulation in ostrich eggshells. *Journal of crystal growth, 233*(3), pp.548-554.

Fontanilla, I.K., 2010. *Achatina* (*Lissachatina*) *fulica* Bowdich: its molecular phylogeny, genetic variation in global populations, and its possible role in the spread of the rat lungworm *Angiostrongylus cantonensis* (Chen). PhD thesis, University of Nottingham.

Foster, L.C., Andersson, C., Høie, H., Allison, N., Finch, A.A. and Johansen, T., 2008. Effects of micromilling on δ^{18}O in biogenic aragonite. *Geochemistry, Geophysics, Geosystems, 9*(4).

Goodfriend, G.A., 1991. Patterns of racemization and epimerization of amino acids in land snail shells over the course of the Holocene. *Geochimica et Cosmochimica Acta, 55*(1), pp.293-302.

Goodfriend, G.A., Hare, P.E. and Druffel, E.R., 1992. Aspartic acid racemization and protein diagenesis in corals over the last 350 years. *Geochimica et Cosmochimica Acta, 56*(10), pp.3847-3850.

Hammouda, S.A., Kadolsky, D., Adaci, M., Mebrouk, F., Bensalah, M., Mahboubi, M.H. and Tabuce, R., 2017. Taxonomic review of the "Bulimes", terrestrial gastropods from the continental Eocene of the Hamada de Méridja (northwestern Sahara, Algeria)(Mollusca: *Stylommatophora*: *Strophocheilidae*?), with a discussion of the genera of the family Vidaliellidae. *PalZ, 91*, pp.85-112.

Hare, P.E., 1963. Amino acids in the proteins from aragonite and calcite in the shells of *Mytilus californianus*. *Science, 139*(3551), pp.216-217.

Hare, P.E., Abelson, P.H., 1967. Racemisation of amino acids in fossil shells. *Carnegie Institute of Washington Year Book, 66*, pp.526-528.

Haugen, J.E. and Sejrup, H.P., 1990. Amino acid composition of aragonitic concholin in the shell of *Arctica islandica*. *Lethaia, 23*(2), pp.133-141.

Hausdorf, B., 2018. The giant African snail *Lissachatina fulica* as potential index fossil for the Anthropocene. *Anthropocene, 23*, pp.1-4.

Hearty, P.J. and Kaufman, D.S., 2009. A *Cerion*-based chronostratigraphy and age model from the central Bahama Islands: Amino acid racemization and ^{14}C in land snails and sediments. *Quaternary Geochronology, 4*(2), pp.148-159.

Hendy, E.J., Tomiak, P.J., Collins, M.J., Hellstrom, J., Tudhope, A.W., Lough, J.M. and Penkman, K.E., 2012. Assessing amino acid racemization variability in coral intra-crystalline protein for geochronological applications. *Geochimica et Cosmochimica Acta, 86*, pp.338-353.

Hill, R.L., 1965. Hydrolysis of proteins. *Advances in protein chemistry, 20*, pp.37-107.

Hodasi, J.K.M., 1984. Some observations on the edible giant land snails of West Africa. *World Animal Review (FAO)*, (52).

Kaufman, D.S. and Manley, W.F., 1998. A new procedure for determining DL amino acid ratios in fossils using reverse phase liquid chromatography. *Quaternary Science Reviews, 17*(11), pp.987-1000.

Kaufman, D.S., 2006. Temperature sensitivity of aspartic and glutamic acid racemization in the foraminifera *Pulleniatina*. *Quaternary Geochronology, 1*(3), pp.188-207.

Kimber, R.W.L. and Griffin, C.V., 1987. Further evidence of the complexity of the racemization process in fossil shells with implications for amino acid racemization dating. *Geochimica et Cosmochimica Acta, 51*(4), pp.839-846.

Kosnik, M.A., Kaufman, D.S. and Hua, Q., 2008. Identifying outliers and assessing the accuracy of amino acid racemization measurements for geochronology: I. Age calibration curves. *Quaternary Geochronology, 3*(4), pp.308-327.

Kowalewska-Groszkowska, M., Mierzwa-Szymkowiak, D. and Zdunek, J., 2018. The crossed-lamellar structure of mollusk shells as biocomposite material. *Composites Theory and Practice, 18*(2), pp.71-76.

Kriausakul, N. and Mitterer, R.M., 1978. Isoleucine epimerization in peptides and proteins: Kinetic factors and application to fossil proteins. *Science, 201*(4360), pp.1011-1014.

Lesbani, A., Tamba, P., Mohadi, R. and Fahmariyanti, F., 2013. Preparation of calcium oxide from *Achatina fulica* as catalyst for production of biodiesel from waste cooking oil. *Indonesian Journal of Chemistry, 13*(2), pp.176-180.

Mead, A.R., 1991. Anatomical criteria in the systematics of the Achatinidae (Pulmonata). *In Proceedings of the 10th International Malacological Congress, Meier-Brook C* (ed). Tubingen pp. 549-553.

Miller, G.H., Beaumont, P.B., Jull, A.J.T. and Johnson, B., 1992. Pleistocene geochronology and palaeothermometry from protein diagenesis in ostrich eggshells: implications for the evolution of modern humans. *Philosophical Transactions of the Royal Society of London. Series B: Biological Sciences, 337*(1280), pp.149-157.

Millman, E., Wheeler, L., Billups, K., Kaufman, D. and Penkman, K.E., 2022. Testing the effect of oxidizing pre-treatments on amino acids in benthic and planktic foraminifera tests. *Quaternary Geochronology, 73*, p.101401.

Mitterer, R.M. and Kriausakul, N., 1984. Comparison of rates and degrees of isoleucine epimerization in dipeptides and tripeptides. *Organic Geochemistry, 7*(1), pp.91-98.

Murray-Wallace, C.V., 1995. Aminostratigraphy of Quaternary coastal sequences in southern Australia—an overview. *Quaternary International, 26*, pp.69-86.

Murray-Wallace, C.V., Richter, J. and Vogelsang, R., 2015. Aminostratigraphy and taphonomy of ostrich eggshell in the sedimentary infill of Apollo 11 Rockshelter, Namibia. *Journal of Archaeological Science: Reports, 4*, pp.143-151.

Neubert, E., Van Damme, D. and van Damme, D., 2012. *Palaeogene continental molluscs of Oman*. Naturhistorisches Museum der Burgergemeinde Bern.

New, E., Yanes, Y., Cameron, R.A., Miller, J.H., Teixeira, D. and Kaufman, D.S., 2019. Aminochronology and time averaging of Quaternary land snail assemblages from colluvial deposits in the Madeira Archipelago, Portugal. *Quaternary Research, 92*(2), pp.483-496.

Ortiz, J.E., Torres, T., Yanes, Y., Castillo, C., Nuez, J.D.L., Ibáñez, M. and Alonso, M.R., 2006. Climatic cycles inferred from the aminostratigraphy and aminochronology of Quaternary dunes and palaeosols from the eastern islands of the Canary Archipelago. *Journal of Quaternary Science: Published for the Quaternary Research Association, 21*(3), pp.287-306.

Ortiz, J.E., Torres, T. and Pérez-González, A., 2013. Amino acid racemization in four species of ostracodes: taxonomic, environmental, and microstructural controls. *Quaternary Geochronology, 16*, pp.129-143.

Ortiz, J.E., Gutiérrez-Zugasti, I., Torres, T., González-Morales, M. and Sánchez-Palencia, Y., 2015. Protein diagenesis in *Patella* shells: implications for amino acid racemisation dating. *Quaternary Geochronology, 27*, pp.105-118.

Ortiz, J.E., Torres, T., Sánchez-Palencia, Y. and Ferrer, M., 2017. Inter-and intra-crystalline protein diagenesis in *Glycymeris* shells: Implications for amino acid geochronology. *Quaternary Geochronology, 41*, pp.37-50.

Ortiz, J.E., Sánchez-Palencia, Y., Gutiérrez-Zugasti, I., Torres, T. and González-Morales, M., 2018. Protein diagenesis in archaeological gastropod shells and the suitability of this material for amino acid racemisation dating: *Phorcus lineatus* (da Costa, 1778). *Quaternary Geochronology, 46,* pp.16-27.

Penkman, K.E.H., 2005. Amino acid geochronology: a closed system approach to test and refine the UK model. PhD thesis, University of Newcastle.

Penkman, K. E. H., Kaufman, D. S., Maddy, D., Collins, M. J., 2008. Closed-system behaviour of the intra-crystalline fraction of amino acids in mollusc shells. Quaternary Geochronology, 31-2), pp.2-25.

Penkman, K.E., Preece, R.C., Keen, D.H., Maddy, D., Schreve, D.C. and Collins, M.J., 2007. Testing the aminostratigraphy of fluvial archives: the evidence from intra-crystalline proteins within freshwater shells. *Quaternary Science Reviews, 26*(22-24), pp.2958-2969.

Penkman, K.E.H., Preece, R.C., Keen, D.H. and Collins, M.J., 2010. Amino acid geochronology of the type Cromerian of West Runton, Norfolk, UK. Quaternary International, 228(1-2), pp.25-37.

Pickford, M., 1995. Fossil land snails of East Africa and their palaeoecological significance. *Journal of African Earth Sciences, 20*(3-4), pp.167-226.

Pickford, M., 2008. Freshwater and terrestrial Mollusca from the Early Miocene deposits of the northern Sperrgebiet, Namibia. *Memoir of the Geological Survey of Namibia, 20*, pp.65-74.

Pickford, M., Senut, B., Mocke, H., Mourer-Chauviré, C., Rage, J.C. and Mein, P., 2014. Eocene aridity in southwestern Africa: timing of onset and biological consequences. *Transactions of the Royal Society of South Africa, 69*(3), pp.139-144.

Pierini, F., Demarchi, B., Turner, J. and Penkman, K., 2016. *Pecten* as a new substrate for IcPD dating: The quaternary raised beaches in the Gulf of Corinth, Greece. *Quaternary Geochronology, 31*, pp.40-52.

Powell, J., Collins, M.J., Cussens, J., MacLeod, N. and Penkman, K.E., 2013. Results from an amino acid racemization inter-laboratory proficiency study; design and performance evaluation. *Quaternary Geochronology, 16*, pp.183-197.

Preece, R.C. and Penkman, K.E.H., 2005. New faunal analyses and amino acid dating of the Lower Palaeolithic site at East Farm, Barnham, Suffolk. *Proceedings of the Geologists' Association, 116*(3-4), pp.363-377.

Raut, S.K. and Barker, G.M., 2002. *Achatina fulica* Bowdich and other Achatinidae as pests in tropical agriculture. p 55–114. Molluscs as Crop Pests. Wallingford, United Kingdom: CAB International.

Roberts, D.L., Bateman, M.D., Murray-Wallace, C.V., Carr, A.S. and Holmes, P.J., 2008. Last interglacial fossil elephant trackways dated by OSL/AAR in coastal aeolianites, Still Bay, South Africa. *Palaeogeography, Palaeoclimatology, Palaeoecology, 257*(3), pp.261-279.

Simms, M.J., 2000. Appendix 7(a) Preliminary Report on the Sediments of Lake Patrick in Barham, L.S., 2000. *The Middle Stone Age of Zambia, South Central Africa*. Western academic & specialist Press. pp. 275-280.

Smith, G.G., Williams, K.M. and Wonnacott, D.M., 1978. Factors affecting the rate of racemization of amino acids and their significance to geochronology. *The Journal of Organic Chemistry, 43*(1), pp.1-5.

Smith, G.G., Evans, R.C., 1980. The effect of structure and conditions on the rate of racemisation of free and bound amino acids. *Biogeochemistry of Amino Acids*, pp.257-282.

Solem, A., 1979. A theory of land snail biogeographic patterns through time. *Pathways in Malacology'.(Eds S Van der Spoel, AC Van Bruggen, J Lever*) pp.225-249.

Sykes, G.A., Collins, M.J. and Walton, D.I., 1995. The significance of a geochemically isolated intracrystalline organic fraction within biominerals. *Organic Geochemistry, 23*(11-12), pp.1059-1065.

Taylor, V.K., Barton, R.N.E., Bell, M., Bouzouggar, A., Collcutt, S., Black, S. and Hogue, J.T., 2011. The Epipalaeolithic (Iberomaurusian) at Grotte des Pigeons (Taforalt), Morocco: a preliminary study of the land Mollusca. *Quaternary International, 244*(1), pp.5-14.

Tomiak, P. J., Penkman, K. E H., Hendy, E. J., Demarchi, B., Murrells, S., Davis, S., McCullagh, P., Collins, M. J. 2013. Testing the limitations of artificial protein degradation kinetics using known-age massive *Porites* coral skeletons. Quaternary Geochronology, 16, pp.87-109.

Torres, T., Ortiz, J.E., Fernández, E., Arroyo-Pardo, E., Grün, R. and Pérez-González, A., 2014. Aspartic acid racemization as a dating tool for dentine: a reality. *Quaternary Geochronology, 22*, pp.43-56.

Towe, K.M., 1980. Preserved organic ultrastructure: an unreliable indicator for Paleozoic amino acid biogeochemistry. *Biogeochemistry of Amino Acids*, pp.65-74.

Vijayan, Keerthy, R. Suganthasakthivel, Fred Naggs, Ian Kendrich Fontanilla, Pritpal Singh Soorae, T. V. Sajeev, and Christopher M. Wade. "Fine-scale geographical sampling and molecular characterization of the giant African land snail in its invasive range in Asia shows low genetic diversity, new haplotypes and the emergence of another haplotype from the Indian Ocean Islands. *Biological Journal of the Linnean Society, 137*(3), pp.421-433.

Wehmiller, J.F., Stecher, H.A., York, L.L. and Friedman, I., 2000. The thermal environment of fossils: effective ground temperatures at aminostratigraphic sites on the US Atlantic Coastal Plain. *Perspectives in Amino Acid and Protein Geochemistry. Oxford University Press, Oxford*, pp.219-250.

Wehmiller, J.F., Harris, W.B., Boutin, B.S. and Farrell, K.M., 2012. Calibration of amino acid racemization (AAR) kinetics in United States mid-Atlantic Coastal Plain Quaternary mollusks using $^{87}Sr/^{86}Sr$ analyses: Evaluation of kinetic models and estimation of regional Late Pleistocene temperature history. *Quaternary Geochronology, 7*, pp.21-36.

Wheeler, L.J., Penkman, K.E. and Sejrup, H.P., 2021. Assessing the intra-crystalline approach to amino acid geochronology of *Neogloboquadrina pachyderma* (sinistral). *Quaternary Geochronology, 61*, pp.101131.

White, T.S., Bridgland, D.R., Limondin-Lozouet, N. and Schreve, D.C., 2017. Fossils from Quaternary fluvial archives: Sources of biostratigraphical, biogeographical and palaeoclimatic evidence. *Quaternary Science Reviews, 166*, pp.150-176.

Wojcieszak, M., Backwell, L., d'Errico, F. and Wadley, L., 2023. Evidence for large land snail cooking and consumption at Border Cave c. 170–70 ka ago. Implications for the evolution of human diet and social behaviour. *Quaternary Science Reviews, 306*, pp.108030.

Zhang, D.D., Zhang, Y., Zhu, A. and Cheng, X., 2001. Physical mechanisms of river waterfall tufa (travertine) formation. *Journal of Sedimentary Research, 71*(1), pp.205-216.

3.5. Supplementary Information

3.5.1. Palaeolake Kafue

The fossils in this study originated from Site 19 sediments associated with Palaeolake Kafue, near to the Twin Rivers kopje. Site 19 represents an outcrop, within a ploughed field, of a fossiliferous 'chalky' limestone at an altitude of 1060 m amsl. Excavations revealed limestone *in situ* at a shallow depth and the outcrop context of the limestone indicates that was overlain by black clay and underlain by similar black clays which were penetrated by a nearby borehole (failed water well) to a depth of 80 metres below the limestone. Loose surface blocks containing well preserved mollusc shells were collected and *in situ* blocks with good preservation (to a depth of around 30 cm) were removed using a hammer, chisel and trowel.

The age of the Site 19 sediments is poorly constrained, but some inferences have been made from radiometric U-series dates from two nearby sites: the Twin Rivers kopje and the Casavera stream. Various U-series dates were obtained from calcite speleothem layers intercalated with bone- and artefact-bearing breccias on the Twin Rivers kopje (Barham and Smart, 1996; Barham, 1998; Barham *et al.*, 2000). Dates range from >400 ka to ~140 ka, but the context of the speleothem layers with the bones and artefacts indicates that the main occupation phase was from ~270-170 ka (Barham *et al.*, 2000). The presence of bushpig (*Potamochoerus porcus*) in the breccias (Bishop and Reynolds, 2000) suggests proximity to water and hence may provide indirect evidence for the existence of the palaeolake at this time.

Two U-series dates were also published for the Casavera stream 'fossil' tufa deposits found along the southern margin of Palaeolake Kafue, ranging in age from ~200–400 ka (Barham *et al.*, 2000: 179). These, now inactive, 'fossil' tufa deposits would have been deposited preferentially on cascades by perennial, carbonate saturated, streams fed by springs emerging from the marble aquifer of the Lusaka Dolomite Formation to the south (Simms, 2000; Zhang *et al.*, 2001). The dated samples are from tufa deposits that overlie pedogenically altered lacustrine carbonates exposed in the Casavera stream near Site 1, at an elevation of 1092 m amsl. These are subaerial tufas that clearly were deposited after lake levels had fallen below this elevation, but they also postdate incision of the Casavera Stream to a depth of several metres into the lacustrine carbonate succession. Hence, these 'fossil' tufa deposits, which occur widely around Palaeolake Kafue, postdate the lacustrine sediments themselves, providing a minimum age.

The top surface of the chalky limestone of Bed 14 at Site 1 (Fig. 3.3B), at 1099 m amsl, has a thin (few cm) stromatolitic crust that indicates a maximum high-stand of ~1100 m amsl (cf. Casanova and Hillaire-Marcel, 1992). This crust and the upper part of the limestone are penetrated by abundant rootlet traces of marginal vegetation, probably reed-dominated, indicating a slight fall in the lake level. The chalky limestone outcrop at Site 19 lies 16 km northwest and at an altitude of 1060 m. More

142

than two metres thick, it too has a thin stromatolitic crust on its top surface and abundant rootlet traces in its upper part. This indicates a significant fall in lake level, to ~40 m below the maximum high-stand represented by Bed 14 at Site 1. However, the nature of the lake sedimentation is such that the Site 19 low-stand limestone may well correspond to palaeosols of Beds 3-6 at Site 1, which indicate a prolonged (>10 ka) period of emergence at Site 1 elevations (Simms, 2000). Loose quartz implements of Middle Stone Age type are found nearby, and presumed to be from Bed 5, suggest that this low-stand episode was broadly coeval with some of the time that the Twin Rivers kopje was occupied, and hence is Middle Pleistocene in age.

3.5.2. Bleaching experiments – amino acid concentrations
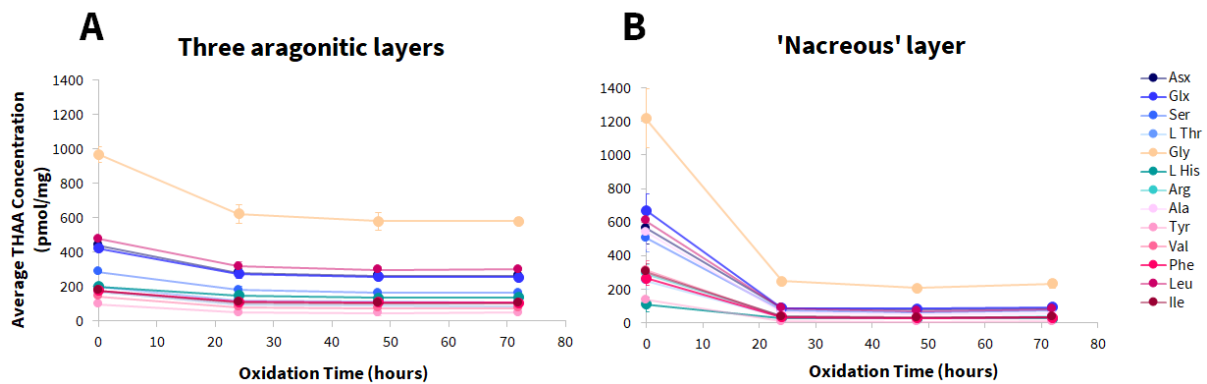
SI Figure 3.1. Average concentrations of all total hydrolysable amino acids (THAA) in modern A*chatina tavaresiana* shell portions (A - 3AL, B - 'nacreous' layer); powdered shell was analysed unbleached (0 hours) and exposed to NaOCl, a strong chemical oxidant, for 24, 48 and 72 hours. Error bars represent the standard deviation about the mean for subsample experimental triplicates. All THAA concentrations are calculated from L + D enantiomers, with the exception of Thr and His, where only the L enantiomer is analysed by the method given in section 3.2.6 and Gly which contains no stereogenic centre and therefore does not have L/D enantiomers. Within 24 hours a decreased, stable concentration of amino acids was achieved in both shell portions, defined as the intra-crystalline protein fraction.

3.5.3. Assessment of protein degradation
3.5.3.1. Elevated temperature kinetic experiments

3.5.3.1.1. Racemisation by temperature
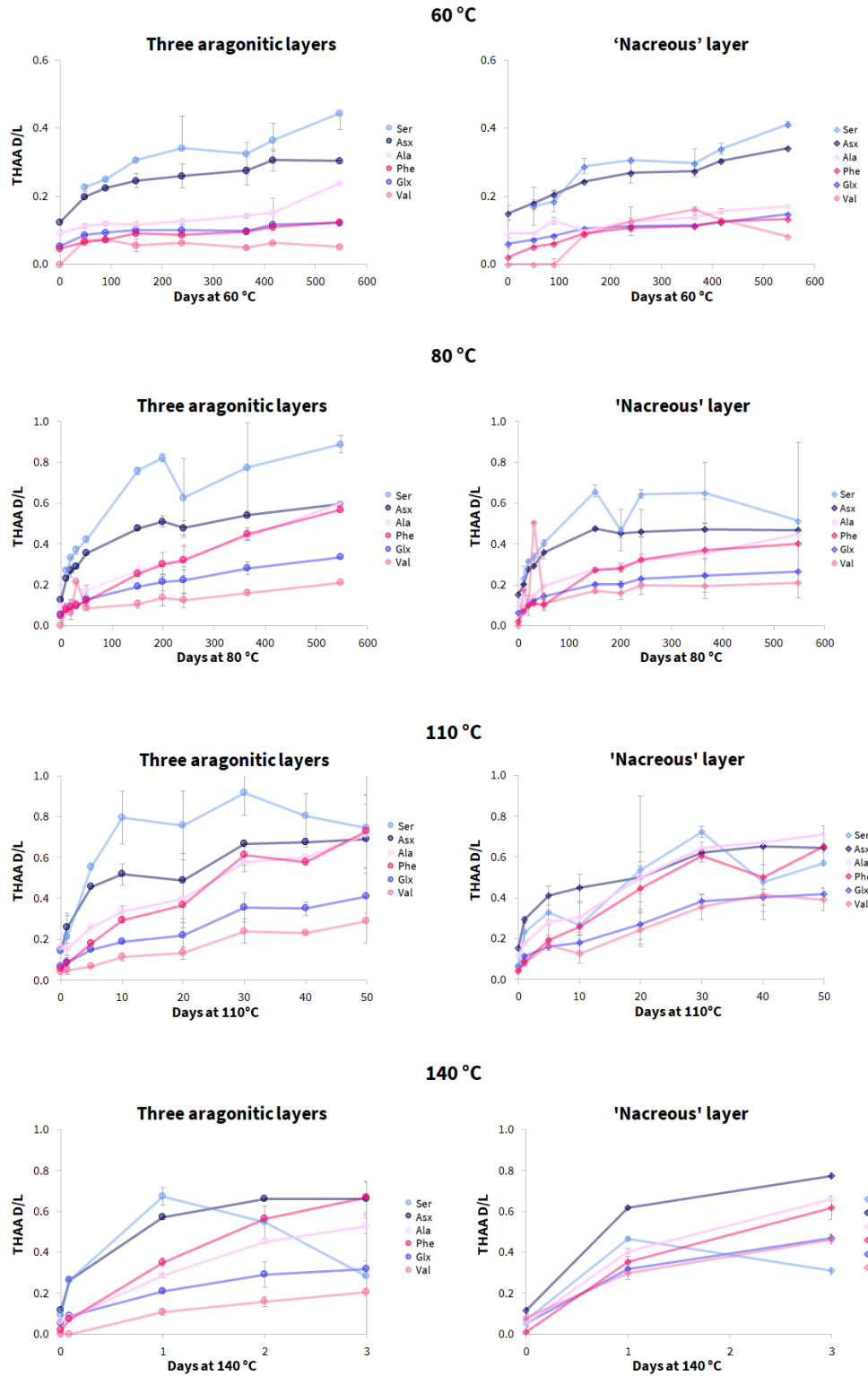
SI Figure 3.2. The average extent of racemisation for the hydrolysable amino acids in the intra-crystalline 3AL shell portion and the 'nacreous' layer of modern A*chatina tavaresiana* during isothermal heating at 60, 80, 110 and 140 °C. Error bars represent the standard deviation about the mean for subsample experimental triplicates.

3.5.3.1.2. Racemisation by time
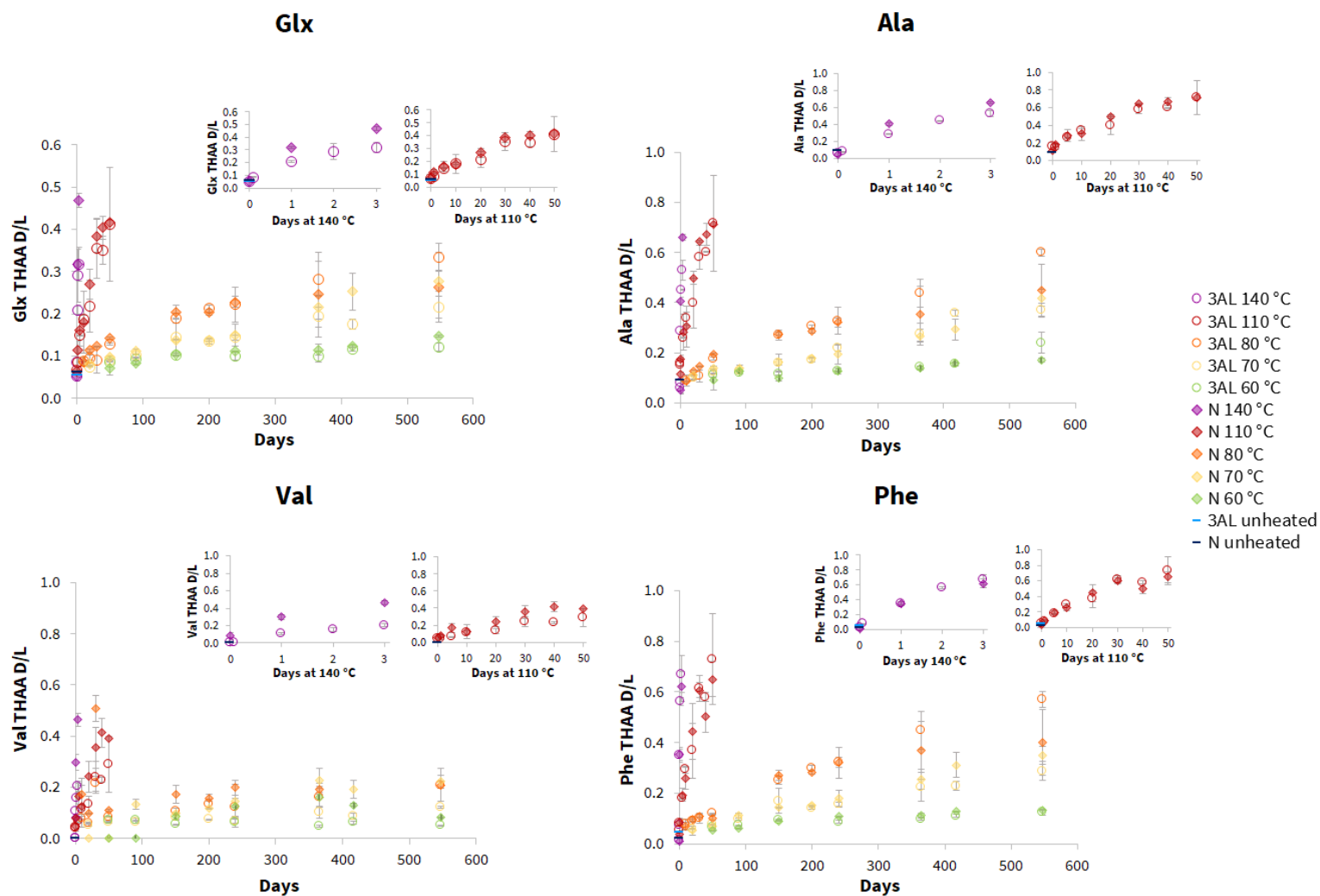
SI Figure 3.3. The average extent of racemisation in Glx, Ala, Val and Phe in intra-crystalline 3AL shell portion and 'nacreous' layer of A*chatina tavaresiana* shell during isothermal heating at 60, 70, 80, 110 and 140 °C. Error bars represent the standard deviation about the mean for subsample experimental triplicates.

3.5.3.1.3. Peptide chain hydrolysis by time
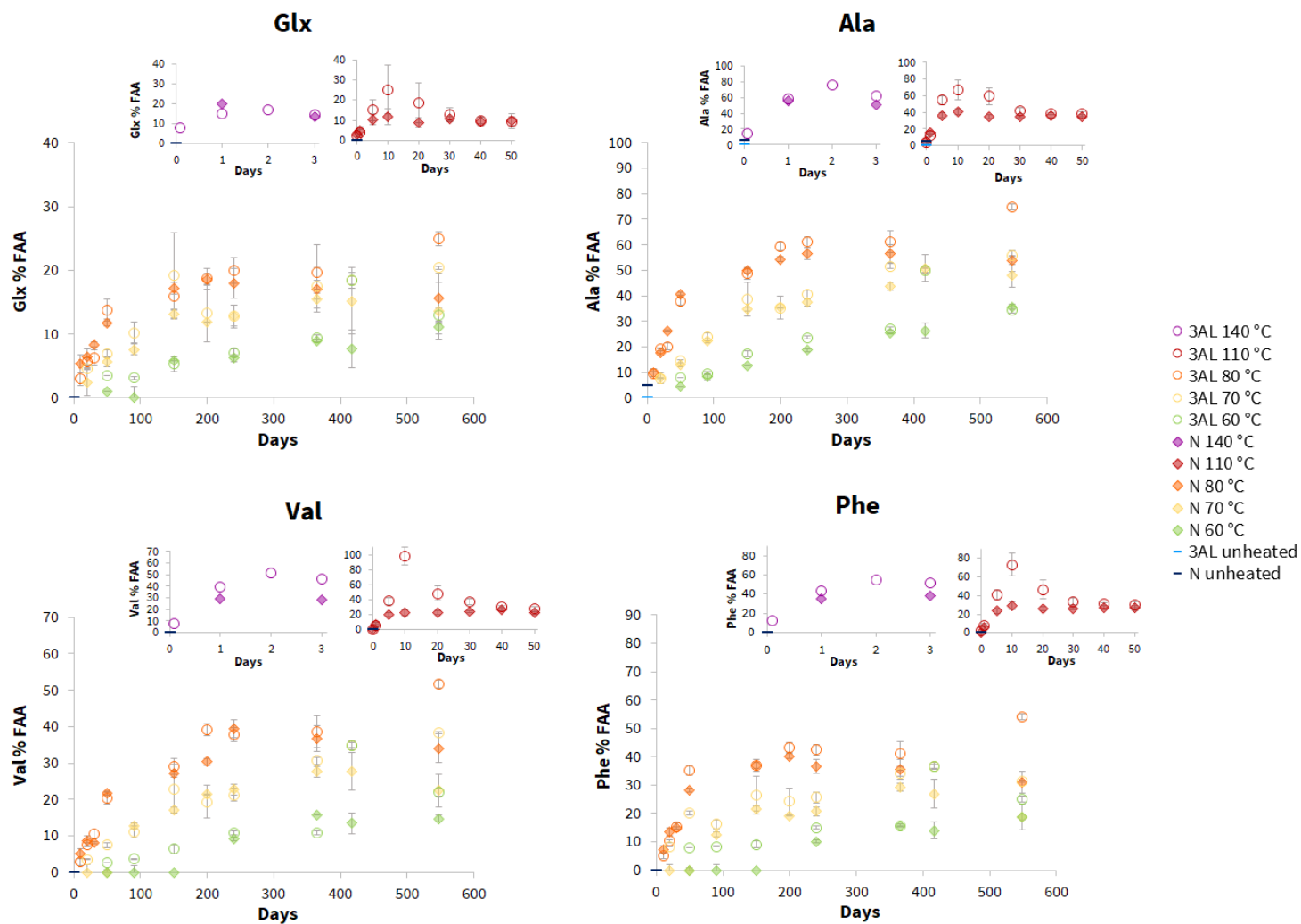
SI Figure 3.4. The average extent of peptide chain hydrolysis in Glx, Ala, Val and Phe in intra-crystalline 3AL shell portion and 'nacreous' layer of A*chatina tavaresiana* shell during isothermal heating at 60, 70, 80, 110 and 140 °C. Error bars represent the standard deviation about the mean for subsample experimental triplicates.

3.5.3.2. Comparison between fossils and modern heated samples

3.5.3.2.1. Concentration
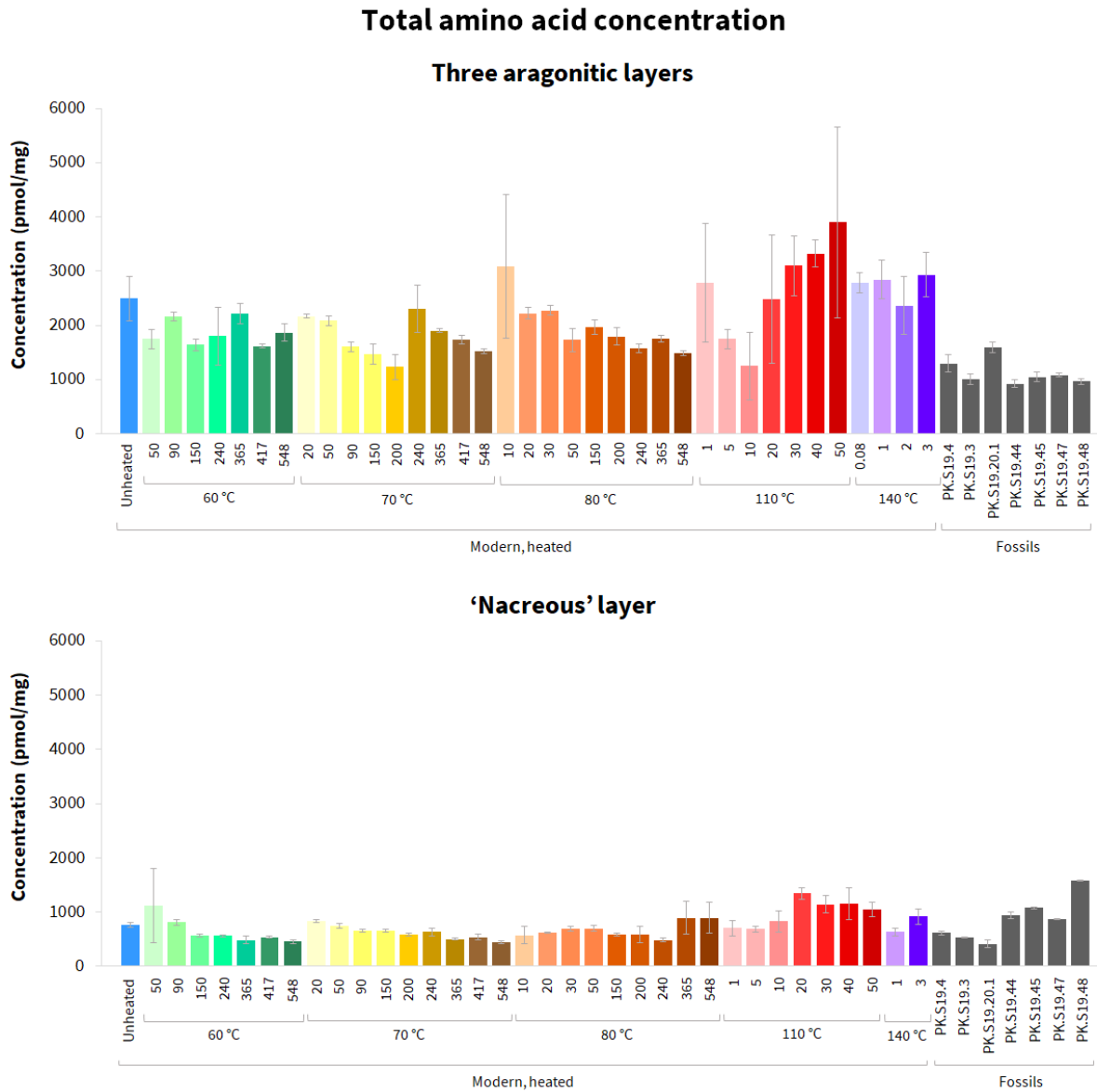
SI Figure 3.5. Comparison between the average total amino acid concentration of modern heated A*chatina tavaresiana* and fossil *Lissachatina* sp. samples in the 3AL and 'nacreous' shell portions. Error bars represent the standard deviation about the mean for subsample experimental triplicates.

3.5.3.2.2. Relative composition

Relative Composition

SI Figure 3.6. Mean relative amino acid abundances for the total hydrolysable amino acids (THAA) in the three aragonitic layer and 'nacreous' shell portions of A*chatina tavaresiana* during heating to 60, 70, 80, 110 and 140 °C and fossil *Lissachatina* sp. samples.

3.5.4. Kinetic behaviour

3.5.4.1. Reaction parameter calculations

There are several mathematical models which can be used to investigate and describe the behaviour of amino acid racemisation (Clarke and Murray-Wallace, 2006); two kinetic models were examined here in order to explore some of the assumptions behind high temperature experiments and the impacts on resulting kinetic parameters. A comprehensive test of all models (including additional models e.g. Bayesian approaches (e.g. Allen *et al.*, 2013) and the 'model-free' approach (e.g. Tomiak *et al.*, 2013)) was not undertaken due to the limitations of this fossil dataset, which contained little stratigraphic control and no calibration of the fossil samples. We therefore selected two commonly occurring models to test the plausibility of the derived kinetic parameters. For simplicity here we use the term "k" to describe the rate of the reaction, but we recognise that because of the complexity of reactions involved in the overall extent of racemisation, it is better considered as k effective (k_{eff}).

Reversible first order kinetics (RFOK) has been shown to describe free amino acids in aqueous solution (Bada and Schroeder, 1975). This mathematical model considers racemisation as described by SI equation 3.1, the interconversion of free amino acids, with equal forward and reverse rates. In proteins, where a range of additional reactions may be simultaneously taking place, racemisation is better described as the apparent reversible first order kinetics ($RFOK_a$) (Clarke and Murray-Wallace, 2006).

$$\text{L – amino acid} \quad \underset{k_2}{\overset{k_1}{\rightleftharpoons}} \text{D – amino acid}$$
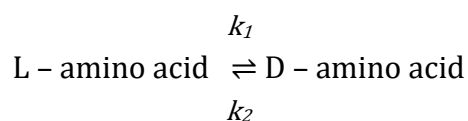
SI Equation 3.1. For reversible first order kinetics, k_1 (forward rate constant) = k_2 (reverse rate constant) for free amino acids in aqueous solution.

$$Ln\left(\frac{1+D/L}{1-D/L}\right) \; + \; c = 2kt$$

SI Equation 3.2. Describes RFOK, where c is a constant to account for laboratory induced racemisation, k is the rate of racemisation ($k_1=k_2$) and t is time.

$RFOK_a$ (SI equation 3.2) has been frequently shown not to accurately describe racemisation of amino acids during protein degradation in biominerals due to the numerous additional chemical interactions and degradation pathways simultaneously occurring (Clarke and Murray-Wallace, 2006). Alternative kinetic models, such as constrained power law kinetics (CPK), attempt to better linearise the data by introducing an alterable power function (n) to improve the data fit (SI equation 3.3).

$$Ln\left(\frac{1+D/L}{1-D/L}\right)^{n} + c = 2kt$$

SI Equation 3.3. Describes CPK, where c is a constant to account for laboratory induced racemisation, k is the rate of racemisation ($k_1=k_2$) and t is time and n is a numerical value used to improve the linearisation between racemisation (D/L) and time.

With a minimum of three temperatures, and making the assumption that the reaction pathways are the same at all temperatures, calculation of the activation energy for racemisation is possible using the Arrhenius equation (3.4).

$$k = Ae^{\frac{-E_a}{RT}}$$

SI Equation 3.4. Arrhenius equation, where k is the rate constant, A is the Arrhenius constant, E_a is the activation energy, R is the universal gas constant and T is temperature.

This high temperature experimental dataset was also investigated for its potential to calculate numerical ages of past climate temperatures for the fossils studies here. Due to the similarity of calculated activation energies for the 3AL shell portion (table 3.3) and the inability to assess which calculated value (from RFOK$_a$ or CPK) was more accurate for the 'nacreous', all subsequent calculations were performed using RFOK data.
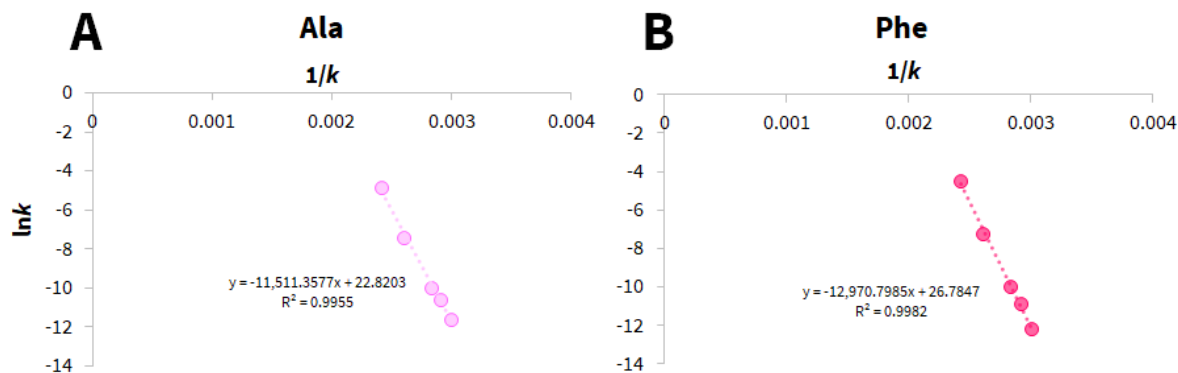
SI Figure 3.7. Arrhenius plots for hydrolysed Ala and Phe in the 3AL shell using RFOK.

Calculated 'kinetic ages' and 'kinetic temperatures' are given in SI table 3.1 for Ala and Phe. This is an additional way in which the functionality of the mathematical models can also be assessed (by comparing the ages (or temperatures) of the same fossil's shell portion between amino acids). The linearity achieved using RFOK$_a$ for both alanine and phenylalanine in the 3AL shell portion was very good ($R^2 > 0.99$, SI Fig. 3.7), but the numerical ages calculated differed notably (SI table 3.1).

SI Table 3.1. 'Kinetic age' and 'kinetic temperature' calculations using two fossils from both their 3AL and 'nacreous' (N), comparing two amino acids. 'Kinetic ages' were calculated using Lusaka, Zambia's current mean annual temperature (MAT, 20.4 °C). 'Kinetic temperatures' were calculated using arbitrary fossil ages of 200 ka and 400 ka for these Late Middle Pleistocene fossils. Note that the 'kinetic age' and 'kinetic temperature' outputs from the mathematical models do not agree with the palaeoenvironmental information for these fossils and should not be interpreted as accurate values for this site.

Fossil ID	Shell fraction	'Kinetic age' (years) using current MAT: 20.4 °C		'Kinetic temperature' (°C) using fossil age: 200 ka		'Kinetic temperature' (°C) using fossil age: 400 ka	
		Ala	Phe	Ala	Phe	Ala	Phe
PK.S19.44	3AL	2705	8697	-8.6	1.0	-12.7	-3.0
	N	1673	1276	-9.1	-11.8	-12.9	-15.7
PK.S19.45	3AL	1724	7524	-11.3	0.1	-15.4	-3.8
	N	2468	2156	-7.0	-8.8	-10.8	-12.8

3.5.5. References

Allen, A.P., Kosnik, M.A. and Kaufman, D.S., 2013. Characterizing the dynamics of amino acid racemization using time-dependent reaction kinetics: a Bayesian approach to fitting age-calibration models. *Quaternary Geochronology, 18*, pp.63-77.

Bada, J.L. and Schroeder, R.A., 1975. Amino acid racemization reactions and their geochemical implications. *Naturwissenschaften, 62*, pp.71-79.

Barham, L.S. and Smart, P.L., 1996. Current events: An early date for the Middle Stone Age of central Zambia. *Journal of Human Evolution, 30*(3), pp.287-290.

Barham, L.S., 1998. Possible early pigment use in south-central Africa. *Current Anthropology, 39*(5), pp.703-710.

Barham, L.S., Simms, M., Gilmour, M., Debenham, N., 2000. Chapter 10 Twin Rivers, excavation and behavioural record in Barham, L.S., 2000. *The Middle Stone Age of Zambia, South Central Africa*. Western academic & specialist Press. pp. 165-216.

Bishop, L.C. and Reynolds, S.C., 2000. Chapter 11 Fauna from Twin Rivers in Barham, L.S., 2000. *The Middle Stone Age of Zambia, South Central Africa*. Western academic & specialist Press. pp. 217-222.

Casanova, J., Hillaire-Marcel, C., 1992. Chronology and paleohydrology of late Quaternary high lake levels in the Manyara basin (Tanzania) from isotopic data (^{18}O, ^{13}C, ^{14}C, Th U) on fossil stromatolites. *Quaternary Research, 38(*2), pp.205–226.

Clarke, S.J. and Murray-Wallace, C.V., 2006. Mathematical expressions used in amino acid racemisation geochronology—a review. *Quaternary Geochronology, 1*(4), pp.261-278.

Simms, M.J., 2000. Appendix 7(a) Preliminary Report on the Sediments of Lake Patrick in Barham, L.S., 2000. *The Middle Stone Age of Zambia, South Central Africa*. Western academic & specialist Press. pp. 275-280.

Tomiak, P. J., Penkman, K. E H., Hendy, E. J., Demarchi, B., Murrells, S., Davis, S., McCullagh, P., Collins, M. J. 2013. Testing the limitations of artificial protein degradation kinetics using known-age massive *Porites* coral skeletons. Quaternary Geochronology, 16, pp.87-109.

Zhang, D.D., Zhang, Y., Zhu, A. and Cheng, X., 2001. Physical mechanisms of river waterfall tufa (travertine) formation. *Journal of Sedimentary Research, 71(*1), pp.205-216.

Chapter 4. Old fossils, new information: insights into site formation processes of two Pleistocene cave sequences in Zambia from enamel amino acid geochronology

Taxonomic re-identifications by morphological analysis were undertaken by SR; all laboratory and data analysis were undertaken by CB; all interpretation and writing were carried out by CB with guidance from MD, TW, LB and KP.

The purpose of this study was originally to investigate whether AAG frameworks could be built from enamel fossils from relevant taxa in this region. Subsequently, the data was used to improve understanding of the chronology of Twin Rivers archaeological site, and for regional site comparisons.

Authorship

Chloë Baldreki[1]*, Marc Dickinson[1], Sally Reynolds[2], Tom S. White[3], Lawrence Barham[4], Kirsty Penkman[1]

[1]Department of Chemistry, University of York, UK
[2]Institute for Studies of Landscape and Human Evolution, Bournemouth University, UK
[3]Principal Curator, non-Insect Invertebrates, Natural History Museum, London, UK
[4] Department of Archaeology, Classics and Egyptology, University of Liverpool, UK

Key words

Abstract

Intra-crystalline protein degradation (IcPD) analysis was undertaken on 80 fossil tooth enamel samples from four taxonomic groups (rhinocerotid, suid, equid, bovid) excavated from two archaeological cave sites in Zambia (Twin Rivers and Mumbwa Caves). Seventy-two (90%) of these fossils showed evidence of closed system behaviour. The fossils' relative extent of protein degradation

153

between the sites was consistent with their known ages, with samples from Twin Rivers (Mid-Pleistocene) showing higher levels of degradation than Mumbwa Caves (late Mid-Pleistocene to late Holocene). At Twin Rivers, a potential trend between IcPD and excavation depth was observed, concordant with the working hypothesis of periodic deposition of sediments as slurry flows into a phreatic passage. However, greater depositional and taphonomic complexity was indicated by relatively wide ranges of IcPD values within individual excavation levels. These results are interpreted partly as the consequence of the excavation methods used, alongside reworking within the deposits, which had not previously been recognised. Whilst lack of stratigraphic control limited the investigation of taxonomic effect, one notable difference in the protein breakdown pattern of peptide chain hydrolysis was observed between rhinocerotid in comparison to the other studied taxa. We therefore recommend taxon-specific enamel amino acid geochronologies (AAGs) are developed in future. Whilst lack of comparator datasets meant it was not possible to create a calibrated, enamel AAG for the South-Central African region from these sites, Twin Rivers provides a case study illustrating the complexity of cave formation processes and the importance of direct dating for interpreting archaeological and palaeontological sequences.

4.1. Introduction

The ability to accurately date archaeological sites and their material is essential to the study of human evolution over the Pleistocene. Caves are common archaeological sites within the Palaeolithic (e.g. Barham and Mitchell, 2008; Dennell, 2009; French, 2021) and can act as excellent fossil repositories, especially in areas of the African continent such as the South-Central region (Fig. 4.1), where fossil preservation is generally poor (Bishop *et al.*, 2016). This region's current ecology, reflecting its topography, is diverse, with tropical deciduous woodlands across the high central plateau grading to dryland savannah on the margins of the Kalahari basin. Large wetlands occur in northern Zambia and in neighbouring northern Botswana today, and evidence has been found for a vast palaeo-wetland during the Pleistocene encompassing the Okavango delta, Makgadikgadi basin, and the Zambezi and Kafue rivers (Chan *et al.*, 2019; Burrough *et al.*, 2022). This wetland would have provided both a migratory corridor between South and East Africa and an ideal environment for mammalian (including hominin) habitation. The region has preserved important Mid-Pleistocene fossils, most notably the Kabwe cranium (*Homo heidelbergensis* (*rhodesiensis*)) (Grün *et al.*, 2020), evidence for the transition from the Early to Middle Stone Age (Duller *et al.*, 2015), the preservation of evidence for early pigment use (Barham, 2002) and woodworking (Barham *et al.*, 2023).
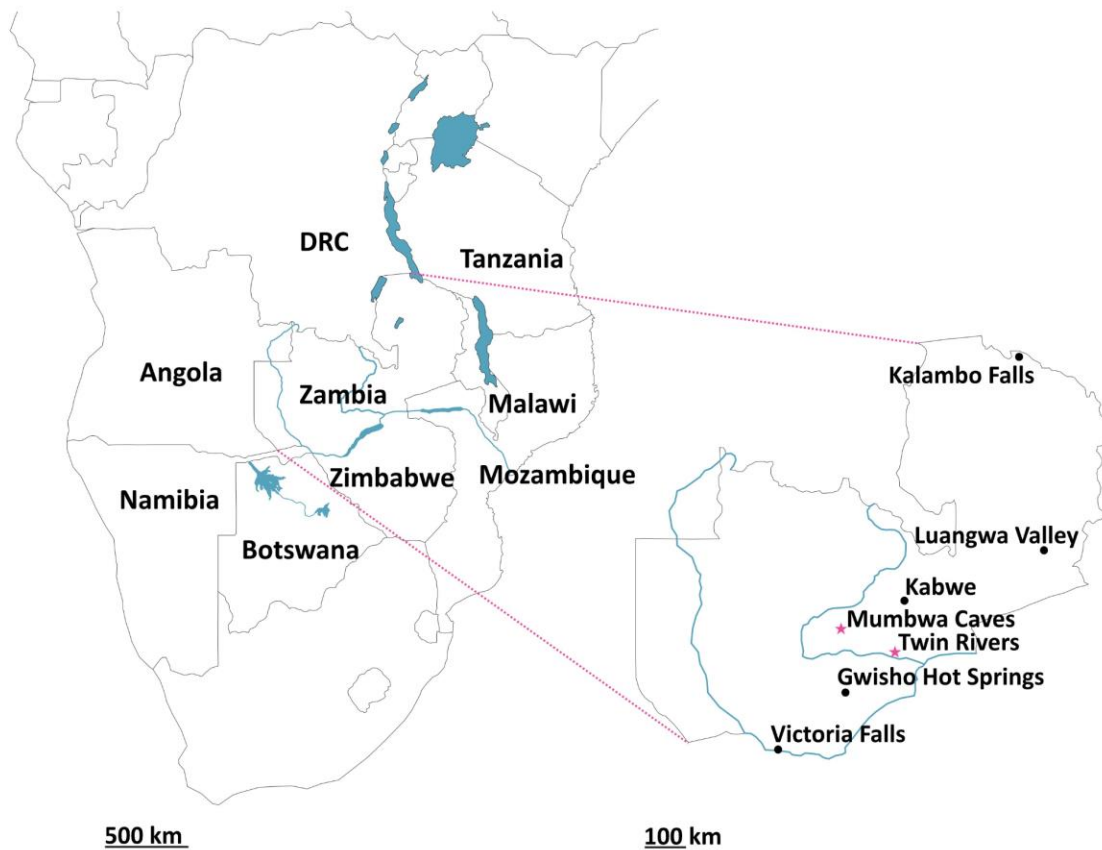
Figure 4.1. Left: Map of southern Africa highlighting the South-Central African region with major current water bodies; Right: Map of Zambia highlighting key archaeological sites. Those included in this study (Twin Rivers and Mumbwa Caves) are highlighted with pink stars.

Many archaeological and palaeoenvironmental sites have poorly constrained chronologies, and cave sites are well known for their complex depositional histories, making dating and accurate site interpretation especially challenging (e.g. Brain, 1983; Reynolds and Kibii, 2011; Val *et al.,* 2015; Marin-Monfort *et al.*, 2022). Direct dating of fossils (as opposed to dating associated sediments and/or flowstones) can enable identification of stratigraphic disruption and place the archaeologically/palaeontologically relevant material within a more detailed stratigraphic context. One such technique, amino acid geochronology (AAG), has the potential to provide direct, relative, dating on fossil biominerals (e.g. Wehmiller, 1977; Bowen *et al.*, 1989; Brooks *et al.*, 1990; Penkman *et al.*, 2007; Hearty and Kaufman, 2009; Torres *et al.*, 2014; Koppel *et al.*, 2016). AAG exploits the time-dependent degradation of proteins (such as amino acid racemisation; AAR) trapped in fossil biominerals (Abelson, 1955; Hare and Mitterer, 1967). As protein degradation is temperature dependent, AAGs are built regionally (Wehmiller and Miller, 2000) and to date only one AAG study in gastropod shell has been published for the South-Central African region (Baldreki *et al.*, 2024).

155

One approach which has been shown to improve the reliability of AAG data in some biominerals is intra-crystalline protein degradation (IcPD), which targets the analysis of protein within the fossil's mineral matrix. This fraction of protein, isolated with the use of a strong chemical oxidant, has been shown to effectively operate as a closed system in many $CaCO_3$ biominerals (e.g. gastropods (Sykes *et al.*, 1995; Penkman *et al.*, 2008; Demarchi *et al.*, 2013a), ostrich eggshell (Crisp *et al.*, 2013), coral (Hendy *et al.*, 2012) and foraminifera (Wheeler *et al.*, 2021)). Where the intra-crystalline fraction is shown to operate as a closed system, leaching of endogenous protein, contamination by exogenous protein and most additional environmental impacts on protein degradation (e.g. pH (Hare and Mitterer, 1969)) are minimised (Towe, 1980). In some biominerals, targeting the intra-crystalline fraction has been shown to improve the accuracy and precision of the data, thereby increasing the reliability of the geochronologies obtained (e.g. Brooks *et al.*, 1990; Penkman *et al.*, 2013; Wheeler *et al.*, 2021). Oxidative treatment is not always suitable or necessary (e.g. Orem and Kaufman, 2011; Torres *et al.*, 2014; Demarchi *et al.*, 2015; Ortiz *et al.*, 2017), and stringent data screening approaches have also been successfully employed for many fossil biominerals (e.g. Brooks *et al.*, 1990; Kaufman, 2006; Kosnik and Kaufman, 2008; Ortiz *et al.*, 2013; 2018; Wheeler, 2022).

Recent methodological advances to the IcPD protocol for the analysis of tooth enamel ($CaPO_4$), has confirmed that this biomineral also has an intra-crystalline protein fraction which effectively behaves as a closed system (Dickinson *et al.*, 2019). This has opened an additional avenue of direct dating for fossil teeth, which are commonly found at archaeological cave sites. The enamel proteome is composed of a small number of proteins, whose primary sequence has been shown to vary by taxa (and therefore infer phylogenetic relationships e.g. Cappellini *et al.*, 2019; Welker *et al.*, 2019). As protein degradation, including racemisation, is influenced by the sequence of amino acids in a peptide chain (Mitterer and Kriausakul, 1984), any taxonomic effect in tooth enamel IcPD ratesneed to be accounted for in any arising amino acid geochronology (Cappellini *et al.*, 2019; Dickinson *et al.*, 2024).

Here we explore the capacity of tooth enamel to build taxa-specific aminostratigraphies for the South-Central African region using IcPD analysis. We tested fossil teeth/fragments of four commonly occurring taxonomic groups (rhinocerotid, equid, suid, bovid) excavated from Twin Rivers and Mumbwa Caves archaeological sites in Zambia (Fig. 4.1). We investigate whether the intra-crystalline fraction of protein behaves as a closed system in these taxa and examine age-related signals of protein degradation. Through these investigations, we demonstrate the use of this AAG approach to examine depositional histories and taphonomies, and inter-site relationships.

4.2. Materials and Methods

4.2.1. Materials

The 80 fossil teeth/fragments included in this study are from two archaeological cave sites in Zambia (Twin Rivers and Mumbwa Caves; Fig. 4.1, Table 4.1, SI Data) and represent commonly found fauna in the region. Both sites provide important regional climate and behavioural records: Mumbwa Caves for the Middle to Late Pleistocene (Burrough *et al.*, 2019) and Twin Rivers for the Middle Pleistocene (Barham, 2000). Both sites were excavated in the 1990s with faunal assemblages reported and discussed in Barham (2000), Klein and Cruz-Uribe, (2000) and Bishop and Reynolds (2000).

4.2.1.1. Mumbwa Caves

Mumbwa Caves in Zambia has had a number of dating techniques applied to its sediments and materials (Barham and Debenham, 2000) including thermoluminescence (TL) on burnt quartz and calcite, radiocarbon on charcoal, optically stimulated luminescence (OSL) on sediment and electron spin resonance (ESR) on enamel, and the stratigraphy is relatively well constrained to a maximum age of >172 ka (Barham, 2000).

Amino acid geochronology was considered during the 1993 excavation, but the only applicable biomineral at the time was ostrich eggshell, which was not present at the site (Brooks *et al.*, 1990; Barham and Debenham, 2000). The enamel IcPD protocol published in 2019 (Dickinson *et al.*, 2019) therefore opened another avenue for dating and depositional history interpretation. Unfortunately, the teeth/fragments used for the previous enamel ESR analysis were not available, and thus IcPD analysis could not be undertaken on these specimens for direct comparison between the two dating techniques. Additionally, the stratigraphic context of each specimen that was available for analysis was unrecoverable, and the loss of contextual information (including taxonomy) meant that individual specimens could not be linked to the published identifications. One intention of this study was therefore to increase the scientific value of these materials through re-identification of their taxonomy and explore their potential to provide useful age information through IcPD analysis.

4.2.1.2. Twin Rivers

The tooth enamel samples analysed in this study from Twin Rivers were excavated from A Block (Fig. 4.2) in 1999. A Block originated as an irregularly shaped phreatic passage and the sediments are thought to have been deposited in periodic, gentle slurry flows. Over time much of the deposits became cemented into breccia with lenses of speleothem separating the breccia into units. The cave roof collapsed at an unknown time, leaving the deposit exposed to weathering. Dynamite was used in the 1950s to excavate much of the deposit (Clark and Brown 2001; blast scree area shown in Fig. 4.2), though none of the material included in this study comes from this excavation. The 1999

excavations focused on shallow (<60 cm) and narrow (<30 cm) pockets of loose sandy sediment between the breccia and the cave walls. The pockets contained sharp stone tools, ochre pieces, and faunal fossils (Barham, 2000). As a hilltop site, the presence of rhinocerotid and giraffid (among others) within the fossil assemblage is thought to have accumulated from predation and/or scavenging activity, including the possibility of (but not limited to) hominin activity. The excavation was named using a hybrid reference system (e.g. E5/E6; Fig. 4.2), with each pocket/cavity discrete from one another. The excavation within each discrete cavity was conducted in horizontal levels in the absence of any visible stratigraphy. There is therefore no correlation between excavation levels of different cavities.
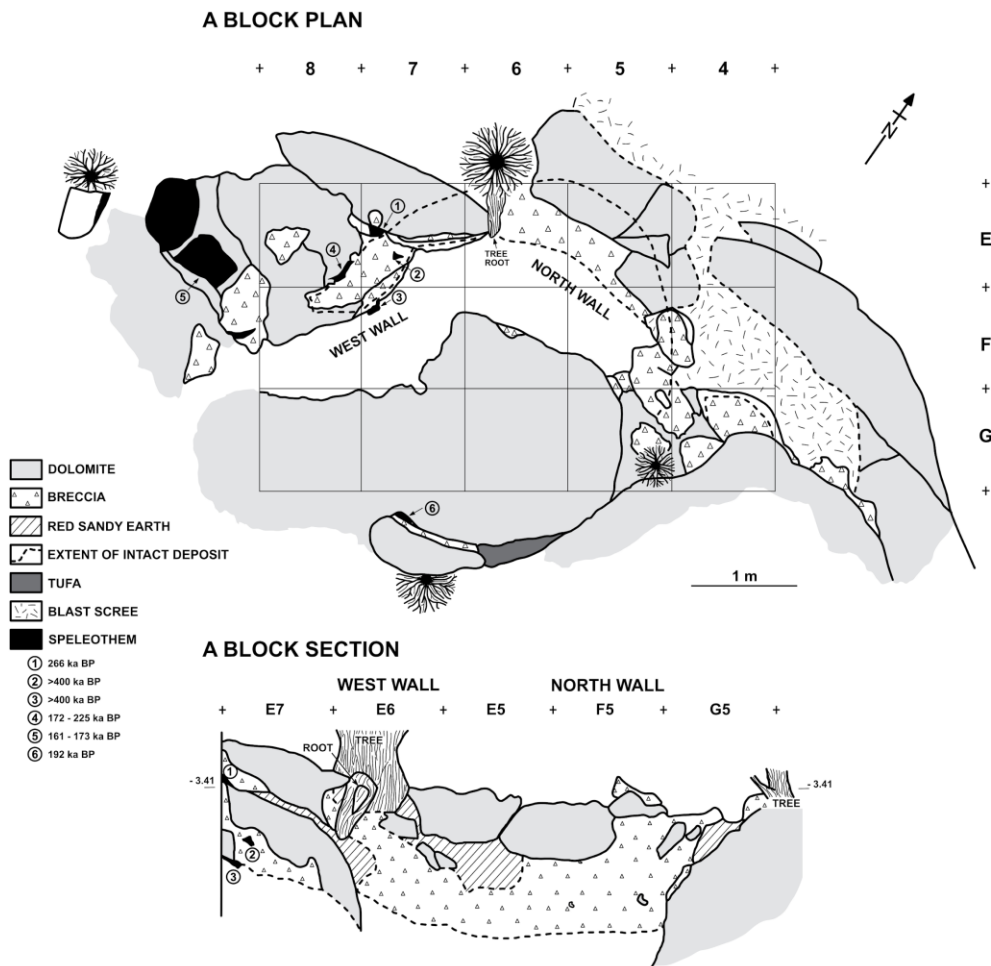
Figure 4.2. Plan and section (west and north walls) of Twin Rivers A Block excavated in 1999. Speleothem are shown with associated uranium-thorium dates (speleothem: sample 1 = 266 ka BP, sample 2 = >400 ka BP, sample 3 = >400 ka BP, sample 4 = 172-225 ka BP, sample 5 = 161-173 ka BP, sample 6 = 192 ka BP). All tooth enamel samples analysed for AAG were excavated from red sandy earth sediments which filled multiple discrete cavities between the cave walls and the rim of the intact breccia. Due to the irregular shape of the cave passage and deposits within, not all excavation cavities and no excavation levels are visible in this section.

158

Previous speleothem U-series dating at the site placed the collapsed cave passage sequence to ~170 - >400 ka (Barham, 2000). The nature of the site meant that, with one exception (266 ka), the flowstones were not directly related to the excavated levels. Whilst their associations were helpful in providing minimum and maximum ages, and ages concordant with increasing depth, they were difficult to directly relate to the archaeological material. Additionally, due to the upper age limitation of the U-series dating undertaken here (>400 ka), the base of the sequence has a minimum age of 400 ka but could represent a much older formation. It was therefore hoped that enamel IcPD could be used as a direct dating technique to improve the understanding of the ages of the faunal material from this site.

4.2.1.3. Taxonomic re-identification

Both the Mumbwa Caves and Twin Rivers teeth/fragments required taxonomic re-identification due to the loss of contextual information. These were visually evaluated by one of us (SCR) who had previously analysed the original faunal material from Twin Rivers in 2000 (Bishop and Reynolds, 2000). Additional published species lists, such as Clark and Brown (2001) were also consulted. The very fragmentary material was assigned to genus only, and specimens were only assigned to species level if the dental morphology was complete enough to permit this (SI Data). For all subsequent sections, data is discussed in terms of the four family groups commonly identified amongst the Twin Rivers and Mumbwa Caves faunal fossil assemblages (rhinocerotid, equid, suid, bovid). These taxa were selected as they have not yet been characterised for enamel amino acid geochronology but form a common component of Pleistocene faunal assemblages in Africa (and elsewhere) and therefore potentially have a wide utility for dating.

Table 4.1. Tooth enamel samples analysed in this study; Numbers in brackets indicate the number of individual teeth/fragments sampled. For more detailed sample information please see the supplementary data.

| Site Name | Excavation | | Taxa |
	Cavity	Level	
Twin Rivers	E5/F5	1	Rhinocerotid (3), Suid (1), Equid (1), Bovid (1)
		2	Bovid (1)
	E4/F4	1	Suid (3), Equid (6)
		3	Rhinocerotid (3), Equid (1), Bovid (1)
	E5/E6	1	Rhinocerotid (3), Equid (1)
		2	Rhinocerotid (2), Equid (4)
		3	Rhinocerotid (5), Suid (2), Bovid (4)
		4	Rhinocerotid (1), Suid (2), Equid (3)
		5	Equid (1), Bovid (1)
	G5	N/A	Bovid (3)
Mumbwa Caves	N/A	N/A	Suid (10), Equid (4), Bovid (13)

4.2.2. Enamel IcPD methodology

All tooth enamel samples were prepared and analysed following the methods of Dickinson *et al.*, (2019).

Approximately 40 mg of enamel (as chips, from a single location) was removed from each tooth/fragment (Table 4.1) using abrasive rotary drill bits on a handheld rotary tool (Dremel drill), before being washed with water (ultrapure, 18.2 MΩ cm^{-1}) and left to air dry. Each enamel sample was powdered with an agate pestle and mortar.

Bleach (12% NaOCl (analytical grade), 50 µL/mg) was added to each accurately weighed powdered sample (in separate 2 mL plastic microcentrifuge tubes) and left on a rotor (constant mild agitation) for 72 hours. The bleach was removed by pipette and each sample was washed five times with water (ultrapure, 18.2 MΩ cm^{-1}), before a final wash with methanol (HPLC-grade) and the powdered sample left to air dry.

Ca. 5 mg subsample replicates (accurate masses noted) of each powdered and bleached sample were weighed out for the analysis of both the free amino acid fraction (FAA) and the total hydrolysable amino acid fraction (THAA). THAA subsample replicates were demineralised in 7 M HCl (20 µL/mg), the vials flushed with N_2 and heated in an oven at 110 °C for 24 hours, prior to drying by centrifugal evaporation. The THAA subsample replicates were then redissolved in 1 M HCl (20 µL/mg) and the FAA subsample replicates demineralised in 1 M HCl (25 µL/mg), prior to the addition of 1 M KOH (28 µL/mg) to all subsamples, which formed a monophasic translucent gel with a viscous consistency. All subsamples were centrifuged at 13,000 rpm for 5 minutes whereupon a biphasic

solution formed (supernatant above a cloudy gel). The supernatant was removed and dried by centrifugal evaporation.

The subsamples were rehydrated in the minimum possible volume (at 10 µL/mg, with 10 µL aliquots additions to achieve dissolution where necessary) of a solution of internal standard (L-homo-arginine (0.01 M), hydrochloric acid (0.01 M) and sodium azide (1.5 mM)). Separation of the chiral isomers of the amino acids (Fig. 4.3) was carried out by fluorescence detection RP-HPLC (Agilent 1100) using a modified Kaufman and Manley (1998) method (Penkman, 2005). As experimental subsample replicates were prepared, no analytical replicates were undertaken. Analytical replicates have been shown to account for only a small portion of the total variability, hence the use of subsample experimental replicates also encompasses analytical variability (Powell *et al.*, 2013).
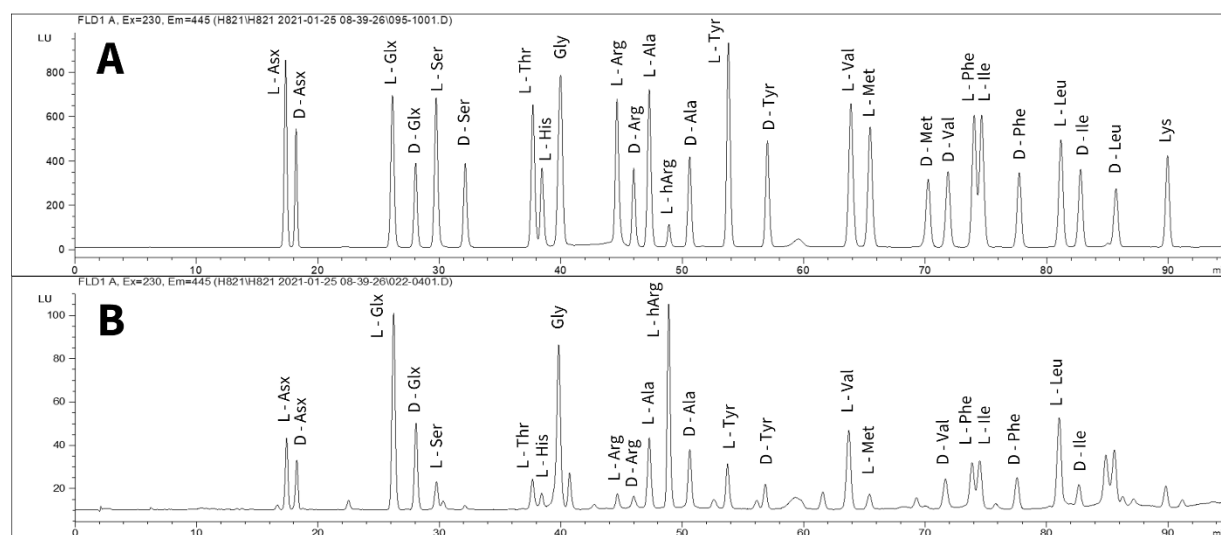
Figure 4.3. Example chromatograms of A – 0.5 standard, B – rhinocerotid THAA sample.

Total amino acid concentration and relative composition calculations were carried out from the enantiomeric chromatographic peaks of Asx, Glx, Ser, Thr, His, Gly, Arg, Ala, Tyr, Val, Met, Phe, Ile and Leu. In the case of Thr and His only the L enantiomer is resolved by this chromatographic method, whilst Gly contains no stereogenic centre and therefore does not have L/D enantiomers (Fig. 4.3). During the laboratory preparation procedures, irreversible deamidation of Asn to Asp and Gln to Glu is induced. It is therefore not possible to distinguish between these chromatographically and are therefore reported as Asx and Glx (Hill, 1965). Sufficient concentration and chromatographic resolution was achieved for the calculation of racemisation and percentage free values for Asx, Glx, Ser, Ala, Val, Phe within the tooth enamel (SI Data).

4.3. Results and Discussion

4.3.1. Assessment of closed system behaviour

The closed-system behaviour of the intra-crystalline fraction of protein from the 80 enamel samples was assessed by looking at key aspects of IcPD data (Penkman *et al.*, 2013): the relationship between the free and total hydrolysable fractions of amino acids (section 4.3.1.1); the relative racemisation rates (section 4.3.1.2); peptide bond hydrolysis (section 4.3.1.3); serine decomposition (section 4.3.1.4) and concentration and relative composition (section 4.3.1.5).

4.3.1.1. Amino acid fraction D/L covariance

When protein degradation occurs within a closed system, a strong positive correlation should be observed in the extent of racemisation between the free and total hydrolysable amino acid fractions (Preece and Penkman, 2005; Penkman *et al.*, 2007). This was observed for the majority of samples (72) in all four taxonomic groups (rhinocerotid, equid, suid, bovid); two amino acids, Asx and Glx, are provided as examples in Fig. 4.4 (see all additional amino acids in SI Figs. 4.1-4). This indicates maintenance of closed system behaviour in these 72 samples over their depositional history. However, eight samples (10%) deviated from the general trend, with large subsample replicate variability for the majority of amino acids in these samples (TR12- Fig. 4.4A; TE2, TE6, TE10, TE12 - Fig. 4.4B; TD6 - Fig. 4.4C; MB1, MB2 - Fig. 4.4D). For seven of these samples, in each case one subsample replicate fell within, and one well outside of the observed correlation range (Fig. 4.4). Open-system behaviour from mineral diagenesis can lead to larger variability in results, and/or off-trend racemisation values (Penkman *et al.*, 2007; Dickinson *et al.*, 2024) and may therefore be an explanation for this data. For one sample (MB1- Fig. 4.4D), unexpectedly high racemisation was observed in only Glx FAA, although replicate precision was high. This sample is discussed further in sections 4.3.1.2 and 4.3.1.5. In either case, these eight samples highlight the importance of undertaking preparative replicate analysis to help identify outliers.
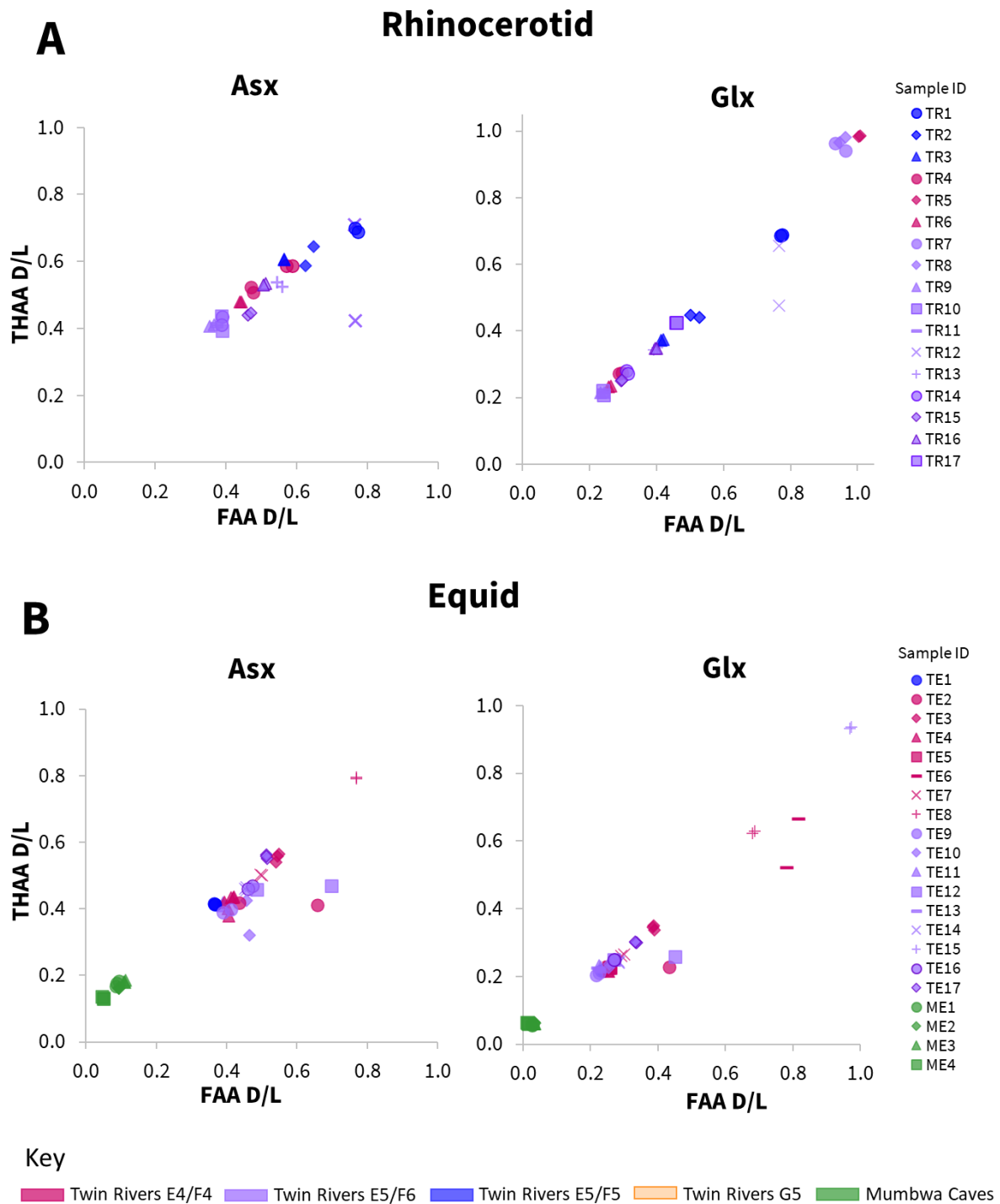
Figure 4a. Relationship between racemisation values (D/L) in free (FAA) vs total hydrolysable (THAA) amino acids, for subsample replicates, in two taxonomic groups of enamel samples (A - rhinocerotid; B – equid), for two example amino acids (Asx, Glx). Mumbwa Caves samples were all excavated from one deposit (Barham, 2000). Twin Rivers samples were excavated from four areas within the A Block cave passage (Barham, 2000).
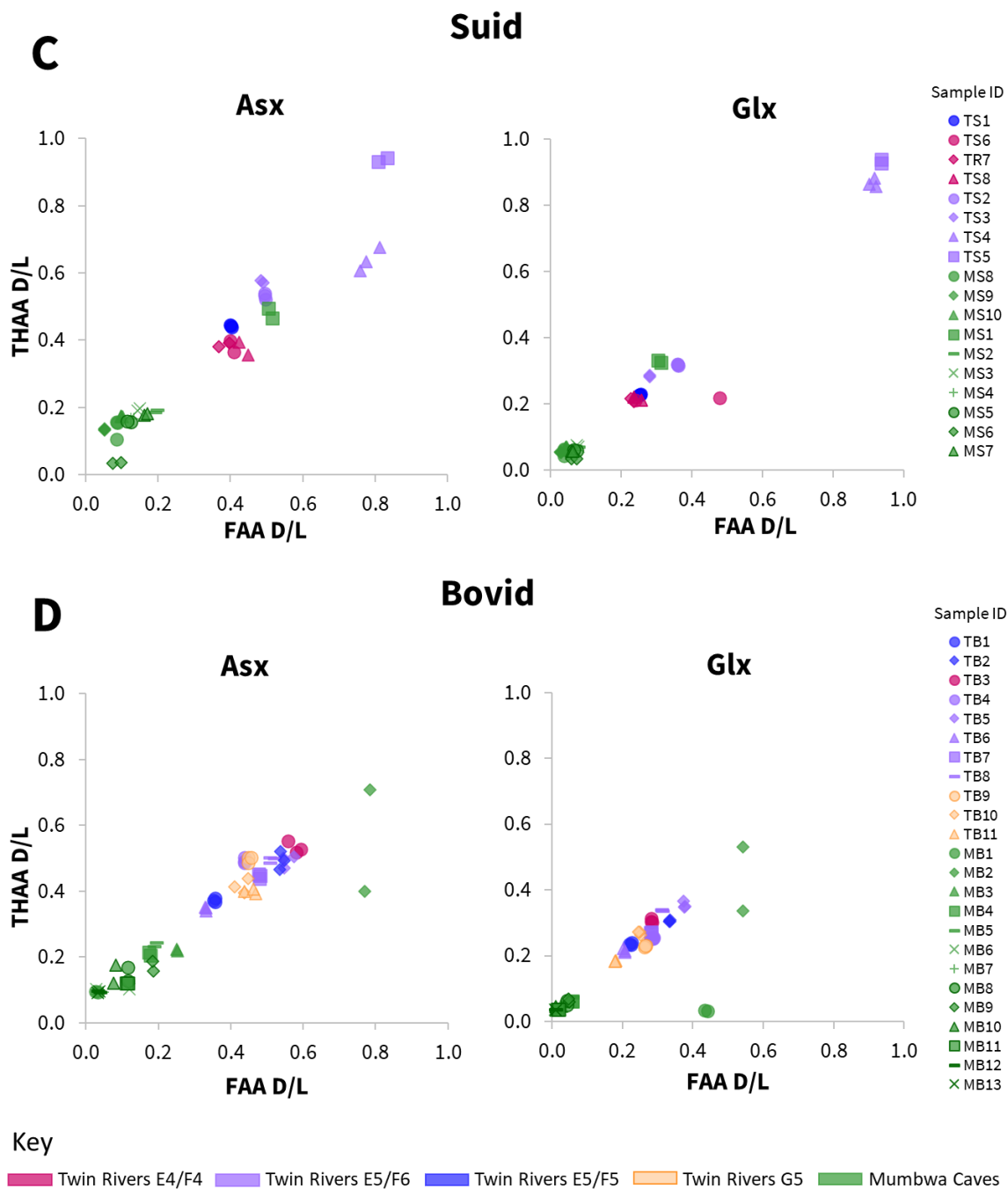
Figure 4b. Relationship between racemisation values (D/L) in free (FAA) vs total hydrolysable (THAA) amino acids, for subsample replicates, in two taxonomic groups of enamel samples (C - suid; D – bovid), for two example amino acids (Asx, Glx). Mumbwa Caves samples were all excavated from one deposit (Barham, 2000). Twin Rivers samples were excavated from four areas within the A Block cave passage (Barham, 2000).

4.3.1.2. Relative rates of racemisation

An additional avenue that can support maintenance of closed-system behaviour is the consistent relative order of amino acid racemisation. Where samples display inconsistencies in the extent of racemisation between amino acids with different relative rates, contamination and/or leaching could be the cause. Relative rates of racemisation in enamel have been shown to display broadly similar trends to other biominerals (Dickinson *et al.*, 2019) and to those reported for free amino acids in an aqueous solution (Asp>Phe>Ala>Glu>Val; Smith and Evans, 1980). This broad trend was also observed in all the taxonomic groups studied here, for example the racemisation was lower in Glx (a slower racemising amino acid) than Asx for nearly all samples (Fig. 4.4). Where near complete racemisation was observed in Glx (D/L ~ 1), Asx concentrations were too low to obtain reliable racemisation data (e.g. rhinocerotid samples TR5, TR7, TR8 - Fig. 4.4A and equid sample TE15 - Fig. 4.4C), consistent with heavily degraded protein trapped within the intra-crystalline fraction (Penkman *et al.*, 2013). Two samples (rhinocerotid TR12 and bovid MB1; already discussed in section 4.3.1.1 for deviations observed in their racemisation data) had relative rates of racemisation that deviated from this trend, with either similar or higher extents of racemisation observed in Glx to Asx, potentially indicative of contamination (Willerslev *et al.*, 2007) and/or mineral diagenesis (Preece and Penkman, 2005).

4.3.1.3. Peptide bond hydrolysis

Peptide chain hydrolysis can be investigated from IcPD data by calculating the relative percentage of free amino acids (%FAA) and allows an additional corroboration of extent of protein degradation. Hydrolysis is, however, considered a less predictable protein degradation mechanism with respect to rates (Walton, 1998), partly because its calculation compounds the errors derived from the low masses and volumes involved (rather than the cancellation achieved in D/L ratios) which occur during the calculation of concentrations (Powell *et al.*, 2013). In addition, FAA formation can be affected by other degradation mechanisms such as decomposition (e.g. Ser decomposition to Ala; Bada *et al.*, 1978) and lactam formation in Glu (Walton, 1998). %FAA therefore results in less precise data than racemisation (e.g. Penkman *et al.*, 2013), which can be observed in the higher subsample variability (Fig. 4.3). Nevertheless, peptide bond hydrolysis remains a useful marker for general protein degradation, and where closed system behaviour is maintained, different protein degradation pathways, such as hydrolysis and racemisation, should be closely related (Penkman *et al.*, 2013).

Most amino acids (with the exception of Ser and Asx, Stephenson and Clarke, 1989; Takahashi *et al.*, 2010; Demarchi *et al.*, 2013b) are not able to racemise when bound within a peptide chain (Smith and Evans, 1980; Mitterer and Kriausakul, 1984), requiring more conformational freedom, either as the terminal amino acid or completely free. Where closed system behaviour has been

maintained and degradation markers only result from endogenous protein, increasing degrees of racemisation should be correlated to increasing degrees of hydrolysis, broadly supported by this data (Fig. 4.5; SI Figs. 4.5-8). In general, for Ala, Val and Phe (SI Figs. 4.5-8), an increase in free amino acid correlated with increased racemisation in all taxa, whilst for Asx (SI Figs. 4.5-8) and Glx (Fig. 4.5), in the suid, equid and bovid, highly racemised samples resulted in a lower percentage of free amino acids (e.g. suid samples TS4, TS5 and equid samplesTE8, TE15, Fig. 4.5). The lower concentration of free amino acid in these samples may be as a result of decomposition typical of later stages of degradation. Differences in degradation patterns were observed for the rhinocerotid data in comparison to suid, equid and bovid, discussed further in section 4.3.2.
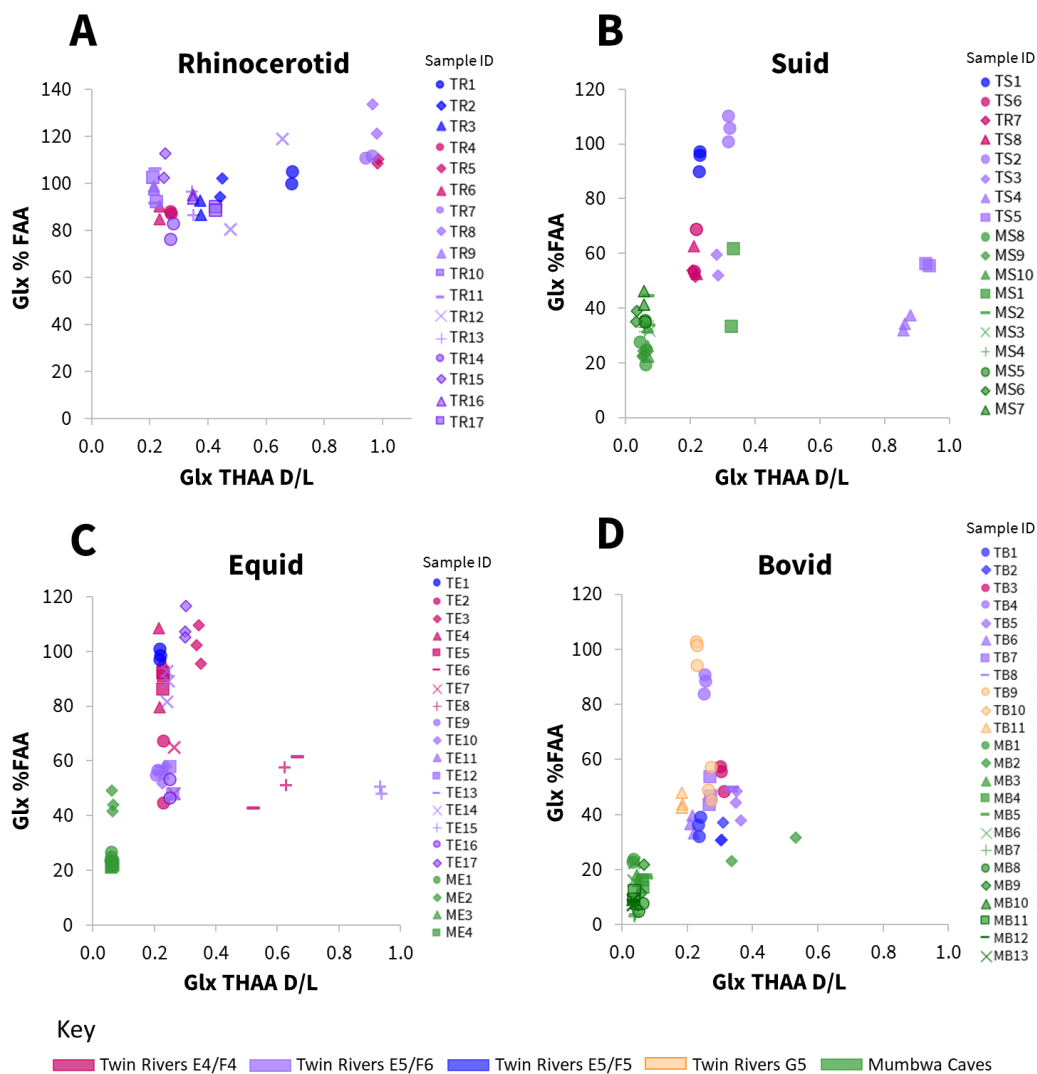
Figure 4.5. Relationship between racemisation values (THAA D/L) in Glx vs the percentage of free Glx, for subsample replicates, in four taxonomic groups of fossil enamel samples (A - rhinocerotid; B - suid; C - equid; D - bovid). Mumbwa Caves samples were all excavated from one deposit (Barham, 2000). Twin Rivers samples were excavated from four areas within the A Block cave passage (Barham, 2000).

4.3.1.4. Serine degradation

During protein diagenesis, dehydration of serine results in the production of alanine (Bada *et al.*, 1978); in a closed system, [Ser]/[Ala] (the concentration of serine divided by alanine) can therefore be used as a measure of protein decomposition. As discussed in section 4.3.1.3, where closed system behaviour is maintained, a relationship would be expected between different protein degradation pathways. As for hydrolysis, the decomposition of serine was closely correlated with racemisation. [Ser]/[Ala] rapidly decreased when Glx THAA D/Ls were low (~ 0.0 – 0.2) and slowed after Glx D/L ~ 0.2 (Fig. 4.6), indicating the retention of degradation products within a closed system (Penkman *et al.*, 2008). For four samples, large differences were observed between subsample replicates (TR12 - Fig. 4.6A, TE6, TE10 - Fig. 4.6C and MB2 - Fig. 4.6D), with one falling within and one outside of the trend; these divergent subsample replicates also showed divergent racemisation data (Fig. 4.4), indicating consistent subsample variability across multiple degradation pathways.
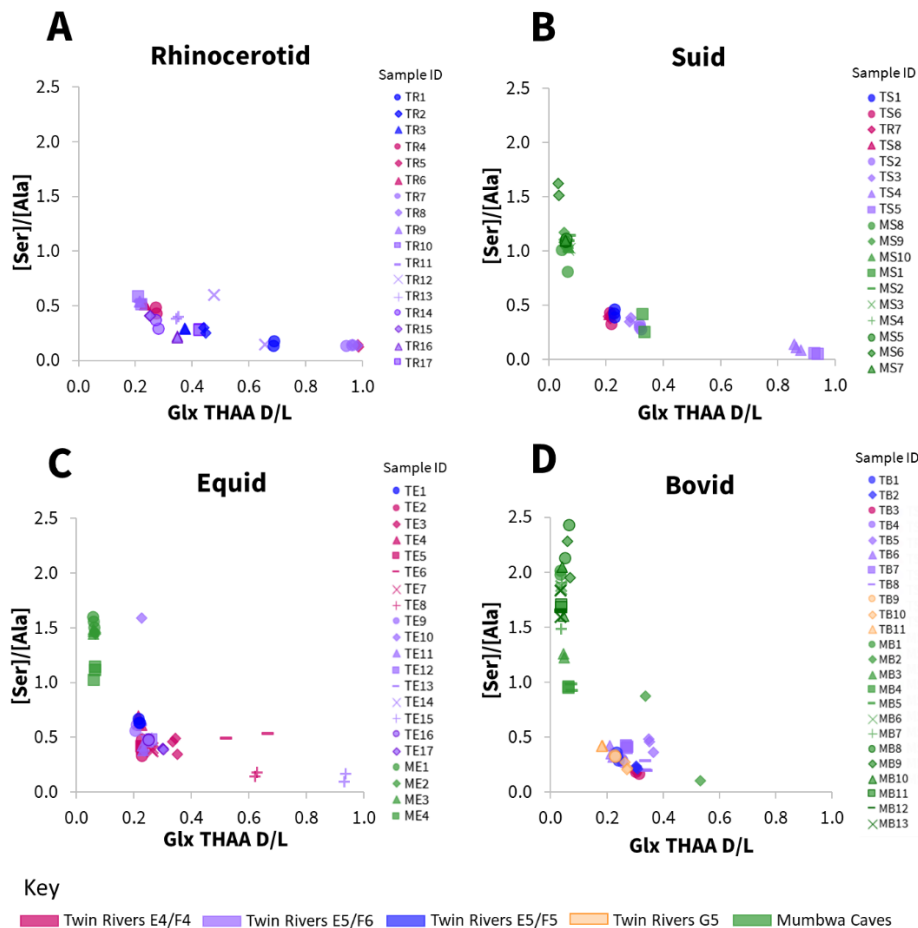
Figure 4.6. Covariance plots of average Glx racemisation vs serine decomposition in four taxonomic groups (A - rhinocerotid; B - suid; C - equid; D - bovid). No rhinocerotid samples were excavated from Mumbwa Caves, which all came from one deposit (Barham, 2000). Twin Rivers samples were excavated from four areas within the A Block cave passage (Barham, 2000).

4.3.1.5. Concentration and Composition

Concentration and relative composition are useful additional tools for closed-system behaviour assessment. As both vary with the extent of degradation, they are therefore best interpreted in combination with additional protein degradation markers. For example, low amino acid concentrations could result from highly degraded protein within a closed-system but may also arise from leaching of material out of an open-system. Similarly, relative amino acid composition can help to indicate when contamination (e.g. from dentine or exogenous sources) may be present in a sample (Dickinson *et al.*, 2019), but profiles will change as a result of degradation (e.g. Ser dehydration to Ala; Bada *et al.*, 1978). Exemplified by the rhinocerotid and equid data (Fig. 4.7; all data shown in SI Figs. 4.9-12), the low THAA concentration and very high relative proportion of Gly observed for rhinocerotid sample TR8 (Fig. 4.7) indicated heavily degraded protein, corroborated by the high levels of racemisation (Fig. 4.4), hydrolysis (Fig. 4.5) and serine decomposition (Fig. 4.6). However, for equid sample TE6 (Fig. 4.7), the low concentration and atypical composition plot (high relative proportions of Leu and Ile) were observed in combination with highly variable (off-trend) racemisation (Fig. 4.4), hydrolysis (Fig. 4.5) and serine decomposition (Fig. 4.6) data, indicating open-system behaviour and/or contamination by exogenous protein.
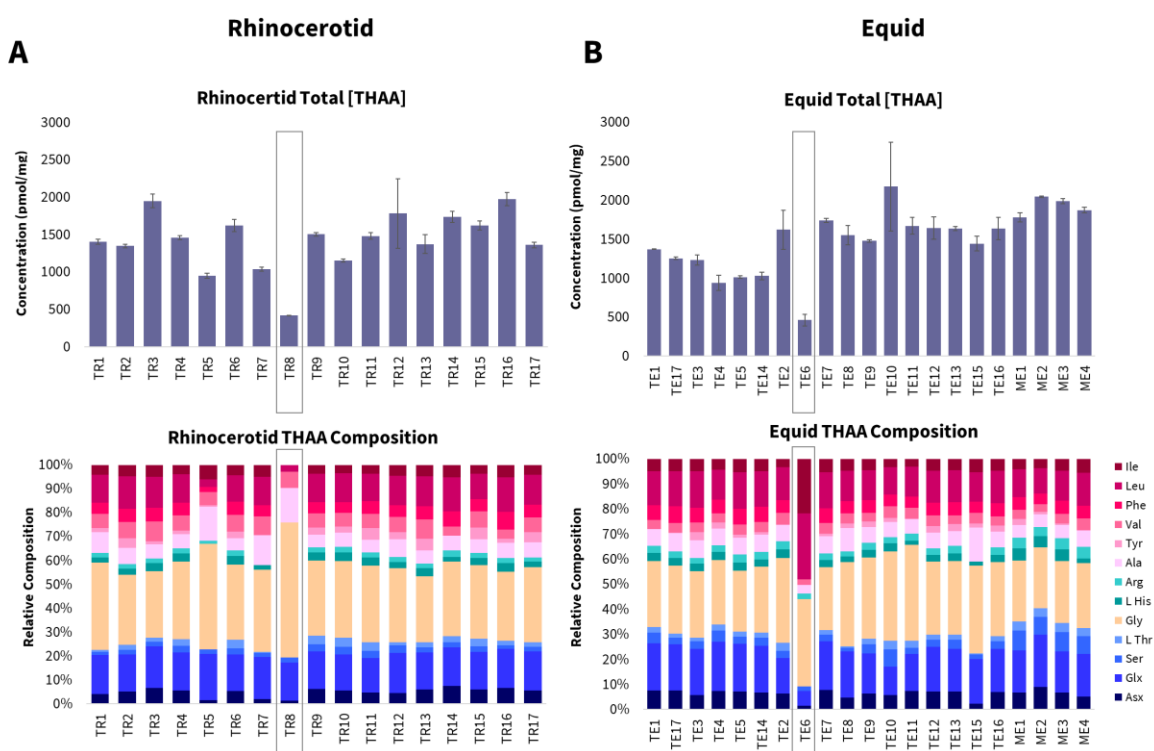
Figure 4.7. Top - average total amino acid concentration, bottom - relative amino acid composition, for each enamel sample (A - rhinocerotid, B - equid). Boxes highlight low concentrations and atypical composition profiles.

4.3.1.6. Summary of identified outliers

Eight enamel samples showed evidence of possible open-system behaviour and/or contamination. This was observed from a combination of large, consistent, replicate variation across multiple degradation pathways, relative rates of racemisation and protein concentration and composition. While all the data is reported in the SI, these eight samples (TR12 (rhinocerotid); TS6 (suid); TE2, TE6, TE10, TE12 (equid); MB1, MB2 (bovid)) were removed from the final dataset used for each taxonomic group in the following sections. The remaining 72 samples, which appeared to adhere to closed-system behaviour (sections 4.3.1.1-5.), were used for subsequent assessment of taxonomic effects (section 4.3.2), the fossils' suitability for an enamel South-Central African amino acid geochronology and investigation of site formation processes (section 4.3.3).

4.3.2. Taxonomic effect

A taxonomic effect of amino acid racemisation has previously been described in a range of taxa (e.g. King and Hare, 1972; Bright and Kaufman, 2011; Ortiz *et al.*, 2013), including enamel (Dickinson *et al.*, 2024). Rates of degradation, including racemisation, are influenced by a protein's primary amino acid sequence (Mitterer and Kriausakul, 1984); as this differs by taxa in the enamel proteome, a taxonomic effect in racemisation may be expected. To investigate whether family level differences could be observed in this dataset, IcPD degradation trends were investigated. For racemisation (Fig. 4.8A and SI Fig. 4.13) and serine decomposition (Fig. 4.8B), no family level taxonomic differences were observed in their overall degradation trends, although the lack of chronological control in the dataset (see section 4.3.3 for discussion) meant that is was not possible to determine if their relative rates between taxonomic groups were different. There was, however, an observable difference in the degradation trend of rhinocerotid hydrolysis in comparison to suid, equid and bovid (Fig. 4.8C and D; SI Figs. 4.14 - 17). For the rhinocerotid samples, very high levels of hydrolysis were observed over a broad range of racemisation values in most amino acids (e.g. >80% FAA between 0.2 - 1.0 D/L, Fig. 4.8D, SI Figs. 4.14 - 17). However, for the other three taxonomic groups (suid, equid, bovid), a different peptide chain hydrolysis (%FAA) degradation trend was observed, with a potential decrease in hydrolysis at higher racemisation values (Fig. 4.8D, SI Figs, 4.14 - 17). These apparently lower extents of hydrolysis in the more degraded samples likely indicate the loss of free amino acids through additional degradation mechanisms. Interestingly, in many $CaCO_3$ biominerals, Glu lactam formation in the free amino acid fraction (Vallentyne, 1964; Walton, 1998) has been inferred from low Glu FAA concentrations, with %FAA plateauing at ~50% (e.g. Penkman *et al.*, 2008; Crisp *et al.*, 2013; Tomiak *et al.*, 2013). This trend, however, is not observable in this dataset. This may suggest a fundamental difference in protein degradation mechanisms between these types of biominerals or could indicate the additional biphasic separation step for enamel (as a $CaPO_4$

biomineral; not included in CaCO$_3$ methodology), could be influencing the observable degradation products.
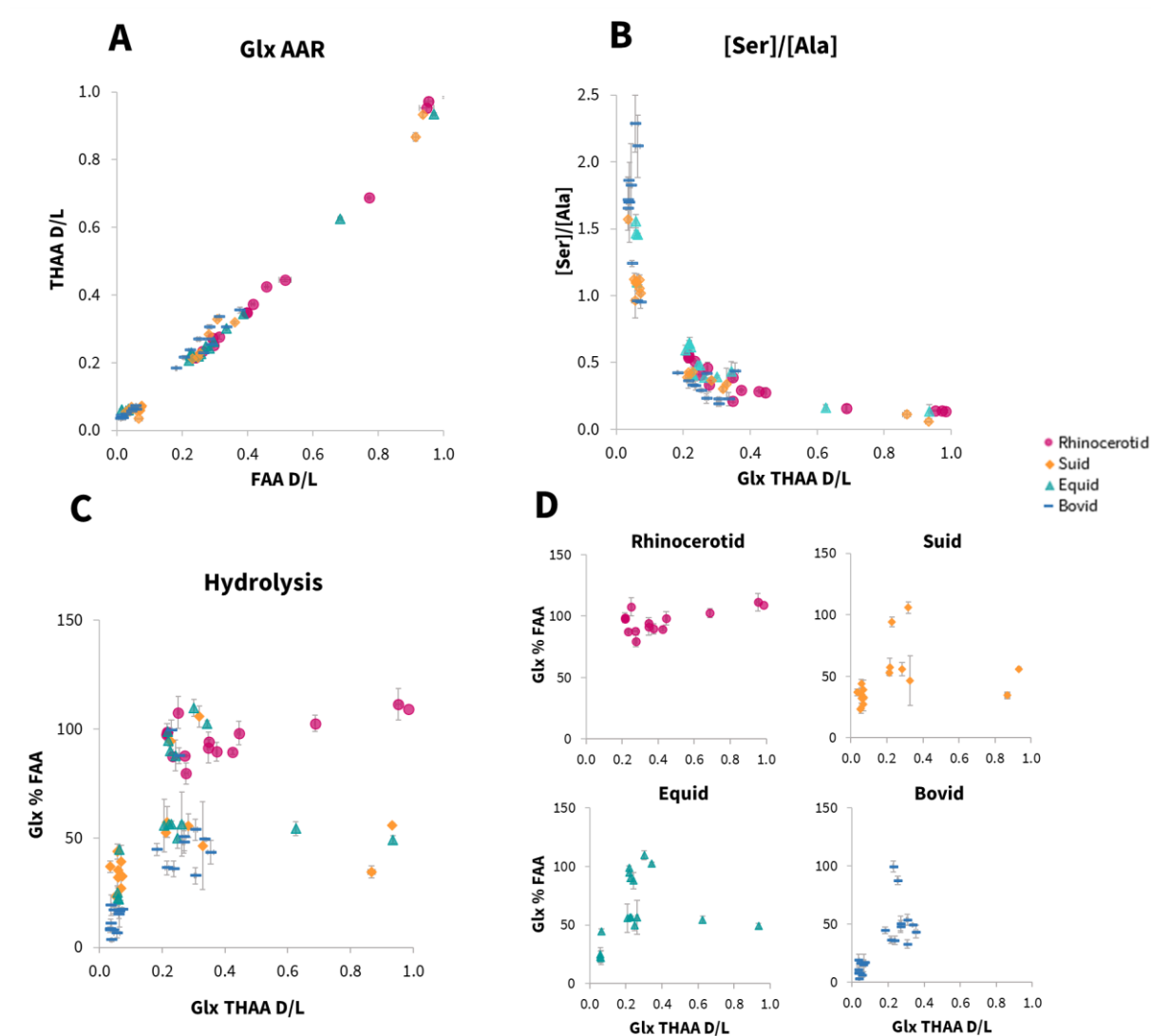
Figure 4.8. Investigation of family level taxonomic effect on the intra-crystalline protein degradation trends in rhinocerotid, suid, equid and bovid enamel samples. A - Relationship between the average free (FAA) vs total hydrolysable (THAA) Glx racemisation values (D/L). B - Relationship between serine decomposition vs total hydrolysable (THAA) Glx racemisation values (D/L). C - Overlay of the relationship between percentage free (%FAA) Glx vs total hydrolysable (THAA) Glx racemisation values (D/L). D - Individual taxonomic plots from C.

The apparent differences in family level taxonomic degradation trends observed in some of the IcPD parameters means that we therefore recommend building enamel amino acid geochronologies within family level taxonomic groups (at a minimum).

4.3.3. Assessment of site chronologies and depositional histories

IcPD analysis of fossil biominerals can provide useful direct dating information, enabling regional comparisons between sites, as well as within-site chronologies. It is not uncommon for sites, especially caves, to have experienced complicated depositional histories. Direct dating using a relative technique (such as IcPD) can be used to investigate individual site depositional histories (e.g. whether events such as bioturbation and erosion may have occurred), to allow a more robust understanding of each site's sedimentary processes.

4.3.3.1. Mumbwa Caves

Relatively low levels of racemisation were observed for all samples from Mumbwa Caves (Fig. 4.8), consistent with the site's relatively young age (a maximum of >172 ka). One notable exception (suid MS1, Fig. 4.9A) had considerably higher D/L values for the majority of amino acids analysed (e.g. Asx Fig. 4.9A). As the stratigraphic information for all Mumbwa Caves samples had been lost, it is not possible to relate the extent of racemisation with relative age, and therefore it is difficult to assess the likelihood of this being a genuine marker of depositional time. It is worth noting that this site has evidence of hearths in multiple archaeological horizons. Any tooth in close proximity to fire during its depositional history, could result in accelerated protein degradation and the extent of racemisation no longer reflecting primarily a signal of time (e.g. Brooks *et al*., 1991; Crisp, 2013). Previous work to identify signatures characteristic of heating has been undertaken on intra-crystalline protein in ostrich eggshell (where high %Glx composition vs Asx D/L and/or low %Ala composition vs Ala D/L observed were indicative of heating; Crisp, 2013); however, we have too little comparative data in this study to investigate any characteristic heat-induced degradation trends in enamel, and it is therefore not currently possible to assess this in any of the samples analysed here, including suid sample MS1. With a range of racemisation values observed, this data does, however, provide an intra-site relative chronology for the material analysed.
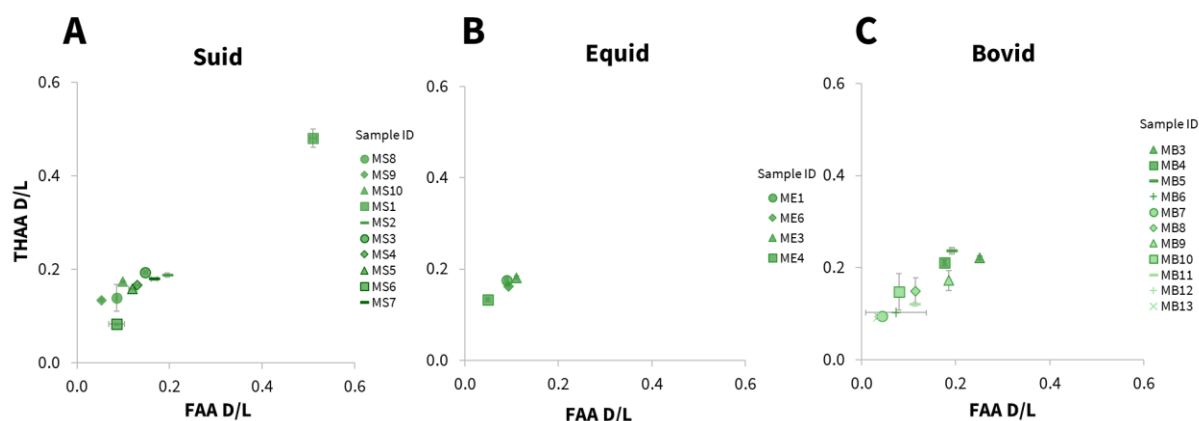
Figure 4.9. Relationship between the average free (FAA) vs total hydrolysable (THAA) Asx racemisation values (D/L) in three taxonomic groups of enamel samples present at Mumbwa Caves (A - suid, B - equid, C - bovid).

4.3.3.2. Twin Rivers

As stratigraphic information was available for the samples from Twin Rivers, the relationship between the extent of protein degradation and excavation depth could be investigated. Only in one excavation cavity (E5/E6), for two of the four taxonomic groups were there enough samples to investigate the relationship between the extent of racemisation and excavation level (Fig. 4.10; SI Fig. 4.18). Whilst each excavation level is likely to be time-averaged, for both rhinocerotid (Fig. 4.10A) and equid (Fig. 4.10B), the sample with the lowest extent of racemisation observed for each excavation level (assumed not to be reworked) increased with depth. This is concordant with the working hypothesis of sediment deposition having washed into the sloping cave passage. There were, however, a number of levels displaying a large spread of racemisation values (e.g. rhinocerotids in E5/E6 level 1 (Fig. 4.10A) and equids in E5/E6 level 4 (Fig. 4.10B; SI Fig. 4.18), beyond what might have been expected from the horizontal excavation stratigraphy. Given these fossils showed closed system behaviour (supported by the conclusions of section 4.3.1), and with no archaeological evidence of heating in A Block at Twin Rivers, we are left with the interpretation that the cave passage may have greater complexity within its depositional history, including considerable reworking of the fossils/sediments within the stratigraphy. The evidence of potential for bioturbation by tree root systems (Fig. 4.2) provides one clear mechanism for this reworking, in addition to the known complexities of cave site taphonomies (e.g. Brain, 1983; Adams *et al*., 2007; Thompson, 2010; Val *et al*., 2015).

172
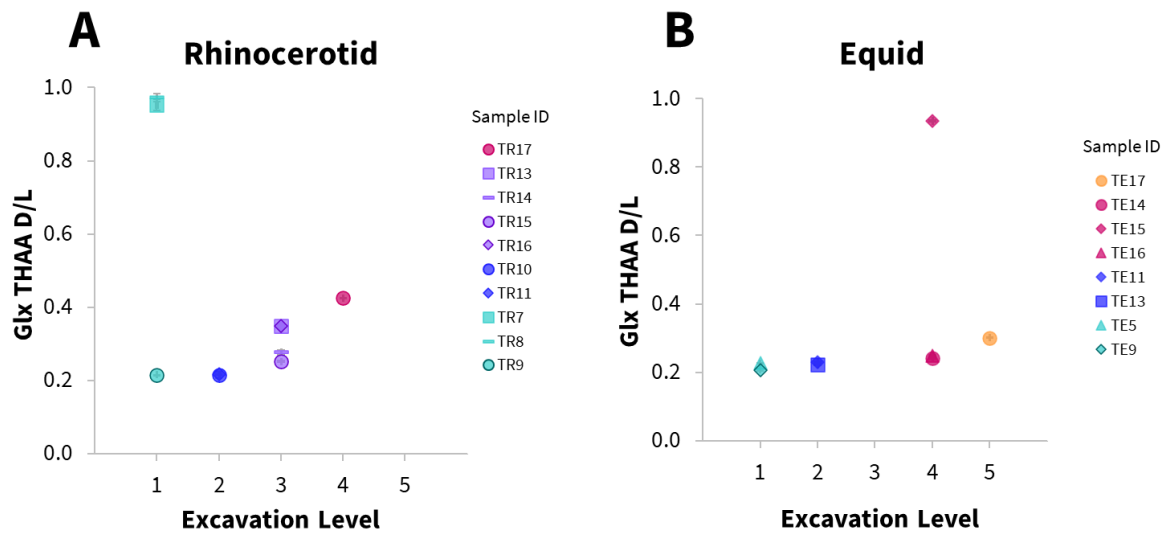
Figure 4.10. Average total hydrolysable amino acid (THAA) racemisation in Glx plotted against excavation level (1 = top 5 = bottom) in one excavation cavity (E5/E6) for rhinocerotid (A) and equid (B) samples. Error bars represent the standard deviation about the mean for subsample experimental replicates.

Whilst the lack of independent evidence of age precludes the ability to use this site to build an amino acid geochronology for the South-Central African region, the IcPD analysis has provided key information to allow a more informed interpretation of the site, by providing relative dates on the fauna for direct comparison. It is also clear that the faunal material covers a range of geological time at this site, with a wide spread of racemisation values observable in the majority of species (Fig. 4.10, SI Fig. 4.18).

4.3.3.3. Between-site comparison

Whilst investigation of Mumbwa Cave's stratigraphic adherence to chronological deposition was not possible, comparison to Twin Rivers, known to be an older archaeological site, was possible. With the exception of one relatively degraded suid sample (MS1; Fig. 4.11), all samples from Mumbwa Caves had racemisation values lower than from Twin Rivers, in agreement with their younger age from previous dating. Interestingly, the published dates from both sites suggest there could be a temporal overlap between the sites (at ~ 170 ka); only in the suid materials is a possible overlap evident (Fig. 4.11).
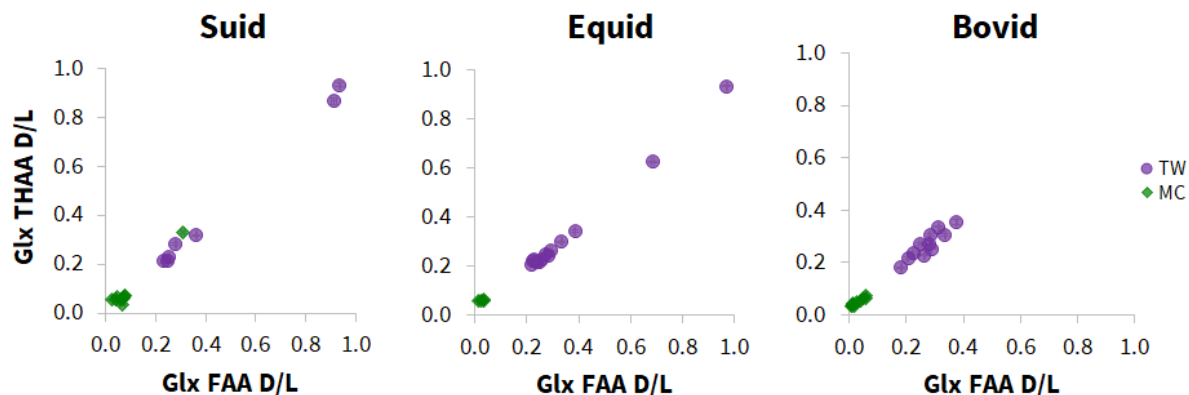
Figure 4.11. Relationship of the average free (FAA) vs total hydrolysable (THAA) Glx racemisation values (D/L) in the three taxonomic groups (suid, equid, bovid) of enamel samples present from both Mumbwa Caves (MC) and Twin Rivers (TW).

As the contextual information is not known for the fossils from Mumbwa Caves, one explanation is that the majority of fossils analysed from Mumbwa Caves represent a younger selection from later in the cave sequence. This could also mean the one exception where there is overlap with Twin Rivers samples (MS1, Fig. 4.11), is an accurate representation of time at ~ 170 ka, and not as a result of proximity to a heat source (as discussed in section 4.3.3.1). However, as the flowstone capping the topmost part of the Twin Rivers A block sequence provides a minimum age of ~170 ka, the fossils excavated below may be older. Further study is required to better understand this dataset, but despite this, the IcPD data enables relative age assignments for this set of samples.

Conclusion

Eighty fossil tooth enamel samples from two archaeological cave sites in the South-Central African region (Twin Rivers and Mumbwa Caves) were analysed for IcPD to investigate their use for amino acid geochronology. Seventy-two of these (90%) showed evidence of closed system behaviour in their intra-crystalline protein fraction. The relative extent of racemisation between sites was consistent with previous dating information. At Twin Rivers, a potential trend between the extent of racemisation in the least degraded samples and excavation depth was observed, concordant with the working hypothesis of a sequential deposition within A Block. Post-depositional processes (including bioturbation by roots and the mixing of deposits on excavation) may account in part for the wide spreads of racemisation values within some individual excavation levels, although greater depositional history complexity is likely. Direct dating of the fauna allowed recognition of this complexity, critical for interpretation.

The unrecoverable contextual information of the Mumbwa Caves material, combined with the data complexities at Twin Rivers, limited investigation of taxonomic variability within the IcPD dataset of enamel. Whilst a more thorough investigation of the taxonomic effect was not possible from these

sites due to the lack of stratigraphic control, one notable degradation pattern difference in peptide chain hydrolysis was observed in the rhinocerotid data, in comparison to the suid, equid and bovid data, leading to the recommendation that taxon-specific enamel AAGs are developed. Although it was not possible to calibrate a regional aminostratigraphy based on these sites, the IcPD data provided key information for site interpretation allowing relative age determination for both individual faunal samples and between-site comparisons. At Twin Rivers the broad range of racemisation values observed in Glx (0.2 - 1.0 D/L), one of the slowest racemising amino acids, indicated the likely presence of fauna over a large portion of the Pleistocene, highlighting enamel's potential for building Quaternary AAGs in warm regions, such as South-Central Africa. This study also provides a case study for the cautious approach needed when interpreting archaeological cave sites, and the value of direct dating material.

Acknowledgements

4.4. References

Adams, J.W., Herries, A.I., Kuykendall, K.L. and Conroy, G.C., 2007. Taphonomy of a South African cave: geological and hydrological influences on the GD 1 fossil assemblage at Gondolin, a Plio-Pleistocene paleocave system in the Northwest Province, South Africa. *Quaternary Science Reviews, 26*(19-21), pp.2526-2543.

Bada, J.L., Shou, M.Y., Man, E.H., and Schroeder, R.A. 1978. Decomposition of hydroxy amino acids in foraminiferal tests: Kinetics, mechanism and geochronological implications. *Earth Planetary Science Letters, 41*(1), pp.67-76.

Baldreki, C., Burnham, A., Conti, M., Wheeler, L., Simms, M.J., Barham, L., White, T.S. and Penkman, K., 2024. Investigating the potential of African land snail shells (Gastropoda: Achatininae) for amino acid geochronology. *Quaternary Geochronology*, *79*, pp.101473.

Barham, L.S., 2000. *The Middle Stone Age of Zambia, South Central Africa*. Western academic & specialist Press.

Barham, L. and Debenham, N. 2000. Chapter 3 Mumbwa Caves Chronology in Barham, L.S., 2000. *The Middle Stone Age of Zambia, South Central Africa*. Western academic & specialist Press. pp.43-50.

Barham, L., 2002. Systematic pigment use in the Middle Pleistocene of South-Central Africa. *Current anthropology*, *43*(1), pp.181-190.

Barham. L. and Mitchell. P., 2008. *The First Africans: African Archaeology from the Earliest Toolmakers to Most Recent Foragers*. Cambridge: Cambridge University Press.

Barham, L., Duller, G.A.T., Candy, I., Scott, C., Cartwright, C.R., Peterson, J.R., Kabukcu, C., Chapot, M.S., Melia, F., Rots, V. and George, N., 2023. Evidence for the earliest structural use of wood at least 476,000 years ago. *Nature, 622*(7981), pp.107-111.

Bishop, L.C. and Reynolds, S.C., 2000. Chapter 11 Fauna from Twin Rivers in Barham, L.S., 2000. *The Middle Stone Age of Zambia, South Central Africa*. Western academic & specialist Press. pp. 217-222.

Bishop, L.C., Barham, L., Ditchfield, P.W., Elton, S., Harcourt-Smith, W.E. and Dawkins, P., 2016. Quaternary fossil fauna from the Luangwa Valley, Zambia. *Journal of Quaternary Science, 31*(3), pp.178-190.

Bowen, D.Q., Hughes, S., Sykes, G.A. and Miller, G.H., 1989. Land-sea correlations in the Pleistocene based on isoleucine epimerization in non-marine molluscs. *Nature, 340*(6228), pp.49-51.

Brain, C.K., 1983. *The hunters or the hunted?: an introduction to African cave taphonomy*. University of Chicago Press.

Bright, J. and Kaufman, D.S., 2011. Amino acid racemization in lacustrine ostracodes, part I: effect of oxidizing pre-treatments on amino acid composition. *Quaternary Geochronology, 6*(2), pp.154-173.

Brooks, A.S., Hare, P.E., Kokis, J.E., Miller, G.H., Ernst, R.D. and Wendorf, F., 1990. Dating Pleistocene archeological sites by protein diagenesis in ostrich eggshell. *Science, 248*(4951), pp.60-64.

Burrough, S.L., Thomas, D.S.G. and Barham, L.S., 2019. Implications of a new chronology for the interpretation of the Middle and Later Stone Age of the upper Zambezi Valley. *Journal of Archaeological Science: Reports, 23*, pp.376-389.

Burrough, S.L., Thomas, D.S., Allin, J.R., Coulson, S.D., Mothulatshipi, S.M., Nash, D.J. and Staurset, S., 2022. Lessons from a lakebed: unpicking hydrological change and early human landscape use in the Makgadikgadi basin, Botswana. *Quaternary Science Reviews, 291*, p.107662.

Cappellini, E., Welker, F., Pandolfi, L., Ramos-Madrigal, J., Samodova, D., Rüther, P.L., Fotakis, A.K., Lyon, D., Moreno-Mayar, J.V., Bukhsianidze, M. and Rakownikow Jersie-Christensen, R., 2019. Early Pleistocene enamel proteome from Dmanisi resolves *Stephanorhinus* phylogeny. *Nature, 574*(7776), pp.103-107.

Chan, E.K., Timmermann, A., Baldi, B.F., Moore, A.E., Lyons, R.J., Lee, S.S., Kalsbeek, A.M., Petersen, D.C., Rautenbach, H., Förtsch, H.E. and Bornman, M., 2019. Human origins in a southern African palaeo-wetland and first migrations. *Nature*, *575*(7781), pp.185-189.

Clark, J.D. and Brown, K,S. 2001. The Twin Rivers Kopje, Zambia: stratigraphy, fauna, and artefact assemblages from the 1954 and 1956 excavations. *Journal of Archaeological Science*, *28*(3), pp.305-330.

Crisp, M., Demarchi, B., Collins, M., Morgan-Williams, M., Pilgrim, E. and Penkman, K., 2013. Isolation of the intra-crystalline proteins and kinetic studies in *Struthio camelus* (ostrich) eggshell for amino acid geochronology. *Quaternary Geochronology*, *16*, pp.110-128.

Crisp, M.K., 2013. Amino acid racemization dating: Method development using African ostrich *(Struthio camelus)* eggshell. PhD thesis, University of York.

Demarchi, B., Rogers, K. Fa, D. A., Finlayson, C. J., Milner, N., Penkman, K. E. H., 2013a. Intra-crystalline protein diagenesis (IcPD) in *Patella vulgata*. Part I: Isolation and testing of the closed system. *Quaternary Geochronology, 16*, pp.144-157.

Demarchi, B., Collins, M., Bergström, E., Dowle, A., Penkman, K., Thomas-Oates, J., Wilson, J., 2013b. New experimental evidence for in-chain amino acid racemization of serine in a model peptide. *Analytical Chemistry, 85*(12), pp.5835-5842 236.

Demarchi, B., Clements, E., Coltorti, M., Van De Locht, R., Kröger, R., Penkman, K. and Rose, J., 2015. Testing the effect of bleaching on the bivalve *Glycymeris*: A case study of amino acid geochronology on key Mediterranean raised beach deposits. *Quaternary Geochronology, 25*, pp.49-65.

Dennell, R., 2008. *The palaeolithic settlement of Asia*. Cambridge: Cambridge University Press.

Dickinson, M.R., Lister, A.M. and Penkman, K.E., 2019. A new method for enamel amino acid racemization dating: a closed system approach. *Quaternary Geochronology, 50*, pp.29-46.

Dickinson, M.R., Scott, K., Adams, N.F., Lister, A.M. and Penkman, K.E.H., 2024. Amino acid dating of Pleistocene mammalian enamel from the River Thames terrace sequence: a multi-taxon approach. *Quaternary Geochronology*, p.101543.

Duller, G.A., Tooth, S., Barham, L. and Tsukamoto, S., 2015. New investigations at Kalambo Falls, Zambia: Luminescence chronology, site formation, and archaeological significance. *Journal of Human Evolution*. 85, pp.111-25.

French, J,C., 2021. *Palaeolithic Europe: A Demographic and Social Prehistory*. Cambridge: Cambridge University Press.

Grün, R., Pike, A., McDermott, F., Eggins, S., Mortimer, G., Aubert, M., Kinsley, L., Joannes-Boyau, R., Rumsey, M., Denys, C., and Brink, J., 2020. Dating the skull from Broken Hill, Zambia, and its position in human evolution. *Nature*, *580*(7803), pp.372-375.

Hare, P.E. and Mitterer, R.M., 1969. Laboratory simulation of amino acid diagenesis in fossils. *Carnegie Institute Washington Year Book*, 67, pp.205-208.

Hearty, P.J. and Kaufman, D.S., 2009. A *Cerion*-based chronostratigraphy and age model from the central Bahama Islands: Amino acid racemization and ^{14}C in land snails and sediments. *Quaternary Geochronology*. *4*(2), pp.148-159.

Hendy, E.J., Tomiak, P.J., Collins, M.J., Hellstrom, J., Tudhope, A.W., Lough, J.M. and Penkman, K.E., 2012. Assessing amino acid racemization variability in coral intra-crystalline protein for geochronological applications. *Geochimica et Cosmochimica Acta, 86*, pp.338-353.

Hill, R.L., 1965. Hydrolysis of proteins. *Advances in Protein Chemistry*, *20*, pp.37-107.

Kaufman, D.S. and Manley, W.F., 1998. A new procedure for determining DL amino acid ratios in fossils using reverse phase liquid chromatography. *Quaternary Science Reviews*. *17*(11), pp.987-1000.

Kaufman, D.S., 2006. Temperature sensitivity of aspartic and glutamic acid racemization in the foraminifera *Pulleniatina*. *Quaternary Geochronology*, *1*(3), pp.188-207.

King, K.J. and Hare, P.E., 1972. Species effects in the epimerization of L-isoleucine in fossil planktonic foraminifera. *Carnegie Institute Washington Year Book*, *71*, pp.596–598.

Klein, R.G. and Cruz-Uribe, K., 2000. Chapter 4 Macromammals and reptiles in Barham, L.S., 2000. *The Middle Stone Age of Zambia, South Central Africa*. Western academic & specialist Press. pp.51-56.

Koppel, B., Szabom K., Moore, W., Morwood, M.J., 2016. Untangling time-averaging in shell middens: defining temporal units using amino acid racemisation. *Journal of Archaeological Science: Reports 7*, pp.741-750.

Kosnik, M.A. and Kaufman, D.S., 2008. Identifying outliers and assessing the accuracy of amino acid racemization measurements for geochronology: II. Data screening. *Quaternary Geochronology*, *3*(4), pp.328-341.

Marin-Monfort, M.D., García-Morato, S., Andrews, P., Avery, D.M., Chazan, M., Horwitz, L.K., Fernández-Jalvo, Y., 2022. The owl that never left! Taphonomy of Earlier Stone Age small mammal assemblages from Wonderwerk Cave (South Africa). *Quaternary International*, *614*, pp.111-25.

Mitterer, R.M. and Kriausakul, N., 1984. Comparison of rates and degrees of isoleucine epimerization in dipeptides and tripeptides. *Organic Geochemistry*, *7*(1), pp.91-98.

Orem, C.A. and Kaufman, D.S., 2011. Effects of basic pH on amino acid racemization and leaching in freshwater mollusk shell. *Quaternary Geochronology, 6*(2), pp.233-245.

Ortiz, J.E., Torres, T. and Pérez-González, A., 2013. Amino acid racemization in four species of ostracodes: taxonomic, environmental, and microstructural controls. *Quaternary Geochronology, 16*, pp.129-143.

Ortiz, J.E., Torres, T., Sánchez-Palencia, Y. and Ferrer, M., 2017. Inter-and intra-crystalline protein diagenesis in *Glycymeris* shells: Implications for amino acid geochronology. *Quaternary Geochronology, 41*, pp.37-50.

Ortiz, J.E., Sánchez-Palencia, Y., Gutiérrez-Zugasti, I., Torres, T. and González-Morales, M., 2018. Protein diagenesis in archaeological gastropod shells and the suitability of this material for amino acid racemisation dating: *Phorcus lineatus* (da Costa, 1778). *Quaternary Geochronology, 46,* pp.16-27.

Penkman, K.E.H., 2005. Amino acid geochronology: a closed system approach to test and refine the UK model. PhD thesis, University of Newcastle.

Penkman, K.E.H., Preece, R.C., Keen, D.H., Maddy, D., Schreve, D.C. and Collins, M.J., 2007. Testing the aminostratigraphy of fluvial archives: the evidence from intra-crystalline proteins within freshwater shells. *Quaternary Science Reviews*, *26*(22-24), pp.2958-2969.

Penkman, K. E. H., Kaufman, D. S., Maddy, D., Collins, M. J., 2008. Closed-system behaviour of the intra-crystalline fraction of amino acids in mollusc shells. *Quaternary Geochronology, 3*(1-2), pp.2-25.

Penkman, K.E., Preece, R.C., Bridgland, D.R., Keen, D.H., Meijer, T., Parfitt, S.A., White, T.S. and Collins, M.J., 2013. An aminostratigraphy for the British Quaternary based on *Bithynia* opercula. *Quaternary Science Reviews, 61,* pp.111-134.

Powell, J., Collins, M.J., Cussens, J., MacLeod, N. and Penkman, K.E., 2013. Results from an amino acid racemization inter-laboratory proficiency study; design and performance evaluation. *Quaternary Geochronology, 16*, pp.183-197.

Preece, R.C. and Penkman, K.E.H., 2005. New faunal analyses and amino acid dating of the Lower Palaeolithic site at East Farm, Barnham, Suffolk. *Proceedings of the Geologists' Association*, *116*(3-4), pp.363-377.

Reynolds, S.C. and Kibii, J.M., 2011. Sterkfontein at 75: review of paleoenvironments, fauna, dating and archaeology from the hominin site of Sterkfontein (Gauteng Province, South Africa). *Palaeontologia africana*, *46*, pp.59-88.

Smith, G.G., Evans, R.C., 1980. The effect of structure and conditions on the rate of racemisation of free and bound amino acids. *Biogeochemistry of Amino Acids*, pp.257-282.

Stephenson, R.C. and Clarke, S., 1989. Succinimide formation from aspartyl and asparaginyl peptides as a model for the spontaneous degradation of proteins. *Journal of Biological Chemistry, 264*(11), pp.6164-6170.

Sykes, G.A., Collins, M.J. and Walton, D.I., 1995. The significance of a geochemically isolated intracrystalline organic fraction within biominerals. *Organic Geochemistry, 23*(11-12), pp.1059-1065.

Takahashi, O., Kobayashi, K. and Oda, A., 2010. Computational insight into the mechanism of serine residue racemization. *Chemistry & Biodiversity, 7*(6), pp.1625-1629.

Thompson, J.C., 2010. Taphonomic analysis of the middle stone age faunal assemblage from Pinnacle Point Cave 13B, Western Cape, South Africa. *Journal of Human Evolution, 59*(3-4), pp.321-339.

Tomiak, P.J., Penkman, K.E., Hendy, E.J., Demarchi, B., Murrells, S., Davis, S.A., McCullagh, P. and Collins, M.J., 2013. Testing the limitations of artificial protein degradation kinetics using known-age massive *Porites* coral skeletons. *Quaternary Geochronology, 16,* pp.87-109.

Torres, T., Ortiz, J.E., Fernández, E., Arroyo-Pardo, E., Grün, R. and Pérez-González, A., 2014. Aspartic acid racemization as a dating tool for dentine: a reality. *Quaternary Geochronology, 22*, pp.43-56.

Towe, K.M., 1980. Preserved organic ultrastructure: an unreliable indicator for Paleozoic amino acid biogeochemistry. *Biogeochemistry of Amino Acids*, pp.65-74.

Val, A., Dirks, P.H., Backwell, L.R., d'Errico, F. and Berger, L.R., 2015. Taphonomic analysis of the faunal assemblage associated with the hominins (*Australopithecus sediba*) from the Early Pleistocene cave deposits of Malapa, South Africa. *PloS one, 10*(6), pp.0126904.

Vallentyne, J.R., 1964. Biogeochemistry of organic matter—II Thermal reaction kinetics and transformation products of amino compounds. *Geochimica et Cosmochimica Acta, 28*(2), pp.157-88.

Walton, D., 1998. Degradation of intracrystalline proteins and amino acids in fossil brachiopods. *Organic Geochemistry, 28*(6), pp.389-410.

Wehmiller, J.F., 1977. *Correlation and chronology of Pacific coast marine terrace deposits of continental United States by fossil amino acid stereochemistry: Technique evaluation, relative ages, kinetic model ages, and geologic implications.* US Department of the Interior, Geological Survey.

Wehmiller, J.F. and Miller, G.H., 2000. Aminostratigraphic dating methods in Quaternary geology. *Quaternary geochronology: methods and applications*, *4*, pp.187-222.

Welker, F., Ramos-Madrigal, J., Kuhlwilm, M., Liao, W., Gutenbrunner, P., de Manuel, M., Samodova, D., Mackie, M., Allentoft, M.E., Bacon, A.M. and Collins, M.J., 2019. Enamel proteome shows that *Gigantopithecus* was an early diverging pongine. *Nature, 576*(7786), pp.262-265.

Wheeler, L.J., Penkman, K.E. and Sejrup, H.P., 2021. Assessing the intra-crystalline approach to amino acid geochronology of *Neogloboquadrina pachyderma* (sinistral). *Quaternary Geochronology, 6,* pp.101131.

Wheeler, L., 2022. Towards an aminostratigraphy of foraminifera for Pleistocene sea-level records: testing the intra-crystalline approach to amino acid racemisation dating. PhD thesis, University of York.

Willerslev, E., Cappellini, E., Boomsma, W., Nielsen, R., Hebsgaard, M.B., Brand, T.B., Hofreiter, M., Bunce, M., Poinar, H.N., Dahl-Jensen, D. and Johnsen, S., 2007. Ancient biomolecules from deep ice cores reveal a forested southern Greenland. *Science, 317*(5834), pp.111-114.

4.5. Supplementary Information

4.5.1. Assessment of closed system behaviour

4.5.1.1. Amino acid fraction D/L covariance
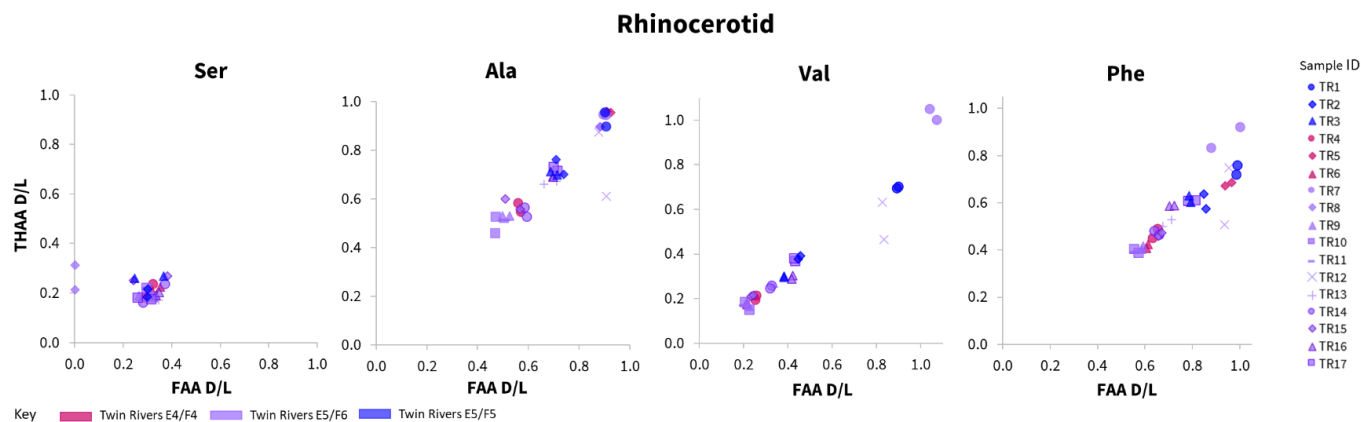
SI Figure 4.1. Relationship between racemisation values (D/L) in free (FAA) vs total hydrolysable (THAA) amino acids, for rhinocerotid subsample replicates, for Ser, Ala, Val and Phe. Twin Rivers samples were excavated from three areas within the A Block cave passage (Barham, 2000).
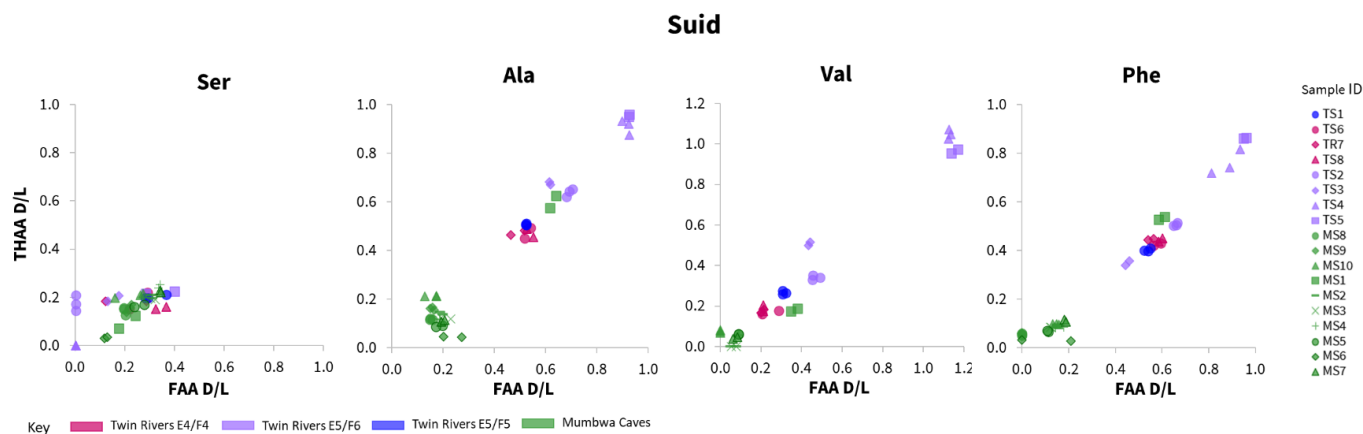
SI Figure 4.2. Relationship between racemisation values (D/L) in free (FAA) vs total hydrolysable (THAA) amino acids, for suid subsample replicates, for Ser, Ala, Val and Phe. Mumbwa Caves samples were all excavated from one deposit (Barham, 2000). Twin Rivers samples were excavated from three areas within the A Block cave passage (Barham, 2000).
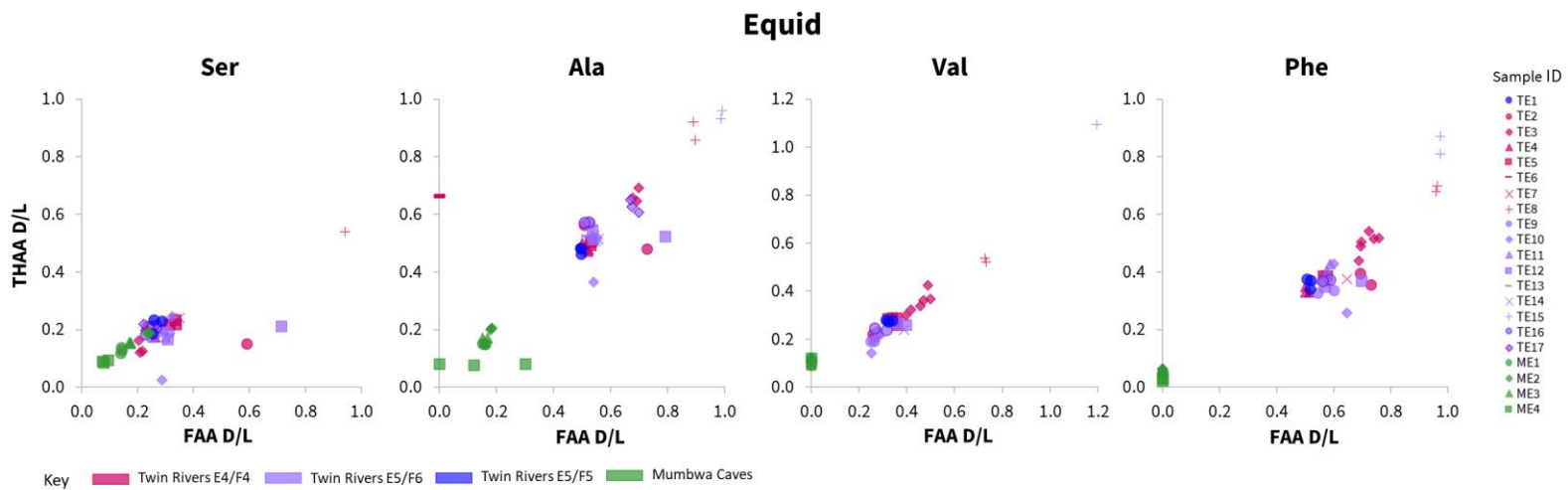
SI Figure 4.3. Relationship between racemisation values (D/L) in free (FAA) vs total hydrolysable (THAA) amino acids, for equid subsample replicates, for Ser, Ala, Val and Phe. Mumbwa Caves samples were all excavated from one deposit (Barham, 2000). Twin Rivers samples were excavated from three areas within the A Block cave passage (Barham, 2000).
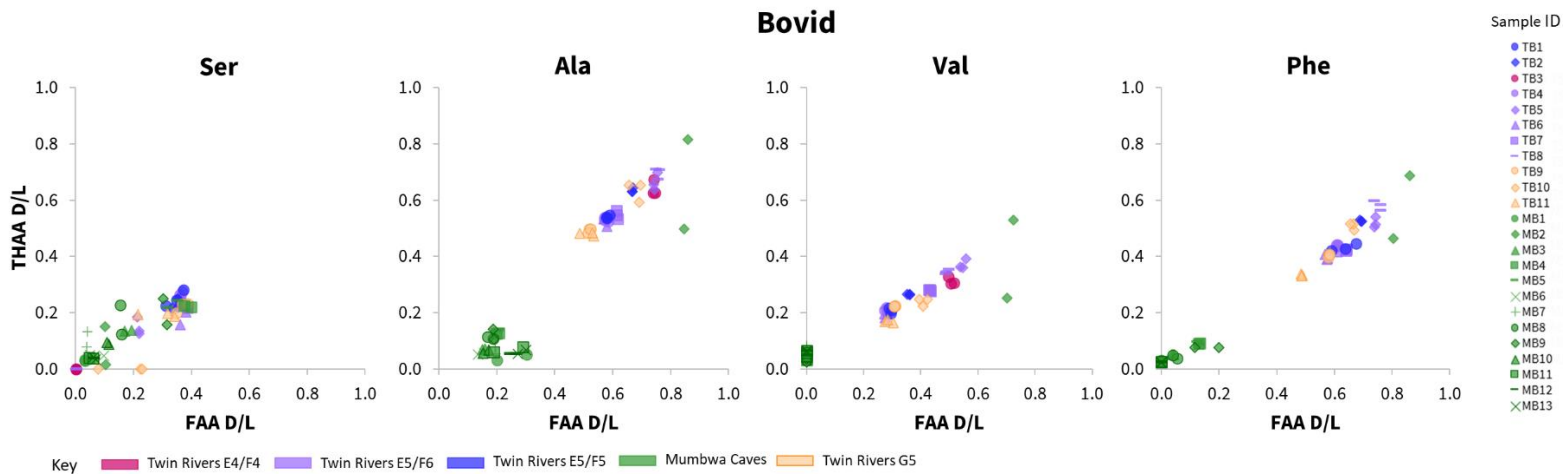
SI Figure 4.4. Relationship between racemisation values (D/L) in free (FAA) vs total hydrolysable (THAA) amino acids, for bovid subsample replicates, for Ser, Ala, Val and Phe. Mumbwa Caves samples were all excavated from one deposit (Barham, 2000). Twin Rivers samples were excavated from four areas within the A Block cave passage (Barham, 2000).

184

4.5.1.2. Peptide bond hydrolysis
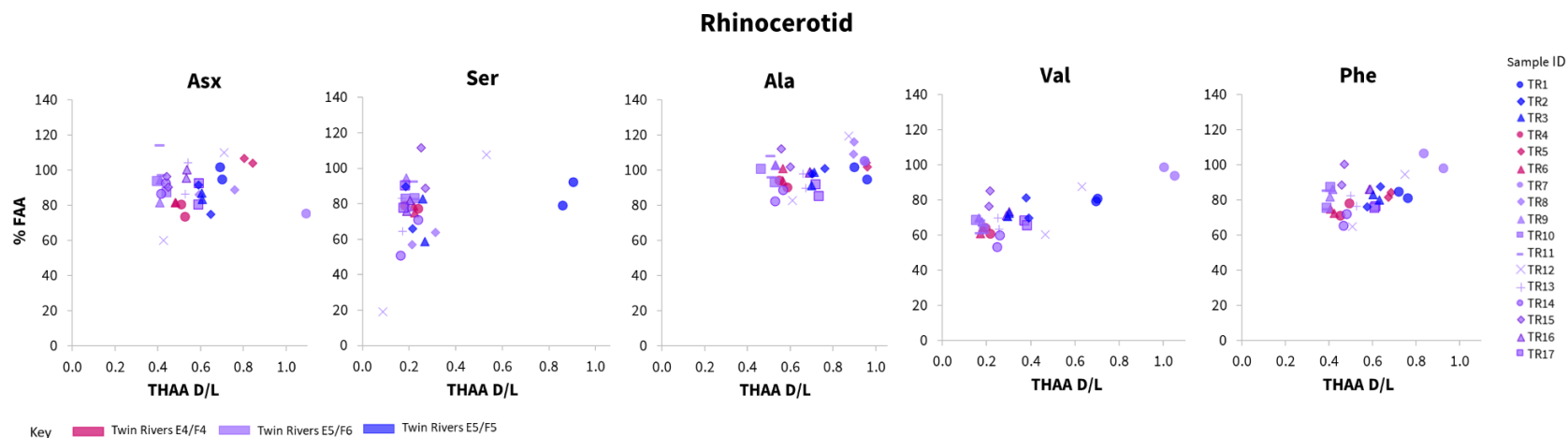
SI Figure 4.5. Relationship between racemisation values (THAA D/L) vs the percentage of free amino acid, for rhinocerotid subsample replicates, in Asx, Ser, Ala, Val and Phe. Twin Rivers samples were excavated from three areas within the A Block cave passage (Barham, 2000).
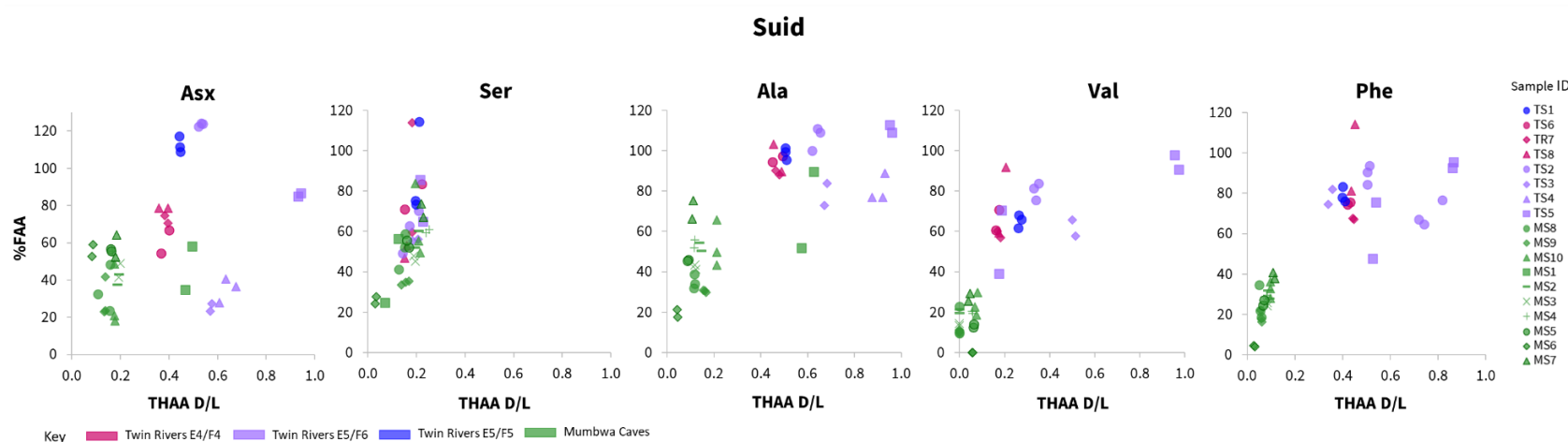
SI Figure 4.6. Relationship between racemisation values (THAA D/L) vs the percentage of free amino acid, for suid subsample replicates, in Asx, Ser, Ala, Val and Phe. Mumbwa Caves samples were all excavated from one deposit (Barham, 2000). Twin Rivers samples were excavated from three areas within the A Block cave passage (Barham, 2000).
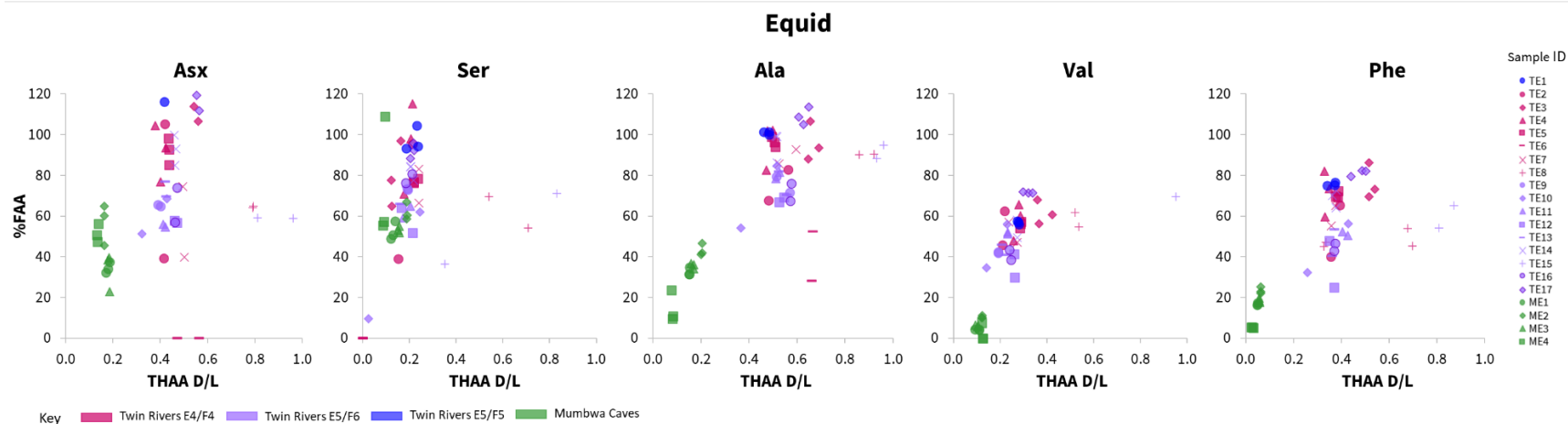
SI Figure 4.7. Relationship between racemisation values (THAA D/L) vs the percentage of free amino acid, for equid subsample replicates, in Asx, Ser, Ala, Val and Phe. Mumbwa Caves samples were all excavated from one deposit (Barham, 2000). Twin Rivers samples were excavated from three areas within the A Block cave passage (Barham, 2000).
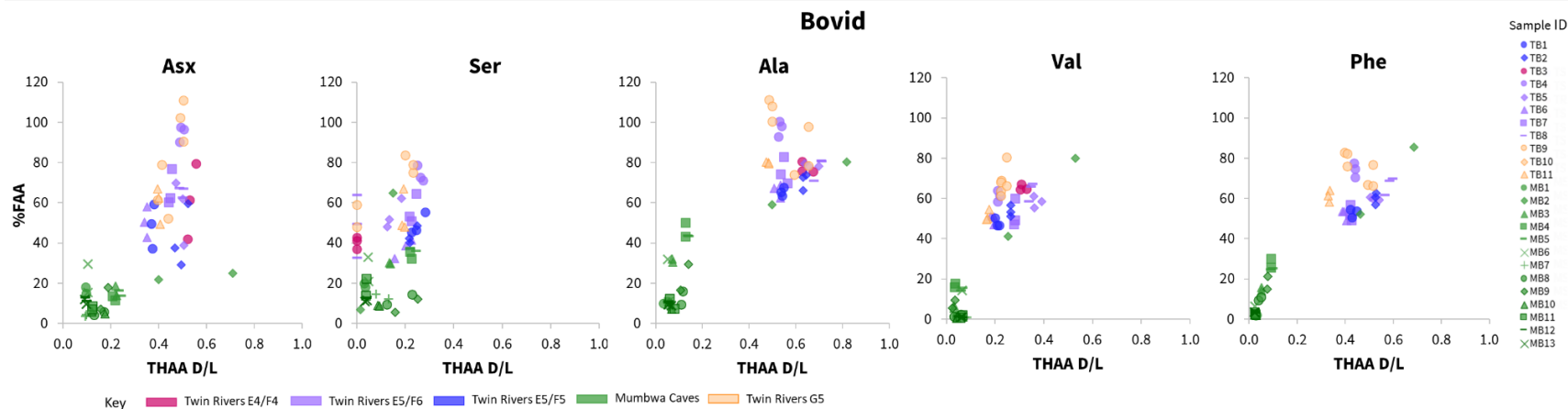
SI Figure 4.8. Relationship between racemisation values (THAA D/L) vs the percentage of free amino acid, for bovid subsample replicates, in Asx, Ser, Ala, Val and Phe. Mumbwa Caves samples were all excavated from one deposit (Barham, 2000). Twin Rivers samples were excavated from four areas within the A Block cave passage (Barham, 2000).

4.5.1.3. Concentration and composition
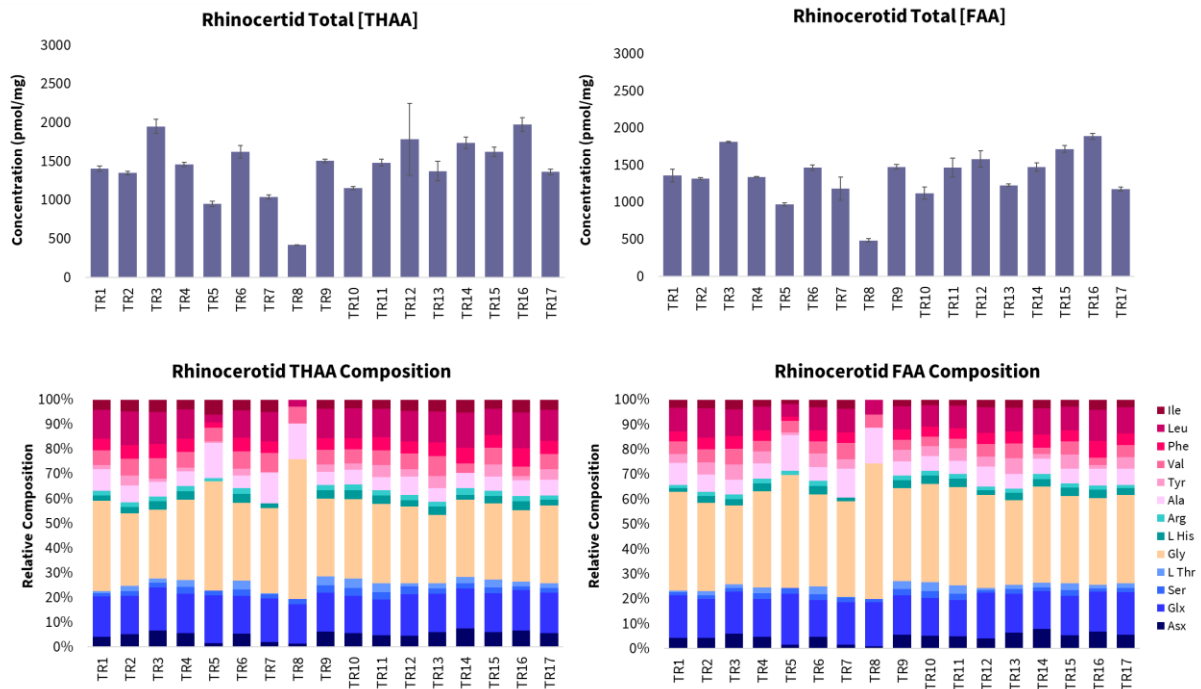
SI Figure 4.9. Average concentration and relative composition for all rhinocerotid enamel samples. Boxes highlight low concentrations and atypical composition profiles associated with low extents of degradation and/or highly variable data. Where low concentration and atypical composition profiles can be observed without boxes, high levels of protein degradation were observed from other indicators such as racemisation.
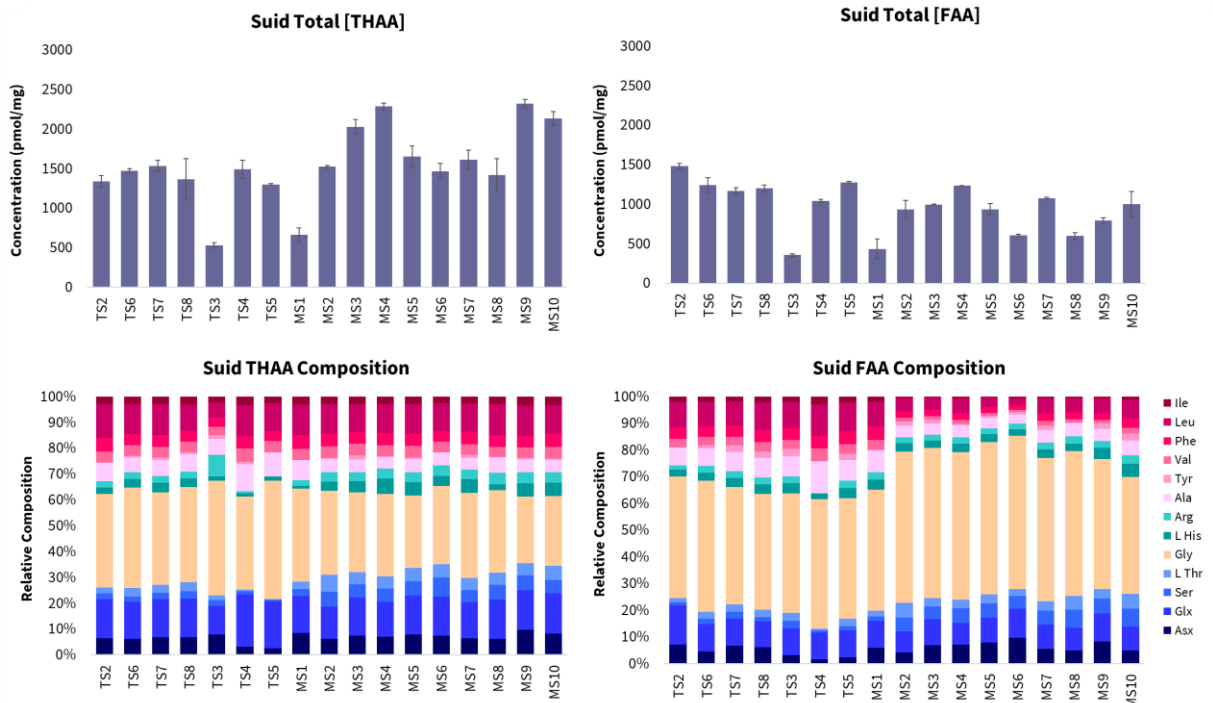
SI Figure 4.10. Average concentration and relative composition for all suid enamel samples. Boxes highlight low concentrations and atypical composition profiles associated with low extents of degradation and/or highly variable data. Where low concentration and atypical composition profiles can be observed without boxes, high levels of protein degradation were observed from other indicators such as racemisation.
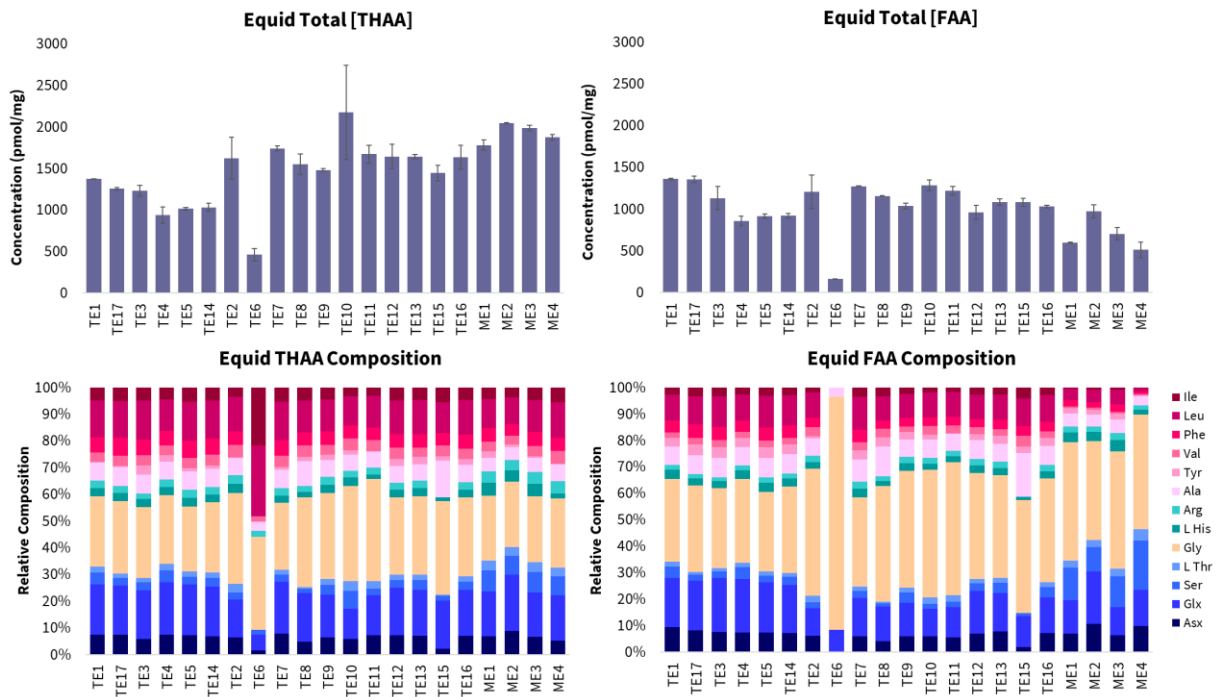
SI Figure 4.11. Average concentration and relative composition for all equid enamel samples. Boxes highlight low concentrations and atypical composition profiles associated with low extents of degradation and/or highly variable data. Where low concentration and atypical composition profiles can be observed without boxes, high levels of protein degradation were observed from other indicators such as racemisation.
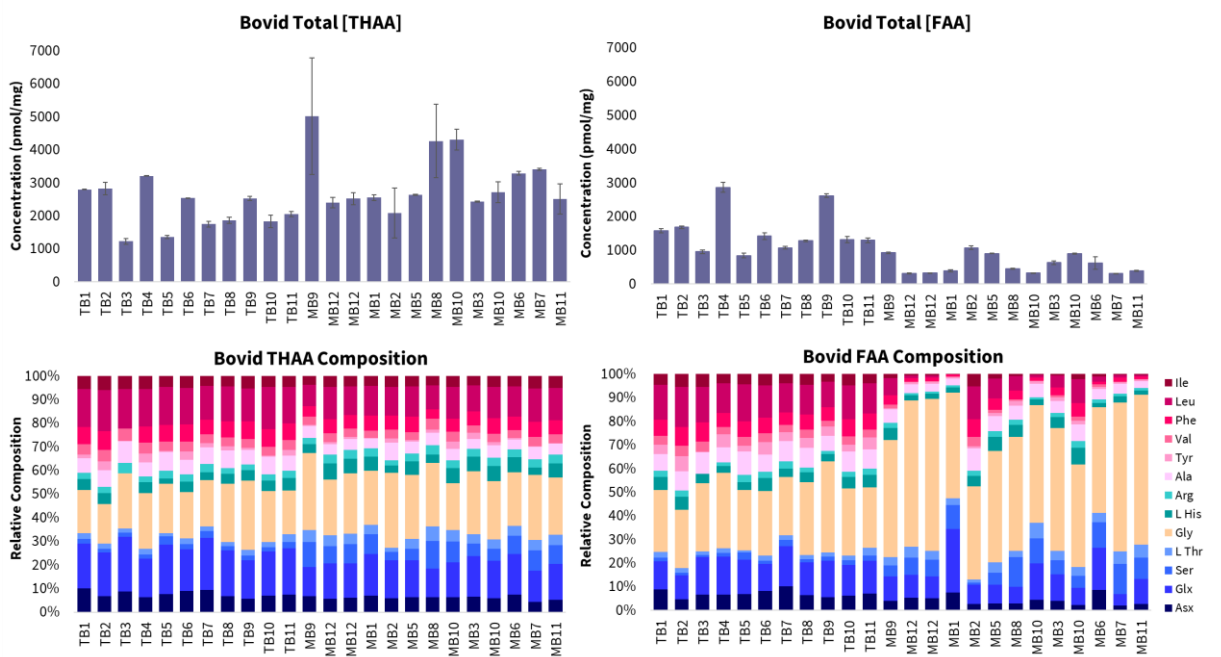
SI Figure 4.12. Average concentration and relative composition for all bovid enamel samples (NB bovid concentration is on a different scale to the rhinocerotid, equid and suid). Boxes highlight low concentrations and atypical composition profiles associated with low extents of degradation and/or highly variable data. Where low concentration and atypical composition profiles can be observed without boxes, high levels of protein degradation were observed from other indicators such as racemisation.
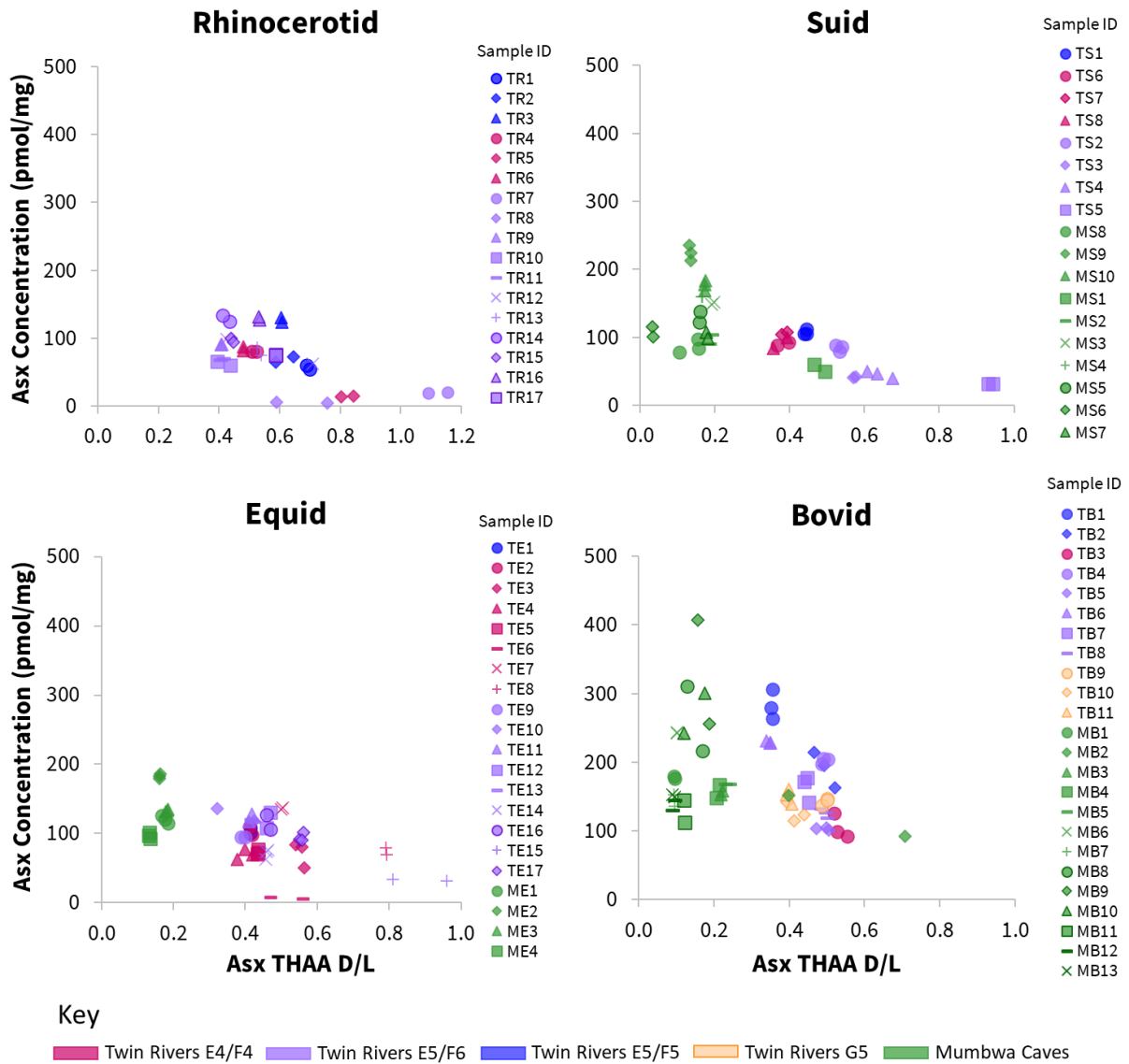
SI Figure 4.13. Relationship between the total hydrolysable Asx racemisation values (D/L) and Asx concentration. Mumbwa Caves samples were all excavated from one deposit (Barham, 2000). Twin Rivers samples were excavated from four areas within the A Block cave passage (Barham, 2000)

4.5.2. Assessment of taxonomic effect

4.5.2.1. Amino acid fraction D/L covariance
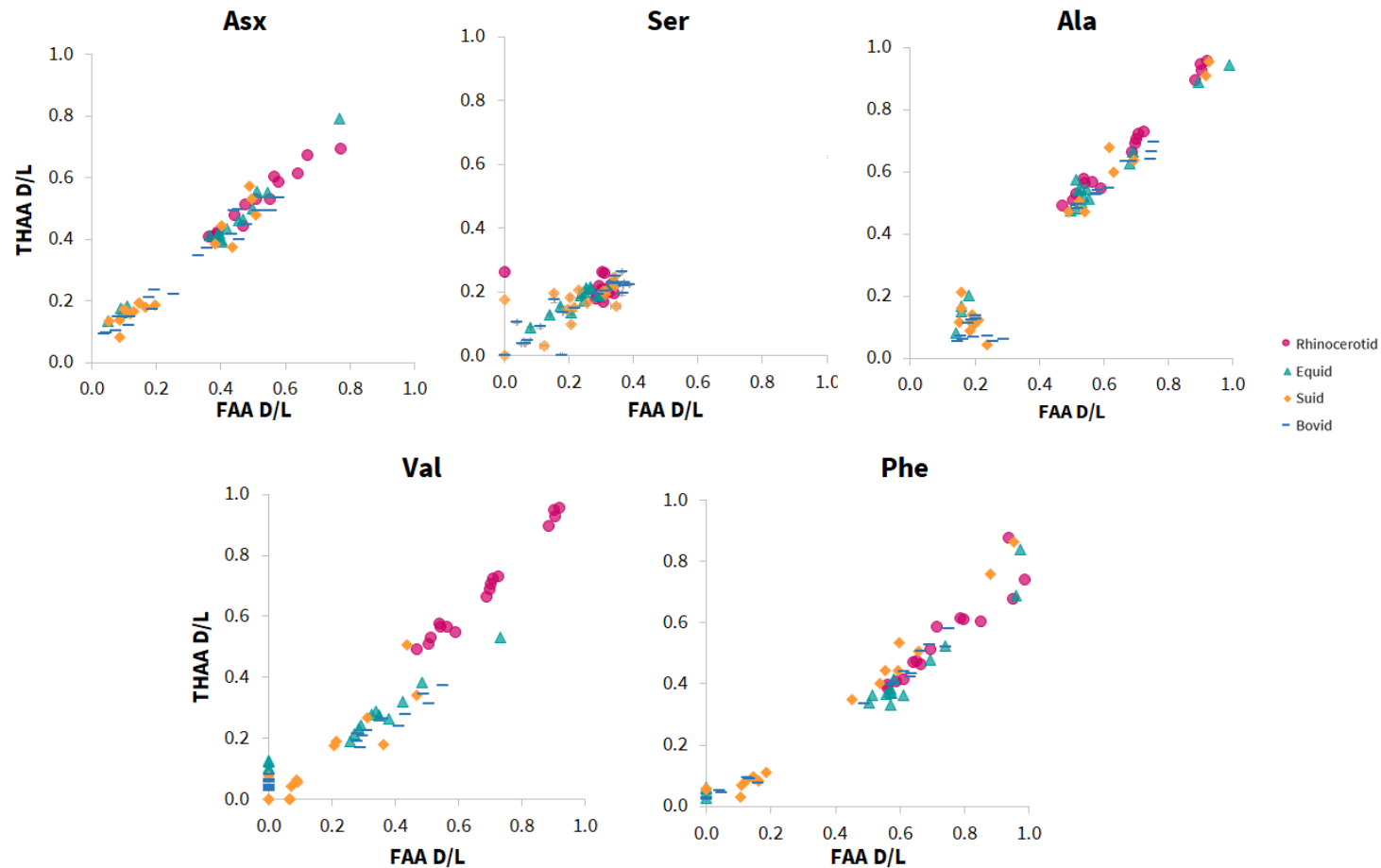
SI Figure 4.14. Comparison of the general amino acid racemisation degradation trend between the four taxonomic groups (rhinocerotid, suid, equid, bovid) of enamel samples present from Mumbwa Caves and Twin Rivers, assessed from the relationship between the average free (FAA) vs total hydrolysable (THAA) racemisation values (D/L) for Asx, Ser, Ala, Val and Phe.

4.5.2.2. Peptide chain hydrolysis
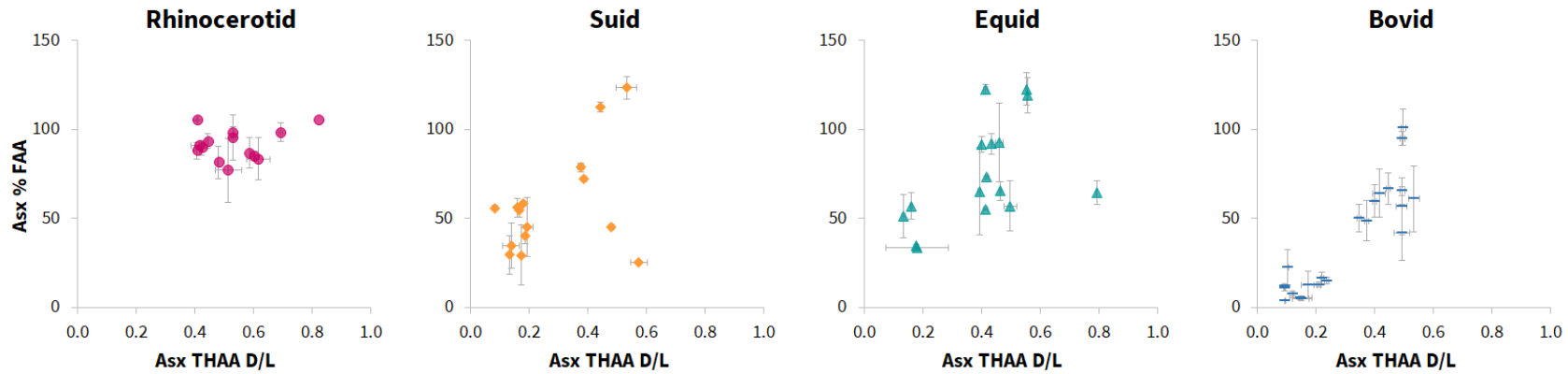
SI Figure 4.15. Comparison of the general peptide chain hydrolysis degradation trend in Asx between the four taxonomic groups (rhinocerotid, suid, equid, bovid) of enamel samples present from Mumbwa Caves and Twin Rivers, assessed from the relationship between the percentage of free Asx (% FAA) vs total hydrolysable Asx (THAA) racemisation values (D/L).
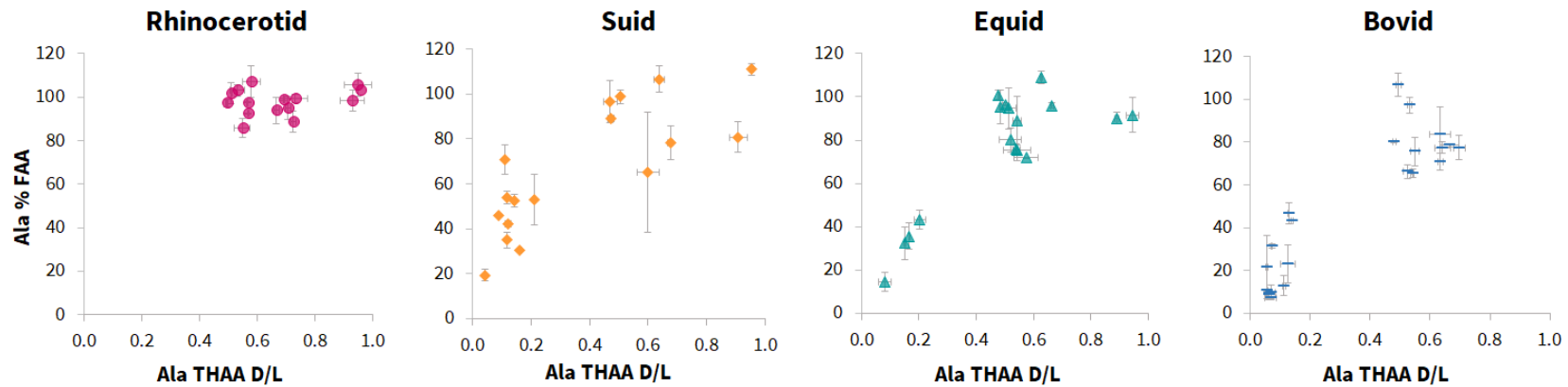
SI Figure 4.16. Comparison of the general peptide chain hydrolysis degradation trend in Ala between the four taxonomic groups (rhinocerotid, suid, equid, bovid) of enamel samples present from Mumbwa Caves and Twin Rivers, assessed from the relationship between the percentage of free Ala (% FAA) vs total hydrolysable Ala (THAA) racemisation values (D/L).

191
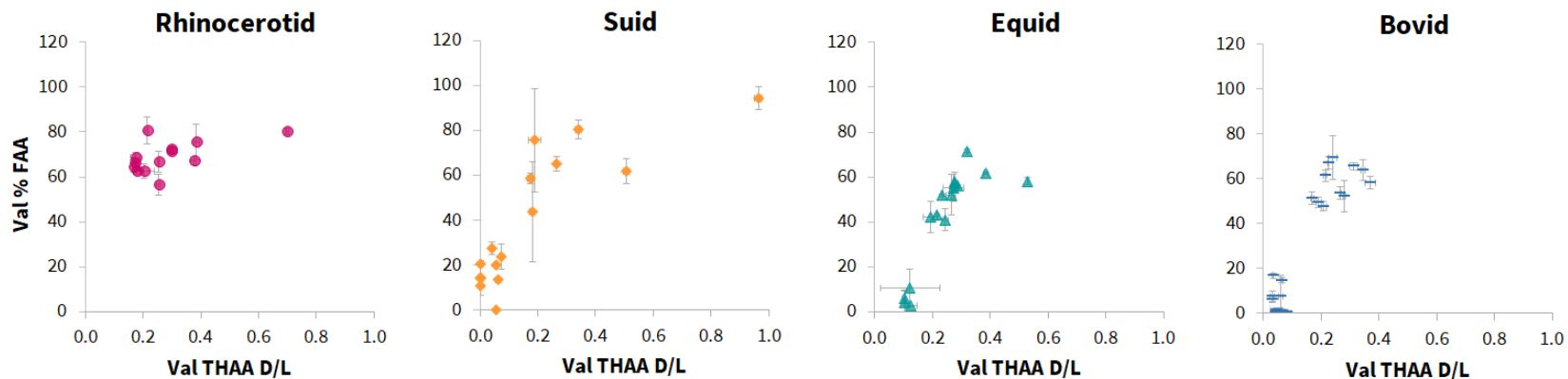
SI Figure 4.17. Comparison of the general peptide chain hydrolysis degradation trend in Val between the four taxonomic groups (rhinocerotid, suid, equid, bovid) of enamel samples present from Mumbwa Caves and Twin Rivers, assessed from the relationship between the percentage of free Val (% FAA) vs total hydrolysable Val (THAA) racemisation values (D/L).
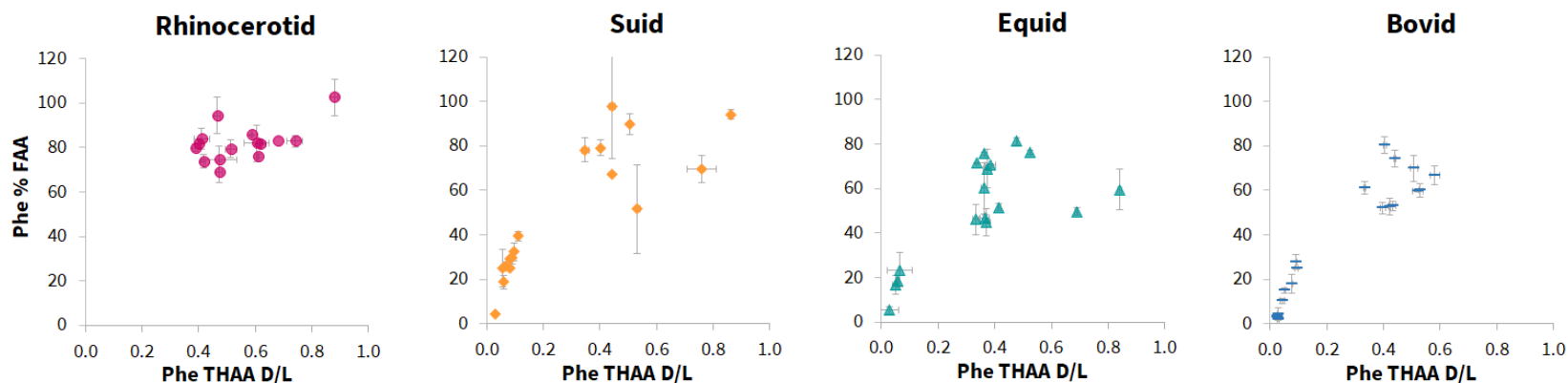
SI Figure 4.18. Comparison of the general peptide chain hydrolysis degradation trend in Phel between the four taxonomic groups (rhinocerotid, suid, equid, bovid) of enamel samples present from Mumbwa Caves and Twin Rivers, assessed from the relationship between the percentage of free Phe (% FAA) vs total hydrolysable Phe (THAA) racemisation values (D/L).

4.5.2.3. Twin Rivers: extent of amino acid racemisation by excavation location
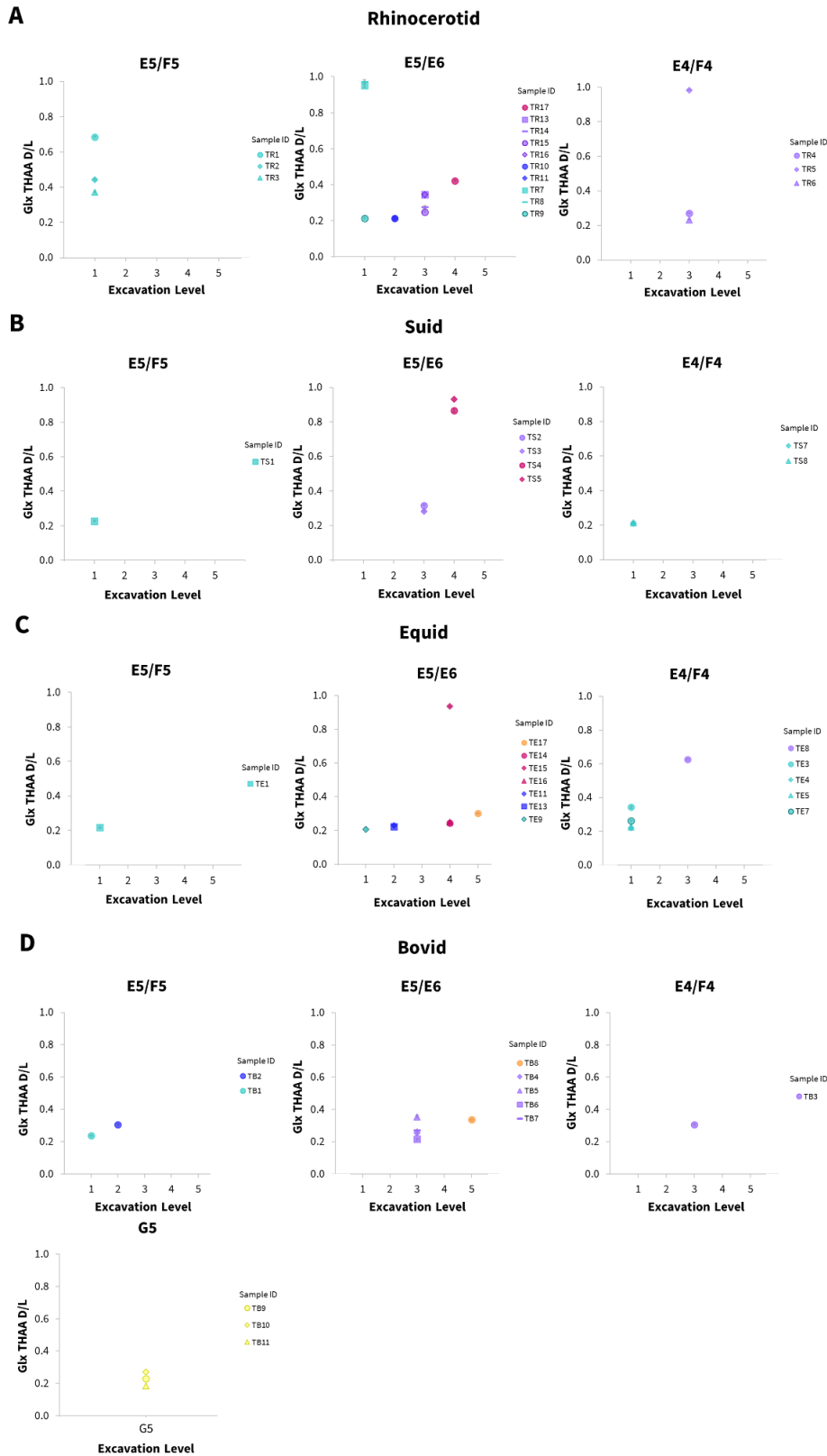
SI Figure 4.19. Average total hydrolysable amino acid (THAA) racemisation in Glx plotted against excavation level (1 = top 5 = bottom) in each excavation cavity (E5/F5, E5/E6, E4/F4, G5) for all samples.

Chapter 5. The use of biomolecular analysis to investigate protein degradation within Rhinocerotidae tooth enamel

This chapter has been written in the style of a research paper, as although it is not yet ready for submission, we ultimately aim to publish the study. All IcPD laboratory procedures, data acquisition, analysis and interpretation were carried out by CB; for the palaeoproteomic work, the laboratory procedures and MS data acquisition were carried out by CB for all of the forced degradation experiments; the palaeoproteomic laboratory procedures and MS data acquisition of the four Zambian fossil specimens was undertaken by a colleague, Fazeelah Munir (Munir, in prep.). All subsequent database searching, data analysis and interpretation was undertaken by CB.

The purpose of this study was to investigate the degradation of protein within Rhinocerotidae tooth enamel, through two complementary biomolecular techniques, the IcPD approach to AAG and palaeoproteomics. Rhinocerotidae was chosen as a taxa present within the archaeological and palaeoenvironmental record of the South-Central African region (chapter 4), but on which no forced degradation experiments had been previously undertaken.

Abstract

Forced degradation experiments are a useful way to investigate protein degradation on accelerated timescales for comparison to fossil diagenesis. Here, Rhinocerotidae tooth enamel samples were isothermally heated at 60, 70 and 80 °C over the course of two years for subsequent complementary chiral amino acid and palaeoproteomic analysis. Using the intra-crystalline protein degradation (IcPD) approach to amino acid geochronology (AAG), the markers of degradation observed through chiral amino acid analysis increased with respect to both time and temperature for samples heated to 70 and 80 °C, although the overall extent of degradation observed was low. Minimal degradation was observed at 60 °C over the two years. The low overall levels of degradation meant comparisons with fossils was challenging, and further studies would be required to more accurately assess whether the mechanisms of degradation were consistent between fossils and at the higher experimental temperatures. Comparison to previously published Elephantidae heating experiments, however, indicated a potential taxonomic effect from the different relative rates of racemisation for Asx and Ser. The low levels of racemisation induced for Rhinocerotidae enamel in this experiment also precluded appropriate mathematical transformations for kinetic modelling. It is therefore recommended that future studies using similar experimental temperatures be planned for a minimum of ten years for more accurate comparison with fossil diagenesis. Through palaeoproteomic analysis by mass spectrometry (MS) of bleached, unheated woolly rhino enamel, it was possible to improve

upon the known enamel proteome sequences. Patterns of degradation at the peptide level were also difficult to study by MS analysis; in addition to the low levels of degradation covered, this was also partly as a result of the limited replication possible in this pilot dataset. However, comparison to fossil samples which had higher levels of degradation showed similar regions of peptide preservation in AMEL, suggesting the heating experiments undertaken in this study may mimic environmental diagenesis. Similar to the chiral amino acid analysis, it is also recommended to undertake forced degradation experiments over longer timescales in future. Undertaking longer studies would also help to further elucidate the relationship between the markers of protein degradation observable through these two complementary techniques.

5.1. Introduction

In recent years, tooth enamel has gained interest among the palaeo-bioanalytical community as a source of endogenous protein, capable of surviving over, at least, the Quaternary. It has been shown to contain an intra-crystalline fraction of protein which adheres to closed-system behaviour (Dickinson *et al.*, 2019), making it the first $CaPO_4$ biomineral appropriate for the intra-crystalline protein degradation (IcPD) approach to amino acid geochronology (AAG). In addition to AAG, palaeoproteomic analysis by mass spectrometry (MS) has also been undertaken for a number of purposes, including taxonomic and sex identification. Evolutionary studies utilising the enamel proteome have been used to investigate and clarify extinct family lineages (e.g. Cappellini *et al.*, 2019; Welker *et al.*, 2019). The small proteome of enamel, which is dominated by amelogenin (AMEL, ~ 90%), has also gained interest from the palaeo community for its sex-specific isoforms (X and Y). This has provided insights into a number of archaeological and palaeontological fields of study, for example challenging gendered assumptions surrounding social relationships (Lugli *et al.*, 2019) and positions of political leadership (Cintas-Peña *et al.*, 2023), as well as sexual dimorphism (Madupe *et al.,* 2023). Chiral amino acid analysis has been incorporated into a number of palaeoproteomic studies, either to indicate the likelihood of successful analysis (Presslee *et al.*, 2021) and/or to support endogeneity (e.g. Cappellini *et al.*, 2019; Welker *et al.*, 2020).

Ancient protein is suggested to be well preserved within biominerals, in part through the physical protection of the mineral structure they reside within (Umamaheswaran and Dutta, 2024). In mammals, enamel is the densest mineral (Lacruz *et al.*, 2017), providing both an excellent repository for ancient protein and high fossil preservation potential. Studying protein diagenesis in tooth enamel is therefore highly valuable for understanding the capabilities and limitations of using this proteome for palaeo-bioanalytical studies. In the laboratory, high temperature experiments can be used to study protein degradation mechanisms on accelerated timescales (e.g. Bada and Schroeder, 1972; Kimber and Griffin, 1987; Canoira *et al.*, 2003; Dobberstein *et al.*, 2009; Crisp *et al.*, 2013; Solazzo *et al.*,

2013; Tomiak *et al.*, 2013; Ortiz *et al.*, 2017; Dickinson *et al.*, 2019). Through the IcPD approach to AAG, a number of degradation mechanisms can be studied at the amino acid level, such as amino acid racemisation, peptide chain hydrolysis, and dehydration of serine and threonine (e.g. Penkman *et al.*, 2008; Penkman *et al.*, 2013; Crisp *et al.*, 2013; Tomiak *et al.*, 2013; Dickinson *et al.*, 2019). Additional degradation mechanisms such as deamidation can be studied at the peptide level by palaeoproteomic MS analysis, allowing broadening the scope of investigation into protein diagenesis.

High temperature experiments are typically undertaken at a minimum of three experimental temperatures to allow for mathematical transformations capable of calculating activation energies for racemisation, and therefore numerical age and environmental temperature calculations for fossils (e.g. Brooks *et al.*, 1990; Kaufman and Miller, 1992; Clarke and Murray-Wallace, 2006; Bravenec *et al.*, 2018). Such calculations rely on several assumptions, and critically that the degradation mechanisms occurring under experimental conditions are reflective of lower temperature environmental diagenesis; this has previously been shown not to be the case for some biominerals, including elephantid tooth enamel (e.g. Tomiak *et al.*, 2013; Dickinson *et al.*, 2019). This study therefore aims to investigate protein diagenesis in lower temperature forced degradation experiments by two complementary techniques, chiral amino acid HPLC analysis and palaeoproteomic MS analysis. As one of the four family groups from South-Central Africa studied in chapter 4, and on which no forced degradation research had previously been undertaken, Rhinocerotidae tooth enamel was chosen for this study. Lower experimental temperatures were chosen in comparison to previous enamel forced degradation experiments (Dickinson *et al.*, 2019), to investigate whether these temperatures better mimic environmental diagenesis and are therefore more appropriate for fossil comparisons.

5.2. Materials and Methods

5.2.1. Materials

Fossil Rhinocerotidae enamel from Twin Rivers archaeological site in Zambia was previously analysed for IcPD (chapter 4). Data from the 16 samples which appear to have adhered to closed system behaviour are included as comparative fossil data, and methodological information for these 16 samples can be found in section 4.2 of chapter 4. These 16 samples were taxonomically identified by their morphology as Rhinocerotidae. Their identity was assumed to be probable white rhino (*Ceratotherium simum*); whilst black rhino (*Diceros bicornis*) could not be ruled out due to its potential presence in the region, as a herbivorous browser, its profile was less in keeping with the other herbivorous grazers within the fossil record at the site (Bishop and Reynolds, 2000). Regardless, due to the near threatened and critically endangered nature of white and black rhinos respectively, and the UK policies for animal material at zoos, it was not possible to obtain sufficient white or black rhino

tooth enamel to undertake forced degradation experiments. Therefore, the most ethically viable option for the study of protein diagenesis in Rhinocerotidae enamel was selected: a Late Pleistocene woolly rhino (*Coelodonta antiquitatis*) tooth (COAN.FE.1, York lot# 20093), which had lost all meaningful stratigraphical context (found in a sand excavation area around Eich on the River Rhine in Germany), was purchased from North Sea Fossils.

5.2.2. Isolation of the intra-crystalline protein fraction

Following the methods of Dickinson *et al*. (2019), approximately 1.8 g of enamel (as chips) was removed from COAN.FE.1 using abrasive rotary drill bits on a handheld rotary tool (Dremel drill), before being washed with water (ultrapure, 18.2 MΩ cm^{-1}) and left to air dry. The enamel sample was powdered with an agate pestle and mortar.

Bleach (12% NaOCl (analytical grade), 50 µL/mg) was added to the accurately weighed powdered sample and left on a rotor (constant, mild agitation) for 72 hours. The bleach was removed by pipette and each sample was washed five times with water (ultrapure, 18.2 MΩ cm^{-1}), before a final wash with methanol (HPLC-grade) and left to air dry.

5.2.3. Elevated temperature experiments

Approximately 6 mg of the powdered, bleached (section 5.2.2) sample was weighed in triplicate for subsequent IcPD analysis (section 5.2.4) and approximately 25 mg in singlicate for subsequent MS analysis (section 5.2.5) in individual sterilised glass vials (Wheaton), prior to the addition of 300 µL water (ultrapure, 18.2 MΩ cm^{-1}). The vials were wrapped with PTFE tape to minimise evaporation loss. The samples were isothermally heated in ovens for the times and temperatures given in table 5.1. These temperatures were chosen as degradation trends observed at higher temperatures (typically 80, 110 and 140 °C) from a number of biominerals (e.g. Tomiak *et al*., 2013), including enamel (Dickinson *et al*., 2019), did not appear to be reflective of the diagenetic mechanisms occurring at lower environmental temperatures. Temperatures closer to environmental conditions (60, 70 and 80 °C) were therefore chosen to investigate whether they better reflected the protein diagenesis in fossil enamel. Upon removal from the ovens, the water was removed by pipette and the samples were left to air dry prior to preparation for analysis (sections 5.2.4-5).

Table 5.1. Elevated temperature conditions for experimental woolly rhino enamel.

Temperature (°C)	Heating Time (days)									
60	-	-	-	50	90	150	-	240	365	730
70	-	20	-	50	90	150	200	240	365	730
80	10	20	30	50	-	150	200	240	365	730

5.2.4. Enamel IcPD methodology (chiral amino acid HPLC analysis)

Subsequent to bleaching and heating (sections 5.2.2 and 5.2.3) and following the methods of Dickinson *et al*., (2019), from each experimental triplicate, *ca*. 2.5 mg (accurate masses noted) was weighed out for analysis of the free amino acid fraction (FAA) and the total hydrolysable amino acid fraction (THAA). THAA subsamples were demineralised in 7 M HCl (20 µL/mg), the vials flushed with N_2 and heated in an oven at 110 °C for 24 hours, prior to drying by centrifugal evaporation. The THAA subsamples were then redissolved in 1 M HCl (20 µL/mg) and the FAA subsamples demineralised in 1 M HCl (25 µL/mg), prior to the addition of 1 M KOH (28 µL/mg) to all subsamples, which formed a monophasic translucent gel with a viscous consistency. The subsamples were centrifuged at 13,000 rpm for 5 minutes whereupon a biphasic solution formed (supernatant above a cloudy gel). The supernatant was removed and dried by centrifugal evaporation.

The samples were rehydrated in the minimum possible volume of a solution of internal standard (L-homo-arginine (0.01 M), hydrochloric acid (0.01 M) and sodium azide (1.5 mM)). Separation of the chiral isomers of the amino acids was carried out by fluorescence detection RP-HPLC (Agilent 1100) using a modified Kaufman and Manley (1998) method (Penkman, 2005). The samples were run alongside standards and blanks.

5.2.5. Enamel MS methodology (palaeoproteomic analysis)

Subsequent to bleaching and heating (sections 5.2.2 and 5.2.3) and following a method adapted from Cappellini *et al*., (2019), 1 mL 10% hydrochloric acid (HCl) was added to approximately 25 mg (accurate masses noted) of the enamel sample before refrigeration (4 °C) overnight.

The sample was centrifuged for 10 minutes before removal of the supernatant into a separate vial (S1) and storage in the freezer. The sample was resuspended in 1 mL 10% HCl prior to refrigeration (4 °C) overnight.

The sample was centrifuged for 10 minutes before removal of the supernatant into a separate vial (S2). S1 was removed from the freezer to thaw prior to centrifugation alongside S2 at 13,000 rpm for 1 hour.

150 µL of methanol (MeOH, LC-MS grade) was added to the ZipTip (Millipore P10 with 0.6 µL C18 resin) and centrifuged at 3000 rpm for 30 seconds before discarding the solvent. This step was repeated twice with AT80 (80% 0.1% trifluoroacetic acid (TFA) in acetonitrile (MeCN, LC-MS grade) 20% 0.1% TFA in water (H_2O, LC-MS grade)) and then 0.1% TFA in H_2O (LC-MS grade). 200 µL increments of the sample supernatant (S1 and S2 combined) were added to the ZipTip, centrifuging at 3000 rpm for 30 seconds before discarding the liquid. 150 µL 0.1% TFA in H_2O (LC-MS grade) was added to the ZipTip and centrifuged at 3000 rpm for 30 seconds before discarding the liquid. This step was repeated.

The sample was then eluted into a clean microcentrifuge tube with the addition of 30 µL of 40% MeCN (LC-MS grade) before centrifugal evaporation to dryness and reconstitution in 50 µL 0.1% TFA in H_2O (LC-MS grade).

6 µL of sample was loaded onto an mClass nanoflow UPLC system (Waters) equipped with a nanoEaze M/Z Symmetry 100 Å C18, 5 µm trap column (180 µm x 20 mm, Waters) and a PepMap, 2 µm, 100 Å, C18 EasyNano nanocapillary column (75 m x 500 mm, Thermo). The trap wash solvent was aqueous 0.05% (v:v) TFA and the trapping flow rate was 15 µL/min. The trap was washed for 5 min before switching flow to the capillary column. Separation used gradient elution of two solvents: solvent A, 0.1% formic acid (FA) in water (LC-MS grade); solvent B, 0.1% FA in MeCN (LC-MS grade). The flow rate for the capillary column was 300 nL/min and the column temperature was 40 °C. The linear multi-step gradient profile was: 3-10% B over 7 mins, 10-35% B over 30 mins, 35-99% B over 5 mins and then proceeded to wash with 99% solvent B for 4 min. The column was returned to initial conditions and re-equilibrated for 15 mins before subsequent injections.

The nanoLC system was interfaced with an Orbitrap Fusion Tribrid mass spectrometer (Thermo) with an EasyNano ionisation source (Thermo). Positive ESI-MS and MS 2 spectra were acquired using Xcalibur software (version 4.0, Thermo). Instrument source settings were: ion spray voltage, 1,900 V; sweep gas, 0 Arb; ion transfer tube temperature; 275 °C. MS 1 spectra were acquired in the Orbitrap with: 120,000 resolution, scan range: m/z 375-1,500; AGC target, $4e^5$; max fill time, 100 ms. Data dependent acquisition was performed in topN mode using a selection of the 12 most intense precursors with charge states above 1. Easy-IC was used for internal calibration. Dynamic exclusion was performed for 50 s post precursor selection and a minimum threshold for fragmentation was set at $5e^3$. MS2 spectra were acquired in the Orbitrap with: 30,000 resolution, max fill time, 100 ms, HCD; activation energy: 32 NCE.

5.3. Results and Discussion

The results of the forced degradation experiments are first discussed individually in terms of each technique (IcPD analysis - section 5.3.1, palaeoproteomic analysis - section 5.3.2), prior to consideration of their relationship to one another (section 5.3.3).

5.3.1 IcPD analysis

5.3.1.1. Degradation markers from IcPD analysis

Multiple parameters of protein degradation (amino acid racemisation, section 5.3.1.1.1; concentration, section 5.3.1.1.2; composition, section 5.3.1.1.3; peptide bond hydrolysis, section 5.3.1.1.4; serine and threonine dehydration, 5.3.1.1.4) can be assessed through the IcPD approach to AAG. Used in combination these can help infer the likelihood of maintenance of a closed system (and therefore the endogeneity of the amino acids observed), as well as tracking the different breakdown reactions.

5.3.1.1.1. Amino acid racemisation

Predictable protein degradation was observed in the THAA and FAA fractions, in terms of increasing racemisation with both increasing temperature (60, 70 and 80 °C) and increasing time at 70 and 80 °C (Fig. 5.1). At 60 °C, over the course of two years, no clear increase in racemisation was observed for any of the amino acids in either the THAA or FAA fraction (Fig. 5.1). Not only was no to little racemisation observed for the majority of amino acids in the FAA fraction at 60 °C, but the overall concentration of free amino acids was also low (section 5.3.1.1.2), indicating only limited peptide bond hydrolysis.

It has previously been noted that tooth enamel provides an excellent repository of ancient protein. Studies reporting very high thermal ages of diagnostically useful protein sequences by mass spectrometry have inferred that under favourable environmental conditions, enamel protein may be able to survive well past the Quaternary (Welker *et al.*, 2019). The lack of racemisation observed at 60 °C and the relatively low levels observed at 70 and 80 °C over two years (Fig. 5.1) therefore isn't entirely unsurprising.
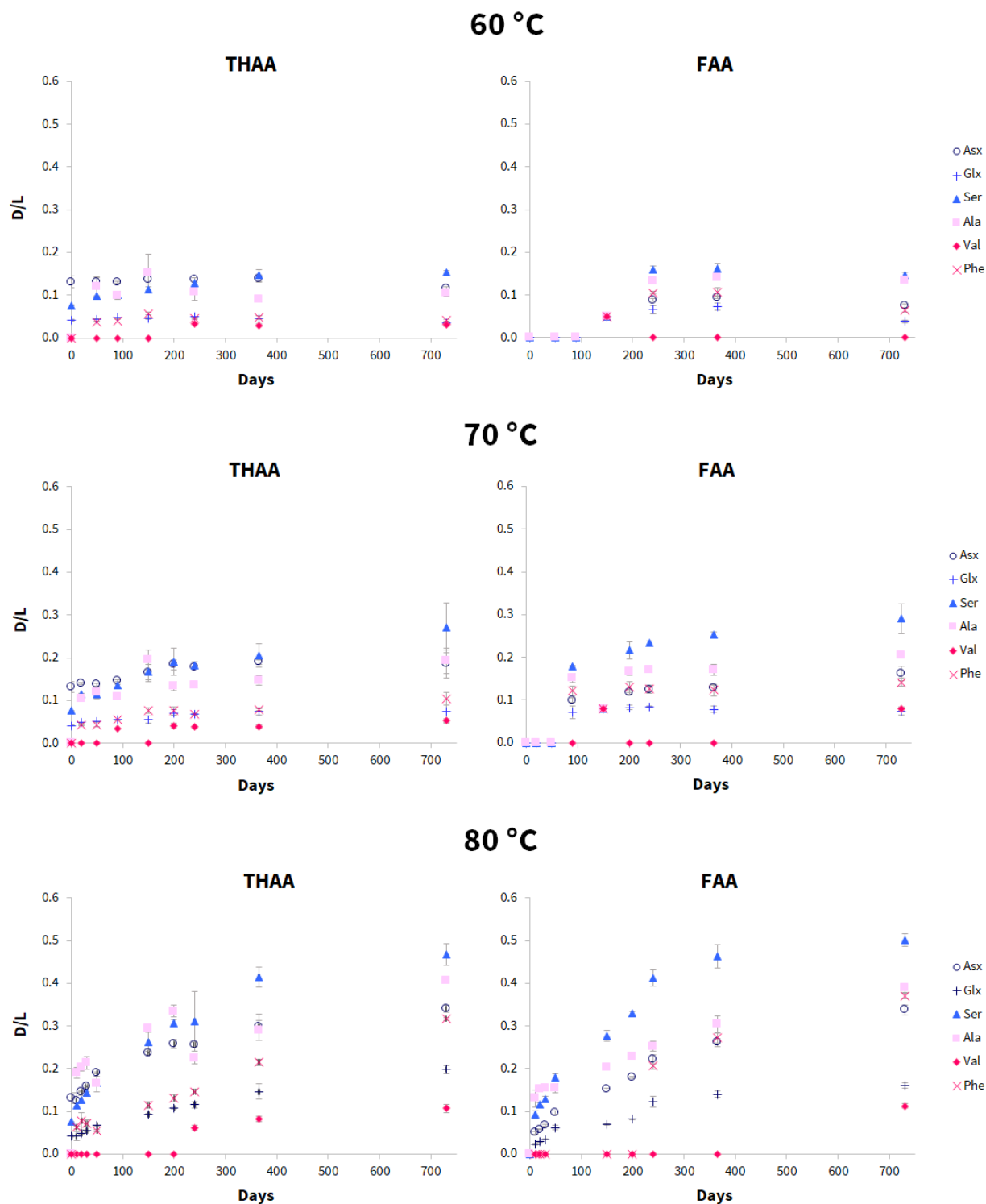
Figure 5.1. The extent of racemisation for the total hydrolysable (left) and free (right) amino acid fractions (THAA and FAA respectively) for amino acids from woolly rhino tooth enamel, during isothermal heating at 60, 70 and 80 °C over two years. Error bars represent the standard deviation about the mean for experimental triplicates. All plots used the same scale for racemisation (D/L) to highlight the increase in racemisation observed with increasing temperature.

In general, the amino acids displayed a similar relative order of racemisation (Fig. 5.1) to those previously reported in Elephantidae tooth enamel at 80 °C (Dickinson *et al.*, 2019) and to free aminos in solution (Asp>Phe>Ala>Glu>Val) (Smith and Evans, 1980). Small differences in the relative order likely result from additional influences of their protein environment, including the primary sequence of amino acids (Mitterer and Kriausakul, 1984), the secondary and tertiary structures (Collins *et al.*, 1999) and additional interactions, such as with the biomineral crystal structure (Demarchi *et al.*, 2016). However, the relative order of amino acid racemisation, whilst similar, was not the same at every time point and temperature measured (Fig. 5.1). This was largely influenced by alanine's racemisation profile over time, which at 80 °C was the fastest racemising amino acid for 30 days in both the free and total hydrolysable amino acid fractions, before being overtaken by serine. Examining the chromatography in detail, the D-Ala peak was in most instances very small, yet broad, and occasionally with fronting and/or tailing shoulders, suggesting co-elution with interfering compounds, possibly other degradation products. The inability to consistently integrate the D-Ala peak, and the knock on effects of these differences on the calculated D/L values, are likely the cause of Ala's racemisation profile at 80 °C.

To study the likelihood of closed-system behaviour in rhinocerotid enamel, the free and total hydrolysable amino acid fractions for each sample were plotted against one another (Fig. 5.2). A strong positive correlation was observed indicating the likelihood of closed-system behaviour (Preece and Penkman, 2005; Penkman *et al.*, 2007), consistent with previously published Elephantidae enamel IcPD data (Dickinson *et al.*, 2019). Ala had a wider strong positive trend between the free and total hydrolysable amino acid fractions in the experimentally heated samples than for the majority of other amino acids (Fig. 5.2). This likely results from the inability to consistently integrate the D-Ala peak as discussed previously, impacting the low levels of racemisation more severely due to the small D-Ala peak. This data therefore suggested that Ala should be treated with caution for Rhinocerotidae enamel IcPD data.

Unfortunately, for the majority of amino acids, the extent of racemisation induced under the experimental conditions undertaken was low. There was therefore no/little overlap between the experimentally heated samples and the Twin Rivers Rhinocerotidae enamel fossils for the majority of amino acids (Fig. 5.2) and it is therefore difficult to draw definitive conclusions from this dataset. However, in general, the fossil data looked consistent with the heated samples, extending the trends observed. To confirm whether this is an accurate interpretation, it is likely that many more years' worth of isothermal heating would be required at 60, 70 and 80 °C to obtain data covering the full extent of racemisation, well beyond the timeframe of a typical PhD or postdoctoral project.
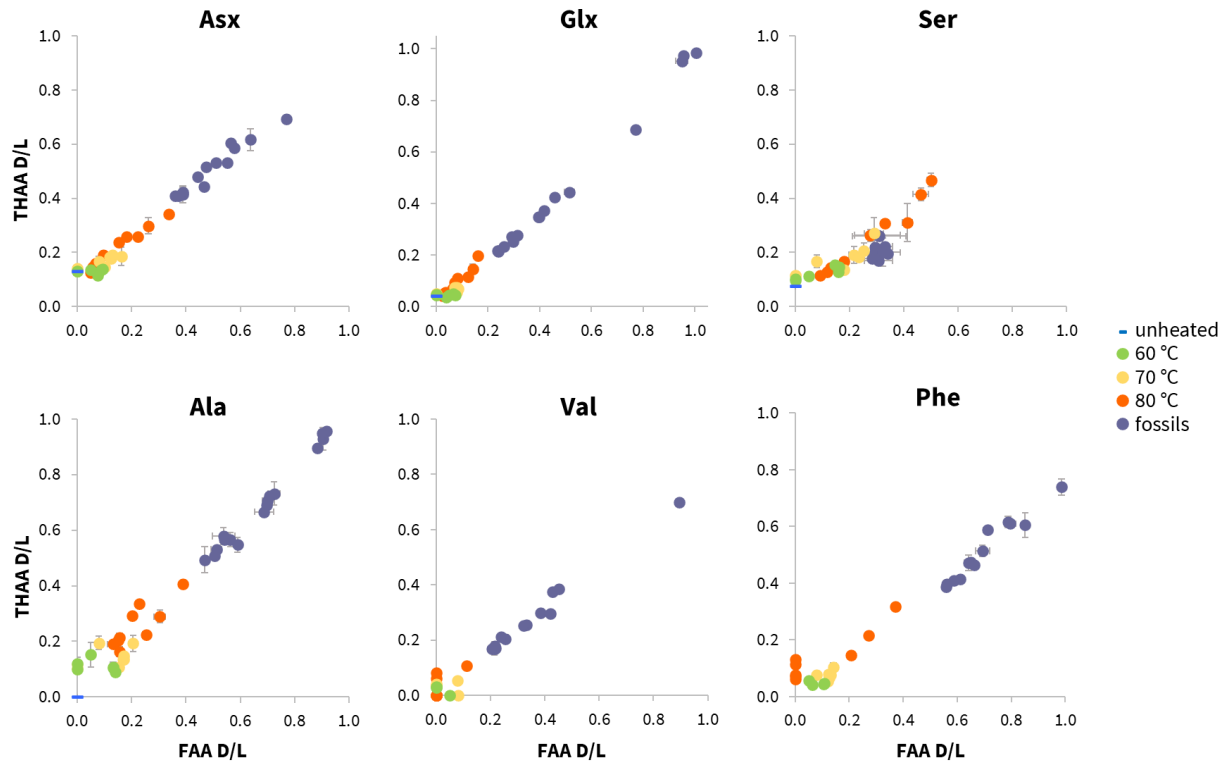
Figure 5.2. Racemisation of free (FAA) vs total hydrolysable (THAA) fraction from experimental samples isothermally heated to 60, 70 and 80 °C over two years in comparison to Zambian fossils. Error bars represent the standard deviation about the mean for subsample experimental replicates.

The only direct comparison possible between the heating experiments undertaken here and those previously undertaken on Elephantidae enamel (Dickinson et al., 2019) was at 80 °C, up to 240 days. Interestingly, for some amino acids (e.g. Glx and Phe), the overall extents of racemisation observed at each timepoint were very similar (Fig. 5.3). For others (e.g. Asx and Ser; interestingly, the only known in chain racemisers (Stephenson and Clarke, 1989; Takahashi et al., 2010; Demarchi et al., 2013)), the relative rates appeared to be different (Fig. 5.3). A taxonomic effect has previously been reported for AAR (e.g. King and Hare, 1972; Bright and Kaufman, 2011; Ortiz et al., 2013) and a potential taxonomic difference in degradation was observed for the fossil Rhinocerotidae enamel studied in chapter 4 (section 4.3.2). Taxonomic differences in enamel proteome sequences does then provide one plausible explanation for the differences in relative rates observed here. Additionally, for amelogenin, which comprises around 90% of the expressed proteome in enamel, sex specific (X and Y) isoforms are present containing differing sequences (e.g. Parker et al., 2019). If these isoforms were also to breakdown at different rates, this may further confound the relative racemisation rates observed. As the biological sex of these two samples (the elephantid and rhinocerotid) is currently unknown, it is therefore unclear whether this could have impacted the observed relative rates for Asx and Ser.

Heating experiments under similar experimental conditions to the woolly rhino enamel described here (60, 70 and 80 °C) were also undertaken on *Achatina* shell (an aragonitic $CaCO_3$ multi-layered biomineral), reported in chapter 3 (Baldreki *et al.*, 2024). Comparison between these biominerals show a large difference in the relative rates of each amino acid's racemisation over time (Fig. 5.3). Significantly lower levels of racemisation (~ ½) were observed in the Rhinocerotidae tooth enamel in comparison to the *Achatina* shell at comparable temperatures and time points, e.g. Asx and Phe at 80 °C over the course of one-year isothermal heating (Fig. 5.3). This data was consistent with that previously reported by Dickinson *et al.* (2019), who compared their enamel data to the relatively faster racemising proteins within *Bithynia* opercula (a calcitic $CaCO_3$ biomineral), bolstering the likelihood of lower rates of racemisation from proteins within tooth enamel more generally.
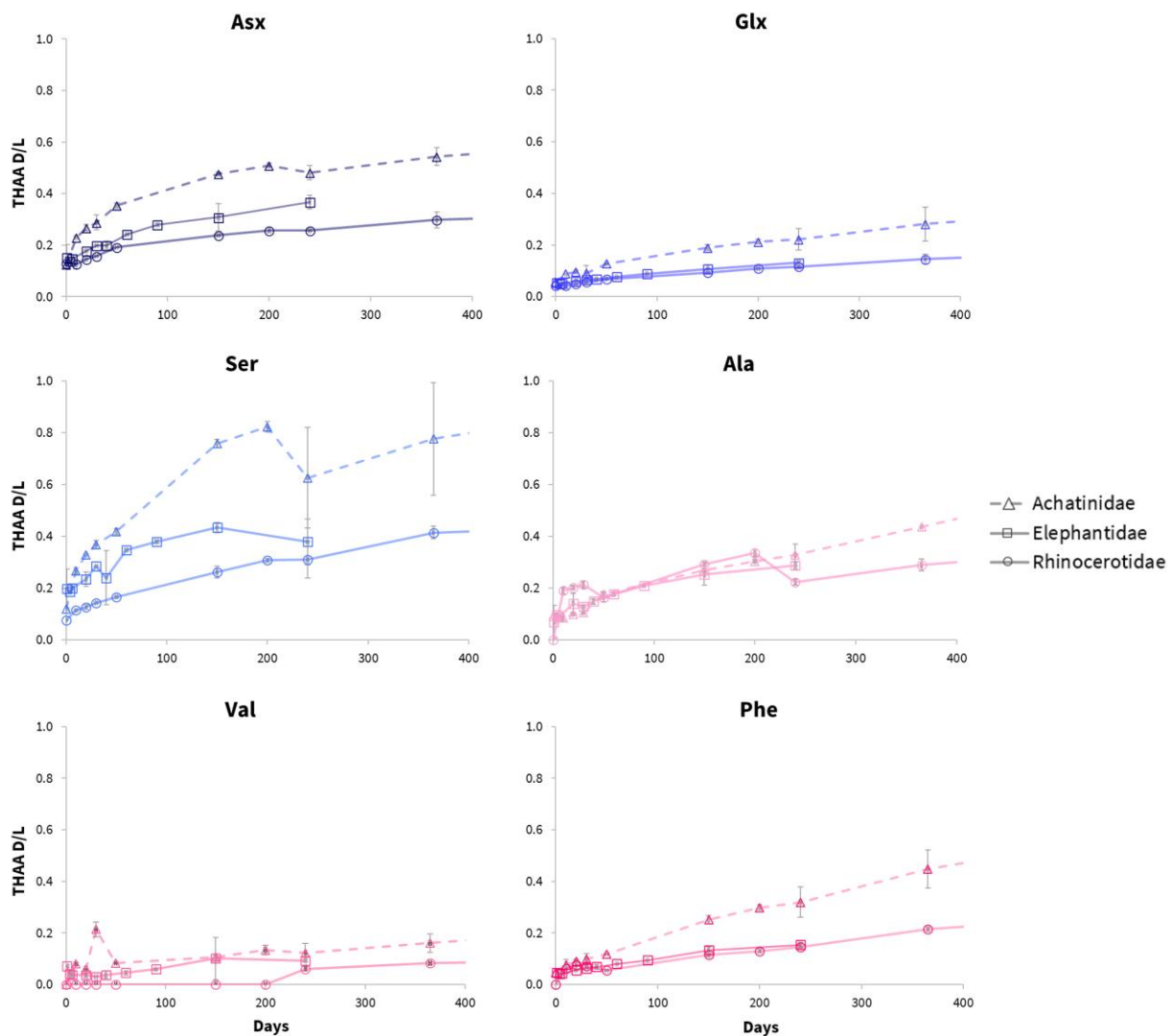
Figure 5.3. Comparison between the extent of racemisation in different amino acids from protein within rhinocerotid and elephantid tooth enamel (solid lines) and *Achatina* shell (three aragonitic layer - '3AL' portion - dotted line) during isothermal heating to 80 °C.

The much lower relative rates of racemisation in enamel may provide a valuable opportunity to increase the dating timescale for AAG, proving especially valuable for warm regions of the globe (such as across Africa), where the maximum dating coverage by AAG would be lower than in temperate latitudes due to warmer environmental conditions. Further discussion is included in section 5.3.1.2.

5.3.1.1.2. Amino acid concentration

Concentrations and relative amino acid abundances, alongside racemisation, can help to provide early indications of both the state of degradation and the likelihood of endogeneity of the observed protein. Calculated concentrations, however, typically contain higher levels of variability than racemisation values, largely because the calculation compounds the errors associated with the low sample masses and volumes, rather than cancelling out as they do in DL ratios (Powell *et al.*, 2013). Nevertheless, calculated concentrations provide highly useful information when in combination with other IcPD parameters.

During the forced degradation experiments, the total concentration of amino acids remained relatively stable over the two-year duration at all experimental temperatures (Fig. 5.4). A possible trend of increasing FAA concentration with time was observable at 80 °C and implications about peptide bond hydrolysis are discussed further in section 5.3.1.1.4. The lack of apparent trends in total amino acid concentration, much like the racemisation data (section 5.3.1.1.1), highlights the slow rates of degradation observed for proteins in tooth enamel, and the likelihood of closed-system intra-crystalline behaviour. It is also highly likely that to track any trends in concentration at the experimental temperatures chosen here, a significantly longer experimental time would be required.
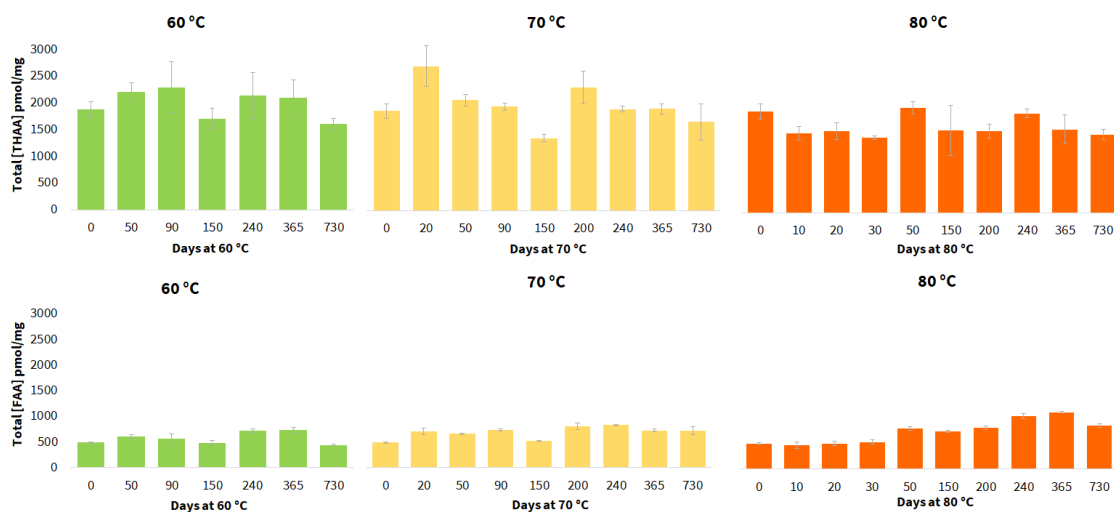
Figure 5.4. Total amino acid concentration of the hydrolysable fraction (top) and free fraction (bottom) during isothermal heating to 60, 70 and 80 °C. Error bars represent the standard deviation about the mean for subsample experimental triplicate.

To assess whether the concentrations in the forced degradation experiments mimicked geological diagenesis, comparison to fossil IcPD data was undertaken. In the absence of a known fossil age (chapter 4, section 4.2.1), the concentrations of individual samples were plotted against the extent of racemisation for each amino acid (Fig. 5.5). For the majority of amino acids, their individual concentrations remained relatively constant across a broad range of racemisation. A trend of decreasing concentration with increasing racemisation was potentially observable for Asx, Glx and Phe (Fig. 5.5). This trend was clearly observable for Ser in the heating experiments, but the fossil data contained relatively low concentrations even at low racemisation values. Ser is a relatively fast racemising amino acid, and unlike most other amino acids, is thought to be able to racemise within a peptide chain (Takahashi *et al.*, 2010; Demarchi *et al.*, 2013). This is reflected in heating experiments, where Ser racemisation profiles in the intra-crystalline fraction of enamel and other biominerals have been shown to increase rapidly and then drop over time (e.g. Orem and Kaufman, 2011; Tomiak *et al.*, 2013; Dickinson *et al.*, 2019), with only the first part of this pattern observable in Fig. 5.1. The latter decrease in the extent of racemisation likely occurs as a result of its susceptibility to additional degradation mechanisms (Akiyama, 1980; Walton, 1998; Orem and Kaufman, 2011; Penkman *et al.*, 2013), removing the racemised Ser from the pool of amino acids. The low levels of Ser racemisation at low concentrations in the fossils (Fig. 5.5), in addition to the fossils' higher levels of racemisation in the other studied amino acids in comparison to the heating experiments (Fig. 5.2), therefore likely reflect high levels of protein diagenesis. A potential increase in Ala concentration with increasing racemisation was also observable. This is likely as a result of a serine and/or threonine decomposition (dehydration) reaction, discussed in section 5.3.1.1.5.
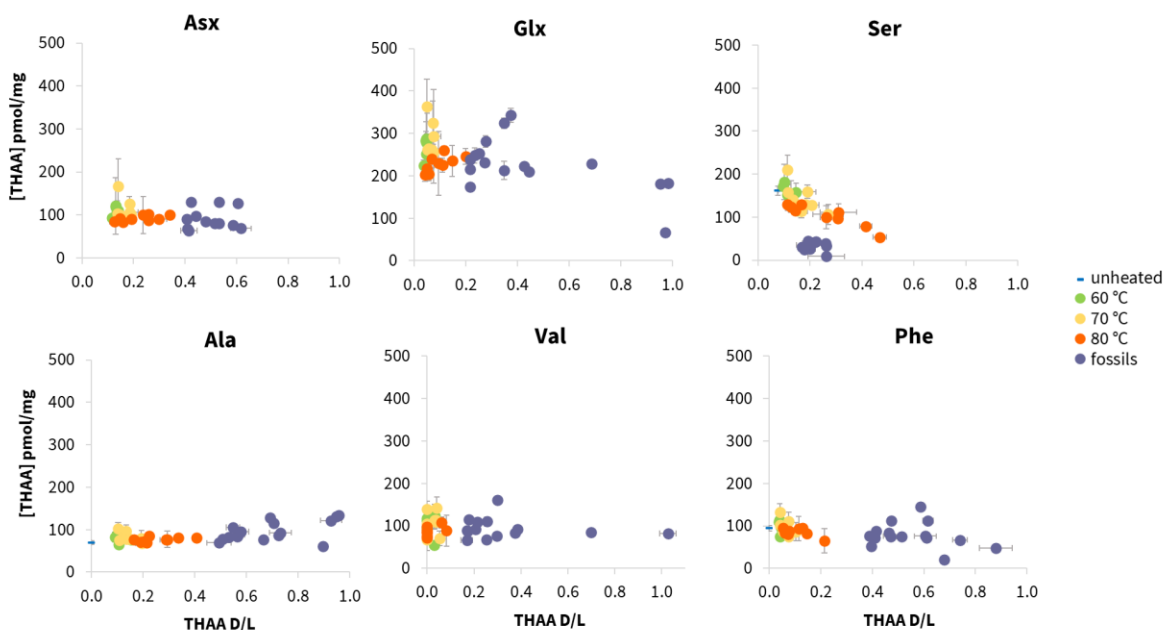
Figure 5.5. Individual amino acid concentrations vs racemisation for amino acids from experimental samples isothermally heated to 60, 70 and 80 °C over two years in comparison to fossils. Error bars represent the standard deviation about the mean for subsample experimental replicates.

5.3.1.1.3. Relative amino acid composition

Relative amino acid composition, alongside concentration, is another parameter which can be investigated from IcPD data, with degradation resulting in characteristic changes in composition (e.g. Bada *et al.*, 1978). Similar to the concentration data discussed in section 5.3.1.1.2, the relative THAA compositions remained relatively consistent over the two-year experiment (Fig. 5.6). The relative stability of the THAA composition profiles (Fig. 5.6) in combination with the concentrations (Fig. 5.4), suggests low levels of protein degradation occurred during this experiment and that minimal (if any) contamination was present, consistent with closed-system behaviour. In the FAA, the least degraded samples were dominated by Gly and to a lesser extent hydrophilic amino acids (Asx, Glx, Ser, Thr). As the heating duration increased, a larger relative proportion of the hydrophobic amino acids was observed (Ile, Leu, Phe, Val, Ala). These amino acids generally have more stable peptide bonds (Sato *et al.*, 2004) and therefore an increase in their relative proportion likely reflects increasing degradation over time (Fig. 5.6).
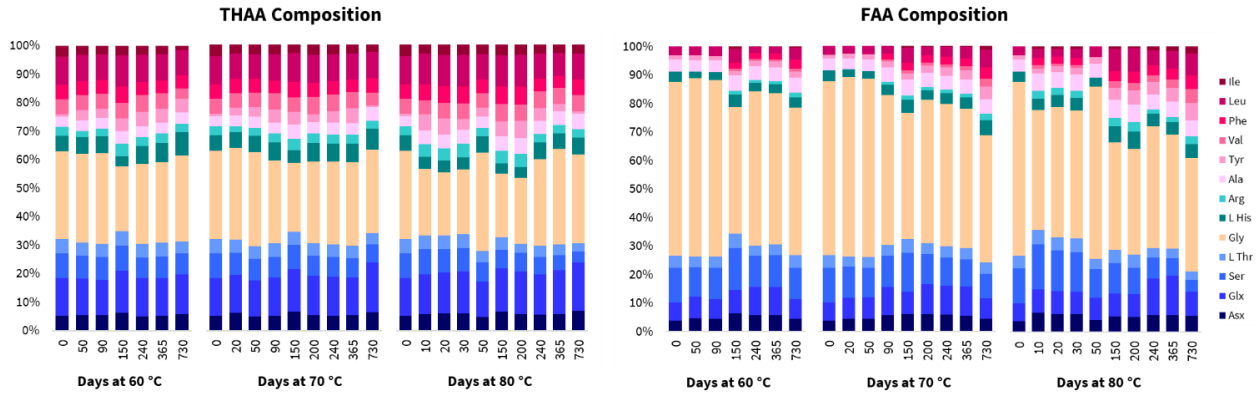
Figure 5.6. Relative amino acid composition during isothermal heating to 60, 70 and 80 °C over two years.

The THAA composition profiles were also similar to fossil Rhinocerotidae samples with comparable levels of racemisation (Fig. 5.7), with the change in composition evident in the most degraded fossil samples likely reflective of high levels of protein degradation. This may indicate the primary sequences of proteins within the enamel proteome are relatively well conserved within the Rhinocerotidae family, and should allow direct comparison of IcPD parameters between its members.
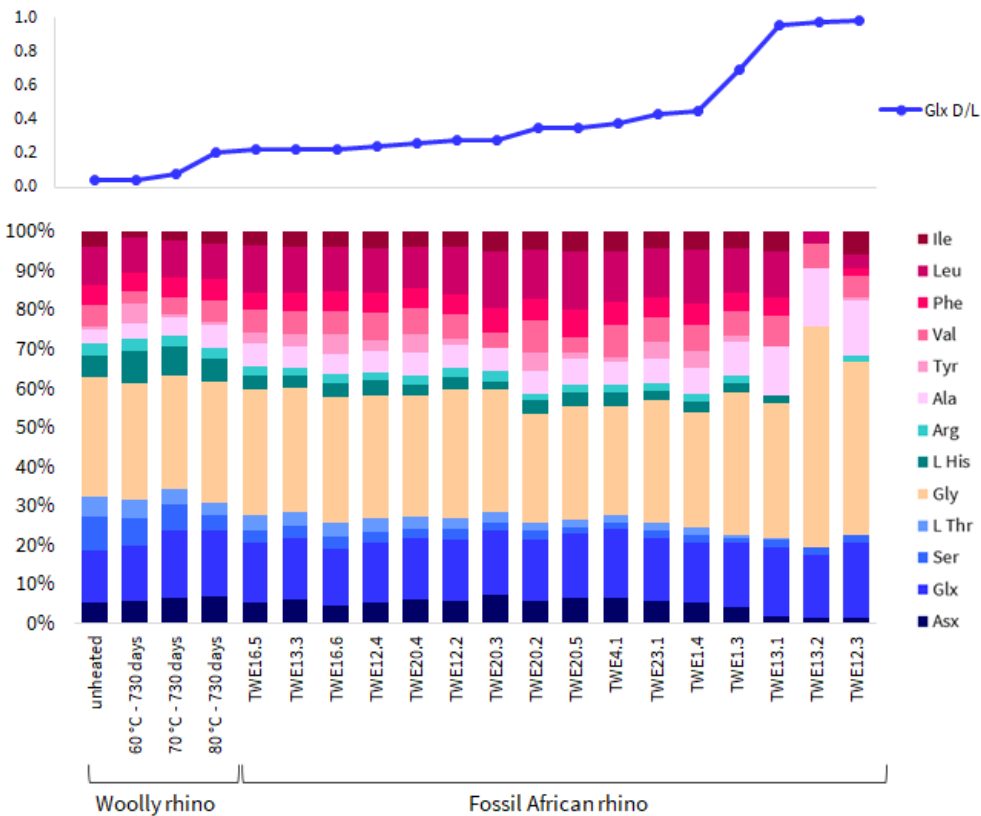
Figure 5.7. Relative amino acid composition of the THAA fraction from woolly rhino enamel unheated and after 2 years of isothermal heating at 60, 70 and 80 °C, in comparison to fossil rhino enamel from Twin Rivers, Zambia. Composition profiles have been ordered from lowest to highest extent of Glx THAA racemisation.

208

5.3.1.1.4. Peptide bond hydrolysis

Peptide bond hydrolysis of the primary protein structure results in the production of shorter peptide chains and ultimately free amino acids. From IcPD analysis, this degradation mechanism can be inferred from calculating the percentage of free amino acids out of the total amino acid concentration observed from the same sample (%FAA).

During the forced degradation experiments, increasing %FAA was observed for all amino acids over the first year, at all temperatures studied (Fig. 5.8). Similar to racemisation (section 5.3.1.1.1), this trend was clearest at 80 °C. This increase in FAA also suggests that the observed degradation occurred within a closed system, with no loss of endogenous amino acids released by hydrolysis.

For some amino acids, a decrease in %FAA was observed at 730 days e.g. Asx, Glx, Ser, Ala (Fig. 5.8). The racemisation of Phe appeared to plateau from 365 to 730 days, whilst an increase was observed for Val (Fig. 5.8). As there were no timepoints in between 365 and 730 days, it is very difficult to assess the cause of these observations. Calculations of %FAA may also further compound the higher variability inherent in the concentration calculations (discussed in section 5.3.1.1.2), giving rise to larger error bars and a less clear degradation profile (Fig. 5.8). These samples were prepared and analysed as two separate batches, a year apart, but there were no indications from standards or blanks run within the HPLC sequences to suggest either as an anomalous batch. Additionally, decreases in %FAA have been previously observed in more highly degraded samples, where additional degradation mechanisms are thought to influence the concentrations of free amino acids (Bada *et al.*, 1978; Walton 1998).
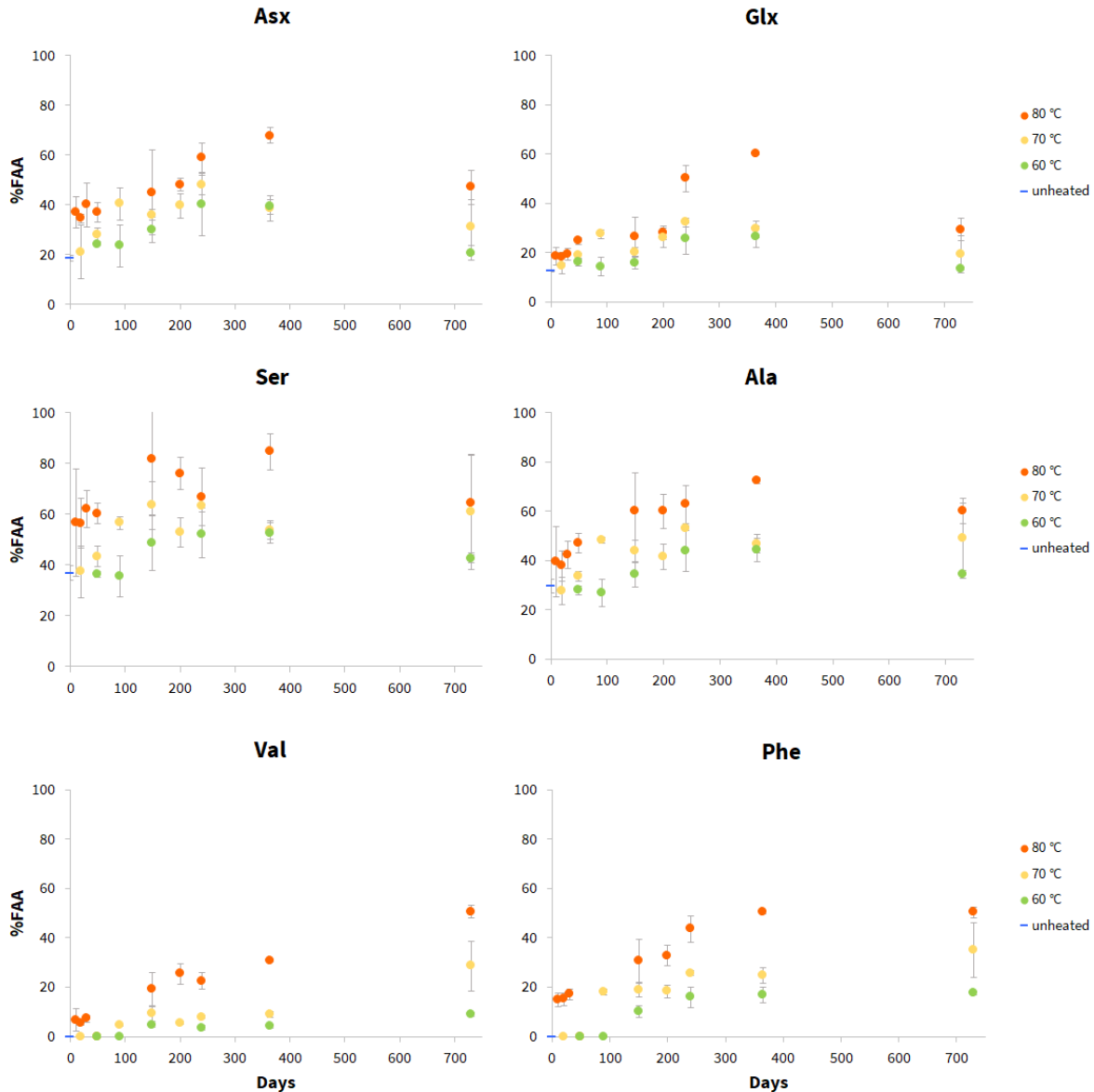
Figure 5.8. The extent of hydrolysis for four amino acids from woolly rhino tooth enamel, during isothermal heating at 60, 70 and 80 °C over two years. Error bars represent the standard deviation about the mean for subsample experimental triplicate.

As for the concentration data, to assess how likely these hydrolysis trends mimicked fossil diagenesis, in the absence of a known fossil age, peptide bond hydrolysis (%FAA) of individual amino acids were plotted against their extent of racemisation (Fig. 5.9). Similar to racemisation (section 5.3.1.1.1), there was no overlapping region of racemisation and %FAA between the heated experimental samples and the fossils for the majority of amino acids (Fig. 5.9). Again, in general it appeared that the fossil data displayed an extension of the trends observed in the heating

experiments, but additional heating experiments over many more years would be required to investigate this further.
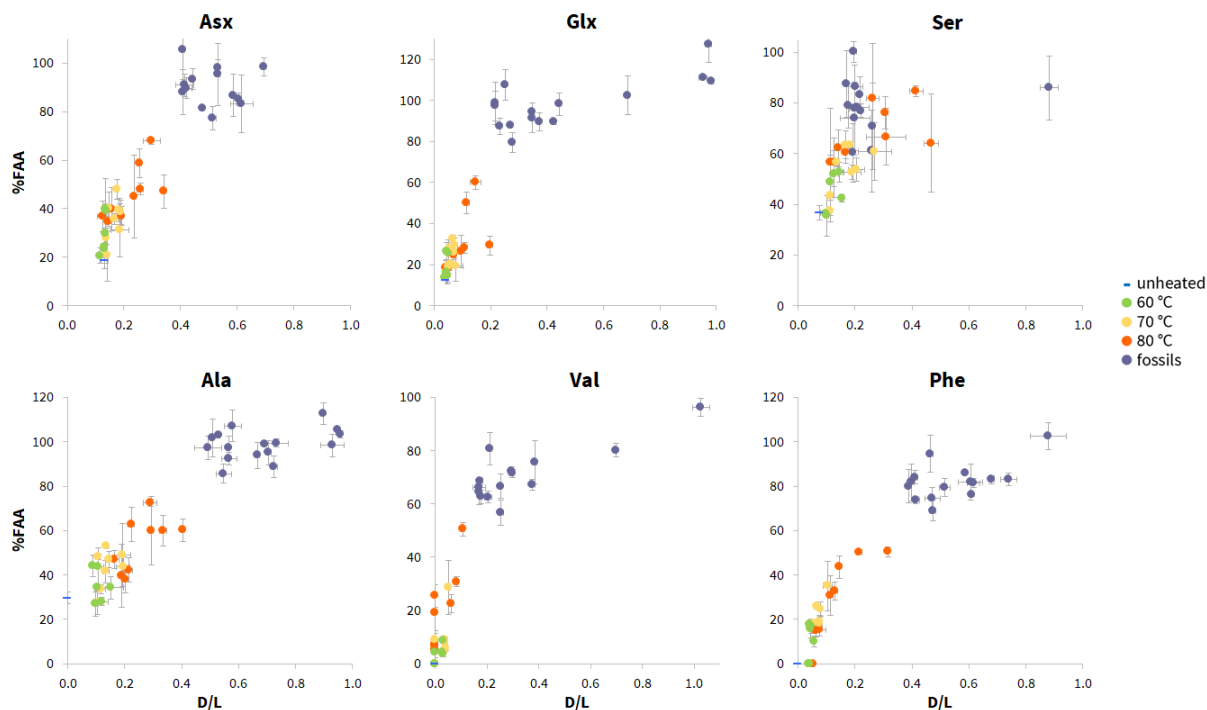
Figure 5.9. Comparison of peptide bond hydrolysis vs racemisation for Individual amino acids from experimental samples isothermally heated at 60, 70 and 80 °C over two years in comparison to fossils. Error bars represent the standard deviation about the mean for subsample experimental replicates.

5.3.1.1.5. Ser and Thr dehydration

Many decomposition reactions take place during protein diagenesis, but one type which can be relatively easily studied through IcPD analysis is the dehydration of serine and threonine, which results in the formation of alanine (Bada *et al.*, 1978). Over the two years of isothermal heating, a trend of decreasing [Ser]/[Ala] and [Thr]/[Ala] was observed at all temperatures (Fig. 5.10), indicating that products of the dehydration pathway of Ser and Thr were likely retained within a closed intra-crystalline system.
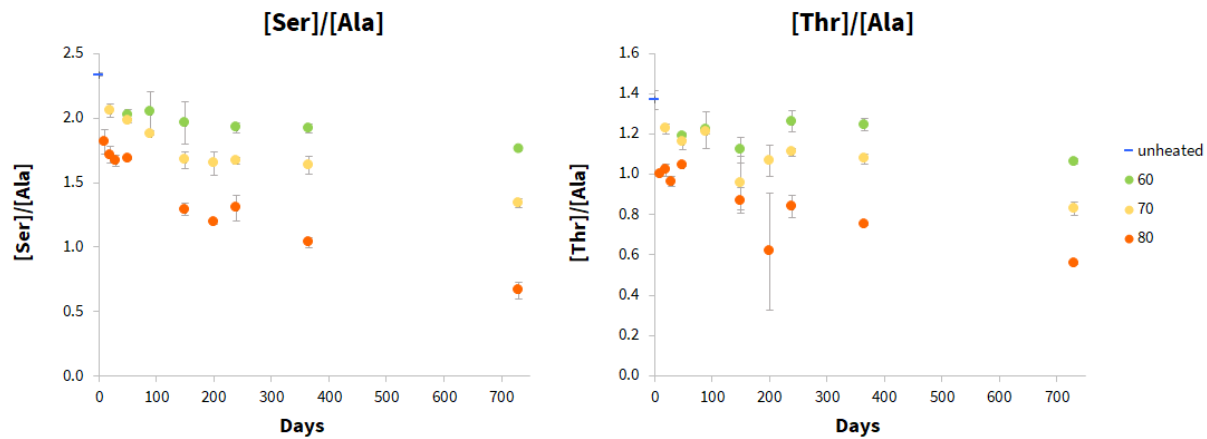
Figure 5.10. The extent of dehydration for Ser (left) and Thr (right) from woolly rhino tooth enamel, during isothermal heating at 60, 70 and 80 °C over two years. Error bars represent the standard deviation about the mean for subsample experimental triplicate.

Similar to the racemisation and hydrolysis data, when the heating experiments were compared to the fossils, there was little to no overlap (Fig. 5.11), confirming the need for longer experiments. However, the fossil data again appeared to extend the trends observed in the heating experiments.
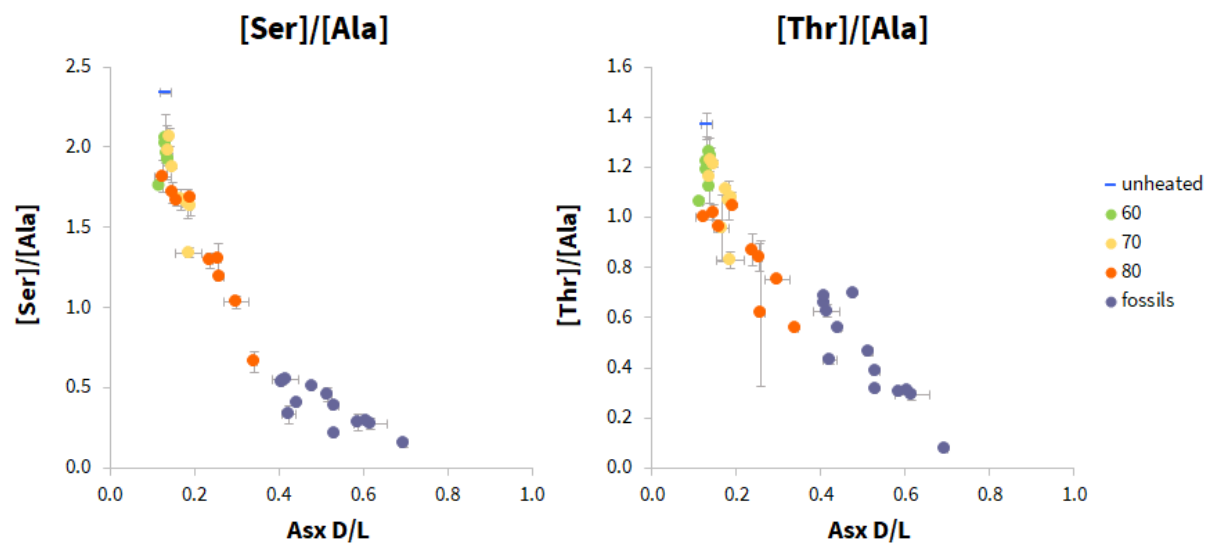
Figure 5.11. Comparison of extent of dehydration for Ser (left) and Thr (right) vs Asx racemisation from experimental samples isothermally heated at 60, 70 and 80 °C over two years in comparison to fossils. Error bars represent the standard deviation about the mean for subsample experimental replicates.

5.3.1.2. Kinetic modelling

5.3.1.2.1. Amino acid racemisation calculations

Amino acid geochronology is used primarily as a relative dating technique, which can be calibrated to numerical ages where independent evidence of age is present. In theory, where the rates of amino acid racemisation from proteins in fossil biominerals can be accurately described by mathematical models, it is possible to calculate numerical dates for fossil data. A variety of mathematical models exist which have been used to investigate the kinetics of racemisation, but their application has achieved mixed results (reviewed in Clarke and Murray-Wallace, 2006). In cases where reliable calibration and/or accelerated degradation experiments have been undertaken which accurately mimic diagenesis in fossils, numerical dates have been applied with success (e.g. Brooks *et al.*, 1990; Ortiz *et al.*, 2004; Kosnik *et al.*, 2008; Wehmiller *et al.*, 2012; Torres *et al.*, 2014). However, in some cases the diagenetic patterns from heating experiments have not been the same as those observed in fossils; in these cases calculations of kinetic parameters have yielded implausible results (e.g. Goodfriend and Meyer, 1991; Tomiak *et al.*, 2013). The results of heating experiments using higher experimental temperatures (80, 110 and 140 °C) on Elephantidae enamel indicated this might be the case for enamel IcPD (Dickinson *et al.*, 2019), hence why lower temperatures (60, 70 and 80 °C) were used in this study. To allow for ease of comparison to this previously reported enamel data, the same kinetic models (reversible first order kinetics (RFOK) and constrained power law kinetics (CPK)) were investigated.

Shown to describe free amino acids in solution (Bada and Schroeder, 1975), RFOK (equation 5.1), is the simplest model, with equal rate constants (k_1 and k_2) for the racemisation between the L and D enantiomers. When used to describe amino acid racemisation as part of protein degradation, apparent reversible first order kinetics (RFOK$_a$) and k effective (k_{eff}) are considered more appropriate terms. This is due to the additional degradation mechanisms which occur concurrently during diagenesis, influencing the observed rates of racemisation during IcPD analysis.

$$L - amino\,acid \underset{k_2}{\overset{k_1}{\rightleftharpoons}} D - amino\,acid$$
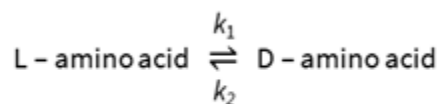
Equation 5.1. Amino acid racemisation reversible first order kinetics

To linearise the racemisation data produced from the heating experiments, D/L values are transformed by equation 5.2 for RFOK$_a$. For each model, the rates of racemisation are considered well described where the transformations achieve linearity.

$$Ln\left(\frac{1+D/L}{1-D/L}\right) + c = 2kt$$

Equation 5.2. Describes RFOK$_a$, where c is a constant to account for laboratory induced racemisation, k is the rate of racemisation ($k_1=k_2$) and t is time.

For the rhinocerotid data, the linearisation achieved with the RFOK$_a$ transformed values was variable between amino acids (e.g. Asx and Phe, Fig. 5.12; Table 5.2). Notably, none of the linearisation transformations performed on any of the amino acids were considered 'good' ($R^2 > 0.97$, as suggested by Crisp *et al.*, (2013)).

Table 5.2. R^2 values determined from plotting the transformed D/L values against time to test for RFOK$_a$ conformity.

Amino acid	60 °C		70 °C		80 °C	
	D/L range	R^2	D/L range	R^2	D/L range	R^2
Asx	0.13 – 0.14	0.3622	0.13 – 0.19	0.5977	0.13 – 0.34	0.8429
Glx	0.04 – 0.05	0.3531	0.04 – 0.07	0.6735	0.04 – 0.20	0.9557
Ala	0.00 – 0.15	0.0532	0.00 – 0.19	0.4229	0.00 – 0.41	0.5960
Phe	0.00 – 0.06	0.1471	0.00 – 0.10	0.6624	0.00 – 0.32	0.9499
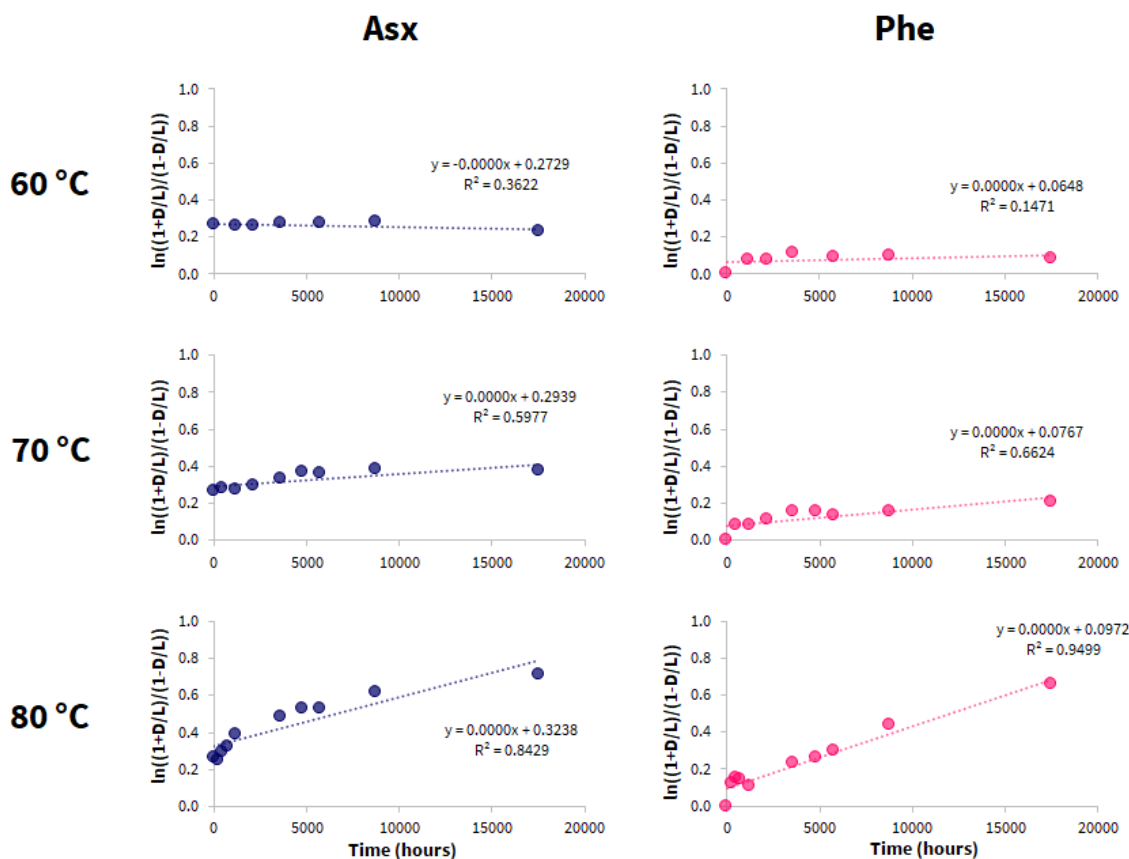
Figure 5.12. Assessment of fit for the linearised relationship between the time spent at three experimental temperatures: 60, 70 and 80 °C, and RFOK transformed (equation 5.2) THAA D/L values for Asx and Phe.

For Asx and Glx, it is likely that the poor fits result, at least in part, to the observed racemisation resulting from aspartic acid and asparagine, and glutamic acid and glutamine respectively (Goodfriend, 1991; Collins *et al.*, 1999). For Asx, the ability for Asn to racemise whilst bound within the peptide chain (Takahashi *et al.*, 2010; Demarchi *et al.*, 2013), may further confound this observed rate signal. For all amino acids, there was a general trend of increasing linearity (R^2) with increasing temperature (e.g. Asx and Phe, Fig. 5.12). This is likely due to the very low levels of racemisation observed over the duration of these low temperature experiments (section 5.3.1.1.1 - Fig. 5.1).

By nature of the simplicity of $RFOK_a$, which is defined for the racemisation of free amino acids only, this mathematical model has previously been shown not to accurately describe amino acid racemisation during the more complex pathways of protein diagenesis (e.g. Clarke and Murray-Wallace, 2006 and references therein). Models such as CPK (equation 5.3) offer transformations which include a power function (n) to improve the linearisation fit of the data.

$$Ln \left(\frac{1+D/L}{1-D/L} \right)^n + c = 2kt$$

Equation 5.3. Describes CPK, where *c* is a constant to account for laboratory induced racemisation, *k* is the rate of racemisation ($k_1=k_2$), *t* is time and *n* is a numerical value used to improve the linearisation between racemisation (D/L) and time.

For the amino acids assessed here, an improved linearisation was achieved using CPK at 70 and 80 °C (Fig. 5.13; Table 5.3). At 60 °C, the improvement of linearisation occurred when the power function 'n' tended towards 0. Therefore, the improved fit at 70 and 80 °C with n>1 resulted in decreased linearity at 60 °C. Similar to $RFOK_a$, at 60 and 70 °C, none of the linearisations would be considered 'good' ($R^2 > 0.97$), though at 80 °C good linearisation was achieved for some amino acids (e.g. Asx Fig. 5.13).

Table 5.3. R^2 values determined from plotting the transformed D/L values against time to test for CPK conformity.

Amino acid	n	60 °C		70 °C		80 °C	
		D/L range	R^2	D/L range	R^2	D/L range	R^2
Asx	5	0.13 – 0.14	0.2540	0.13 – 0.19	0.6242	0.13 – 0.34	0.9887
Glx	2	0.04 – 0.05	0.3177	0.04 – 0.07	0.7002	0.04 – 0.20	0.9984
Ala	2	0.00 – 0.15	0.0041	0.00 – 0.19	0.5053	0.00 – 0.41	0.7810
Phe	2	0.00 – 0.06	0.0945	0.00 – 0.10	0.8761	0.00 – 0.32	0.9671
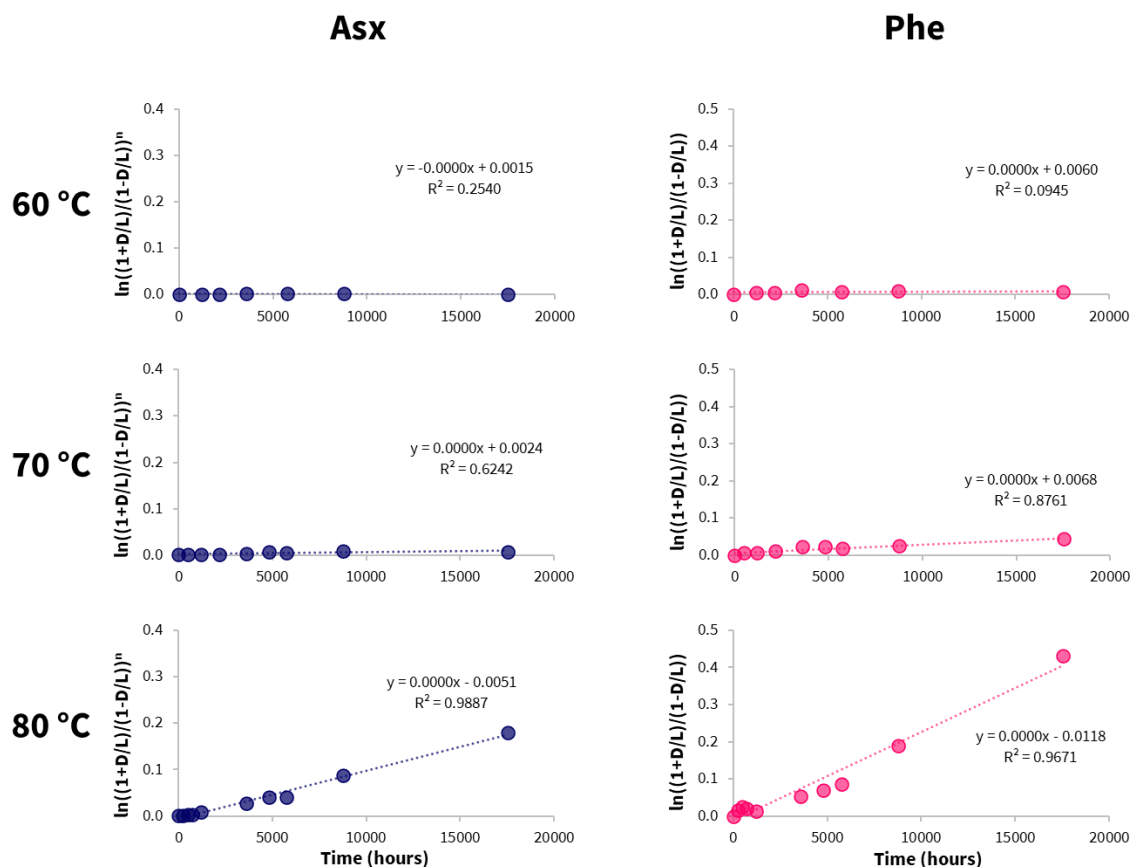
Figure 5.13. Assessment of fit for the linearised relationship between the time spent at three experimental temperatures: 60, 70 and 80 °C, and CPK transformed (equation 5.3) THAA D/L values for Asx (n = 5) and Phe (n = 2).

Overall, both $RFOK_a$ and CPK achieved relatively poor linearisation on transformation for the majority of data. Crisp *et al*., (2013) suggested that only transformed data with an $R^2 > 0.97$ was appropriate for use in subsequent racemisation activation energy calculations and those to predict fossil age or palaeoenvironmental temperature. However, to explore the potential utility of this approach, these data have still been undertaken below as an academic exercise, but subsequent calculations must be considered in light of the limitations around the extent of racemisation observed in this dataset and poor linearity achieved in data transformations.

Theoretically, it is possible to calculate the activation energy of racemisation using the Arrhenius equation (5.4) using data derived from heating experiments. The accuracy of the derived activation energies for each amino acid is dependent on a number of factors. These include using a minimum of three experimental temperatures and the assumption that the rate (k) has been accurately described by the transformed data at each experimental temperature. In addition, it requires the mechanisms for racemisation to be consistent between all experimental temperatures and fossils under environmental conditions.

$$k = Ae^{\frac{-E_a}{RT}}$$

Equation 5.4. Arrhenius equation, where k is the rate constant, A is the Arrhenius constant, E_a is the activation energy, R is the universal gas constant and T is temperature.

What is immediately noticeable from the calculated activation energies for racemisation is the difference between models for every amino acid (table 5.2). It is not uncommon to obtain differences in calculated values between models. For example, Dickinson *et al.*, (2019) reported calculated activation energies for Glx racemisation as 123 kJ mol^{-1} from RFOK$_a$ and 143 kJ mol^{-1} from CPK from elephantid enamel experiments. The value observed for Glx in rhinocerotid enamel at 152 kJ mol^{-1} using RFOK$_a$ is much more similar to previous enamel experiments than for CPK at 205 kJ mol^{-1} (table 5.2). In either case, higher activation energies would be expected from the slower rates of racemisation observed for Asx in Fig. 5.3, section 5.3.1.1.1, although the accuracy of these calculated values is highly questionable based upon the poor linearisation achieved with the rhinocerotid data. Relatedly, the linearisation of the transformed elephantid data was much higher: $R^2 > 0.97$ in most cases (Dickinson *et al.*, 2019), and likely results from the higher overall extents of racemisation achieved with the higher experimental temperatures used in the study (80, 110 and 140 °C). The large differences in calculated activation energy for racemisation in rhinocerotid enamel between models observed here for all amino acids (table 5.4), does, however, indicate that the mathematical transformations are unlikely to be appropriate for data with poor linearisations, as Crisp *et al.,* (2013) previously suggested. Given the low levels of breakdown observed over these experiments, much longer isothermal heating at these lower temperatures would be required to more reliably investigate kinetic modelling.

Table 5.4. Activation energies calculated from the Arrhenius equation (5.4) using the transformed racemisation data from three experimental temperatures (60, 70 and 80 °C).

Amino acid	Kinetic model	Model fit (R^2)	Calculated E_a (kJ mol-1)
Asx	RFOK$_a$	1.0000	137.7
	CPK	0.9946	287.4
Glx	RFOK$_a$	0.9980	151.6
	CPK	0.9947	204.5
Ala	RFOK$_a$	0.9884	108.3
	CPK	0.9765	233.3
Phe	RFOK$_a$	0.9999	130.5
	CPK	0.9999	232.7

To further assess the differences observed between the two mathematical models, numerical ages were calculated for two fossils; the least degraded Rhinocerotidae tooth from Twin Rivers

archaeological site in Zambia and the Dmanisi Rhinocerotidae tooth published in Cappellini *et al.*, (2019). These teeth were chosen as the least degraded Rhinocerotidae fossil samples; however, it should be noted that the extent of racemisation observed in these fossils was above the level induced in the heating experiments and the subsequent calculations are therefore extrapolations and not interpolations.

The 'kinetic ages' of these two fossils were calculated using the current mean annual temperature of Zambia (MAT, 20.4 °C) for the Twin Rivers fossil and estimated MAT of Dmanisi from palaeoclimate reconstructions (13.1 °C, Blain *et al.*, 2014). Whilst these MATs are unlikely to be the average regional temperatures over the changing climate of the Quaternary (and beyond), they provide an acceptable proxy for the calculations.

If a model were to describe the rate of each amino acid accurately, it would be expected that the calculated 'kinetic ages' between the amino acids would be consistent with each other. This was not the case for either model (table 5.5), with highly variable ages from different amino acids within both fossils, suggesting that neither model was able to accurately describe the rates of racemisation for all amino acids based on the heating experiments undertaken in this study. Similar to the activation energy calculations, large differences in 'kinetic ages' were calculated between the two models for all amino acids in the fossils (table 5.5).

The fossil from Twin Rivers archaeological site in Zambia was excavated from A block and whilst not directly related to the fossils, U-series dating of speleothem flowstones placed the sequence to 172 - > 400 ka (Barham, 2000). The Dmanisi Rhinocerotidae fossil was dated to approximately 1.77 Ma using $^{40}Ar/^{39}Ar$ in combination with palaeomagnetism and biozonation (Gabunia *et al.*, 2000; Ferring *et al.*, 2011). The dates obtained from the CPK calculations were therefore implausible in all cases, based on the known dating of the sites and in many cases the dates which significantly predate the evolutionary divergence of Rhinocerotidae at around 55 Ma (Bai *et al.*, 2020). The 'kinetic ages' obtained from the RFOK$_a$ model were much closer to plausible, with the Glx value for the Twin Rivers fossil falling within with the previous U-series dates, although the Dmanisi tooth was calculated to be 620 ka younger than the known site dates.

Table 5.5. 'Kinetic age' calculations using two rhinocerotid fossils. Note that the 'kinetic age' outputs from the mathematical models should not be interpreted as accurate values for these sites.

Fossil	Asx			Glx			Ala			Phe		
	D/L	ROFK$_a$ 'Age'	CPK 'Age'	D/L	ROFK$_a$ 'Age'	CPK 'Age'	D/L	ROFK$_a$ 'Age'	CPK 'Age'	D/L	ROFK$_a$ 'Age'	CPK 'Age'
TWE16.5	0.41	101 ka	3.7 Ga	0.21	186 ka	8.3 Ma	0.49	12 ka	27.2 Ma	0.40	48 ka	38.1 Ma
Dmanisi	0.38	392 ka	173 Ga	0.26	1.15 Ma	171 Ma	0.58	47 ka	814 Ma	0.38	176 ka	861 Ma

These calculated 'kinetic ages' highlight the need for forced degradation experiments at lower temperatures, such as those undertaken here (60, 70 and 80 °C), to be planned for considerable longer-term. Extrapolating from the extents of racemisation observed (Fig. 5.1), it is likely that at a minimum, four years of isothermal heating at 80 °C, six years at 70 °C and ten years at 60 °C, would be required to cover a greater extent of racemisation. In this way, comparison between heating experiments and fossil degradation could be undertaken more thoroughly, and potentially allow more concrete conclusions on the similarity of degradation mechanisms to enable a better assessment of the appropriateness of kinetic modelling.

5.3.2. Mass spectrometry analysis

Multiple pathways of protein degradation can also be investigated from MS analysis of the enamel proteome. Palaeoproteomics studies proteins qualitatively via their peptides, allowing multiple proteins (including contamination) to be identified within each sample. Palaeoproteomics therefore allows a complementary set of degradation information to be studied individually within enamel. Alongside chiral amino acid analysis, peptide chain hydrolysis can be inferred from MS analysis through assessment of peptide chain length (e.g. Cappellini *et al.*, 2019; Madupe *et al.*, 2023). Additional degradation mechanisms can also be studied through MS, such as asparagine and glutamine deamidation (e.g. Simpson *et al.*, 2016; Chowdhury and Buckley, 2022), and oxidation of methionine, histidine and tryptophan (e.g. Mackie *et al.*, 2018). Protein regions where peptides are preserved and routinely detected are also studied (Demarchi *et al.*, 2016), with the potential for corroboration with other diagenetic markers.

5.3.2.1. Building Woolly Rhino Enamel Protein Sequences

Pleistocene woolly rhino (*Coelodonta antiquitatis*) teeth were purchased from North Sea Fossils, as the closest ethically available proxy for Pleistocene African material. Unfortunately, to date, the enamel proteome has only been well studied and characterised in a handful of taxa (e.g. Termine *et al.*, 1980; Nagano *et al.*, 2009; Nielsen-Marsh *et al.*, 2009). Only ten reviewed (SwissProt) amelogenin sequences are available on UniProt to date (UniProt, 2024), with the majority of extant species missing protein sequences. Obtaining an accurate enamel proteome for extinct species is often entirely unrealistic. Thankfully, a recent study by Cappellini *et al.,* (2019) investigated the phylogeny of the *Stephanorhinus* genus by proteomic analysis of the dental enamel, and incorporated enamel protein sequences extracted from high-coverage genomic data for all extant rhinos and two extinct rhinos (*Coelodonta antiquitatis* and *Stephanorhinus kirchbergensis*). In many cases, however, including for the woolly rhino, only partial enamel protein sequences were generated/are available.

Prior to commencing the forced degradation experiments, bleached, unheated enamel was first analysed by MS (as detailed in section 5.2.5) and searched against the database included in the Cappellini *et al.*, (2019) supplementary information, appended with common laboratory contaminants. Using a cautious 0.5% false discovery rate (FDR) filter (Burger, 2018), the protein identified with the highest coverage was white rhino AMELX at 57% from a total of 243 matched peptides (Fig. 5.14A). Only 80 peptides matched to the woolly rhino AMELX sequence, giving rise to a 34% coverage (Fig. 5.14B). This large difference in peptide number and coverage is largely due to the incomplete woolly rhino AMELX sequence ('X's highlighted in red in Fig. 5.14C), limiting the ability to match peptides through database searching.
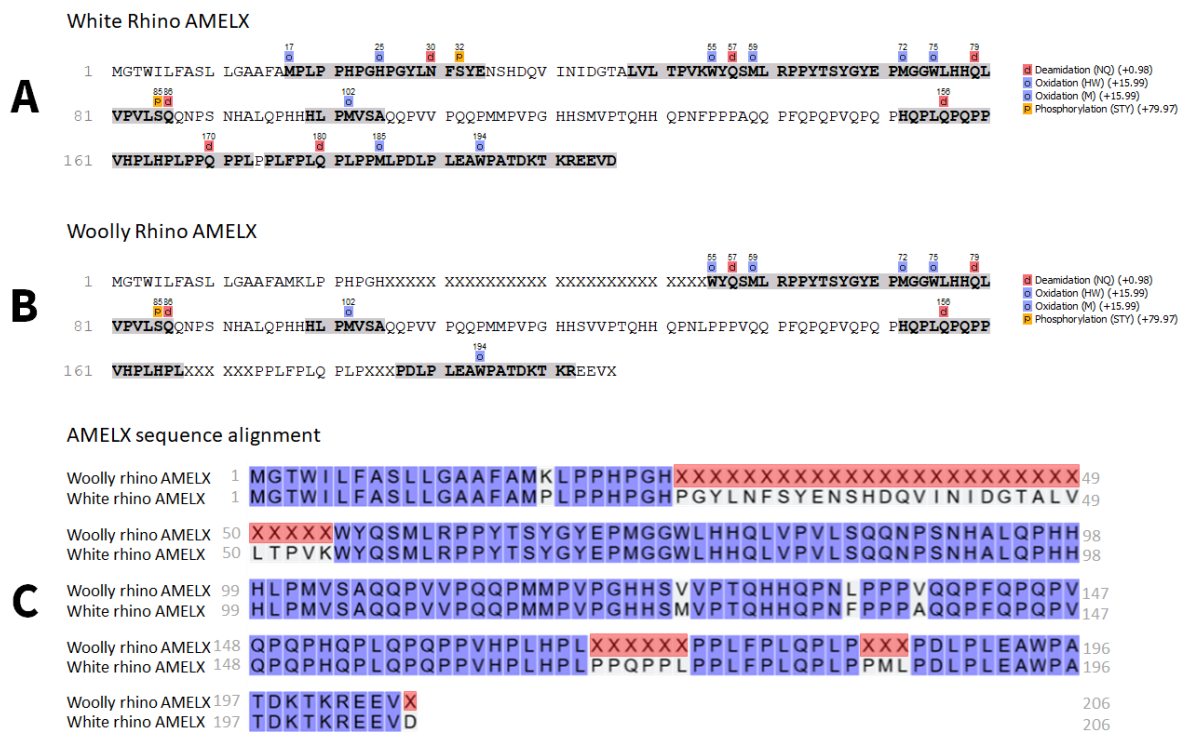
Figure 5.14. Comparison of the white rhino (A) and woolly rhino (B) AMELX protein sequence coverage from peptides identified through database searching (denoted by bold amino acids highlighted in dark grey) from the MS analysis of bleached, unheated woolly rhino tooth enamel. The AMELX sequence alignment (C) from the fasta database (used for searching the data against) shows shared sequences in purple and unknown sections in red.

Improvement of the woolly rhino AMELX sequence was therefore undertaken through a process of scrutinising the data over several iterations. This was undertaken at 0.5% FDR and peptides were only included where high levels of b and y ion identifications were observed (section 1.3.4.1.2). For example, multiple peptides with high levels of b and y ions were observed for the amino acids at positions 168 - 173, 184 - 186 and 206 (examples shown in Fig. 5.15), allowing these unknown regions of the sequence to be filled in.
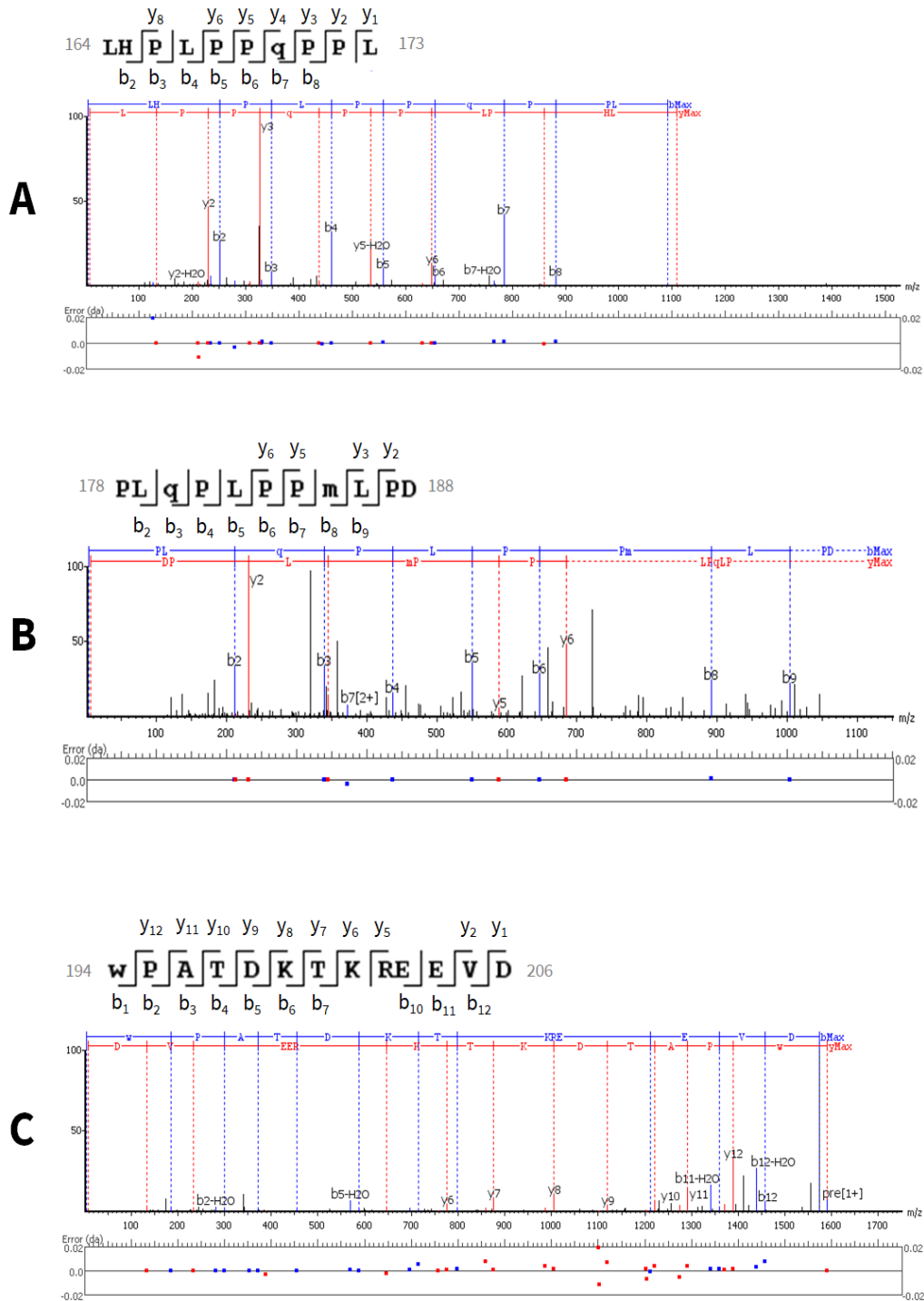
Figure 5.15. Mass spectra for white rhino AMELX peptides observed in unknown regions of the woolly rhino AMELX sequence. These example peptides covered the unknown sequence positions 168-173 (A), 184-186 (B) and 206 (D).

Re-searching the data against a database containing an updated version of the woolly rhino AMELX sequence resulted in an increased coverage from 34% (from 80 peptide matches), to 56% (with

220 peptide matches). Interestingly, this was still below the sequence coverage and peptide number for white rhino AMELX at 57% from 241 peptides. When studying the regions of coverage, it was apparent that the additional coverage in the white rhino sequence resulted from a one amino acid difference at position 18: lysine (K) in woolly rhino and proline (P) in white rhino (Fig. 5.16A). This single amino acid difference was not observed in either of the additional Rhinocerotidae with known sequences of amino acids in this region (Sumatran and Merck's rhino, Fig. 5.16B).
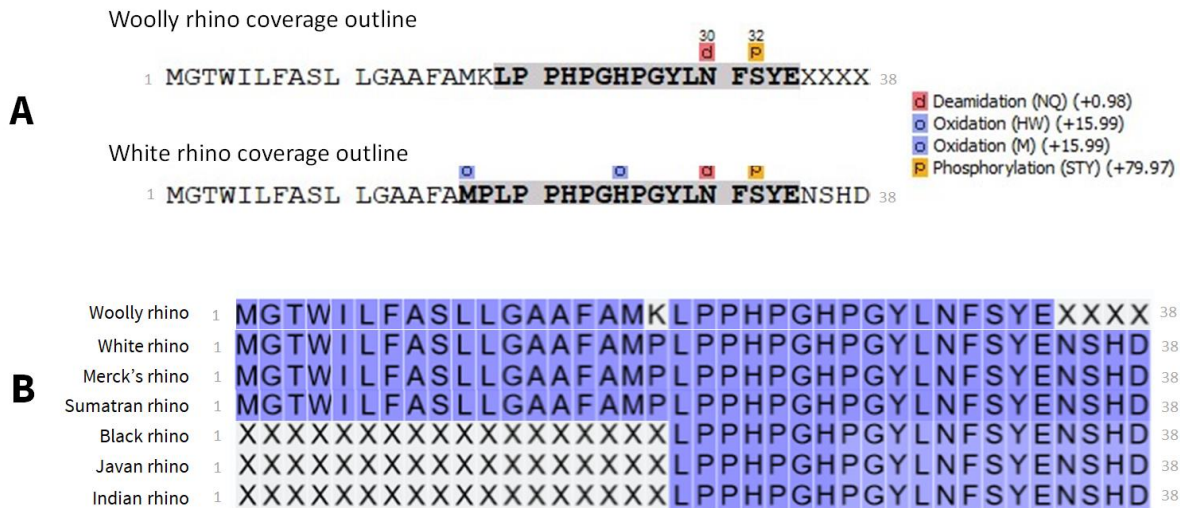
Figure 5.16. A - Comparison of the sequence coverage for white and woolly rhino AMELX from peptides identified in this study through database searching (denoted by the bold amino acids highlighted in dark grey), over positions 1 - 38. B – The fasta database sequences of different rhinocerotids AMELX, aligned from positions 1 – 38 showing shared sequences highlighted in purple.

28 peptides were observed covering the region of the single amino acid difference in white rhino AMELX at 0.5% FDR, and the peptide identifications were convincing on visual assessment of the MS2 spectra (e.g. Fig. 5.17). With the exception of white rhino, all Rhinocerotidae enamel protein sequences in the database were extracted from high-coverage genomic data. These translations are complex, and it is not uncommon for amino acid sequence errors to arise (e.g. Yates *et al.*, 1995; Kumar *et al.*, 2016). Given no peptides were observed containing a lysine (K) at position 18, and 28 peptides were identified containing a proline (P) at this position (e.g. Fig 5.17), it seems likely that woolly rhino AMELX does not contain a species-specific amino acid difference at the position and does contain a proline at position 18.

222
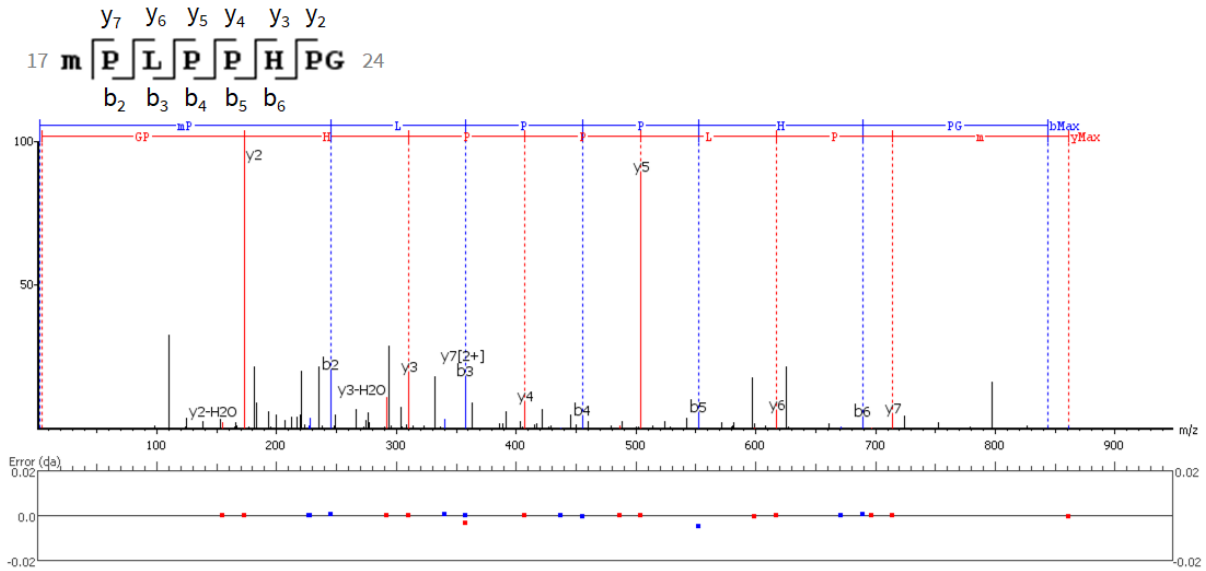
Figure 5.17. A MS2 spectra of one of the 28 peptides identified in the region of the one amino acid difference (position 18) of the white rhino AMELX sequence.

The use of a 0.5% FDR for this task was chosen to increase the stringency of the assessment of unknown sections of the protein sequence in woolly rhino AMELX. As many proteomic studies use a default of 1% FDR for data analysis (Burger, 2018), this filter was also applied to study the impact on the data. When filtering to 1% FDR, the woolly rhino AMELX sequence (containing the single amino acid difference at position 18) increased modestly to 60% coverage from 234 peptides, whilst the white rhino AMELX coverage increased by 10% to 67% from 256 peptides (Fig. 5.18).
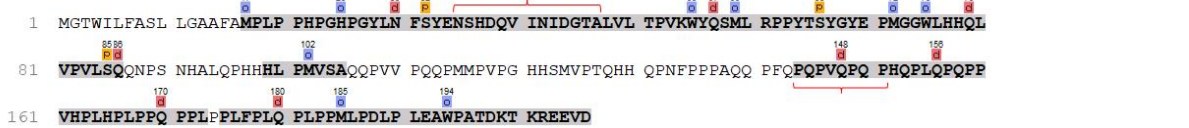
Figure 5.18. Comparison of white rhino AMELX coverage when filtering the data with different false discovery rates (0.5% and 1%). Sections of the sequence bracketed in red display the differences in confident peptide identifications at 0.5% and 1% FDR.

The increased sequence coverage at 1 % FDR at positions 35 – 47 in white rhino AMELX (Fig. 5.18) was provided only by one peptide which contained no b or y ion coverage in the MS2 (Fig. 5.19).

Confident coverage in this region of the sequence therefore could not be met and so was left unknown in woolly rhino AMELX (Fig. 5.14).
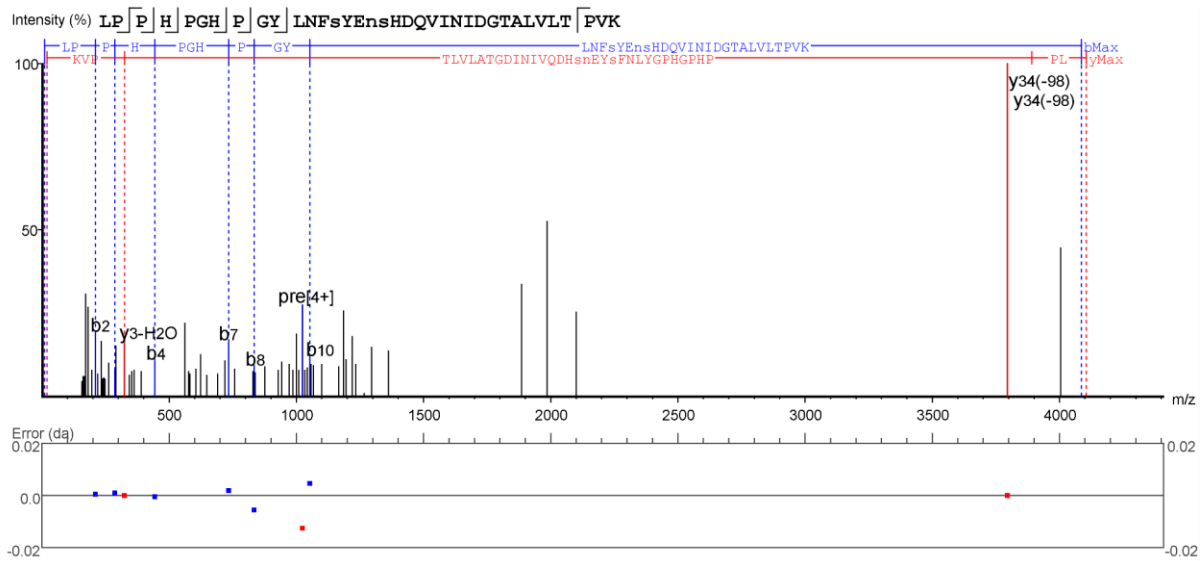
Figure 5.19. Mass spectrum for the single peptide observed at 1% FDR covering previously AA's 11-54.

5.3.2.2. Replicate repeatability

To assess instrument variability and sample storage stability, a second preparation of bleached, unheated woolly rhino enamel was prepared and injected in singlicate. The sample was stored in the freezer and during the next batch of analysis the same sample was analysed in triplicate. A lower coverage (44%) and peptide number (94) was observed for the first analysis of the second preparation of the woolly rhino enamel in comparison to the analysis undertaken for the initial assessment and protein sequence building (section 5.3.2.1), where 57% coverage was observed from 243 peptides at 0.5% FDR. Whilst it is possible that small differences in sample size and instrument performance may have contributed, this difference is likely to be largely as a result of the sample having been more dilute (~ 1.5 x more so) to allow for analytical replicate assessment. Post freezer storage, a decrease in both protein coverage and number of peptides was observed (Fig. 5.20). This was most dramatic for the number of peptides, where less than half of the original number was observed. One of the three analytical replicates had especially low coverage and peptide number ('2_1' Fig. 5.20), and it seems likely this outlier arose from an instrument mis-injection.

%Coverage Repeatability

Peptides Repeatability
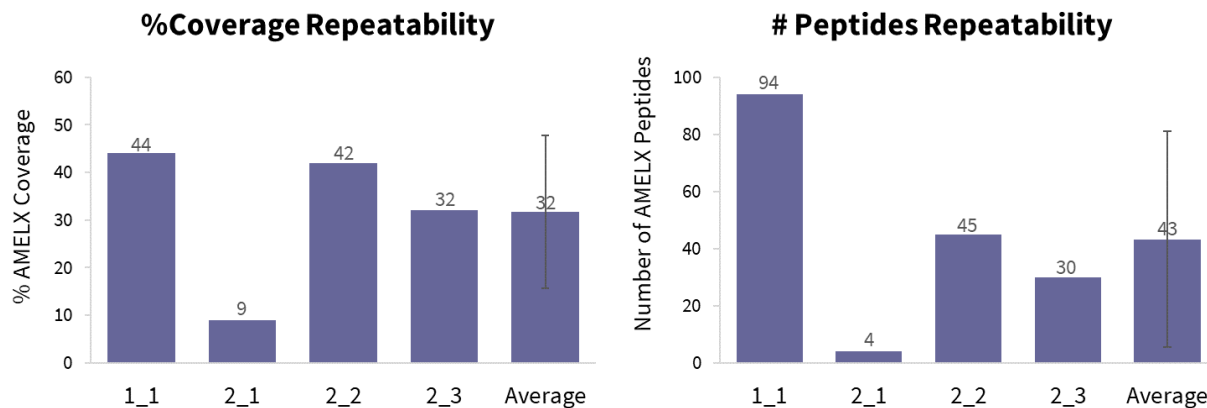
Figure 5.20. Assessment of instrument variability and sample storage stability of two instrument acquisitions of a single sample, in analytical singlicate for the first analysis (1_1) and analytical triplicate for the second analysis (2_1, 2_2 and 2_3), which was undertaken after sample freezer storage. Graphs display the number of identified AMELX peptides in each sample at 0.5% FDR (right) and the percentage of the AMELX sequence they cover (left). The average is calculated as the mean of all four analytical replicates, and the error bar represents one standard deviation about this mean.

The sample preparation for this analysis was carried out in standard 1.5 mL plastic microcentrifuge tubes (eppendorf) and it is probable that a large proportion of the decrease in peptide number post-freezer storage resulted from binding loss to the plastic (Kraut *et al.*, 2009). For future analysis of the enamel proteome, it is therefore recommended to undertake sample preparation with specialised consumables (e.g. eppendorf lo-bind microcentrifuge tubes (Grzeskowiak *et al.*, 2016)) and to undertake analysis as soon after sample preparation as is practically possible. Consideration of starting sample amounts, in addition to final rehydration volumes, is also recommended to improve the likelihood of observable peptides. This is especially important where samples in higher states of degradation are to be analysed.

As only one experimental and analytical replicate was undertaken for each sample, the results of the heating experiments below are considered in light of the high instrument variability observed.

5.3.2.3. Elevated temperature experiments

Similar to the IcPD work, material was designated for MS analysis during the heating experiments to investigate protein degradation mechanisms observable at the peptide level, for comparison to fossil samples. Due to sample and cost limitations, only one experimental replicate was prepared in the laboratory for each heating temperature and time point. Additionally, only one analytical replicate per sample was analysed by LC-MS/MS.

5.3.2.2.1. AMELX Coverage

The coverage and number of associated peptides in AMELX displayed similar trends after isothermal heating at 60, 70 and 80 °C over 730 days (Fig. 5.21). In both cases, a decrease in coverage and total peptide number was observed on initial heating at all temperatures, whilst at longer durations of isothermal heating, a possible temperature trend was observed, with more peptides and a higher % coverage observed at 60°C than at 70°C, and even fewer at 80°C (Fig. 5.21). However, due to the nature of this experimental design (single experimental and analytical replicate), it is challenging to draw conclusions from the observed data given the high levels of analytical variability observed. It may also be the case, that as for much of the IcPD data (section 5.3.1.1), the experimental conditions undertaken here were not sufficient to induce clear markers of degradation observable by MS analysis.
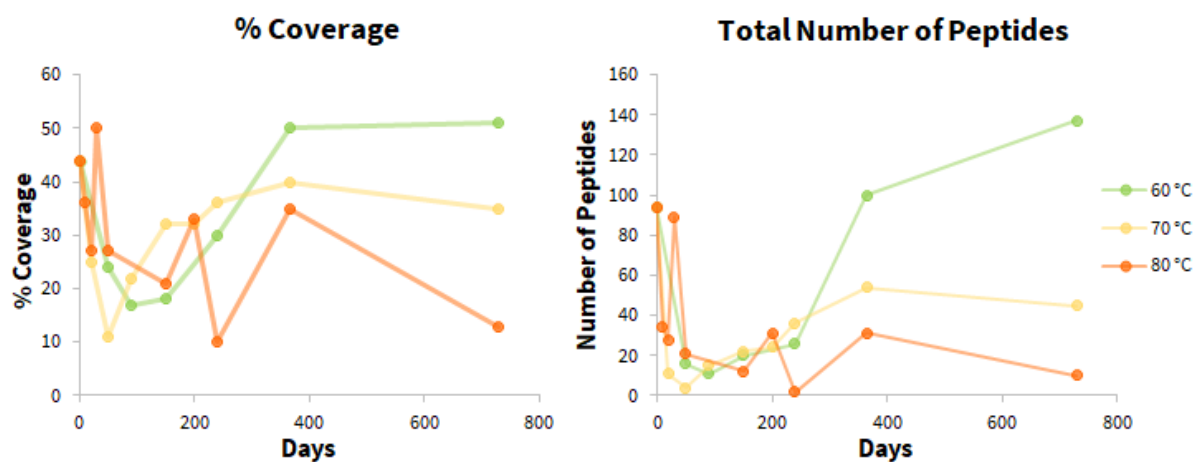
Figure 5.21. The percent coverage (left) and total number of peptides (right) observed for AMELX from woolly rhino enamel during isothermal heating to 60, 70 and 80 °C over two years.

5.3.2.2.2. Diagenetoforms

Post-translational modifications (PTMs) are amino acid modifications which occur *in vivo*, altering the protein properties for numerous biological reasons (Walsh *et al.*, 2005). Diagenetoforms is the term given to 'PTMs' which occur post *vivo*; those amino acid alterations are associated with diagenesis (Cleland *et al.*, 2021), but are also termed 'PTMs' in the software database search terminology. All data searches undertaken here included three 'PTMs'. Phosphorylation at serine, threonine and/or tyrosine (STY) was included as a 'true' PTM which occurs *in vivo* and has also been observed in ancient enamel proteins previously (e.g. Welker *et al.*, 2019; 2020). Oxidation of methionine, histidine and tryptophan (MHW), and deamidation of asparagine and glutamine (NQ) were included as common diagenetoforms to investigate whether any trends could be observed due to forced degradation.

Deamidation has been relatively well studied by the palaeoproteomic community, including attempts to utilise the extent of deamidation for dating (e.g. Robinson and Robinson, 2004; Van Doorn *et al*., 2012; Ramsøe *et al*., 2020). Although a relationship between age and extent of deamidation exists, due to high variability, it is not considered a reliable indicator of extent of protein diagenesis in isolation (Simpson, 2015). Here, the overall extent of deamidation (Fig. 5.22A) displayed a very similar trend to the total number of peptides observed (Fig. 5.21). However, total deamidation counts might be expected to be higher where a larger number of peptides and higher sequence coverage was observed. Therefore, the amount of deamidation per peptide and per AMELX sequence coverage were plotted (Fig. 5.22B and C). Here, a decrease in the amount of deamidation was still observed on initial heating, but was followed by a steady increase in deamidation for all experimental temperatures (Fig. 5.22B and C). Once again it is difficult to assess whether this is a true trend reflective of degradation, or a result of analytical variability. To assess this, experimental replicates and longer isothermal heating times would be recommended for future studies to more reliably investigate any potential trends.
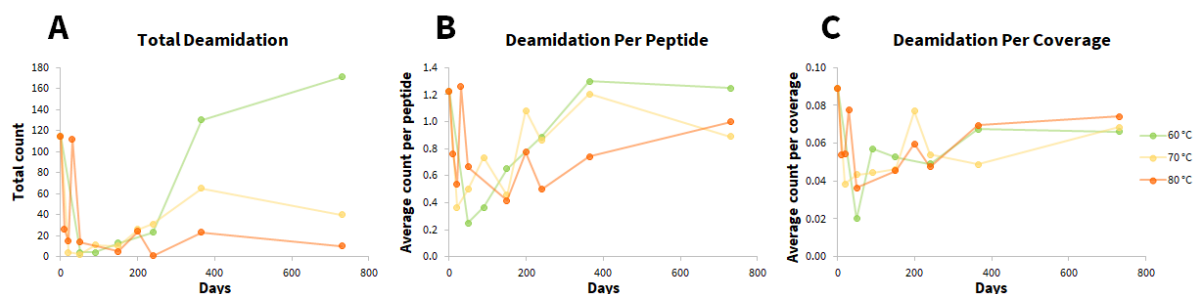
Figure 5.22. Assessment of AMELX deamidation of asparagine and glutamine during isothermal heating of woolly rhino enamel at 60, 70 and 80 °C over two years. A – the total number of deamidated Asn or Gln identifications in AMELX peptides from database searching at 0.5% FDR, B – the total number of deamidated Asn or Gln identifications divided by the total number of AMELX peptides observed for each sample from database searching at 0.5% FDR, C – the total number of deamidated Asn or Gln identifications divided by the percentage of AMELX sequence coverage observed for each sample from database searching at 0.5% FDR.

Very similar data was also observed for oxidation on histidine, tryptophan and methionine over the course of isothermal heating (Fig. 5.23).
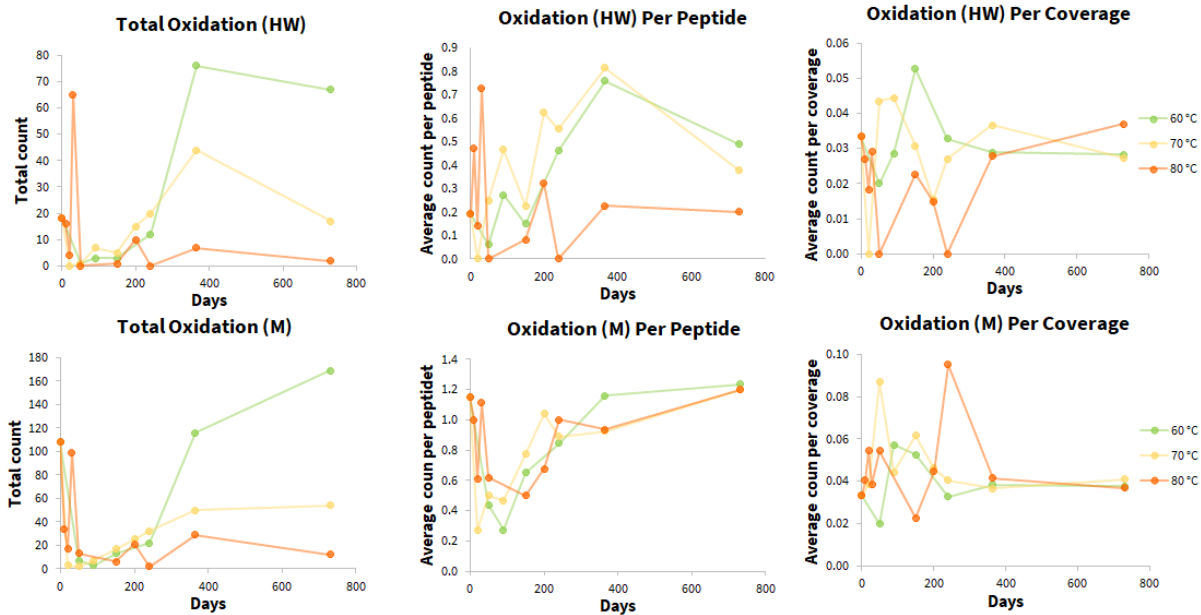
Figure 5.23. Assessment of AMELX oxidation of histidine, tryptophan (HW) and methionine (M) during isothermal heating of woolly rhino enamel to 60, 70 and 80 °C over two years. Total oxidation is the total number of oxidations at His and Trp (top) or Met (bottom) in AMELX peptides from database searching at 0.5% FDR. Oxidation per peptide is the total number of oxidation sites identified for His and Trp (top) or Met (bottom) in AMELX peptides divided by the total number of AMELX peptides observed for each sample from database searching at 0.5% FDR. Oxidation per coverage is the total number of oxidation sites identified for His and Trp (top) or Met (bottom) in AMELX peptides divided by the percentage of AMELX sequence coverage observed for each sample from database searching at 0.5% FDR.

5.3.2.2.3. Peptide Length

Peptide chain hydrolysis is one mechanism of protein degradation which in IcPD data can be assessed by looking at the percentage of free amino acids (section 5.3.1.1.4). With palaeoproteomics, it is also possible to investigate hydrolysis from studying the lengths of peptide chains over time. When the raw number of peptide lengths observed at each heating temperature and time were plotted, at 60 and 70 °C an increase in the majority of peptide lengths was observed over time (Fig. 5.24), reflective of the overall increasing number of peptides observed during heating (Fig. 5.21). Trends were difficult to assess at 80 °C where no clear patterns in peptide length over time was observed (Fig. 5.24).

228
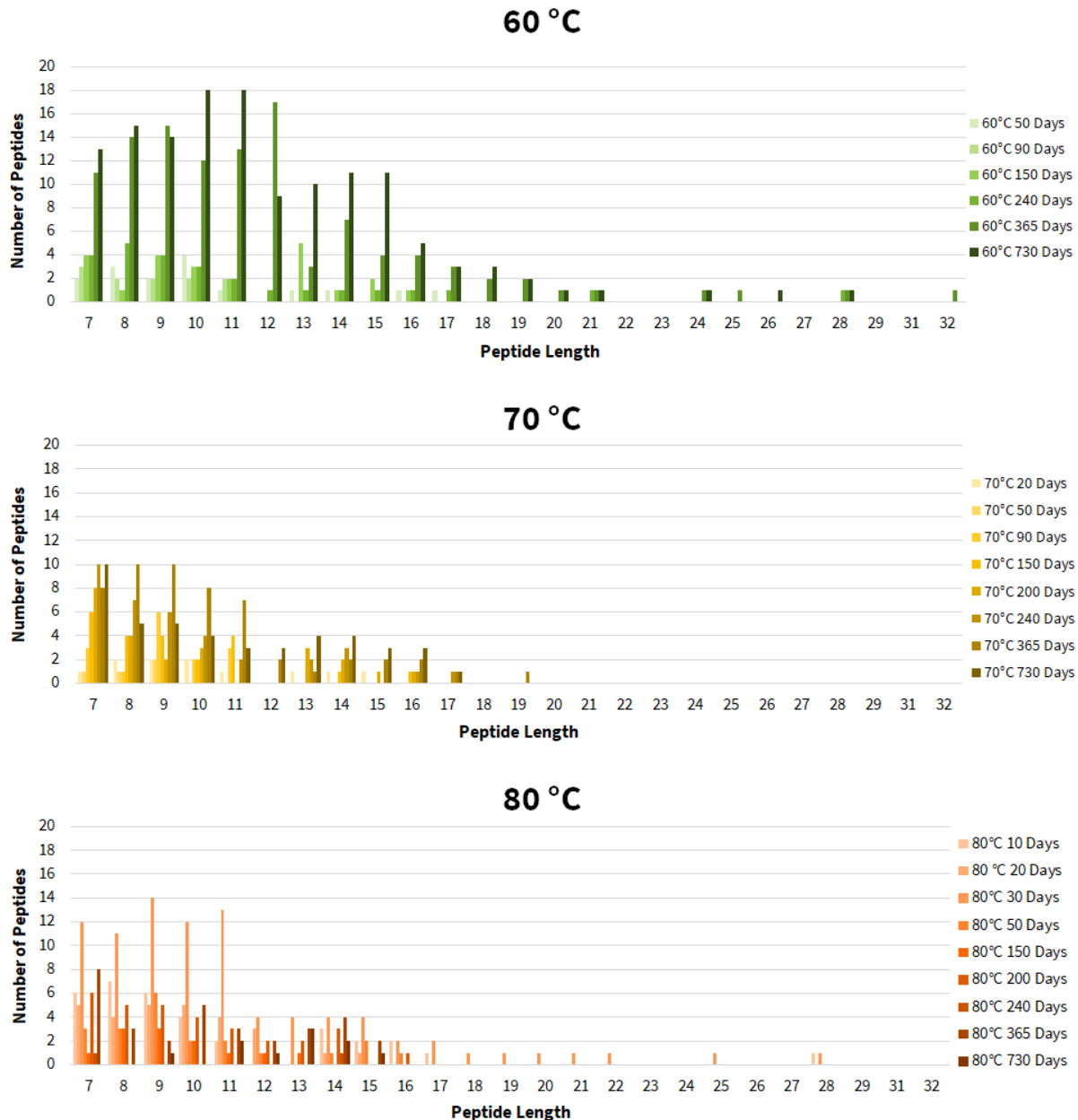
Figure 5.24. Number of peptides observed at different peptide lengths (number of amino acids) over the course of isothermal heating of woolly rhino enamel to 60, 70 and 80 °C over two years.

As the overall total number of peptides also increased with isothermal heating at 60 °C after 1 year (Fig. 5.2.1), and trends in overall peptide number were hard to ascertain more generally (section 5.3.2.2.1), the percentage of peptides by length out of the total observed peptides was plotted to investigate whether any proportional trends were observable (Fig. 5.25). Similarly to the analysis of diagenetoforms, it was difficult to infer any trends in peptide chain hydrolysis, as no clear patterns were visible in the proportion of peptides at differing lengths during isothermal heating at any experimental temperature over time (Fig. 5.25).
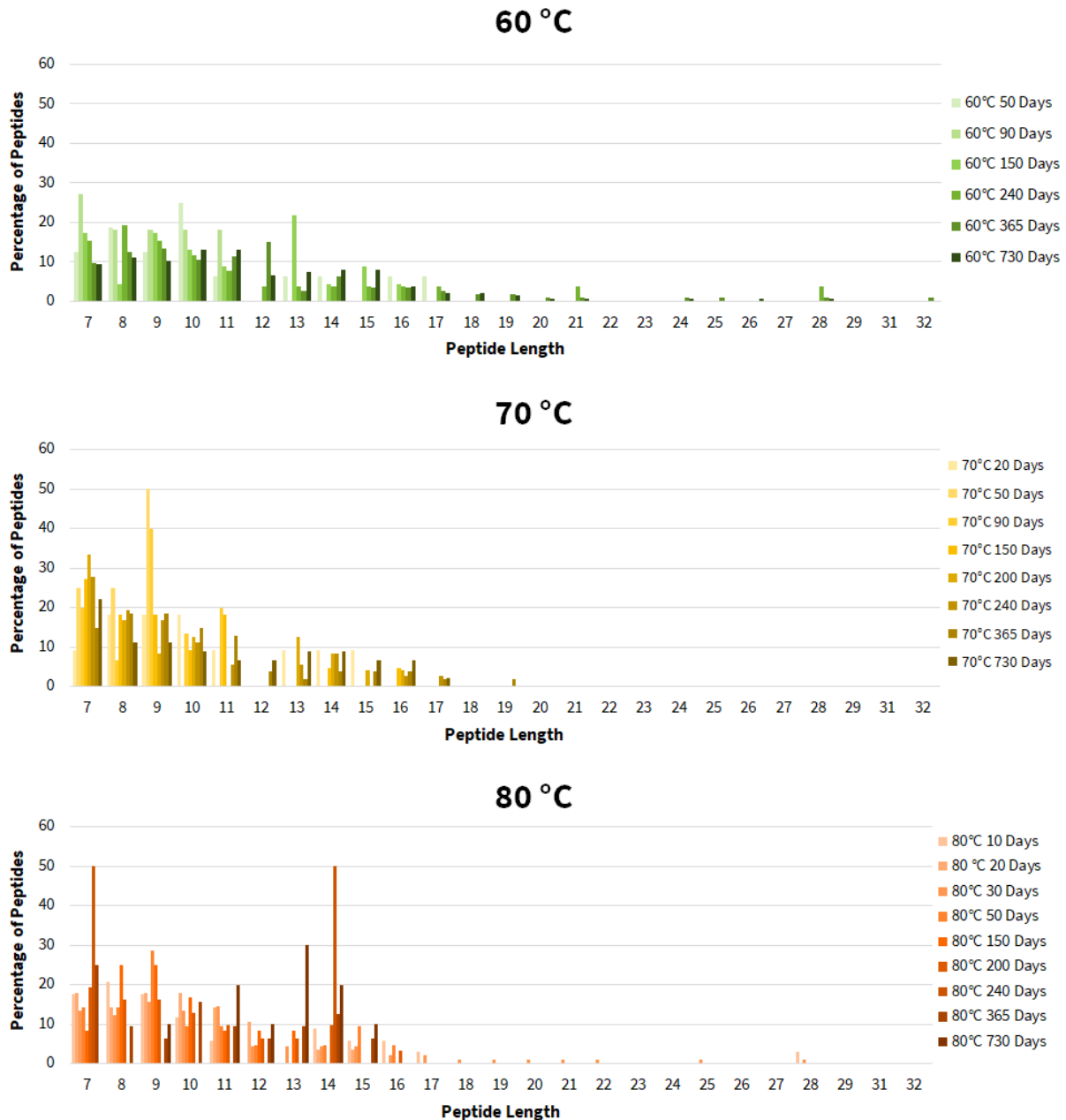
Figure 5.25. The percentage of different peptide lengths (number of amino acids) observed over the course of isothermal heating of woolly rhino enamel to 60, 70 and 80 °C over two years.

In general, observable peptides during LC-MS/MS analysis are typically between ~ 7 - 30 amino acids long, although as is the case here, it can be possible to see longer peptides (Figs. 5.24 and 5.25). The enzyme free approach was undertaken in this study, as proteins within enamel are known to be partially broken down during the maturation process of enamel (Lacruz *et al.*, 2017). They are therefore generally already at appropriate peptide lengths for analysis, and previous studies have used this approach to yield high quality data (e.g. Cappellini *et al.*, 2019; Welker *et al.*, 2020; Madupe *et*

al., 2023). It is, however, possible that an increase of medium length and longer peptides over time could be as a result of peptide chain hydrolysis from peptides that were originally too long to be visible by mass spectrometry. It is also likely that the temperatures and experimental duration undertaken here are insufficient to infer trends in peptide chain hydrolysis from increasing numbers of shorter peptide lengths. As with the investigation of protein coverage (section 5.3.2.2.2) and diagenetoforms (section 5.3.2.2.3), it is recommended that any future studies wishing to undertake forced degradation experiments through isothermal heating, use significantly longer experimental timepoints and with a minimum of three experimental replicates.

5.3.3. IcPD - MS relationship

As few unequivocal degradation trends were observable from the MS analysis undertaken in this study (section 5.3.2), it is not possible to draw many conclusions when comparing against the complementary IcPD analysis. Some relationships, such as amino acid concentration or extent of racemisation, could be compared to aspects of the MS analysis results such as protein coverage. In general, no clear trend was observable between these parameters (Fig. 5.26), but it can be concluded that AMEL peptides were consistently observed in MS analysis where the total THAA concentration was above 1500 pmol/mg, as well as where Asx D/L was below 0.35 (Fig. 5.26).
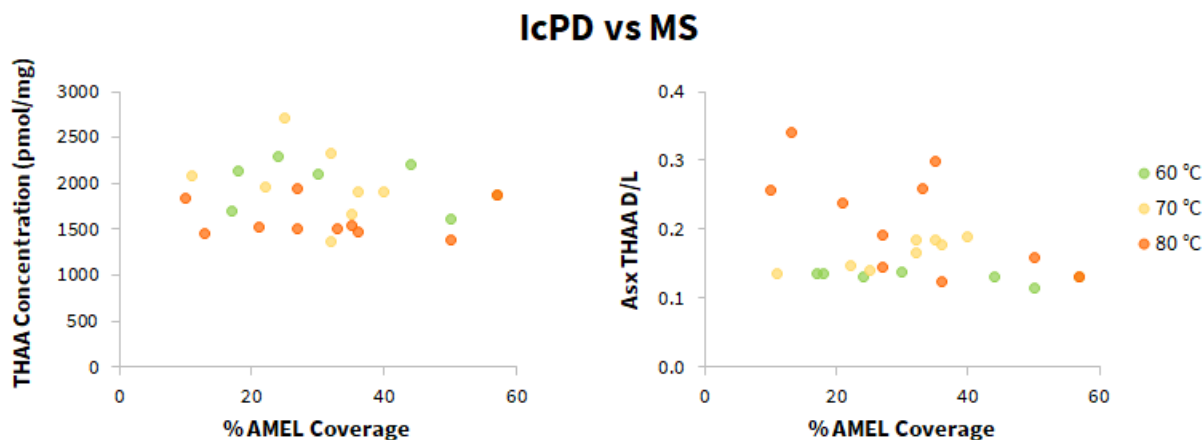
Figure 5.26. Comparison between AMEL coverage (MS) with total THAA concentration (IcPD) - left and Asx THAA D/L (IcPD) - right during isothermal heating of woolly rhino enamel at 60, 70 and 80 °C.

IcPD analysis had been undertaken on Rhinocerotidae (*Stephanorhinus*) tooth enamel, and reported in the Cappellini *et al.,* (2019) paper alongside the MS results to corroborate the likelihood of protein endogeneity. This 1.77-Ma old fossil had a THAA Asx D/L value of 0.38, just above the highest level of racemisation achieved during the forced degradation experiments. It also had a total THAA concentration of ~ 1280 pmol/mg. Searching the raw MS data file for Dm.5/157-16635 (stagetip 870) through PEAKS and filtering to 0.5% FDR gave rise to 67% AMELX coverage from 319 peptides. These

results were better than any of the samples analysed here, including the unheated baseline sample (57% AMELX coverage from 241 peptides, section 5.3.2.1). However, there were a number of differences in the original preparation of the Dmanisi Rhinocerotidae sample that likely gave rise to this. Most notably, ~ 250 mg of sample was demineralised, with no bleaching step for this fossil. As we wanted to directly compare peptides from the same intra-crystalline fraction in both the RP-HPLC and MS analysis in this study, approximately 10-fold less (~ 25 mg) sample was demineralised after bleaching of the powdered enamel. The regions of coverage were, however, very similar (Fig. 5.27), indicating the regions of peptide preservation were consistent between the forced degradation samples studied here and the Dmanisi fossil sample.
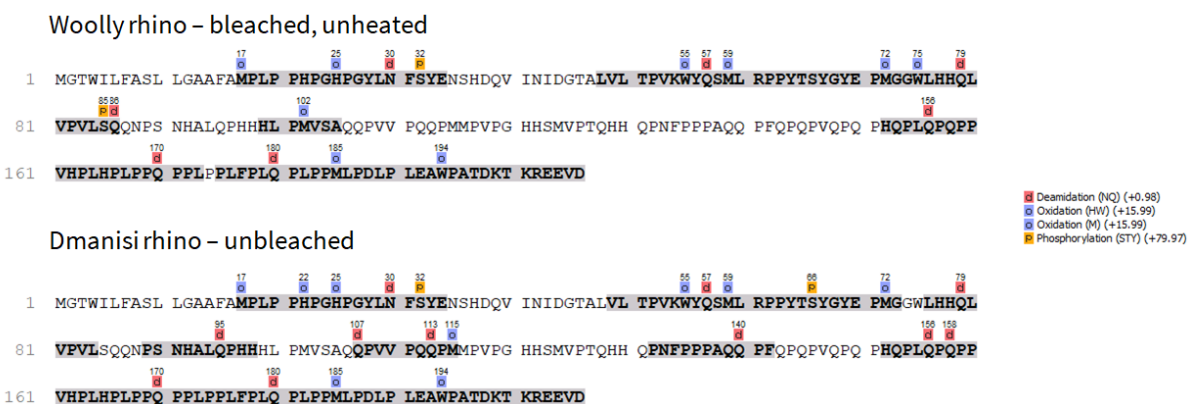
Figure 5.27. Outline of AMELX coverage for bleached, unheated woolly rhino enamel sample (top) and unbleached Dmanisi rhino (Dm.5/157-16635 (stagetip 870)) enamel sample (bottom).

Four of the enamel Rhinocerotidae samples analysed for IcPD in chapter 4 were also analysed by MS (table 5.4) by Fazeelah Munir (Munir, in prep.) using a similar protocol to sections 5.2.2 and 5.2.5, although no 72 hour bleaching step was included and ~ 3 fold higher starting material (~ 80 mg) was used. Database searching and data analysis was undertaken by me for comparison to the IcPD data.

Five or more AMELX peptides were observed for three out of four samples (Fig. 5.28), whilst no peptides were observed for the fourth sample. For these four samples, there appeared to be no relationship between the extent of amino acid racemisation or total amino acid concentration and the outcome of the MS results (e.g. Asx in table 5.4).

Table 5.4. Comparison IcPD results (Asx THAA D/L and total THAA concentration) with number of observed peptides during MS analysis for four fossil Rhinocerotidae samples from Twin Rivers, Zambia.

Fossil Sample	MS Analysis	IcPD Analysis	
	Number of peptides	Asx THAA D/L	Total THAA concentration (pmol/mg)
TWE13.3	5	0.41	~ 1505
TWE20.4	0	0.44	~ 1620
TWE20.2	14	0.53	~ 1375
TWE4.1	5	0.61	~ 1950

Interestingly, the region of observed peptides was consistent between the three Zambian fossil samples and similar to the most degraded sample from this study (Fig. 5.28), indicating this region of AMEL may have the best preservation potential within the enamel proteome for MS analysis.
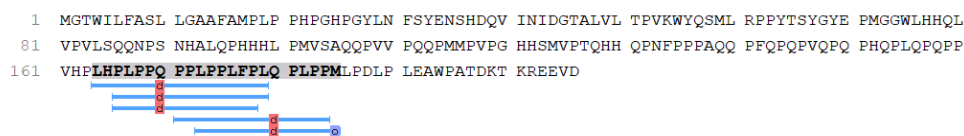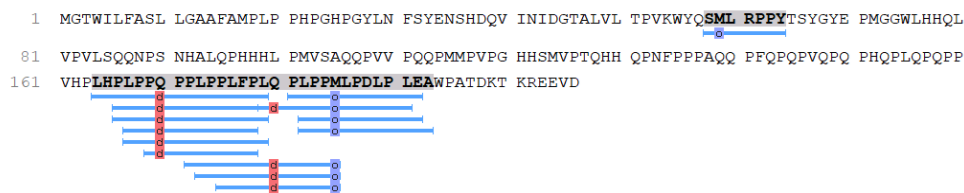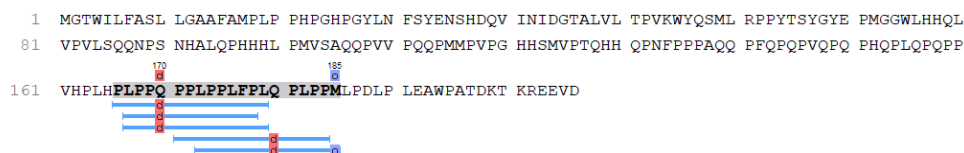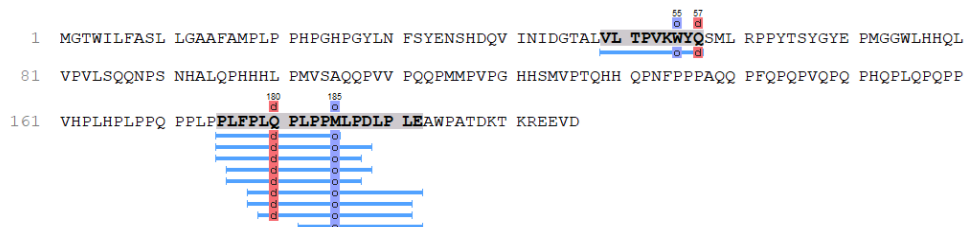
Figure 5.28. Regions of AMELX peptide coverage for three fossil Rhinocerotidae enamel samples from Twin Rivers, Zambia and woolly rhino tooth enamel heated at 80 °C for 2 years.

Conclusion

The IcPD approach to AAG and palaeoproteomics was undertaken on Rhinocerotidae enamel samples heated at 60, 70 and 80 °C for two years to study protein degradation on an accelerated timescale for comparison to fossils.

Increasing markers of IcPD degradation were observed with respect to both temperature and time for racemisation, peptide chain hydrolysis and Ser and Thr dehydration. The relative composition and total amino acid concentrations remained relatively stable over the course of the study. Overall, the extent of degradation observed was low, and there was little overlap of degradation (racemisation, hydrolysis, Ser and Thr dehydration) with the rhinocerotid fossils available, making comparisons challenging. The low levels of racemisation achieved in this study rendered the transformed data inappropriate for kinetic modelling. To more accurately study whether forced degradation experiments at lower experimental temperatures are reflective of environmental diagenesis and therefore appropriate for kinetic modelling, it is recommended future studies are planned for significantly longer timescales. Extrapolating from extents of racemisation observed in this study, it is likely that at a minimum, four years of isothermal heating at 80 °C, six years at 70 °C and ten years at 60 °C, would be required to cover a greater extent of racemisation.

Through MS analysis of bleached, unheated woolly rhino enamel, it was possible to improve upon the previously known enamel proteome sequences, and should higher sample amounts be used and/or without bleaching, further improvements could be made. Patterns of degradation were difficult to elucidate from the palaeoproteomic MS results, partly as a result of the pilot experimental design undertaken (single experimental and analytical replicates), and the low levels of degradation. However, comparisons to fossil samples at higher extents of degradation indicated similar regions of peptide preservation in AMEL, suggesting the heating experiments undertaken in this study may be somewhat reflective of environmental diagenesis. For future degradation studies intended for palaeoproteomic MS analysis, a minimum of three experimental replicates are recommended, in addition to optimisation of the methodologies for the best recovery of markers of endogenous protein degradation. As with the IcPD data, it is also recommended to undertake future forced degradation experiments over longer timescales.

Due to the generally low levels of degradation observed by IcPD and MS, it was not possible to draw many conclusions about their relationship. However, as displayed by the forced degradation experiments, it is likely that enamel samples with total THAA concentrations above 1500 pmol/mg and Asx THAA D/L below 0.35 from IcPD chiral amino acid analysis would yield endogenous enamel peptides during MS analysis. Future studies over longer timescales, will likely help to further elucidate their relationship.

5.4. References

Akiyama, M., 1980. Diagenetic decomposition of peptide-linked serine residues in the fossil scallop shells. *Biogeochemistry of amino acids*, pp.115-120.

Bada, J.L. and Schroeder, R.A., 1972. Racemization of isoleucine in calcareous marine sediments: kinetics and mechanism. *Earth and Planetary Science Letters, 15*(1), pp.1-11.

Bada, J.L. and Schroeder, R.A., 1975. Amino acid racemization reactions and their geochemical implications. *Naturwissenschaften, 62*, pp.71-79.

Bada, J.L., Shou, M.Y., Man, E.H., and Schroeder, R.A. 1978. Decomposition of hydroxy amino acids in foraminiferal tests: Kinetics, mechanism and geochronological implications. *Earth Planetary Science Letters, 41*(1), pp.67-76.

Bai, B., Meng, J., Zhang, C., Gong, Y.X. and Wang, Y.Q., 2020. The origin of Rhinocerotoidea and phylogeny of Ceratomorpha (Mammalia, Perissodactyla). *Communications Biology, 3*(1), p.509.

Baldreki, C., Burnham, A., Conti, M., Wheeler, L., Simms, M.J., Barham, L., White, T.S., Penkman, K., 2024. Investigating the potential of African land snail shells (Gastropoda: Achatininae) for amino acid geochronology. *Quaternary Geochronology, 79*, pp.101473.

Barham, L.S., 2000. *The Middle Stone Age of Zambia, South Central Africa*. Western academic & specialist Press.

Bishop, L.C. and Reynolds, S.C., 2000. Chapter 11 Fauna from Twin Rivers in Barham, L.S., 2000. *The Middle Stone Age of Zambia, South Central Africa*. Western academic & specialist Press. pp. 217-222.

Blain, H.A., Agustí, J., Lordkipanidze, D., Rook, L. and Delfino, M., 2014. Paleoclimatic and paleoenvironmental context of the Early Pleistocene hominins from Dmanisi (Georgia, Lesser Caucasus) inferred from the herpetofaunal assemblage. *Quaternary science reviews*, *105*, pp.136-150.

Bravenec, A.D., Ward, K.D. and Ward, T.J., 2018. Amino acid racemization and its relation to geochronology and archaeometry. *Journal of separation science, 41*(6), pp.1489-506.

Brooks, A.S., Hare, P.E., Kokis, J.E., Miller, G.H., Ernst, R.D. and Wendorf, F., 1990. Dating Pleistocene archeological sites by protein diagenesis in ostrich eggshell. *Science*, *248*(4951), pp.60-64.

Bright, J. and Kaufman, D.S., 2011. Amino acid racemization in lacustrine ostracodes, part I: effect of oxidizing pre-treatments on amino acid composition. *Quaternary Geochronology, 6*(2), pp.154-173.

Burger, T., 2018. Gentle introduction to the statistical foundations of false discovery rate in quantitative proteomics. *Journal of proteome research, 17*(1), pp.12-22.

Canoira, L., García-Martínez, M.J., Llamas, J.F., Ortíz, J.E. and Torres, T.D., 2003. Kinetics of amino acid racemization (epimerization) in the dentine of fossil and modern bear teeth. *International journal of chemical kinetics, 35*(11), pp.576-591.

Cappellini, E., Welker, F., Pandolfi, L., Ramos-Madrigal, J., Samodova, D., Rüther, P.L., Fotakis, A.K., Lyon, D., Moreno-Mayar, J.V., Bukhsianidze, M. and Rakownikow Jersie-Christensen, R., 2019. Early Pleistocene enamel proteome from Dmanisi resolves *Stephanorhinus* phylogeny. *Nature, 574*(7776), pp.103-107.

Chowdhury, M.P. and Buckley, M., 2022. Trends in deamidation across archaeological bones, ceramics and dental calculus. *Methods, 200*, pp.67-79.

Cintas-Peña, M., Luciañez-Triviño, M., Montero Artús, R., Bileck, A., Bortel, P., Kanz, F., Rebay-Salisbury, K. and García Sanjuán, L., 2023. Amelogenin peptide analyses reveal female leadership in Copper Age Iberia (c. 2900–2650 BC). *Scientific Reports, 13*(1), pp.9594.

Clarke, S.J. and Murray-Wallace, C.V., 2006. Mathematical expressions used in amino acid racemisation geochronology—a review. *Quaternary Geochronology*, *1*(4), pp.261-278.

Cleland, T.P., Schroeter, E.R. and Colleary, C., 2021. Diagenetiforms: a new term to explain protein changes as a result of diagenesis in paleoproteomics. *Journal of proteomics*, *230*, pp.103992.

Collins, M.J., Waite, E.R. and Van Duin, A.C.T., 1999. Predicting protein decomposition: the case of aspartic–acid racemization kinetics. *Philosophical Transactions of the Royal Society of London. Series B: Biological Sciences*, *354*(1379), pp.51-64.

Crisp, M., Demarchi, B., Collins, M., Morgan-Williams, M., Pilgrim, E. and Penkman, K., 2013. Isolation of the intra-crystalline proteins and kinetic studies in *Struthio camelus* (ostrich) eggshell for amino acid geochronology. *Quaternary Geochronology. 1*(16), pp.110-28.

Demarchi, B., Collins, M., Bergström, E., Dowle, A., Penkman, K., Thomas-Oates, J., Wilson, J., 2013. New experimental evidence for in-chain amino acid racemization of serine in a model peptide. *Analytical Chemistry, 85*(12), pp.5835-5842 236.

Demarchi, B., Hall, S., Roncal-Herrero, T., Freeman, C. L., Woolley, J., Crisp, M. K., Wilson, J., Fotakis, A., Fischer, R., Kessler, B. M., Jersie-Christensen, R. R., Olsen, J. V., Haile, J., Thomas, J., Marean, C. W., Parkington, J., Presslee, S., Lee-Thorp, J., Ditchfield, P., Hamilton, J. F., Ward, M. W., Wang, C. M.,

Shaw, M. D., Harrison, T., Dominguez-Rodrigo, M., Macphee, R. D. E., Kwekason, A., Ecker, M., Horwitz, L. K., Chazan, M., Kroger, R., Thomas-Oates, J., Harding, J. H., Cappellini, E., Penkman, K., Collins, M. J., 2016. Protein sequences bound to mineral surfaces persist into deep time. *elife, 5*, p.e17092.

Dickinson, M.R., Lister, A.M. and Penkman, K.E., 2019. A new method for enamel amino acid racemization dating: a closed system approach. *Quaternary Geochronology, 50*, pp.29-46.

Dobberstein, R.C., Collins, M.J., Craig, O.E., Taylor, G., Penkman, K.E. and Ritz-Timme, S., 2009. Archaeological collagen: Why worry about collagen diagenesis?. *Archaeological and Anthropological Sciences*, *1*, pp.31-42.

Gabunia, L., Vekua, A., Lordkipanidze, D., Swisher III, C.C., Ferring, R., Justus, A., Nioradze, M., Tvalchrelidze, M., Antón, S.C., Bosinski, G. and Joris, O., 2000. Earliest Pleistocene hominid cranial remains from Dmanisi, Republic of Georgia: taxonomy, geological setting, and age. *Science*, *288*(5468), pp.1019-1025.

Goodfriend, G.A., 1991. Patterns of racemization and epimerization of amino acids in land snail shells over the course of the Holocene. *Geochimica et Cosmochimica Acta*, *55*(1), pp.293-302.

Goodfriend, G.A. and Meyer, V.R., 1991. A comparative study of the kinetics of amino acid racemization/epimerization in fossil and modern mollusk shells. *Geochimica et Cosmochimica Acta*, *55*(11), pp.3355-3367.

Grzeskowiak, R., Hamels, S. and Gancarek, E., 2016. Comparative Analysis of Protein Recovery Rates in Eppendorf LoBind® and Other "Low Binding" Tubes. *AG Application Note*.

Kaufman, D.S. and Manley, W.F., 1998. A new procedure for determining DL amino acid ratios in fossils using reverse phase liquid chromatography. *Quaternary Science Reviews. 17*(11), pp.987-1000.

Kaufman, D.S. and Miller, G.H., 1992. Overview of amino acid geochronology. *Comparative Biochemistry and Physiology Part B: Comparative Biochemistry*, *102*(2), pp.199-204.

Kimber, R.W. and Griffin, C.V., 1987. Further evidence of the complexity of the racemization process in fossil shells with implications for amino acid racemization dating. *Geochimica et Cosmochimica Acta, 51*(4), pp.839-846.

King, K.J. and Hare, P.E., 1972. Species effects in the epimerization of L-isoleucine in fossil planktonic foraminifera. *Carnegie Institute Washington Year Book*, *71*, pp.596–598.

Kosnik, M.A., Kaufman, D.S. and Hua, Q., 2008. Identifying outliers and assessing the accuracy of amino acid racemization measurements for geochronology: I. Age calibration curves. *Quaternary Geochronology*, *3*(4), pp.308-327.

Kraut, A., Marcellin, M., Adrait, A., Kuhn, L., Louwagie, M., Kieffer-Jaquinod, S., Lebert, D., Masselon, C.D., Dupuis, A., Bruley, C. and Jaquinod, M., 2009. Peptide storage: are you getting the best return on your investment? Defining optimal storage conditions for proteomics samples. *Journal of proteome research*, *8*(7), pp.3778-3785.

Kumar, D., Bansal, G., Narang, A., Basak, T., Abbas, T. and Dash, D., 2016. Integrating transcriptome and proteome profiling: Strategies and applications. *Proteomics*, *16*(19), pp.2533-2544.

Lacruz, R.S., Habelitz, S., Wright, J.T. and Paine, M.L., 2017. Dental enamel formation and implications for oral health and disease. *Physiological reviews*, *97*(3), pp.939-993.

Lugli, F., Di Rocco, G., Vazzana, A., Genovese, F., Pinetti, D., Cilli, E., Carile, M.C., Silvestrini, S., Gabanini, G., Arrighi, S. and Buti, L., 2019. Enamel peptides reveal the sex of the Late Antique 'Lovers of Modena'. *Scientific reports*, *9*(1), pp.13130.

Mackie, M., Rüther, P., Samodova, D., Di Gianvincenzo, F., Granzotto, C., Lyon, D., Peggie, D.A., Howard, H., Harrison, L., Jensen, L.J. and Olsen, J.V., 2018. Palaeoproteomic profiling of conservation layers on a 14th century Italian wall painting. *Angewandte Chemie International Edition, 57*(25), pp.7369-7374.

Madupe, P.P., Koenig, C., Patramanis, I., Rüther, P.L., Hlazo, N., Mackie, M., Tawane, M., Krueger, J., Taurozzi, A.J., Troché, G.B. and Kibii, J., 2023. Enamel proteins reveal biological sex and genetic variability within southern African *Paranthropus. bioRxiv*, pp.2023-3007.

Mitterer, R.M. and Kriausakul, N., 1984. Comparison of rates and degrees of isoleucine epimerization in dipeptides and tripeptides. *Organic Geochemistry*, *7*(1), pp.91-98.

Munir F. In prep. Understanding protein diagenesis and its relevance to palaeoproteomics and geochronology in tooth enamel. PhD thesis, University of York.

Nagano, T., Kakegawa, A., Yamakoshi, Y., Tsuchiya, S., Hu, J.C., Gomi, K., Arai, T., Bartlett, J.D. and Simmer, J.P., 2009. Mmp-20 and Klk4 cleavage site preferences for amelogenin sequences. *Journal of dental research, 88*(9), pp.823-828.

Nielsen-Marsh, C.M., Stegemann, C., Hoffmann, R., Smith, T., Feeney, R., Toussaint, M., Harvati, K., Panagopoulou, E., Hublin, J.J. and Richards, M.P., 2009. Extraction and sequencing of human and

Neanderthal mature enamel proteins using MALDI-TOF/TOF MS. *Journal of Archaeological Science, 36*(8), pp.1758-1763.

Orem, C.A. and Kaufman, D.S., 2011. Effects of basic pH on amino acid racemization and leaching in freshwater mollusk shell. *Quaternary Geochronology*, *6*(2), pp.233-245.

Ortiz, J.E., Torres, T., Julià, R., Delgado, A., Llamas, F.J., Soler, V. and Delgado, J.. 2004. Numerical dating algorithms of amino acid racemization ratios from continental ostracodes. Application to the Guadix-Baza Basin (southern Spain). *Quaternary Science Reviews*, *23*(5-6), pp.717-730.

Ortiz, J.E., Torres, T. and Pérez-González, A., 2013. Amino acid racemization in four species of ostracodes: taxonomic, environmental, and microstructural controls. *Quaternary Geochronology, 16*, pp.129-143.

Ortiz, J.E., Torres, T., Sánchez-Palencia, Y. and Ferrer, M., 2017. Inter-and intra-crystalline protein diagenesis in *Glycymeris* shells: Implications for amino acid geochronology. *Quaternary Geochronology, 1*(41) pp.37-50.

Parker, G.J., Yip, J.M., Eerkens, J.W., Salemi, M., Durbin-Johnson, B., Kiesow, C., Haas, R., Buikstra, J.E., Klaus, H., Regan, L.A. and Rocke, D.M., 2019. Sex estimation using sexually dimorphic amelogenin protein fragments in human enamel. *Journal of Archaeological Science, 101*, pp.169-180.

Penkman, K.E.H., 2005. Amino acid geochronology: a closed system approach to test and refine the UK model. PhD thesis, University of Newcastle.

Penkman, K. E. H., Kaufman, D. S., Maddy, D., Collins, M. J., 2008. Closed-system behaviour of the intra-crystalline fraction of amino acids in mollusc shells. *Quaternary Geochronology, 31*(2), pp.2-25.

Penkman, K.E., Preece, R.C., Bridgland, D.R., Keen, D.H., Meijer, T., Parfitt, S.A., White, T.S. and Collins, M.J., 2013. An aminostratigraphy for the British Quaternary based on *Bithynia* opercula. *Quaternary Science Reviews*, *61*, pp.111-134.

Penkman, K.E., Preece, R.C., Keen, D.H., Maddy, D., Schreve, D.C. and Collins, M.J., 2007. Testing the aminostratigraphy of fluvial archives: the evidence from intra-crystalline proteins within freshwater shells. *Quaternary Science Reviews, 26*(22-24), pp.2958-2969.

Powell, J., Collins, M.J., Cussens, J., MacLeod, N. and Penkman, K.E., 2013. Results from an amino acid racemization inter-laboratory proficiency study; design and performance evaluation. *Quaternary Geochronology, 16*, pp.183-197.

Preece, R.C. and Penkman, K.E.H., 2005. New faunal analyses and amino acid dating of the Lower Palaeolithic site at East Farm, Barnham, Suffolk. *Proceedings of the Geologists' Association, 116*(3-4), pp.363-377.

Presslee, S., Penkman, K., Fischer, R., Richards-Slidel, E., Southon, J., Hospitaleche, C.A., Collins, M. and MacPhee, R., 2021. Assessment of different screening methods for selecting palaeontological bone samples for peptide sequencing. *Journal of proteomics*, *230*, pp.103986.

Ramsøe, A., van Heekeren, V., Ponce, P., Fischer, R., Barnes, I., Speller, C. and Collins, M.J., 2020. DeamiDATE 1.0: Site-specific deamidation as a tool to assess authenticity of members of ancient proteomes. *Journal of Archaeological Science*, *115*, pp.105080.

Robinson, N.E. and Robinson, A., 2004. Molecular clocks: deamidation of asparaginyl and glutaminyl residues in peptides and proteins. *Althouse press.*

Sato, N., Quitain, A.T., Kang, K., Daimon, H. and Fujie, K., 2004. Reaction kinetics of amino acid decomposition in high-temperature and high-pressure water. *Industrial & Engineering Chemistry Research, 43*(13), pp.3217-3222.

Simpson, J.P., 2015. Investigating the relationship between glutamine deamidation and collagen breakdown in bone. PhD thesis, University of York.

Simpson, J.P., Penkman, K.E.H., Demarchi, B., Koon, H., Collins, M.J., Thomas-Oates, J., Shapiro, B., Stark, M. and Wilson, J., 2016. The effects of demineralisation and sampling point variability on the measurement of glutamine deamidation in type I collagen extracted from bone. *Journal of archaeological science*, *69*, pp.29-38.

Smith, G.G., Evans, R.C., 1980. The effect of structure and conditions on the rate of racemisation of free and bound amino acids. *Biogeochemistry of Amino Acids*, pp.257-282.

Solazzo, C., Dyer, J.M., Clerens, S., Plowman, J., Peacock, E.E. and Collins, M.J., 2013. Proteomic evaluation of the biodegradation of wool fabrics in experimental burials. *International Biodeterioration & Biodegradation*, *80*, pp.48-59.

Stephenson, R.C. and Clarke, S., 1989. Succinimide formation from aspartyl and asparaginyl peptides as a model for the spontaneous degradation of proteins. *Journal of Biological Chemistry, 264*(11), pp.6164-6170.

Takahashi, O., Kobayashi, K. and Oda, A., 2010. Computational insight into the mechanism of serine residue racemization. *Chemistry & Biodiversity*, *7*(6), pp.1625-1629.

Termine, J.D., Belcourt, A.B., Christner, P.J., Conn, K.M. and Nylen, M.U., 1980. Properties of dissociatively extracted fetal tooth matrix proteins. I. Principal molecular species in developing bovine enamel. *Journal of Biological Chemistry, 255*(20), pp.9760-9768.

Tomiak, P.J., Penkman, K.E., Hendy, E.J., Demarchi, B., Murrells, S., Davis, S.A., McCullagh, P. and Collins, M.J., 2013. Testing the limitations of artificial protein degradation kinetics using known-age massive *Porites* coral skeletons. *Quaternary Geochronology, 16*, pp.87-109.

Torres, T., Ortiz, J.E., Fernández, E., Arroyo-Pardo, E., Grün, R. and Pérez-González, A., 2014. Aspartic acid racemization as a dating tool for dentine: a reality. *Quaternary Geochronology*, *22*, pp.43-56.

Umamaheswaran, R. and Dutta, S., 2024. Preservation of proteins in the geosphere. *Nature Ecology & Evolution*, pp.1-8.

UniProt (2024), *UniProtKB*. Available at: https://www.uniprot.org/uniprotkb?query=amelogenin&facets=reviewed%3Atrue (Accessed 17 May 2024)

Van Doorn, N.L., Wilson, J., Hollund, H., Soressi, M. and Collins, M.J., 2012. Site-specific deamidation of glutamine: a new marker of bone collagen deterioration. *Rapid communications in mass spectrometry*, *26*(19), pp.2319-2327.

Walsh, C.T., Garneau-Tsodikova, S. and Gatto Jr, G.J., 2005. Protein posttranslational modifications: the chemistry of proteome diversifications. *Angewandte Chemie International Edition, 44*(45), pp.7342-7372.

Walton, D., 1998. Degradation of intracrystalline proteins and amino acids in fossil brachiopods. *Organic Geochemistry*, *28*(6), pp.389-410.

Welker, F., Ramos-Madrigal, J., Kuhlwilm, M., Liao, W., Gutenbrunner, P., de Manuel, M., Samodova, D., Mackie, M., Allentoft, M.E., Bacon, A.M. and Collins, M.J., 2019. Enamel proteome shows that *Gigantopithecus* was an early diverging pongine. *Nature*, *576*(7786), pp.262-265.

Welker, F., Ramos-Madrigal, J., Gutenbrunner, P., Mackie, M., Tiwary, S., Rakownikow Jersie-Christensen, R., Chiva, C., Dickinson, M.R., Kuhlwilm, M., de Manuel, M. and Gelabert, P., 2020. The dental proteome of Homo antecessor. *Nature*, *580*(7802), pp.235-238.

Wehmiller, J.F., Harris, W.B., Boutin, B.S. and Farrell, K.M., 2012. Calibration of amino acid racemization (AAR) kinetics in United States mid-Atlantic Coastal Plain Quaternary mollusks using

[87]Sr/[86]Sr analyses: Evaluation of kinetic models and estimation of regional Late Pleistocene temperature history. *Quaternary Geochronology*, *7,* pp.21-36.

Yates, J.R., Eng, J.K. and McCormack, A.L., 1995. Mining genomes: correlating tandem mass spectra of modified and unmodified peptides to sequences in nucleotide databases. *Analytical chemistry*, *67*(18), pp.3202-3210.

Chapter 6. Conclusions and future work

6.1. Conclusions

The South-Central African region contains many important archaeological and palaeoenvironmental sites (e.g. Woodward, 1921; Fagan *et al.*, 1966; Barham, 2002; Duller *et al.*, 2015; Richter *et al.*, 2022; Fletcher *et al.*, 2022; Barham *et al.*, 2023), although the chronology of the region is not well understood. Dating is crucial to understand each site to its fullest, and especially to relate wider mammalian (including hominin) evolutionary patterns. A number of regional sites were excavated in the 1990s, including Twin Rivers and nearby Palaeolake Kafue, with archived fossil material available for further study.

The aim of this thesis was to explore the potential of this material for palaeoenvironmental and biomolecular analyses using techniques which have advanced in the intervening years, in order to add palaeoclimate, taxonomic and geochronological insights.

Molluscan assemblages were extracted from Pleistocene sediments which had been previously excavated from Palaeolake Kafue in southern Zambia (Chapter 2). Palaeoenvironmental analysis of this assemblage resulted in the identification of a mixture of species, indicative of varied past climates. These included terrestrial taxa (*Achatina* spp., *Afroguppya rumrutiensis*), as well as those with a preference for lake- or river- margin vegetation (*Helicarion issangoensis*, *Succinea* sp.) and freshwater taxa (*Planorbis* sp.). Notably, this assemblage provided the first record of *Helicarion issangoensis* (the first of any helicarionid to be listed) from Zambia, highlighting the need for more detailed studies of the Pleistocene fossil record and on current fauna for comparative analysis. One commonly occurring taxa identified from these Pleistocene sediments, *Achatina* spp., which can also be found widespread across the African continent (Fontanilla, 2010), was therefore chosen for assessment for its suitability for the IcPD approach to AAG.

Achatininae shell contains a complex multi-layered $CaCO_3$ microstructure, which can complicate the application of amino acid geochronology if sampling is not consistent (e.g. Sejrup and Haugen, 1994; Goodfriend *et al.*, 1997; Torres *et al.*, 2013). To assess a suitable sampling strategy, comparison was made between the three aragonitic layer (3AL) shell portion and the 'nacreous' layers alone (Chapter 3). Achatininae shell was shown to have an intra-crystalline fraction of protein, which appeared to adhere to closed-system behaviour in the 3AL shell portion. The 'nacreous' layer did not adhere well to closed system behaviour, possibly due to complications arising from difficulties sampling the very thin shell (~ 250 μm thick) and potential mineral diagenesis during drilling observed through XRD analysis. During heating experiments, predictable degradation of protein was observed (in terms of racemisation and hydrolysis), with respect to both temperature and time. Different relative rates of racemisation were observed for proteins in the 'nacreous' layer and the 3AL in modern shells at different temperatures. Additionally, a different pattern of behaviour was observed

in the fossils, indicating the heating experiments undertaken were not wholly representative of the diagenesis observed in the fossils and are not strictly comparable. As well as possible temperature related protein degradation differences, the lack of correspondence could also be as a result of taxonomic differences between the modern *Achatina tavaresiana* and fossil *Lissachatina* sp. studied. This prevented accurate extrapolation of fossil parameters (numerical dating) from mathematical modelling of high temperature kinetic experiments. However, the consistent degradation patterns and closed-system behaviour of the 3AL shell portion of Achatininae demonstrated that it has the potential to provide chronological data for the South-Central African region, and beyond.

Mammalian tooth enamel, recently shown to be an appropriate biomineral for the IcPD approach to AAG (Dickinson *et al.*, 2019), is a commonly excavated fossil from archaeological and palaeoenvironmental sites. Application of this newly developed technique to previously excavated material from the Zambian archaeological sites of Twin Rivers and Mumbwa Caves (Chapter 4), gave the opportunity to provide additional site information, key for accurate interpretation. Of the 80 fossil tooth enamel samples from four taxonomic groups (bovids, equids, suids, rhinocerotids), 72 of these (90%) showed evidence of closed system behaviour in their intra-crystalline protein fraction. At Twin Rivers, a potential trend between excavation depth and the extent of racemisation in the least degraded samples was observed, concordant with the working hypothesis of a sequential deposition within A Block. Post-depositional processes (including bioturbation by roots and the mixing of deposits on excavation) may account in part for the wide spreads of racemisation values within some individual excavation levels, although greater depositional history complexity is likely. Direct dating of the fauna allowed recognition of this complexity for the first time, critical for accurate site interpretation. Whilst the contextual information of the Mumbwa Caves material was unrecoverable, the material provided a regional comparison which was consistent with previous dating information. Investigation of taxonomic variability within the IcPD dataset was limited due to the lack of chronological constraint at both sites. However, one notable degradation pattern difference in peptide chain hydrolysis was observed in the rhinocerotid data, in comparison to the suid, equid and bovid data, leading to the recommendation that taxon-specific enamel AAGs are developed. In the Twin Rivers dataset, the broad range of racemisation values observed in Glx (0.2 - 1.0 D/L), one of the slowest racemising amino acids, indicated the likely presence of fauna over the Pleistocene. This highlights enamel's potential for building Quaternary AAGs in warm regions, such as South-Central Africa, enabling direct dating on mammalian material, on which evolutionary, palaeoenvironmental and isotopic studies are conducted.

Alongside amino acid geochronology, a second biomolecular technique which can be undertaken on proteins in fossil tooth enamel is mass spectrometric palaeoproteomics. Used together, these complementary techniques allow the analysis of proteins at the amino acid and peptide level respectively (Chapter 5). Forced degradation experiments at relatively low temperatures

(60, 70 and 80 °C) were undertaken on Rhinocerotidae tooth enamel to study the protein degradation in a new taxa, for comparison to fossils. Markers of IcPD increased with respect to both temperature and time for racemisation, peptide chain hydrolysis and Ser and Thr dehydration. Overall, despite the experiments lasting two years, the extent of degradation observed was low, with the relative composition and total amino acid concentrations remaining relatively stable over the course of the study. Little to no overlap was observed between the forced degradation data and the available fossil dataset (for racemisation, hydrolysis, Ser and Thr dehydration), making comparisons challenging; however, the fossils appeared to extend the trends. The low levels of racemisation achieved in this study also rendered the transformed data inappropriate for kinetic modelling. It is therefore recommended that future studies are planned for significantly longer timescales (a minimum of ten years) when using these lower experimental temperatures (60, 70 and 80 °C).

A potential taxonomic difference in the relative rates of racemisation were also observed for two amino acids (Asx and Ser) when comparing Rhinocerotidae and Elephantidae experimental data, strengthening the recommendation to build taxa-specific AAGs from mammalian tooth enamel. Through MS analysis of bleached, unheated woolly rhino enamel, it was possible to improve upon the known enamel proteome sequences and should higher sample amounts be used and/or without bleaching, further improvements could be made. Patterns of degradation were difficult to elucidate from the palaeoproteomic MS results, partly as a result of the pilot experimental design undertaken (single experimental and analytical replicates), and the low levels of degradation. However, comparisons to fossil samples at higher extents of degradation indicated similar regions of peptide preservation in AMEL, suggesting the heating experiments undertaken in this study may be somewhat reflective of environmental diagenesis. For future degradation studies intended for palaeoproteomic MS analysis, a minimum of three experimental replicates are recommended, in addition to optimisation of the methodologies for the best recovery of markers of endogenous protein degradation. As with the IcPD data, it is also recommended to undertake future forced degradation experiments over longer timescales. Due to the generally low levels of degradation observed by IcPD and MS in this study, it was not possible to draw many conclusions about their relationship. However, it is likely that enamel samples with total THAA concentrations above ~1500 pmol/mg and Asx THAA D/L below 0.35 would yield endogenous enamel peptides during MS analysis. Future studies over longer timescales will likely help to further elucidate their relationship.

This thesis demonstrates the importance of accurate recording and archival of all excavated material from archaeological and palaeoenvironmental sites, to allow future studies the opportunity to further both site and scientific understanding, as more knowledge and techniques are developed.

6.2. Future work

The scope of this thesis changed during the course of this project, in part due to the significant restrictions of the COVID-19 pandemic. Some future work is therefore based on some of the original project plans, whilst others are natural progressions of the results presented in this thesis.

As the assemblage extracted from the Palaeolake Kafue Site 1 Pleistocene sediments was not large enough to make detailed claims about past climate and environmental conditions, the insight from the relatively limited amount of material recovered indicates that one area of future work would be to undertake additional purposely designed fieldwork. Excavating Pleistocene sediments from more sites around Palaeolake Kafue and over longer, defined sequences would allow a more in depth palaeoenvironmental analysis of the molluscan assemblages and the potential to better characterise the Ancient Lake, of which little is known. Undertaking ecological surveys of current molluscan species from the region would also vastly improve the records in South-Central Africa, an underrepresented region of research. Further palaeoenvironmental analysis could also reveal additional species on which to investigate their potential for AAG.

Achatininae shell showed potential for building amino acid geochronologies, which is particularly important as its shells are widespread across Africa. However, it was not possible to test its applicability within the region due to the lack of fossils from a well chronologically constrained site. It would therefore be valuable to extend this study to include sites where this is the case, such as Panga ya Saidi (Shipton *et al*., 2018; Rowson *et al*., 2024). Different patterns of degradation were also observed at different temperatures during the heating experiments, and to the fossils, rendering the heating experiments inappropriate for kinetic modelling. Additional forced degradation experiments at lower temperatures, such as those undertaken for enamel in chapter 5 (60, 70 and 80 °C), could be undertaken to investigate whether the protein degradation at lower experimental temperatures better mimicked fossil diagenesis and are therefore appropriate for kinetic modelling and ultimately the production of numerical dates.

Chapter 4 showed the potential of fossil tooth enamel from four taxa (bovids, equids, suids and rhinocerotids) to investigate cave site taphonomies/depositional histories using the IcPD approach to AAG. Future work with fossil enamel from additional sites within this region might allow a regional framework to be built. Additionally, should analysis from sites with well constrained chronologies be possible, this would enable further investigation into taxonomic effects, potentially supplemented by forced degradation experiments on a broader range of taxa. Undertaking additional forced degradation experiments at higher temperatures could allow further investigation of temperature dependent protein degradation mechanisms, whilst longer forced degradation experiments on tooth enamel at the lower experimental temperatures used in this study would induce higher levels of protein degradation, and allow better assessment of whether these conditions were

suitable for kinetic modelling and therefore numerical age calculations for fossils. Longer experimental durations of forced heating experiments would also help to investigate the relationship between the IcPD approach to AAG and palaeoproteomics, two complementary techniques applicable to several biominerals.

6.3. References

Barham, L., 2002. Systematic pigment use in the Middle Pleistocene of south-central Africa. *Current anthropology, 43*(1), pp.181-190.

Barham, L., Duller, G.A.T., Candy, I., Scott, C., Cartwright, C.R., Peterson, J.R., Kabukcu, C., Chapot, M.S., Melia, F., Rots, V. and George, N., 2023. Evidence for the earliest structural use of wood at least 476,000 years ago. *Nature, 622*(7981), pp.107-111.

Duller, G.A., Tooth, S., Barham, L. and Tsukamoto, S., 2015. New investigations at Kalambo Falls, Zambia: Luminescence chronology, site formation, and archaeological significance. *Journal of Human Evolution, 85*, pp.111-125.

Fagan, B.M., Van Noten, F.L. and Vynckier, J.R., 1966, December. Wooden Implements from Late Stone Age Sites at Gwisho Hot-springs, Lochinvar, Zambia. In *Proceedings of the Prehistoric Society* (Vol. 32, pp. 246-261). Cambridge University Press.

Fletcher, R., Barham, L., Duller, G. and Jain, M., 2022. Nothing set in stone: Chaines operatoires of later stone age sequences from the Luangwa valley and Muchinga Escarpment, Zambia. *South African Archaeological Bulletin* 77(217), pp.89–114.

Fontanilla, I.K., 2010. *Achatina* (*Lissachatina*) *fulica* Bowdich: its molecular phylogeny, genetic variation in global populations, and its possible role in the spread of the rat lungworm *Angiostrongylus cantonensis* (Chen). PhD thesis, University of Nottingham.

Goodfriend, G.A., Flessa, K.W. and Hare, P.E., 1997. Variation in amino acid epimerization rates and amino acid composition among shell layers in the bivalve Chione from the Gulf of California. *Geochimica et Cosmochimica Acta, 61*(7), pp.1487-1493.

Richter, M., Tsukamoto, S., Chapot, M.S., Duller, G.A. and Barham, L.S., 2022. Electron spin resonance dating of quartz from archaeological sites at Victoria Falls, Zambia. *Quaternary Geochronology, 72*, p.101345.

Rowson, B., Law, M., Miller, J., White, T., Shipton, C., Crowther, A., Ndiema, E., Petraglia, M. and Boivin, N.L., 2024. A Quaternary sequence of terrestrial molluscs from East Africa: a record of diversity, stability, and abundance since Marine Isotope Stage 5 (78,000 BP). *Archiv für Molluskenkunde, 153*(1), pp.61-86.

Sejrup, H.P. and Haugen, J.E., 1994. Amino acid diagenesis in the marine bivalve Arctica islandica Linné from northwest European sites: only time and temperature?. *Journal of Quaternary Science, 9*(4), pp.301-309.

Shipton, C., Roberts, P., Archer, W., Armitage, S.J., Bita, C., Blinkhorn, J., Courtney-Mustaphi, C., Crowther, A., Curtis, R., Errico, F.D. and Douka, K., 2018. 78,000-year-old record of Middle and Later Stone Age innovation in an East African tropical forest. *Nature Communications, 9*(1), p.1832.

Torres, T., Ortiz, J.E. and Arribas, I., 2013. Variations in racemization/epimerization ratios and amino acid content of *Glycymeris* shells in raised marine deposits in the Mediterranean. *Quaternary Geochronology, 16*, pp.35-49.

Woodward, A.S., 1921. A new cave man from Rhodesia, South Africa. *Nature, 108*(2716), pp.371-372.